

Adaptive Finite Element Computation of Eigenvalues

D I S S E R T A T I O N

zur Erlangung des akademischen Grades
Dr. rer. nat.
im Fach Mathematik

eingereicht an der
Mathematisch-Naturwissenschaftlichen Fakultät II
der Humboldt-Universität zu Berlin

von
Dipl.-Math. Dietmar Gallistl

Präsident der Humboldt-Universität zu Berlin:
Prof. Dr. Jan-Hendrik Olbertz

Dekan der Mathematisch-Naturwissenschaftlichen Fakultät II:
Prof. Dr. Elmar Kulke

Gutachter:

1. Prof. Dr. Carsten Carstensen, Humboldt-Universität zu Berlin
2. Prof. Dr. Volker Mehrmann, Technische Universität Berlin
3. Prof. Dr. Jinchao Xu, The Pennsylvania State University

Tag der Verteidigung: 16. Juli 2014

Zusammenfassung

Gegenstand dieser Arbeit ist die numerische Approximation von Eigenwerten elliptischer Differentialoperatoren mittels der adaptiven Finite-Elemente-Methode (AFEM). Durch lokale Netzverfeinerung können derartige Verfahren den Rechenaufwand im Vergleich zu uniformer Verfeinerung deutlich reduzieren und sind daher von großer praktischer Bedeutung. Diese Arbeit behandelt adaptive Algorithmen für Finite-Elemente-Methoden (FEMs) für drei selbstadjungierte Modellprobleme: den Laplaceoperator, das Stokes-System und den biharmonischen Operator.

In praktischen Anwendungen führen Störungen der Koeffizienten oder der Geometrie auf Eigenwert-Haufen (Cluster). Dies macht simultanes Markieren im adaptiven Algorithmus notwendig. In dieser Arbeit werden optimale Konvergenzraten für einen praktischen adaptiven Algorithmus für Eigenwert-Cluster des Laplaceoperators (konforme und nichtkonforme \mathcal{P}_1 -FEM), des Stokes-Systems (nichtkonforme \mathcal{P}_1 -FEM) und des biharmonischen Operators (Morley-FEM) bewiesen. Fehlerabschätzungen in der L^2 -Norm und Bestapproximations-Resultate für diese Nichtstandard-Methoden erfordern neue Techniken, die in dieser Arbeit entwickelt werden. Dadurch wird der Beweis optimaler Konvergenzraten ermöglicht.

Die Optimalität bezüglich einer nichtlinearen Approximationsklasse betrachtet die Approximation des invarianten Unterraums, der von den Eigenfunktionen im Cluster aufgespannt wird. Der Fehler der Eigenwerte kann dazu in Bezug gesetzt werden: Die hierfür notwendigen Eigenwert-Fehlerabschätzungen für nichtkonforme Finite-Elemente-Methoden werden in dieser Arbeit gezeigt.

Die numerischen Tests für die betrachteten Modellprobleme legen nahe, dass der vorgeschlagene Algorithmus, der bezüglich aller Eigenfunktionen im Cluster markiert, einem Markieren, das auf den Vielfachheiten der Eigenwerte beruht, überlegen ist. So kann der neue Algorithmus selbst im Fall, dass alle Eigenwerte im Cluster einfach sind, den vorasymptotischen Bereich signifikant verringern.

Abstract

The numerical approximation of the eigenvalues of elliptic differential operators with the adaptive finite element method (AFEM) is of high practical interest because the local mesh-refinement leads to reduced computational costs compared to uniform refinement. This thesis studies adaptive algorithms for finite element methods (FEMs) for three model problems, namely the eigenvalues of the Laplacian, the Stokes system and the biharmonic operator.

In practice, little perturbations in coefficients or in the geometry immediately lead to eigenvalue clusters which requires the simultaneous marking in adaptive finite element methods. This thesis proves optimality of a practical adaptive algorithm for eigenvalue clusters for the conforming and nonconforming \mathcal{P}_1 FEM for the eigenvalues of the Laplacian, the nonconforming \mathcal{P}_1 FEM for the eigenvalues of the Stokes system and the Morley FEM for the eigenvalues of the biharmonic operator. New techniques from the medius analysis enable the proof of L^2 error estimates and best-approximation properties for these nonstandard finite element methods and thereby lead to the proof of optimality. The optimality in terms of the concept of nonlinear approximation classes is concerned with the approximation of invariant subspaces spanned by eigenfunctions of an eigenvalue cluster. In order to obtain eigenvalue error estimates, this thesis presents new estimates for nonconforming finite elements which relate the error of the eigenvalue approximation to the error of the approximation of the invariant subspace.

Numerical experiments for the aforementioned model problems suggest that the proposed practical algorithm that uses marking with respect to all eigenfunctions within the cluster is superior to marking that is based on the multiplicity of the eigenvalues: Even if all exact eigenvalues in the cluster are simple, the simultaneous approximation can reduce the pre-asymptotic range significantly.

Contents

Contents	v
1. Introduction	1
2. Preliminaries	9
2.1. Function Spaces and Operators	9
2.2. Adaptive Finite Element Meshes in Any Space Dimension	11
2.3. Data Structures	16
2.4. Frequently Used Results	17
3. Eigenvalue Clusters	21
3.1. Discrete Eigenvalue Problem	21
3.2. Equivalence of Seminorms	25
3.3. Upper and Lower Spectral Bounds	27
3.4. Adaptive Algorithms	29
4. Conforming \mathcal{P}_1 FEM for the Eigenvalues of the Laplacian	33
4.1. Conforming Discretisation	33
4.2. Adaptive Algorithm	35
4.3. Theoretical Error Estimator	38
4.4. Contraction Property	41
4.5. Optimal Convergence Rates	43
5. Nonconforming \mathcal{P}_1 FEM for the Eigenvalues of the Laplacian	47
5.1. The Nonconforming \mathcal{P}_1 Finite Element Space	47
5.2. Conforming Companion Operators	48
5.3. Discrete Distance Control	50
5.4. Nonconforming FEM for the Poisson Model Problem	53
5.5. Discretisation of the Laplace Eigenvalue Problem	55
5.6. Adaptive Algorithm and Approximation Classes	56
5.7. Theoretical Error Estimator and Discrete Reliability	58
5.8. Contraction Property	59
5.9. Optimal Convergence Rates	62
6. Eigenvalues of the Stokes System	65
6.1. Nonconforming Discretisation of the Stokes Equations	65
6.2. Discretisation of the Stokes Eigenvalue Problem	69
6.3. Adaptive Algorithm	70
6.4. Theoretical Error Estimator and Discrete Reliability	72
6.5. Contraction Property and Optimal Convergence Rates	75

CONTENTS

7. Biharmonic Eigenvalue Problem	79
7.1. Morley Finite Element Method	79
7.2. Conforming Companion Operator	84
7.3. Discrete Helmholtz Decompositions	87
7.4. Morley FEM for the Linear Biharmonic Equation	91
7.5. Biharmonic Eigenvalue Problem	93
7.6. Error Estimator and Adaptive Algorithm	94
7.7. Discrete Reliability and Optimal Convergence Rates	95
7.8. Extension to Buckling Problems	98
8. Eigenvalue Error Estimates for Nonconforming FEMs	101
8.1. A Nonstandard Quasi-Ritz Projection	101
8.2. Eigenvalues of the Laplacian	104
8.3. Stokes System	108
8.4. Biharmonic Operator	110
9. Numerical Experiments	113
9.1. Numerical Realisation	113
9.2. Eigenvalues of the Laplacian	116
9.3. Eigenvalues of the Stokes System	122
9.4. Eigenvalues of the Biharmonic Operator	124
9.5. Inexact Solution of the Algebraic Eigenvalue Problems	128
9.6. Conclusions from the Computational Experiments	134
Bibliography	137
A. Table of Common Notation	145
B. Implementation	149
B.1. Structure of the Implementation	149
B.2. Reproduction of the Numerical Experiments	151
C. Data Medium Containing the Software	153
List of Figures	155
List of Tables	157

1. Introduction

The numerical solution of selfadjoint eigenvalue problems with the finite element method (FEM) is fundamental in computational science and engineering with many applications ranging from time-harmonic to stability analysis. Corner singularities in nonsmooth domains make an appropriate mesh-adaptation inevitable for affordable computational costs. Nonconforming finite element methods are the first choice for many problems in computational fluid dynamics (here in the form of the Stokes equations) or in computational structural mechanics (here in the form of the Kirchhoff plate model). Figure 1.1 displays an example for the superiority of adaptive mesh-refinement with the Morley finite element for the first eigenvalue of an L-shaped Kirchhoff plate. In the double logarithmic convergence history plot (right), uniform refinement yields a convergence rate of $-1/4$ with respect to the number of degrees of freedom (ndof), whereas adaptive refinement leads to the optimal decay rate -1 . The computation of guaranteed lower bounds, which is highly relevant in

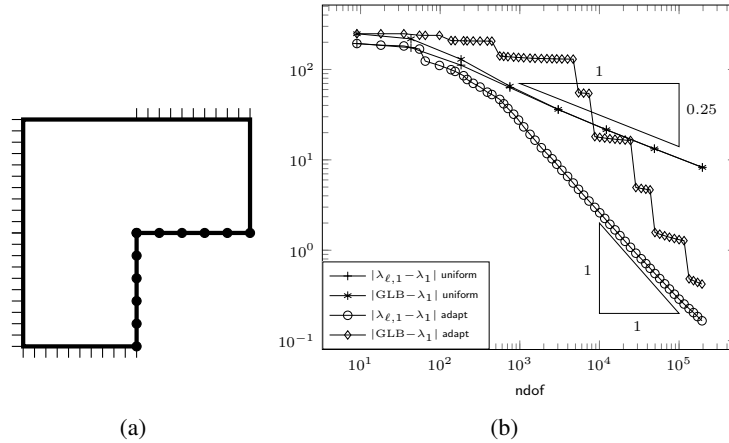


Figure 1.1.: L-shaped domain with clamped (|||||), simply supported (•••••) and free (—) boundary and convergence history for the first eigenvalue of the biharmonic operator and the guaranteed lower bound (GLB) after Carstensen and Gallistl [2014] for uniform and adaptive mesh-refinement.

many practical applications for instance in the bifurcation analysis in the buckling of plates for a stability design in computational mechanics, is one motivation for the nonconforming Morley FEM. Figure 1.1 also shows the convergence of the guaranteed lower bound (GLB) after Carstensen and Gallistl [2014].

This thesis studies the adaptive finite element approximation of selfadjoint eigenvalue problems and proves optimal convergence rates of adaptive finite element methods for three model eigenvalue problems, namely the eigenvalues of the Laplacian, the Stokes system and the biharmonic operator. The main aspects in the presented work are the analysis of nonconforming finite element methods and the treatment of clustered eigenvalues.

1. Introduction

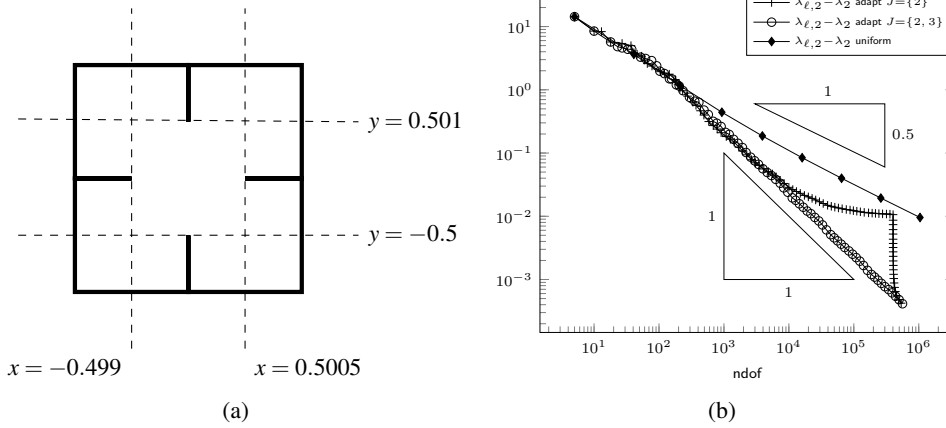


Figure 1.2.: Numerical test on a perturbed geometry. Uniform mesh-refinement (\blacklozenge) leads to a sub-optimal convergence rate. Adaptive mesh-refinement which takes into account the residuals of only one discrete eigenfunction leads to the plateau in the convergence graph (+). Marking with respect to all discrete eigenfunctions in the cluster (o) leads to the optimal rate from the very beginning.

In practice, little perturbations in coefficients or in the geometry immediately lead to an eigenvalue cluster of finite length. Figure 1.2 displays an example with a narrow eigenvalue cluster where the algorithm of Dai et al. [2013] may fail in its original version. The small non-symmetry in the geometry generates an eigenvalue cluster of two simple eigenvalues

$$\lambda_2 = 17.6557, \quad \lambda_3 = 17.6660.$$

The optimality results of Dai et al. [2008] and Carstensen and Gedicke [2012] for simple eigenvalues apply under the critical condition on the initial mesh to be sufficiently fine. A numerical computation with a coarse initial mesh (5 degrees of freedom) and conforming \mathcal{P}_1 finite elements shows a large plateau up to 400 000 degrees of freedom in the convergence history (Figure 1.2b) of the eigenvalue error $|\lambda_{\ell,2} - \lambda_2|$ in the case that the adaptive mesh-refinement is driven by the error estimator contributions of the second discrete eigenfunction $u_{\ell,2}$ only. This numerical experiment reveals an unacceptable behaviour between 10 000 and 400 000 degrees of freedom for the algorithms of [Dai et al., 2008, Carstensen and Gedicke, 2012, Dai et al., 2013].

Adaptive mesh-refinement with respect to the error estimator contributions of both discrete eigenfunctions $u_{\ell,2}$ and $u_{\ell,3}$ leads to the optimal convergence rate even for very coarse meshes. A heuristic explanation of this phenomenon will be given in Section 9.2. This pre-asymptotic failure of the known algorithms up to 400 000 degrees of freedom motivates the study and design of adaptive FEMs for eigenvalue clusters. A first-glance generalisation of the analysis of Dai et al. [2013] from multiple eigenvalues to clusters encounters the difficulty that the cluster width should not enter in the analysis as an additive term (cf. Remark 4.13).

To illuminate the differences to the analysis of Dai et al. [2013], the first main aspect of this thesis is the analysis of the conforming \mathcal{P}_1 FEM computation of the eigenvalues of the Laplace operator. A cluster-robust reliability proof for the error estimator requires

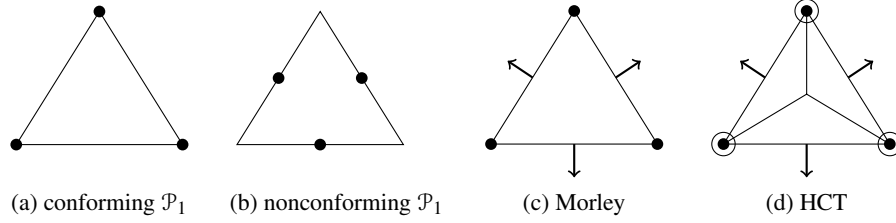


Figure 1.3.: Mnemonic diagrams of some finite elements.

a new mathematical methodology (see Remark 4.13). The focus of the thesis, however, is on the a posteriori and optimality analysis of adaptive nonstandard finite elements for some eigenvalue problems in continuum mechanics, namely the Stokes and the biharmonic eigenvalue problem. The results are valid for the situation of eigenvalue clusters, but are also the first contributions for the case of simple eigenvalues.

One motivation for the use of nonconforming methods, especially for higher-order problems, is that they allow an easier implementation compared to conforming finite elements. Figures 1.3c and 1.3d show the nonconforming Morley FEM in comparison to the conforming Hsieh-Clough-Tocher FEM based on a macro element. The computation of guaranteed lower eigenvalue bounds is a second motivation for nonconforming FEMs. The separation and resolution of the real eigenvalues requires known upper and lower eigenvalue bounds. The min-max principle shows that upper eigenvalue bounds can be computed with any conforming FEM. Besides the easier practical implementation, nonconforming FEMs allow a convenient computation of lower eigenvalue bounds. This observation was first theoretically justified by Armentano and Durán [2004] for singular eigenfunctions in an asymptotic regime. The recent works of Carstensen and Gedicke [2014], Carstensen and Gallistl [2014] and Liu and Oishi [2013] establish guaranteed lower eigenvalue bounds on arbitrarily coarse meshes. For nonconforming methods, the constants of the L^2 error estimates for the related interpolation operators are known explicitly. The projection properties of those operators lead to the lower bounds of Carstensen and Gedicke [2014] and Carstensen and Gallistl [2014]. These results should be seen in comparison to the work of Liu and Oishi [2013] for the conforming \mathcal{P}_1 FEM with an L^2 error estimate for the Galerkin projection. The involved constant depends on the mesh and has to be computed as an eigenvalue of a large-scale matrix. The advantage of nonconforming FEMs is that the interpolation functionals are well-defined for functions of minimal regularity and, therefore, the error estimates are valid element-wise. This thesis provides a unified framework for the aforementioned results and establishes lower bounds for the eigenvalues of the Stokes system as a new application,

Historical Overview

A basic overview of the finite element approximation of compact symmetric eigenvalue problems can be found in the textbook of Strang and Fix [1973]. A more abstract approach is summarised in the monograph of Chatelin [1983] and in the review articles of Babuška and Osborn [1991] and Boffi [2010]. An a priori error analysis for the nonconforming

1. Introduction

FEM of eigenvalue problems dates back to Rannacher [1979]. The first a posteriori error estimates for eigenvalue problems were obtained by Verfürth [1994] within a general framework for nonlinear problems and by [Larson, 2000] by means of a duality technique while later Durán et al. [2003] employed techniques from the analysis of linear problems plus elementary algebra and higher-order convergence in the L^2 norm for the proof of a posteriori error bounds. Heuveline and Rannacher [2001] established a posteriori error bounds for nonsymmetric eigenvalue problems. The convergence of adaptive FEMs for eigenvalue problems was proven by Garau et al. [2009], Giani and Graham [2009] and Carstensen and Gedicke [2011]. An adaptive FEM based on the saturation assumption was proposed in [Carstensen et al., 2014d]. The proof of optimal convergence rates of AFEM for simple eigenvalues was given by Dai et al. [2008] and Carstensen and Gedicke [2012] for conforming FEMs and by Carstensen, Gallistl, and Schedensack [2014c] for a nonconforming FEM in the particular case of the first eigenvalue of the Laplacian. The first optimal convergence result of adaptive conforming finite element schemes with a multiple eigenvalue [Dai et al., 2013] suggests to use one bulk criterion for all discrete eigenfunctions in the algorithm for automatic mesh refinement.

Optimal convergence rates for the Stokes equations [Hu and Xu, 2013a] and the linear biharmonic problem [Hu et al., 2012] were recently established for the linear case. The recent work [Carstensen et al., 2014a] presents an axiomatic framework that unifies the optimality proofs that trace back to Stevenson [2007] and Cascon et al. [2008]. This approach also covers the optimality of the adaptive FEM computation of simple eigenvalues of the Laplacian of [Dai et al., 2008, Carstensen and Gedicke, 2012].

Ever since the pioneering work of Stevenson [2007], it has been understood that one key ingredient for the proof of optimal convergence rates of adaptive FEMs is the discrete reliability. For the nonconforming \mathcal{P}_1 FEM on simply-connected domains in two space dimensions, the discrete reliability can be proven by means of the discrete Helmholtz decomposition of Arnold and Falk [1989]. Only very recently, discrete reliability for multiply-connected domains in any space dimension $d \geq 2$ was proven by Carstensen, Gallistl, and Schedensack [2013a]. The main technical tool in the proof is a transfer operator between the non-nested finite element spaces. The design of an analogous operator for the Morley FEM appears more difficult because of the lack of a conforming subspace.

Main Results

One of the main aspects in the convergence analysis for eigenvalue problems is the error analysis of the eigenfunctions in the L^2 norm. The Aubin-Nitsche duality technique controls the L^2 error by the error in the energy norm times some power of the global mesh-size for conforming finite element methods. This methodology is not applicable to nonconforming FEMs because nonconforming functions are not admissible test functions in the continuous setting. This thesis enfolds conforming companion techniques to prove the L^2 control. For the nonconforming \mathcal{P}_1 FEM, the operator of Carstensen, Gallistl, and Schedensack [2014c] is generalised to any space dimension $d \geq 2$. For the biharmonic eigenvalue problem and the Morley FEM from Figure 1.3c, a new C^1 -conforming companion operator is developed based on the Hsieh-Clough-Tocher macro FEM [Ciarlet, 1978] (see Figure 1.3d) and polynomial bubble functions of order 6. This enables the proof of an L^2 error estimate even for singular solutions with H^{2+s} regularity for $0 < s \leq 1$. The proofs

employ techniques from the medius analysis [Braess, 2009, Gudi, 2010, Carstensen et al., 2012b]. This means that, in contrast to classical a priori estimates, the results are true for any regularity of the eigenfunctions.

These results allow for the first optimality proofs for adaptive finite element computation of the Stokes and the biharmonic eigenvalue problems. The discrete reliability proof for the Morley FEM in this thesis is based on a novel discrete Helmholtz decomposition that generalises the recent decomposition of Carstensen, Gallistl, and Hu [2014b] to the case of simply supported and free boundary conditions.

In the adaptive scheme, the computable error estimator depends on the choice of the discrete eigenfunctions and is therefore not suitable for a convergence analysis based on a contraction property as in [Cascon et al., 2008, Stevenson, 2007]. This thesis follows the idea from [Dai et al., 2013] to employ a theoretical non-computable error estimator which allows a proof of equivalence to the refinement indicator of the adaptive algorithm. It turns out that the analysis of [Dai et al., 2013] is not directly applicable to the case of clustered eigenvalues. In contrast to the case of one multiple eigenvalue, care has to be taken that the reliability and equivalence estimates of the error estimator do not include the cluster width as an additive term. This thesis proves the first optimality result for adaptive finite element approximation of clustered eigenvalues with respect to the concept of nonlinear approximation classes.

One subtle aspect is the dependence of the parameters on the fineness of the initial mesh and the initial resolution of the cluster and its width. Therefore, the analysis in this thesis is explicit in all quantities that describe the eigenvalue cluster. To give an illustration of the dependence of the initial mesh-size, all constants in the optimality analysis for the conforming FEM for the Laplace eigenvalue problem are traced explicitly.

The optimality analysis is merely concerned with the approximation of the eigenfunctions. In order to obtain the optimal convergence rate for the eigenvalues, error estimates are needed that relate the eigenvalue error to the approximation error of the eigenfunctions within the cluster independent of the approximation error of all previous eigenfunctions. Such a result for conforming discretisations was obtained by Knyazev and Osborn [2006]. Since this result makes use of the conformity by exploiting the min-max principle, their theorem cannot be directly applied to nonconforming finite elements. This thesis gives an extension of that result to nonconforming finite element spaces by applying the original result of Knyazev and Osborn [2006] to a modified setting where the spectrum with respect to the sum of the continuous and the finite element space is considered. The careful application of conforming companion operators enables certain L^2 and best-approximation results that eventually lead to the control of the eigenvalue error by the approximation error of the eigenvalue cluster.

Structure of the Thesis

Chapter 2 introduces the necessary notation and preliminaries on finite element meshes in \mathbb{R}^d and their adaptive refinement and recalls some relevant inequalities. Chapter 3 outlines an abstract framework for the discretisation of eigenvalue clusters and provides an equivalence of error estimators. Section 3.3 presents an abstract approach to justify guaranteed lower eigenvalue bounds. The AFEM loop is introduced in Section 3.4. Chapter 4 proves optimal convergence rates of AFEM for the conforming \mathcal{P}_1 discretisation of the eigenval-

1. Introduction

ues of the Laplacian. Chapter 5 introduces the nonconforming \mathcal{P}_1 FEM space and two non-standard results, namely the existence of conforming companion operators and the discrete distance control [Carstensen, Gallistl, and Schedensack, 2013a]. The remaining parts of Chapter 5 prove optimality of the adaptive nonconforming FEM for the eigenvalues of the Laplacian. Chapter 6 presents a new application to the eigenvalues of the Stokes system. Chapter 7 focuses on fourth-order eigenvalue problems and presents several new results on the nonconforming Morley finite element methods, namely an error estimate for the Morley interpolation operator, the existence of C^1 -conforming companion operators and a discrete Helmholtz decomposition. These results enable the proof of optimal convergence rates of the Morley FEM for the eigenvalues of the biharmonic operator. The optimality proofs in the Chapters 4, 5, 6, and 7 are based on the discrete reliability and the contraction property whose proofs can be found in the respective sections. Chapter 8 is devoted to error estimates which relate the eigenvalue error to the angle between the invariant subspaces in the case of nonconforming FEMs. Chapter 9 presents numerical tests for the model problems of this thesis on non-convex domains. It investigates the performance of the proposed algorithm for eigenvalue clusters in comparison to algorithms that rely on the multiplicity of the exact eigenvalues. Furthermore, the inclusion of an inexact linear-algebraic solve is investigated empirically. A table of basic notation is given in Appendix A. Appendix B gives an outline how to reproduce the numerical results with the software provided on an attached data medium (Appendix C).

Conclusions and Outlook

This thesis proves optimality of adaptive finite element methods for eigenvalue clusters of self-adjoint differential operators. The numerical experiments indicate that the requirements on the initial mesh-size for the proposed algorithm are somehow weaker in comparison with algorithms that are based on the multiplicity of the exact eigenvalues.

In order to achieve optimal computational complexity, the AFEM loop has to be combined with an iterative eigenvalue solver and some termination criterion as proposed in [Miedlar, 2011]. The accuracy of the linear-algebraic solution is controlled by some parameter \varkappa . The optimality of algorithms of this type for sufficiently small $\varkappa \ll 1$ was analysed by Carstensen and Gedicke [2012] for conforming FEMs and by Carstensen, Gallistl, and Schedensack [2014c] for nonconforming FEMs. The results of this thesis is carried out for the case $\varkappa = 0$, i.e., under the theoretical assumption that the discrete eigenvalue problems are solved exactly. The analysis can be extended to inexact solve with similar perturbation arguments as in [Carstensen and Gedicke, 2012, Carstensen, Gallistl, and Schedensack, 2014c]. The thesis proposes an adaptive algorithm which includes the iterative solve. This may be the first step towards optimal computational complexity for eigenvalue clusters.

The analysis of this thesis reveals that optimal convergence rates can be proven in the case of low-order finite elements whereas the treatment of higher-order methods remains an open problem, cf. Remark 4.21.

The analysis of non-selfadjoint eigenvalue problems encounters several additional difficulties which cannot be covered with the analysis of this thesis. Recent developments on homotopy-based methods [Carstensen et al., 2011] are the objective of future research. Nonlinear eigenvalue problems are a further challenge with high relevance in industrial

applications [Apel et al., 2002]. For most of these problems, the development of adaptive methods is still in its infancy and far from industrial practice.

Acknowledgement

The author thanks Professor C. Carstensen for the supervision of this thesis and Professor V. Mehrmann for the collaboration in the project C22 “Adaptive solution of parametric eigenvalue problems for partial differential equations ” within the DFG Research Center MATHEON. Moreover, the author thankfully acknowledges the support of the Deutsche Forschungsgemeinschaft (DFG), the support by the Chinesisch-Deutsches Zentrum (project “The Adaptive Finite Element Method for the Fourth Order Problem”, grant no. GZ578), and by the Indian Department of Science and Technology (DST) (National programme on differential equations) which enabled the participation in several workshops.

2. Preliminaries

This chapter clarifies the notation on function spaces (Section 2.1) and gives an overview of adaptive mesh-refinement in any space dimension (Section 2.2) and related data structures (Section 2.3). Section 2.4 reports some important results that will be frequently employed throughout the thesis.

The notation is summarised in the tables of Appendix A.

2.1. Function Spaces and Operators

Let $\Omega \subseteq \mathbb{R}^d$ be a bounded open domain with polyhedral Lipschitz boundary. Throughout this thesis, $d \geq 2$ denotes the space dimension. The notation $a \lesssim b$ denotes an inequality $a \leq Cb$ up to a multiplicative constant C that does not depend on the mesh-size or the eigenvalue cluster; $a \approx b$ abbreviates $a \lesssim b \lesssim a$.

Lebesgue and Sobolev Spaces

Standard notation on Lebesgue and Sobolev spaces [Adams and Fournier, 2003, Evans, 2010] applies throughout this thesis. Let $(\omega, \mathfrak{F}, \mu)$ be a measure space and let $(X, \|\cdot\|)$ be a finite-dimensional real Banach space $X \subseteq \mathbb{R}^{M \times N}$. For any μ -measurable function $f : \omega \rightarrow X$, the Lebesgue integral is denoted by $\int_{\omega} f d\mu$ and, if $\mu(\omega) < \infty$, $\int_{\omega} f d\mu := \mu(\omega)^{-1} \int_{\omega} f d\mu$ denotes the integral mean. The L^2 seminorm is defined by

$$\|f\|_{L^2(\omega)} := \left(\int_{\omega} \|f\|^2 d\mu \right)^{1/2}.$$

Although neither the target set X nor the used measure may appear in this notation, they will be clear from the context. The space of equivalence classes of square integrable functions up to equality almost everywhere reads as

$$L^2(\omega; X) := \{f : \omega \rightarrow X \mid f \text{ is measurable and } \|f\|_{L^2(\omega)} < \infty\} / \{\|\cdot\|_{L^2(\omega)} = 0\}$$

and $L^2(\omega) := L^2(\omega; \mathbb{R})$. The subset of $L^2(\omega; X)$ -functions with vanishing integral is denoted by $L_0^2(\omega; X)$ and $L_0^2(\omega) := L_0^2(\omega; \mathbb{R})$. The space of (equivalence classes of) essentially bounded measurable functions is denoted by $L^\infty(\omega)$ and the set of X -valued functions whose components belong to $L^\infty(\omega)$ is denoted by $L^\infty(\omega; X)$. The essential supremum is denoted by $\|\cdot\|_{L^\infty(\omega)}$ or $\|\cdot\|_\infty$.

For a Lebesgue-measurable set $\omega \subseteq \mathbb{R}^d$ and a Lebesgue-measurable function $f : \omega \rightarrow X$ with values in a finite-dimensional real Banach space X , the integral with respect to the d -dimensional Lebesgue measure is denoted by $\int_{\omega} f dx$. The d -dimensional Lebesgue measure of ω is denoted by $\text{meas}(\omega)$. The integral over a $(d-1)$ -dimensional hypersurface Γ with respect to the $(d-1)$ -dimensional Hausdorff measure reads as $\int_{\Gamma} f ds$ and the $(d-1)$ -dimensional Hausdorff measure of Γ is denoted by $\text{meas}_{d-1}(\Gamma)$.

2. Preliminaries

The set of infinitely differentiable functions from ω to X with compact support in ω is denoted by $\mathcal{D}(\omega; X)$ while $\mathcal{D}(\omega) := \mathcal{D}(\omega; \mathbb{R})$. For any $f \in \mathcal{D}(\omega)$ and any multi-index $\alpha = (\alpha_1, \dots, \alpha_d) \in \mathbb{N}_0^d$ of length $|\alpha| := \sum_{j=1}^d \alpha_j$, the partial derivative with respect to α is defined via

$$D^\alpha f := \frac{\partial^{|\alpha|} f}{\partial x^\alpha} := \frac{\partial^{|\alpha|} f}{\partial x^{\alpha_1} \dots \partial x^{\alpha_d}}.$$

For a bounded open Lipschitz domain $\omega \subseteq \mathbb{R}^d$, a function $f \in L^2(\omega)$ is called k times weakly differentiable with respect to α , if there exists some $g \in L^2(\omega)$ such that

$$\int_{\omega} f D^\alpha \varphi dx = (-1)^k \int_{\omega} g \varphi dx \quad \text{for all } \varphi \in \mathcal{D}(\omega).$$

The function $\partial^{|\alpha|} f / \partial x^\alpha := D^\alpha f := g$ is called k -th weak derivative with respect to α .

The Sobolev space $H^k(\omega)$ is defined by

$$H^k(\omega) := \{f \in L^2(\omega) \mid \text{for all } \alpha \in \mathbb{N}_0^d \text{ with } |\alpha| \leq k \text{ there exists } D^\alpha f \in L^2(\omega)\}.$$

The set of X -valued functions whose components belong to $H^k(\omega)$ is denoted by $H^k(\omega; X)$. The finite-dimensional Banach space $X \subseteq \mathbb{R}^{M \times N}$ may be identified with \mathbb{R}^m for some $m \in \mathbb{N}$. Define for any $f = (f_1, \dots, f_m) \in H^k(\omega; X)$ the norm

$$\|f\|_{H^k(\omega)} := \left(\sum_{|\alpha| \leq k} \sum_{j=1}^m \|D^\alpha f_j\|_{L^2(\omega)}^2 \right)^{1/2}.$$

The closure of $\mathcal{D}(\omega; X)$ with respect to the norm $\|\cdot\|_{H^k(\omega)}$ is denoted by $H_0^k(\omega; X)$ and $H_0^k(\omega) := H_0^k(\omega; \mathbb{R})$.

For $k \in \mathbb{N}$ and $0 < s \leq 1$ define the Sobolev space

$$H^{k+s}(\omega) := \{v \in L^2(\omega) \mid \|v\|_{H^{k+s}(\omega)} < \infty\}$$

for the Sobolev–Slobodeckij norm

$$\|v\|_{H^{k+s}(\omega)} := \left(\|v\|_{H^k(\omega)}^2 + \sum_{|\alpha|=k} \int_{\omega} \int_{\omega} \frac{|D^\alpha v(\xi) - D^\alpha v(\eta)|^2}{|\xi - \eta|^{d+2s}} dx(\xi) dx(\eta) \right)^{1/2}.$$

Differential Operators

Definition 2.1 (derivative, divergence). For a sufficiently smooth function $f : \Omega \rightarrow \mathbb{R}^m$, the first (weak) derivative is denoted by Df and the second derivative is denoted by $D^2 f$. For a sufficiently smooth vector field $\beta : \Omega \rightarrow \mathbb{R}^d$, the divergence reads as $\operatorname{div} \beta := \sum_{j=1}^d \partial \beta_j / \partial x_j$. For a sufficiently smooth tensor field $\sigma : \Omega \rightarrow \mathbb{R}^{d \times d}$, the divergence is applied row-wise, i.e., $\operatorname{div} \sigma := (\operatorname{div} \sigma_{1\bullet}, \dots, \operatorname{div} \sigma_{d\bullet})$. The Laplacian reads as $\Delta := \operatorname{div} D^\top$ and the biharmonic operator (also called the bi-Laplacian operator) is defined as $\Delta^2 := \Delta \Delta$. \blacklozenge

Remark 2.2. If $f : \Omega \rightarrow \mathbb{R}^m$ for $m \geq 1$, then Df always denotes the Jacobian $Df : \Omega \rightarrow \mathbb{R}^{m \times d}$. \blacklozenge

Definition 2.3 (Curl operator). Let $d = 2$ and define for any smooth function $f : \Omega \rightarrow \mathbb{R}$ its Curl as

$$\text{Curl } f := (-\partial f / \partial x_2 \quad \partial f / \partial x_1).$$

For a sufficiently smooth vector field $\beta : \Omega \rightarrow \mathbb{R}^2$, define

$$\text{Curl } \beta := \begin{pmatrix} -\partial \beta_1 / \partial x_2 & \partial \beta_1 / \partial x_1 \\ -\partial \beta_2 / \partial x_2 & \partial \beta_2 / \partial x_1 \end{pmatrix}. \quad \blacklozenge$$

2.2. Adaptive Finite Element Meshes in Any Space Dimension

This section describes the data structures and refinement rules for adaptive mesh-generation in d space dimensions. This refinement algorithm traces back to Maubach [1995] and Traxler [1997]. The presentation in this section follows the description of Stevenson [2008] and recalls some results from Carstensen, Gallistl, and Schedensack [2013a].

Regular Triangulations

Definition 2.4 (tagged simplex). A tagged simplex $(z_0, \dots, z_d; \gamma)$ is a $(d+2)$ -tuple with vertices $(z_0, \dots, z_d) \in (\mathbb{R}^d)^{d+1}$, which do not lie on a $(d-1)$ -dimensional hyperplane, and a type $\gamma \in \{0, \dots, d-1\}$. \blacklozenge

The mapping

$$\text{dom} : (\mathbb{R}^d)^{d+1} \times \{0, \dots, d-1\} \rightarrow 2^{\mathbb{R}^d}$$

extracts the corresponding (closed) simplex $\text{dom}(z_0, \dots, z_d; \gamma) := \text{conv}\{z_0, \dots, z_d\}$ from a tagged simplex $(z_0, \dots, z_d; \gamma)$.

If there is no risk of confusion, a tagged simplex is identified with its domain. Given tagged simplices T, T' , define for abbreviation $\partial T := \partial \text{dom}(T)$, $T \cap T' := \text{dom}(T) \cap \text{dom}(T')$, $T \cup T' := \text{dom}(T) \cup \text{dom}(T')$, $v|_T := v|_{\text{dom}(T)}$, $\text{int}(T) := \text{int}(\text{dom}(T))$. Let furthermore $z \in T$ abbreviate $z \in \text{dom}(T)$.

Definition 2.5 (regular triangulation). A finite set \mathcal{T} of tagged simplices is called regular triangulation of Ω , if it covers the domain in the sense that $\overline{\Omega} = \bigcup_{T \in \mathcal{T}} \text{dom}(T)$ and any two distinct simplices $(T_1, T_2) \in \mathcal{T}^2$ with $T_1 = (z_0, \dots, z_d; \gamma_1)$ and $T_2 = (y_0, \dots, y_d; \gamma_2)$ with $T_1 \neq T_2$ are either disjoint or share exactly one lower-dimensional surface in the sense that there exist $n \in \{1, \dots, d\}$ and $(j_1, \dots, j_n) \in \{0, \dots, d\}^n$ and $(k_1, \dots, k_n) \in \{0, \dots, d\}^n$ such that

$$T_1 \cap T_2 = \text{conv}\{z_{j_1}, \dots, z_{j_n}\} = \text{conv}\{y_{k_1}, \dots, y_{k_n}\}. \quad \blacklozenge$$

Definition 2.6 (vertices and hyper-faces). Given a tagged simplex $T = (z_0, \dots, z_d; \gamma)$, its set of vertices is denoted by

$$\mathcal{N}(T) := \{z_0, \dots, z_d\}.$$

The set of hyper-faces reads as

$$\mathcal{F}(T) := \{\text{conv}(\mathcal{N}(T) \setminus \{z_k\}) \mid k \in \{0, \dots, d\}\}. \quad \blacklozenge$$

2. Preliminaries

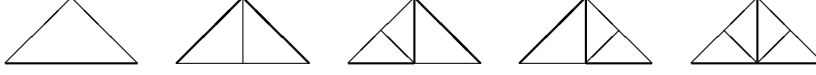


Figure 2.1.: Possible refinements of a triangle T in one level in 2D. The thick lines indicate the refinement edges of the sub-triangles.

Bisection

Definition 2.7 (bisection of a simplex). Let $T = (z_0, \dots, z_d; \gamma)$ be a tagged simplex. The two tagged simplices

$$\begin{aligned} & \left(z_0, \frac{z_0 + z_d}{2}, z_1, \dots, z_\gamma, z_{\gamma+1}, \dots, z_{d-1}; (\gamma+1) \bmod d \right) \quad \text{and} \\ & \left(z_d, \frac{z_0 + z_d}{2}, z_1, \dots, z_\gamma, z_{d-1}, \dots, z_{\gamma+1}; (\gamma+1) \bmod d \right) \end{aligned} \quad (2.1)$$

are called the children of T . (By convention, the finite sequence $(z_{\gamma+1}, \dots, z_{d-1})$ and (z_1, \dots, z_γ) is void for $\gamma = d-1$ and $\gamma = 0$, respectively.) Any child of some child of T is called grandchild; conversely, T is called a parent (resp. grandparent) of each of its two children (resp. four grandchildren). A simplex generated from T by a finite number of applications of (2.1) is called a descendant of T . \blacklozenge

The following proposition ensures that grandchildren do not share hyper-faces with their grandparents.

Proposition 2.8. Any grandchild T of a tagged simplex K satisfies $\mathcal{F}(T) \cap \mathcal{F}(K) = \emptyset$.

Proof. This follows from the definition of the bisection rule (2.1). A detailed proof is given in [Carstensen, Gallistl, and Schedensack, 2013a, Proposition 2.1]. \blacksquare

Initial Conditions

The initial condition from [Stevenson, 2008, p. 232] described in Definition 2.10 below guarantees that successive refinements of a regular triangulation \mathcal{T} lead to regular triangulations. The notion of a reflected neighbour [Stevenson, 2008] is required for the statement of that initial condition. Note that, given a tagged simplex $T = (z_0, \dots, z_d; \gamma)$, the simplex

$$T_R := (z_d, z_1, \dots, z_\gamma, z_{d-1}, z_{d-2}, \dots, z_{\gamma+1}, z_0; \gamma)$$

with $\text{dom}(T_R) = \text{dom}(T)$ has the same children as T .

Definition 2.9 (neighbour, reflected neighbour). Two tagged simplices T, K are called neighbours, if they share a common $(d-1)$ -dimensional surface (i.e., a hyper-face in the sense of Definition 2.6). Two neighbouring tagged simplices T and K are called reflected neighbours, if the ordered sequence of vertices of either T or T_R coincides with that of K on all but one position. \blacklozenge

The following initial condition from [Stevenson, 2008] is crucial for the regularity of refinements.

Definition 2.10 (initial condition). A regular triangulation \mathcal{T} is said to satisfy the initial condition, if all simplices in \mathcal{T} are of the same type γ and any two neighbouring tagged simplices $T = (y_0, \dots, y_d; \gamma)$ and $K = (z_0, \dots, z_d; \gamma)$ satisfy

(a) If $\text{conv}\{y_0, y_d\} \subseteq T \cap K$ or $\text{conv}\{z_0, z_d\} \subseteq T \cap K$, then T and K are reflected neighbours.

(b) If $\text{conv}\{y_0, y_d\} \not\subseteq T \cap K \neq \emptyset$ and $\text{conv}\{z_0, z_d\} \not\subseteq T \cap K$, then any two neighbouring children of T and K are reflected neighbours. \blacklozenge

This condition guarantees that uniform refinements of a triangulation \mathcal{T} are regular [Stevenson, 2008, Theorem 4.3] which transfers to the refinement routine of the following subsection.

Admissible Triangulations

Throughout this thesis, the initial regular triangulation \mathcal{T}_0 of Ω is assumed to satisfy the initial condition from Definition 2.10. A regular triangulation \mathcal{T} is called an admissible refinement of \mathcal{T}_0 if it is a regular triangulation and it was created by refining \mathcal{T}_0 with a successive application of the bisection rule (2.1).

The set of all admissible triangulations is denoted by \mathbb{T} . This set is known to be uniformly shape-regular [Stevenson, 2008] in the sense that the ratio of the diameter and the radius of the largest inscribed ball is uniformly bounded only dependent on \mathcal{T}_0 . For any $\mathcal{T} \in \mathbb{T}$,

$$\mathbb{T}(\mathcal{T}) := \{\mathcal{T}' \in \mathbb{T} \mid \mathcal{T}' \text{ is an admissible refinement of } \mathcal{T}\}.$$

Let, for any $m \in \mathbb{N}$, the set of triangulations in \mathbb{T} whose cardinality differs from that of \mathcal{T}_0 by m or less be denoted by

$$\mathbb{T}(m) := \{\mathcal{T} \in \mathbb{T} \mid \text{card}(\mathcal{T}) - \text{card}(\mathcal{T}_0) \leq m\}.$$

Definition 2.11 (overlay). Given two admissible triangulations $(\mathcal{T}, \mathcal{K}) \in \mathbb{T}^2$, the overlay $\mathcal{T} \otimes \mathcal{K}$ is defined as the smallest common refinement of \mathcal{T} and \mathcal{K} in the sense that $\mathcal{T} \otimes \mathcal{K} \in \mathbb{T}$ satisfies

$$\mathbb{T}(\mathcal{T}) \cap \mathbb{T}(\mathcal{K}) = \mathbb{T}(\mathcal{T} \otimes \mathcal{K}). \quad \blacklozenge$$

Lemma 2.12. Any $(\mathcal{T}, \mathcal{K}) \in \mathbb{T}^2$ satisfy

$$\text{card}(\mathcal{T} \otimes \mathcal{K}) - \text{card}(\mathcal{T}) \leq \text{card}(\mathcal{K}) - \text{card}(\mathcal{T}_0). \quad (2.2)$$

Proof. See Lemma 3.7 of [Cascon et al., 2008]. \blacksquare

Notice that $\mathcal{T}_1 \in \mathbb{T}(\mathcal{T}_2)$ and $\mathcal{T}_2 \in \mathbb{T}(\mathcal{T}_1)$ implies $\mathcal{T}_1 = \mathcal{T}_2$. For any $T \in \mathcal{T}$, the routine $\text{refine}(\mathcal{T}, T)$ from [Stevenson, 2008, p. 235] computes a refinement $\widehat{\mathcal{T}} \in \mathbb{T}(\mathcal{T})$ such that $T \in \mathcal{T} \setminus \widehat{\mathcal{T}}$. It is repeated here for convenient reading. For a simplex $T = \text{conv}\{z_0, \dots, z_d\}$, the edge $\text{conv}\{z_0, z_d\}$ is called its refinement edge.

Algorithm 2.13 ($\text{refine}(\mathcal{T}, T)$).

Input: $\mathcal{T} \in \mathbb{T}$ and $T \in \mathcal{T}$

set $K := \emptyset$, $R := \{T\}$

while $R \neq \emptyset$ **do**

2. Preliminaries

```

Rnew :=  $\emptyset$ 
for  $T' \in R$  do
  for  $T'' \in \mathcal{T}$  that are neighbours of  $T'$  with  $T'' \notin R \cup K$  do
    if  $T''$  and  $T'$  have the same refinement edge then
      Rnew := Rnew  $\cup \{T''\}$ 
    else
       $\mathcal{T} := \text{refine}(\mathcal{T}, T'')$ 
      add to Rnew the child of  $T''$  that is a neighbour of  $T'$ 
    end if
  end for
end for
K := K  $\cup$  R and R := Rnew
end while
for  $T' \in K$  do
  bisect  $T'$  into children  $T'_1, T'_2$  and update  $\mathcal{T} := (\mathcal{T} \setminus \{T'\}) \cup \{T'_1, T'_2\}$ 
end for
Output:  $\mathcal{T}$ 

```

The following proposition proven in [Stevenson, 2008, Theorem 5.1] assures the minimality of this routine. In case that $T \notin \mathcal{T}$ set $\text{refine}(\mathcal{T}, T) := \mathcal{T}$.

Proposition 2.14. *The output $\widehat{\mathcal{T}} := \text{refine}(\mathcal{T}, T)$ is a regular triangulation $\widehat{\mathcal{T}} \in \mathbb{T}$ and is minimal in the sense that any other refinement $\widetilde{\mathcal{T}} \in \mathbb{T}(\mathcal{T})$ with $T \in \mathcal{T} \setminus \widetilde{\mathcal{T}}$ is a refinement $\widetilde{\mathcal{T}} \in \mathbb{T}(\widehat{\mathcal{T}})$ of $\widehat{\mathcal{T}}$.* ■

For a set of simplices $\mathcal{M} \subseteq \mathcal{T}$, the routine $\text{refine}(\mathcal{T}, \mathcal{M})$ runs the following loop.

Algorithm 2.15 ($\text{refine}(\mathcal{T}, \mathcal{M})$).

Input: $\mathcal{T} \in \mathbb{T}$ and $\mathcal{M} \subseteq \mathcal{T}$

Set $\widetilde{\mathcal{T}} := \mathcal{T}$

while $\mathcal{M} \cap \widetilde{\mathcal{T}} \neq \emptyset$ **do**

choose $T \in \mathcal{M} \cap \widetilde{\mathcal{T}}$

compute $\widetilde{\mathcal{T}} := \text{refine}(\widetilde{\mathcal{T}}, T)$

end while

Output: $\widetilde{\mathcal{T}}$

This loop computes a refinement $\widehat{\mathcal{T}} \in \mathbb{T}(\mathcal{T})$ of \mathcal{T} by applying $\text{refine}(\widetilde{\mathcal{T}}, T)$ for simplices in \mathcal{M} and results in a triangulation in which all simplices of $\mathcal{M} \subseteq \mathcal{T} \setminus \widehat{\mathcal{T}}$ are refined. The following proposition guarantees that the result is independent of the order of $T \in \mathcal{M} \cap \widetilde{\mathcal{T}}$ in the loop of refine and furthermore states the minimality of refine for any input set $\mathcal{M} \subseteq \mathcal{T}$.

Proposition 2.16. *The output $\widehat{\mathcal{T}} := \text{refine}(\mathcal{T}, \mathcal{M})$ does not depend on the selection of $T \in \mathcal{M} \cap \widetilde{\mathcal{T}}$ in Algorithm 2.15. The output $\widehat{\mathcal{T}} := \text{refine}(\mathcal{T}, \mathcal{M})$ is minimal in the sense that any other refinement $\mathcal{T}' \in \mathbb{T}(\mathcal{T})$ with $\mathcal{M} \subseteq \mathcal{T} \setminus \mathcal{T}'$ is a refinement $\mathcal{T}' \in \mathbb{T}(\widehat{\mathcal{T}})$.*

Proof. See Propositions 2.2 and 2.4 of [Carstensen, Gallistl, and Schedensack, 2013a]. ■

The following fundamental result proven by Binev et al. [2004] for $d = 2$ and by Stevenson [2008] for $d \geq 2$, is one of the main tools for the proof of optimal convergence rates.

Theorem 2.17 (Binev et al. [2004], Stevenson [2008]). *Let $(\mathcal{T}_j \mid j \in \mathbb{N}_0) \in \mathbb{T}^{\mathbb{N}_0}$ be a sequence of regular triangulations and let $(\mathcal{M}_j \mid j \in \mathbb{N}_0)$ be a sequence of subsets $\mathcal{M}_j \subseteq \mathcal{T}_j$ (for all $j \in \mathbb{N}_0$) such that*

$$\mathcal{T}_{j+1} = \text{refine}(\mathcal{T}_j, \mathcal{M}_j) \quad \text{for all } j \in \mathbb{N}_0.$$

Then there exists a constant C_{BDV} solely dependent on \mathcal{T}_0 such that, for any $\ell \in \mathbb{N}$, it holds that

$$\text{card}(\mathcal{T}_\ell) - \text{card}(\mathcal{T}_0) \leq C_{\text{BDV}} \sum_{j=0}^{\ell-1} \text{card}(\mathcal{M}_j). \quad \blacksquare$$

One-Level Refinements

The remaining parts of this section present a result of a private communication with Stevenson [2013].

Definition 2.18 (level). Let $\mathcal{T} \in \mathbb{T}$ be an admissible triangulation refined from \mathcal{T}_0 . For any $T \in \mathcal{T}$ there exists an ancestor $K \in \mathcal{T}_0$ with $T \subseteq K$. The level of T , is defined by

$$\ell(T) := \text{meas}(T) / \text{meas}(K).$$

In other words, $\ell(T)$ is the number of applications of the bisection rule (2.1) that are needed to obtain T from K . \blacklozenge

Lemma 2.19. *Let $T \in \mathcal{T}$ and $\mathcal{T}' := \text{refine}(\mathcal{T}, T)$. If $T' \in \mathcal{T}'$ is newly created by this call of $\text{refine}(\mathcal{T}, T)$, i.e., $T' \in \mathcal{T}' \setminus \mathcal{T}$, then*

- (a) $\ell(T') \leq \ell(T) + 1$,
- (b) $\text{dist}(T', T) \lesssim 2^{-\ell(T')/d}$.

Moreover,

- (c) *there exists a constant $C > 0$ such that, for all $\mathcal{T} \in \mathbb{T}$ and any $(T, K) \in \mathcal{T}^2$ with $T \cap K \neq \emptyset$, it holds that $|\ell(T) - \ell(K)| \leq C$;*
- (d) *there exists a constant $c > 0$ such that, for all $\mathcal{T} \in \mathbb{T}$ and any $(T, K) \in \mathcal{T}^2$ with $\ell(T) > \ell(K) + C$, it holds that $\text{dist}(K, T) \geq c2^{-\ell(K)/d}$.*

Proof. The first two assertions follow from [Stevenson, 2008, Thms. 5.1–5.2]. Properties (c)–(d) follow from the shape-regularity. \blacksquare

The following proposition implies that the number of refinements of any $K \in \mathcal{T}$ generated by a call of $\text{refine}(\mathcal{T}, T)$ is uniformly bounded.

Proposition 2.20. *Let $T \in \mathcal{T}$ and $\mathcal{T}' = \text{refine}(\mathcal{T}, T)$. Let $K \in \mathcal{T}$ and $K' \in \mathcal{T}'$ with $K' \subseteq K$ be its descendant in the sense of Definition 2.7. Then it holds that*

$$\ell(K') - \ell(K) \lesssim 1.$$

2. Preliminaries

Proof. If $\ell(K') = \ell(K)$, the assertion is trivially satisfied. Hence, assume $\ell(K) + 1 \leq \ell(K')$. By (a) from Lemma 2.19, $\ell(K') \leq \ell(T) + 1$ and so $\ell(K) \leq \ell(T)$. Recall the constant C from Lemma 2.19.

Case 1. If $\ell(T) \leq \ell(K) + C$, then (a) from Lemma 2.19 implies that $\ell(K') \leq \ell(T) + 1$ and, hence, $\ell(K') \leq \ell(K) + C + 1$.

Case 2. If $\ell(T) > \ell(K) + C$, then (d) implies that $\text{dist}(T, K) \gtrsim 2^{-\ell(K)/d}$, whence

$$\text{dist}(T, K') \gtrsim 2^{-\ell(K)/d}.$$

On the other hand, (b) states that

$$\text{dist}(K', T) \lesssim 2^{-\ell(K')/d}.$$

The foregoing two inequalities imply

$$2^{-\ell(K)/d} \lesssim 2^{-\ell(K')/d}$$

and so $\ell(K') - \ell(K) \lesssim 1$. ■

The following proposition generalises Proposition 2.20 to the case of a marked set $\mathcal{M} \subseteq \mathcal{T}$.

Proposition 2.21. *Let $\mathcal{T}' \in \mathbb{T}(\mathcal{T})$ be some one-level refinement of \mathcal{T} , i.e., there exists a subset $\mathcal{M} \subseteq \mathcal{T}$ with $\mathcal{T}' = \text{refine}(\mathcal{T}, \mathcal{M})$, and let $K \in \mathcal{T}$, $K' \in \mathcal{T}'$ with $K' \subseteq K$, i.e., K' is a descendant of K . Then, there exists a constant $C > 0$ with*

$$\ell(K') - \ell(K) \leq C.$$

Proof. It holds that

$$\mathcal{T}' = \bigotimes_{T \in \mathcal{M}} \text{refine}(\mathcal{T}, T),$$

i.e., \mathcal{T}' is the overlay of all $\text{refine}(\mathcal{T}, T)$ with $T \in \mathcal{M}$. The concept of binary trees [Binev et al., 2004] shows that there exists $T \in \mathcal{M}$ with $K' \in \text{refine}(\mathcal{M}, T)$. Thus, Proposition 2.20 proves the assertion. ■

2.3. Data Structures

Definition 2.22 (piecewise polynomials). Let $\mathcal{T}_\ell \in \mathbb{T}$. For any subset $\omega \subseteq \Omega$, the space of polynomial functions of total degree $\leq k$ is denoted by $\mathcal{P}_k(\omega)$. Let $X \subseteq \mathbb{R}^{M \times N}$ be a finite-dimensional Banach space. The X -valued functions whose components belong to $\mathcal{P}_k(\omega)$ are denoted by $\mathcal{P}_k(\omega; X)$. For a regular triangulation \mathcal{T}_ℓ of Ω , the spaces of piecewise polynomials read as

$$\begin{aligned} \mathcal{P}_k(\mathcal{T}_\ell) &:= \{v \in L^\infty(\Omega) \mid \forall T \in \mathcal{T}_\ell, v|_T \in \mathcal{P}_k(T)\}, \\ \mathcal{P}_k(\mathcal{T}_\ell; X) &:= \{v \in L^\infty(\Omega; X) \mid \forall T \in \mathcal{T}_\ell, v|_T \in \mathcal{P}_k(T; X)\}. \end{aligned}$$

The L^2 -orthogonal projection onto the space $\mathcal{P}_k(\mathcal{T}_\ell)$ (or $\mathcal{P}_k(\mathcal{T}_\ell; X)$) is denoted by Π_ℓ^k or $\Pi_{\mathcal{T}_\ell}^k$. ◆

Definition 2.23 (midpoints). The centre of gravity of a simplex T (resp. a hyper-face F) is denoted by $\text{mid}(T)$ (resp. $\text{mid}(F)$). \blacklozenge

Definition 2.24 (notation of vertices and hyper-faces). Let $\omega \subseteq \Omega$ and $\Gamma \subseteq \partial\Omega$. Define $\mathcal{N}_\ell := \mathcal{N}(\mathcal{T}_\ell) := \cup_{T \in \mathcal{T}_\ell} \mathcal{N}(T)$ as the set of vertices of \mathcal{T}_ℓ . The set of vertices that belong to ω is denoted by $\mathcal{N}_\ell(\omega) := \mathcal{N}_\ell \cap \omega$. The hyper-faces of \mathcal{T}_ℓ are denoted by $\mathcal{F}_\ell := \mathcal{F}(\mathcal{T}_\ell) := \cup_{T \in \mathcal{T}_\ell} \mathcal{F}(T)$. The hyper-faces that lie inside Ω read as $\mathcal{F}_\ell(\Omega) := \{F \in \mathcal{F}_\ell \mid F \not\subseteq \partial\Omega\}$ and the hyper-faces that belong to Γ read as $\mathcal{F}_\ell(\Gamma) := \{F \in \mathcal{F}_\ell \mid \text{meas}_{d-1}(F \cap \Gamma) > 0\}$. Furthermore, define $\mathcal{F}_\ell(\Omega \cup \Gamma) := \mathcal{F}_\ell(\Omega) \cup \mathcal{F}_\ell(\Gamma)$. \blacklozenge

Definition 2.25 (patches). Let $z \in \mathcal{N}_\ell$, $F \in \mathcal{F}_\ell$ and $T \in \mathcal{T}_\ell$. The set of simplices that share z reads as $\mathcal{T}_\ell(z) := \{K \in \mathcal{T}_\ell \mid z \in K\}$. The set of simplices that share F is defined as $\mathcal{T}_\ell(F) := \{K \in \mathcal{T}_\ell \mid F \in \mathcal{F}(K)\}$. The patches ω_z , ω_F and ω_T read as

$$\begin{aligned}\omega_z &:= \text{int}(\cup \mathcal{T}_\ell(z)), \\ \omega_F &:= \text{int}(\cup \mathcal{T}_\ell(F)), \\ \omega_T &:= \text{int}(\cup \{K \in \mathcal{T}_\ell \mid T \cap K \neq \emptyset\}).\end{aligned}\quad \blacklozenge$$

Definition 2.26 (mesh-size). For $T \in \mathcal{T}_\ell$ define $h_T := \text{meas}(T)^{1/d}$. For $F \in \mathcal{F}_\ell$ define $h_F := \text{diam}(F)$. The piecewise constant function $h_\ell := h_{\mathcal{T}_\ell} \in \mathcal{P}_0(\mathcal{T}_\ell)$ is defined by $h_{\mathcal{T}_\ell}|_T := h_T$ for each $T \in \mathcal{T}_\ell$. \blacklozenge

Definition 2.27 (normals and jumps). Any $F \in \mathcal{F}(\mathcal{T}_\ell)$ is associated to a fixed orientation of the unit normal \mathbf{v}_F on F ; on the boundary, \mathbf{v}_F is the outer unit normal of Ω . For an interior hyper-face $F \not\subseteq \partial\Omega$ the orientation is fixed through the choice of the simplices $T_+ \in \mathcal{T}_\ell$ and $T_- \in \mathcal{T}_\ell$ with $F = T_+ \cap T_-$ and $\mathbf{v}_F = \mathbf{v}_{T_+}|_F$ (i.e. \mathbf{v}_F points outwards of T_+). In this situation, $[v]_F := v|_{T_+} - v|_{T_-}$ denotes the jump across F . For a hyper-face $F \subseteq \partial\Omega$ on the boundary, the jump across this hyper-surface F is $[v]_F := v$. \blacklozenge

Definition 2.28 (piecewise action of differential operators). Let \mathcal{T}_ℓ be a regular triangulation. The piecewise action of a differential operator is indicated by the subscript NC, i.e., the piecewise versions of D , D^2 , div , Δ , Δ^2 , Curl read as D_{NC} , D_{NC}^2 , div_{NC} , Δ_{NC} , Δ_{NC}^2 , Curl_{NC} , e.g., $(D_{\text{NC}}v)|_T = D(v|_T)$ for any $T \in \mathcal{T}_\ell$. \blacklozenge

Definition 2.29 (oscillations). Let $(p, k) \in \mathbb{N}_0^2$ and $f \in L^2(\Omega; X)$. For a regular triangulation \mathcal{T}_ℓ of Ω the oscillations are defined as

$$\text{osc}_{p,k}^2(f, \mathcal{T}_\ell) := \|h_\ell^k(1 - \Pi_\ell^p)f\|_{L^2(\Omega)}^2 \quad \text{and} \quad \text{osc}_{p,k}(f, \mathcal{T}_\ell) := \sqrt{\text{osc}_{p,k}^2(f, \mathcal{T}_\ell)}. \quad \blacklozenge$$

2.4. Frequently Used Results

This section reports some important estimates and identities that are used throughout the analysis of this thesis.

Proposition 2.30 (Young inequality). Any $(a, b, \varepsilon) \in \mathbb{R}^3$ with $\varepsilon > 0$ satisfy

$$2ab \leq \varepsilon a^2 + \varepsilon^{-1}b^2.$$

Proof. The formula $0 \leq (\varepsilon^{1/2}a - \varepsilon^{-1/2}b)^2 = \varepsilon a^2 + \varepsilon^{-1}b^2 - 2ab$ proves the result. \blacksquare

2. Preliminaries

Proposition 2.31 (trace identity, trace inequality). *Let T be a simplex with $F \in \mathcal{F}(T)$ and $P_F \in \mathcal{N}(T) \setminus \{F\}$ the vertex opposite to $F \in \mathcal{F}(T)$. Then any $v \in H^1(\text{int}(T))$ satisfies the trace identity*

$$\oint_F v ds = \int_T v dx + \frac{1}{d} \int_T Dv(\bullet - P_F) dx$$

as well as the trace inequality

$$\|v\|_{L^2(F)}^2 \lesssim h_T^{-1} \|v\|_{L^2(T)}^2 + h_T \|Dv\|_{L^2(T)}^2.$$

Proof. The proof of the trace identity follows from the integration by parts formula, see [Carstensen and Funken, 2000]. The trace inequality is a consequence of that identity and the Young inequality. For a proof see, e.g., [Di Pietro and Ern, 2012]. ■

Proposition 2.32 (discrete Friedrichs inequality). *Let \mathcal{T}_ℓ be a regular triangulation of Ω . Any piecewise smooth $v \in L^2(\Omega)$, in the sense that $v|_{\text{int}(T)} \in H^1(\text{int}(T))$ for any $T \in \mathcal{T}_\ell$, with $\int_{\partial\Omega} v ds = 0$ satisfies*

$$\|v\|_{L^2(\Omega)} \lesssim \left(\sum_{F \in \mathcal{F}_\ell(\Omega)} h_F^{d-2} (f_F[v]_F ds)^2 \right)^{1/2} + \|D_{\text{NC}} v\|_{L^2(\Omega)}$$

where the constant hidden in the notation \lesssim only depends on Ω and the shape-regularity of \mathcal{T}_ℓ . If Ω is a simplex, any piecewise smooth $v \in L^2(\Omega)$ satisfies

$$\begin{aligned} \|v\|_{L^2(\Omega)} &\lesssim \text{diam}(\Omega)^{(2-d)/2} \left| \int_{\partial\Omega} v ds \right| \\ &\quad + \text{diam}(\Omega) \left(\left(\sum_{F \in \mathcal{F}_\ell(\Omega)} h_F^{d-2} (f_F[v]_F ds)^2 \right)^{1/2} + \|D_{\text{NC}} v\|_{L^2(\Omega)} \right) \end{aligned}$$

where the constant hidden in the notation \lesssim only depends on the shape-regularity of \mathcal{T}_ℓ .

Proof. The proof can be found in [Brenner and Scott, 2008, Thm. 10.6.12] or [Brenner, 2003]. The dependence on $\text{diam}(\Omega)$ in the second inequality can be obtained by tracing the dependence of $\text{diam}(\Omega)$ in the proof of [Brenner and Scott, 2008, Thm. 10.6.12] for the volume term and by a scaling argument for the boundary term. ■

The following proposition is a consequence of a result of Kato [1966, Thm. 6.34 in Chapter 1, §6].

Proposition 2.33 (Kato [1966]). *Let $(H, \langle \cdot, \cdot \rangle_H)$ be a Hilbert space with induced norm $\|\cdot\|_H$ and let $X \subseteq H$, $Y \subseteq H$ be finite-dimensional subspaces with $\dim X = \dim Y < \infty$. Let P_X and P_Y denote the orthogonal projections onto X and Y , respectively. Then it holds that*

$$\|P_X - P_Y\|_H \leq \|(1 - P_X)P_Y\|_H = \|(1 - P_Y)P_X\|_H$$

where $\|\cdot\|_H$ abbreviates the operator norm $\|\cdot\|_{\mathcal{L}(H,H)}$.

Proof. Theorem 6.34 of [Kato, 1966, Chapter 1, §6, p. 56] states that the condition

$$\delta_1 := \|(1 - P_Y)P_X\|_H < 1$$

and $\dim X = \dim Y < \infty$ imply that $P_Y|_X : X \rightarrow Y$ is an isomorphism and

$$\|P_X - P_Y\|_H = \|(1 - P_X)P_Y\|_H = \|(1 - P_Y)P_X\|_H.$$

(Here, the finite dimension of X and Y is required to see that an injective mapping is an isomorphism.) By symmetry this is also true in case that $\delta_2 := \|(1 - P_X)P_Y\|_H < 1$. In the remaining case that $\min\{\delta_1, \delta_2\} \geq 1$, the fact that P_X and P_Y are orthogonal projections leads to $\delta_1 = \delta_2 = 1$. In this case, the stated inequality is proven following the arguments of [Kato, 1966]. For any $w \in H$, the Pythagoras theorem shows

$$\|(P_X - P_Y)w\|_H^2 = \|(1 - P_Y)P_X w - P_Y(1 - P_X)w\|_H^2 = \|(1 - P_Y)P_X w\|_H^2 + \|P_Y(1 - P_X)w\|_H^2.$$

Hence, the fact that the projections P_X and $(1 - P_X)$ are idempotent and the Cauchy inequality imply

$$\|(P_X - P_Y)w\|_H^2 \leq \|(1 - P_Y)P_X\|_H^2 \|P_X w\|_H^2 + \|P_Y(1 - P_X)\|_H^2 \|(1 - P_X)w\|_H^2.$$

A direct calculation reveals that $\|P_Y(1 - P_X)\|_H = \|(1 - P_X)P_Y\|_H = \delta_2 = 1$. This and $\|(1 - P_Y)P_X\|_H = \delta_1 = 1$ imply with the Pythagoras theorem that

$$\|(P_X - P_Y)w\|_H^2 \leq \|P_X w\|_H^2 + \|(1 - P_X)w\|_H^2 = \|w\|_H^2.$$

This concludes the proof. ■

Corollary 2.34. *Let $(H, \langle \cdot, \cdot \rangle_H)$ be a Hilbert space with induced norm $\|\cdot\|_H$ and let $X \subseteq H$, $Y \subseteq H$, $Z \subseteq H$ be finite-dimensional subspaces with $\dim X = \dim Y = \dim Z < \infty$. Then it holds that*

$$\begin{aligned} \sup_{\substack{x \in X \\ \|x\|_H=1}} \inf_{y \in Y} \|x - y\|_H &= \sup_{\substack{y \in Y \\ \|y\|_H=1}} \inf_{x \in X} \|y - x\|_H \quad \text{and} \\ \sup_{\substack{x \in X \\ \|x\|_H=1}} \inf_{y \in Y} \|x - y\|_H &\leq \sup_{\substack{x \in X \\ \|x\|_H=1}} \inf_{z \in Z} \|x - z\|_H + \sup_{\substack{z \in Z \\ \|z\|_H=1}} \inf_{y \in Y} \|z - y\|_H. \end{aligned}$$

Proof. Let P_X , P_Y and P_Z denote the orthogonal projection onto X , Y and Z , respectively. The stated identity directly follows from Proposition 2.33

$$\sup_{\substack{x \in X \\ \|x\|_H=1}} \inf_{y \in Y} \|x - y\|_H = \|(1 - P_Y)P_X\|_H = \|(1 - P_X)P_Y\|_H = \sup_{\substack{y \in Y \\ \|y\|_H=1}} \inf_{x \in X} \|y - x\|_H.$$

Similarly, the stated inequality follows from the triangle inequality

$$\|(1 - P_Y)P_X\|_H \leq \|(1 - P_Y)P_Z\|_H + \|(1 - P_Y)(P_Z - P_X)\|_H \leq \|(1 - P_Y)P_Z\|_H + \|P_Z - P_X\|_H$$

and the inequality of Proposition 2.33. ■

2. Preliminaries

Remark 2.35 (angles). One can reformulate the results of Proposition 2.33 and Corollary 2.34 in terms of the largest principal angle between subspaces with

$$\sin^2 \angle(X, Y) = \|(1 - P_Y)P_X\|_H^2 = \sup_{\substack{x \in X \\ \|x\|_H=1}} \inf_{y \in Y} \|x - y\|_H^2.$$

Indeed, for any $x \in X \setminus \{0\}$ with orthogonal projection $y := P_Y x \neq 0$ onto Y , the definition of the angle and $|\langle x, y \rangle_H| = \|P_Y x\|_H \|y\|_H$ lead to

$$\sin^2 \angle(x, y) = 1 - \frac{\langle x, y \rangle_H^2}{\|x\|_H^2 \|y\|_H^2} = 1 - \frac{\|P_Y x\|_H^2}{\|x\|_H^2} = \frac{\|x - P_Y x\|_H^2}{\|x\|_H^2} = \sin^2 \angle(\text{span}\{x\}, Y).$$

If $P_Y x = 0$, then x is orthogonal onto Y and, thus, $\sin^2 \angle(x, y) = 1 = \sin^2 \angle(\text{span}\{x\}, Y)$. ♦

3. Eigenvalue Clusters

This chapter discusses the abstract discretisation of selfadjoint eigenvalue problems. Section 3.1 introduces the notation for eigenvalue clusters and states some important results. Section 3.2 is devoted to the comparison of seminorms. These results will be needed for the equivalence of computable and non-computable error estimators in the analysis of adaptive algorithms. Section 3.3 presents an abstract framework for the computation of lower eigenvalue bounds. Section 3.4 describes the general loop of an adaptive algorithm.

3.1. Discrete Eigenvalue Problem

Let $(V, a(\cdot, \cdot))$ be a separable Hilbert space over \mathbb{R} with induced norm $\|\cdot\|_a$ and let $b(\cdot, \cdot)$ be a scalar product on V with induced norm $\|\cdot\|_b$ such that the embedding $(V, \|\cdot\|_a) \hookrightarrow (V, \|\cdot\|_b)$ is compact. This thesis is concerned with eigenvalue problems of the form: Find eigenpairs $(\lambda, u) \in \mathbb{R} \times V$ with $\|u\|_b = 1$ such that

$$a(u, v) = \lambda b(u, v) \quad \text{for all } v \in V. \quad (3.1)$$

It is well known from the spectral theory of selfadjoint compact operators [see, e.g., Kato, 1966, Chatelin, 1983] that the eigenvalue problem (3.1) has countably many eigenvalues, which are real and positive with $+\infty$ as only possible accumulation point. Suppose that the eigenvalues are enumerated as

$$0 < \lambda_1 \leq \lambda_2 \leq \lambda_3 \leq \dots$$

and let (u_1, u_2, u_3, \dots) be some b -orthonormal system of corresponding eigenfunctions. For any $j \in \mathbb{N}$, the eigenspace corresponding to λ_j is defined as

$$E(\lambda_j) := \{u \in V \mid (\lambda_j, u) \text{ satisfies (3.1)}\} = \text{span}\{u_k \mid k \in \mathbb{N} \text{ and } \lambda_k = \lambda_j\}.$$

In the present case of an eigenvalue problem of (the inverse of) a compact operator, the spaces $E(\lambda_j)$ have finite dimension. The discretisation of (3.1) is based on a family (over a countable index set I) of separable (not necessarily finite-dimensional) Hilbert spaces V_ℓ with scalar products $a_{\text{NC}}(\cdot, \cdot)$ and $b_{\text{NC}}(\cdot, \cdot)$ on $V + V_\ell$ with induced norms $\|\cdot\|_{a, \text{NC}}$ and $\|\cdot\|_{b, \text{NC}}$ such that a_{NC} and b_{NC} coincide with a and b when restricted to V

$$a_{\text{NC}}|_{V \times V} = a \quad \text{and} \quad b_{\text{NC}}|_{V \times V} = b.$$

The discrete eigenvalue problem seeks eigenpairs $(\lambda_\ell, u_\ell) \in \mathbb{R} \times V_\ell$ with $\|u_\ell\|_{b, \text{NC}} = 1$ such that

$$a_{\text{NC}}(u_\ell, v_\ell) = \lambda_\ell b_{\text{NC}}(u_\ell, v_\ell) \quad \text{for all } v_\ell \in V_\ell. \quad (3.2)$$

The discrete eigenvalues can be enumerated

$$0 < \lambda_{\ell,1} \leq \lambda_{\ell,2} \leq \lambda_{\ell,3} \dots$$

3. Eigenvalue Clusters

with corresponding b_{NC} -orthonormal eigenfunctions $(u_{\ell,1}, u_{\ell,2}, u_{\ell,3}, \dots)$. For a cluster of eigenvalues $\lambda_{n+1}, \dots, \lambda_{n+N}$ of length $N \in \mathbb{N}$, define the index set $J := \{n+1, \dots, n+N\}$ and the spaces

$$W := \text{span}\{u_j \mid j \in J\} \quad \text{and} \quad W_\ell := \text{span}\{u_{\ell,j} \mid j \in J\}.$$

The eigenspaces $E(\lambda_j)$ may differ for different $j \in J$.

Assume that the cluster is contained in a compact interval $[A, B]$ in the sense that

$$\{\lambda_j \mid j \in J\} \cup \{\lambda_{\ell,j} \mid \ell \in I, j \in J\} \subseteq [A, B].$$

Therefore,

$$\sup_{\ell \in I} \max_{(j,k) \in J^2} \max \left\{ \lambda_k^{-1} \lambda_{\ell,j}, \lambda_{\ell,j}^{-1} \lambda_k \right\} \leq B/A. \quad (3.3)$$

Recall that $\dim(V_\ell) \in \mathbb{N} \cup \{\infty\}$ and let $J^C := \{1, \dots, \dim(V_\ell)\} \setminus J$ denote the complement of J . Assume that the cluster is separated from the remaining part of the spectrum in the sense that there exists a separation bound

$$M_J := \sup_{\ell \in I} \sup_{j \in J^C} \max_{k \in J} \frac{\lambda_k}{|\lambda_{\ell,j} - \lambda_k|} < \infty. \quad (\text{H1})$$

Definition 3.1 (quasi-Ritz projection). Given $f \in V$, let $u \in V$ denote the unique solution to

$$a(u, v) = b(f, v) \quad \text{for all } v \in V.$$

The quasi-Ritz projection $R_\ell u \in V_\ell$ is defined as the unique solution to

$$a_{\text{NC}}(R_\ell u, v_\ell) = b_{\text{NC}}(f, v_\ell) \quad \text{for all } v_\ell \in V_\ell. \quad \blacklozenge$$

Remark 3.2. In the case that $V_\ell \subseteq V$, R_ℓ is the Ritz projection, also called Galerkin or Ritz-Galerkin projection. The operator R_ℓ describes the discrete solution operator in the case that possibly $V_\ell \not\subseteq V$, which is the case for the nonconforming finite element methods considered in this thesis. In the latter case, the Galerkin orthogonality

$$a_{\text{NC}}(u - R_\ell u, v_\ell) = 0 \quad \text{for all } v_\ell \in V_\ell$$

is *not* valid in general. \blacklozenge

Let P_ℓ denote the b_{NC} -orthogonal projection onto W_ℓ and define

$$\Lambda_\ell := P_\ell \circ R_\ell. \quad (3.4)$$

For any eigenfunction $u \in W$, the function $\Lambda_\ell u \in W_\ell$ is regarded as its approximation. This approximation does not depend on the basis of W_ℓ . Notice that $\Lambda_\ell u$ is neither computable without knowledge of u nor necessarily an eigenfunction.

The following result is essentially contained in the book of Strang and Fix [1973] for a conforming finite element discretisation of the Laplace eigenvalue problem and in [Carstensen and Gedicke, 2011]. The proof presented here extends the arguments of Strang and Fix [1973] to a more abstract situation.

Proposition 3.3. Any eigenpair $(\lambda, u) \in \mathbb{R} \times W$ of (3.1) with $\|u\|_b = 1$ satisfies

$$\begin{aligned} \|R_\ell u - \Lambda_\ell u\|_{b, \text{NC}} &\leq M_J \|u - R_\ell u\|_{b, \text{NC}} \quad \text{and} \\ \|u - P_\ell u\|_{b, \text{NC}} &\leq \|u - \Lambda_\ell u\|_{b, \text{NC}} \leq (1 + M_J) \|u - R_\ell u\|_{b, \text{NC}}. \end{aligned}$$

Proof. Set $v_\ell := R_\ell u - \Lambda_\ell u$ and recall $\dim(V_\ell) \in \mathbb{N} \cup \{\infty\}$. Since the eigenfunctions $(u_{\ell, j} \mid j = 1, \dots, \dim(V_\ell))$ form a b_{NC} -orthonormal system of V_ℓ and v_ℓ is b_{NC} -orthogonal on W_ℓ , there exist coefficients $(\alpha_j \mid j \in J^C)$ such that

$$v_\ell = \sum_{j \in J^C} \alpha_j u_{\ell, j} \quad \text{and} \quad \sum_{j \in J^C} \alpha_j^2 = \|v_\ell\|_{b, \text{NC}}^2.$$

The definition of R_ℓ and the symmetry show that

$$(\lambda_{\ell, j} - \lambda) b_{\text{NC}}(R_\ell u, u_{\ell, j}) = \lambda b_{\text{NC}}(u - R_\ell u, u_{\ell, j}).$$

This and the orthogonality of v_ℓ and $\Lambda_\ell u$ lead to

$$\|v_\ell\|_{b, \text{NC}}^2 = b_{\text{NC}}(R_\ell u, \sum_{j \in J^C} \alpha_j u_{\ell, j}) = b_{\text{NC}}(u - R_\ell u, \sum_{j \in J^C} \alpha_j \frac{\lambda}{\lambda_{\ell, j} - \lambda} u_{\ell, j}).$$

The Cauchy inequality, the estimate (H1) from page 22 and the b_{NC} -orthogonality of the discrete eigenfunctions therefore show

$$\|v_\ell\|_{b, \text{NC}} \leq M_J \|u - R_\ell u\|_{b, \text{NC}}.$$

The second claimed chain of inequalities follows from the projection property of P_ℓ and the triangle inequality. \blacksquare

The following algebraic identity applies frequently in the analysis. It states the important property that, although $\Lambda_\ell u$ is no eigenfunction in general, $\Lambda_\ell u$ satisfies an equation that is similar to an eigenfunction property.

Lemma 3.4. Any eigenpair $(\lambda, u) \in \mathbb{R} \times V$ of (3.1) satisfies

$$a_{\text{NC}}(\Lambda_\ell u, v_\ell) = \lambda b_{\text{NC}}(P_\ell u, v_\ell) \quad \text{for all } v_\ell \in V_\ell.$$

In other words, R_ℓ and P_ℓ commute, $P_\ell \circ R_\ell = R_\ell \circ P_\ell$.

Proof. The representation of $\Lambda_\ell u$ in terms of the b_{NC} -orthonormal basis $(u_{\ell, j})_{j \in J}$ reads as

$$\Lambda_\ell u = \sum_{j \in J} \alpha_j u_{\ell, j} \quad \text{with } \alpha_j = b_{\text{NC}}(R_\ell u, u_{\ell, j}) \quad \text{for all } j \in J.$$

The symmetry of a_{NC} and b_{NC} proves for any $j \in J$ that

$$\alpha_j = b_{\text{NC}}(R_\ell u, u_{\ell, j}) = \lambda_{\ell, j}^{-1} a_{\text{NC}}(R_\ell u, u_{\ell, j}) = \lambda_{\ell, j}^{-1} \lambda b_{\text{NC}}(u, u_{\ell, j}).$$

Therefore, the discrete eigenvalue problem reveals

$$a_{\text{NC}}(\Lambda_\ell u, v_\ell) = \sum_{j \in J} \alpha_j \lambda_{\ell, j} b_{\text{NC}}(u_{\ell, j}, v_\ell) = \lambda \sum_{j \in J} b_{\text{NC}}(b_{\text{NC}}(u, u_{\ell, j}) u_{\ell, j}, v_\ell) = \lambda b_{\text{NC}}(P_\ell u, v_\ell). \quad \blacksquare$$

3. Eigenvalue Clusters

The following theorem of Knyazev and Osborn [2006] gives an abstract eigenvalue error estimate in case $V_\ell \subseteq V$.

Theorem 3.5 (Corollary 3.4 of [Knyazev and Osborn, 2006]). *Suppose $V_\ell \subseteq V$ and let, for $p \in \mathbb{N}$, λ_p be an eigenvalue of (3.1) with multiplicity $q \in \mathbb{N}$, so that*

$$\lambda_{p-1} < \lambda_p = \dots = \lambda_{p+q-1} < \lambda_{p+q}$$

(with the convention $\lambda_0 := 0$) and suppose that

$$\min_{j=1, \dots, p-1} |\lambda_{\ell, j} - \lambda_p| \neq 0.$$

Let $T : V \rightarrow V$ denote the solution operator of the associated linear problem, i.e., for given $f \in V$, $Tf \in V$ solves

$$a(Tf, v) = b(f, v) \quad \text{for all } v \in V.$$

Then, for any $k \in \{p, \dots, p+q-1\}$, the following estimate holds

$$\begin{aligned} & \frac{\lambda_{\ell, k} - \lambda_p}{\lambda_{\ell, k}} \\ & \leq \left(1 + \max_{j=1, \dots, p-1} \frac{\lambda_{\ell, j}^2 \lambda_p^2}{|\lambda_{\ell, j} - \lambda_p|^2} \sup_{\substack{f \in \text{span}\{u_{\ell, 1}, \dots, u_{\ell, p-1}\} \\ \|f\|_a = 1}} \|(1 - R_\ell)Tf\|_a^2 \right) \sup_{\substack{u \in E(\lambda_p) \\ \|u\|_a = 1}} \inf_{\substack{v_\ell \in V_\ell \\ \|v_\ell\|_a = 1}} \|u - v_\ell\|_a^2 \end{aligned}$$

where the maximum and supremum in the parentheses are 0 for $p = 1$. ■

Remark 3.6. In this thesis, the first supremum will usually be estimated through (a power of) some Friedrichs-type constant although it can be seen that in case of a finite element space V_ℓ this quantity even decays as a certain power of the maximum mesh-size. ◆

Remark 3.7. In [Knyazev and Osborn, 2006] the result of Theorem 3.5 is stated for a finite-dimensional space V_ℓ , but it is valid even if V_ℓ has infinite dimension. Only the finite dimension of the eigenspaces is required. One way to see this is to trace carefully the arguments in the proof of Knyazev and Osborn [2006]. For the reader's convenience, another argument is given here that reduces the stated result for $\dim V_\ell = \infty$ to the finite-dimensional case. To this end, consider the finite-dimensional subspace

$$\tilde{V}_\ell := \text{span}\{u_{\ell, 1}, \dots, u_{\ell, p+q-1}, R_\ell u_p, \dots, R_\ell u_{p+q-1}, R_\ell T u_{\ell, p}, \dots, R_\ell T u_{\ell, p-1}\} \subseteq V_\ell.$$

The finite-dimensional space \tilde{V}_ℓ is constructed in such a way that the first $p+q-1$ eigenvalues $\lambda_{\ell, 1}, \dots, \lambda_{\ell, p+q-1}$ that are relevant for the statement of Theorem 3.5 are attained in \tilde{V}_ℓ and similarly all further quantities in the estimate are attained in this finite-dimensional space. For instance,

$$\sup_{\substack{u \in E(\lambda_p) \\ \|u\|_a = 1}} \inf_{\substack{v_\ell \in V_\ell \\ \|v_\ell\|_a = 1}} \|u - v_\ell\|_a^2 = \sup_{\substack{u \in E(\lambda_p) \\ \|u\|_a = 1}} \|u - R_\ell u\|_a^2 = \sup_{\substack{u \in \text{span}\{u_p, \dots, u_{p+q-1}\} \\ \|u\|_a = 1}} \|u - R_\ell u\|_a^2$$

is realised in \tilde{V} . Theorem 3.5 can be employed for \tilde{V}_ℓ in its original version and is thereby also valid for V_ℓ because the claimed inequality is the same. ◆

Remark 3.8. In Chapter 8 below, Theorem 3.5 will be applied to the case that $V \subseteq \widehat{V}_\ell := V + V_\ell$ where V itself is a subspace of the enhanced space \widehat{V}_ℓ . ◆

3.2. Equivalence of Seminorms

This section is devoted to the comparison of seminorms for the eigenfunctions. The first lemma gives a criterion that ensures that the image of a basis under Λ_ℓ and P_ℓ forms a linear independent set. It generalises [Carstensen and Gedicke, 2011, Prop. 3.2].

Lemma 3.9. *Suppose that*

$$\varepsilon := \max_{j \in J} \|u_j - \Lambda_\ell u_j\|_{b, \text{NC}} \leq \sqrt{1 + 1/(2N)} - 1 \quad \text{for all } \ell \in I. \quad (\text{H2})$$

Then, both $(P_\ell u_j)_{j \in J}$ and $(\Lambda_\ell u_j)_{j \in J}$ form a basis of W_ℓ . For any $w_\ell \in W_\ell$ with $\|w_\ell\|_{b, \text{NC}} = 1$, the coefficients of the representation $w_\ell = \sum_{j \in J} \beta_j P_\ell u_j$ and $w_\ell = \sum_{j \in J} \gamma_j \Lambda_\ell u_j$ are controlled as

$$\max \left\{ \sum_{j \in J} |\beta_j|^2, \sum_{j \in J} |\gamma_j|^2 \right\} \leq 2 + 4N \quad \text{for } N = \text{card}(J). \quad (3.5)$$

Remark 3.10. For the proof of Lemma 3.9 it is sufficient that (H2) holds for a fixed $\ell \in I$. However, for the applications in this thesis, the assumption (H2) is required to hold uniformly in $\ell \in I$. \blacklozenge

Remark 3.11. Lemma 3.9 refines [Carstensen and Gedicke, 2011, Prop. 3.2] in that it replaces the assumption of ε to be sufficiently small by an explicit upper bound for ε . The proof employs Gershgorin's theorem. Proofs of linear independence that use this argument can be found in [Carstensen and Gedicke, 2014, Carstensen and Gallistl, 2014]. \blacklozenge

Proof of Lemma 3.9. The proof is carried out for Λ_ℓ only. Analogous arguments and $\max\{\|u_j - P_\ell u_j\|_{b, \text{NC}} \mid j \in J\} \leq \varepsilon$ yield the result for P_ℓ .

For any $(j, k) \in J^2$, the triangle inequality plus $\|u_j\|_b = 1$ and the definition of ε reveal (δ_{jk} denotes the Kronecker δ)

$$\begin{aligned} |b_{\text{NC}}(\Lambda_\ell u_j, \Lambda_\ell u_k) - \delta_{jk}| &= |b_{\text{NC}}(\Lambda_\ell u_j - u_j, \Lambda_\ell u_k) + b_{\text{NC}}(u_j, \Lambda_\ell u_k - u_k)| \\ &\leq \varepsilon(1 + \|\Lambda_\ell u_k\|_{b, \text{NC}}) \\ &\leq \varepsilon(2 + \|u_k - \Lambda_\ell u_k\|_{b, \text{NC}}) \leq \varepsilon(2 + \varepsilon). \end{aligned} \quad (3.6)$$

For any $j \in J$ it follows from (H2) and (3.6) that

$$\frac{2N - 1}{2N} \leq 1 - \varepsilon(2 + \varepsilon) \leq b_{\text{NC}}(\Lambda_\ell u_j, \Lambda_\ell u_j)$$

and

$$\sum_{k \in J \setminus \{j\}} |b_{\text{NC}}(\Lambda_\ell u_j, \Lambda_\ell u_k)| \leq (N - 1)\varepsilon(2 + \varepsilon) \leq \frac{N - 1}{2N}.$$

Thus, the Gershgorin theorem [see, e.g., Stoer and Bulirsch, 2002] implies that all eigenvalues of the matrix

$$(b_{\text{NC}}(\Lambda_\ell u_j, \Lambda_\ell u_k))_{(j, k) \in J^2}$$

are positive and, hence, $(\Lambda_\ell u_j)_{j \in J}$ is a basis of W_ℓ . Let $w_\ell \in W_\ell$ with $\|w_\ell\|_{b, \text{NC}} = 1$ and $w_\ell = \sum_{j \in J} \gamma_j \Lambda_\ell u_j$ for coefficients $(\gamma_j \mid j \in J)$.

For any $k \in J$ it holds that

$$b_{\text{NC}}(\Lambda_\ell u_k, w_\ell) = \sum_{j \in J} \gamma_j b_{\text{NC}}(\Lambda_\ell u_k, \Lambda_\ell u_j) = \gamma_k + \sum_{j \in J} \gamma_j (b_{\text{NC}}(\Lambda_\ell u_k, \Lambda_\ell u_j) - \delta_{jk}).$$

3. Eigenvalue Clusters

Hence, the triangle and Young inequalities (Proposition 2.30) together with (3.6) and $\|\Lambda_\ell u_k\|_{b, \text{NC}} \leq 1 + \varepsilon$ prove

$$\begin{aligned} |\gamma_k|^2 &\leq \left(|b_{\text{NC}}(\Lambda_\ell u_k, w_\ell)| + \sum_{j \in J} |\gamma_j| |b_{\text{NC}}(\Lambda_\ell u_k, \Lambda_\ell u_j) - \delta_{jk}| \right)^2 \\ &\leq 2|b_{\text{NC}}(\Lambda_\ell u_k, w_\ell)|^2 + 2N \sum_{j \in J} |\gamma_j|^2 |b_{\text{NC}}(\Lambda_\ell u_k, \Lambda_\ell u_j) - \delta_{jk}|^2 \\ &\leq 2(1 + \varepsilon)^2 + 2N(\varepsilon(2 + \varepsilon))^2 \sum_{j \in J} |\gamma_j|^2. \end{aligned}$$

The summation over $k \in J$ yields

$$\sum_{k \in J} |\gamma_k|^2 \leq 2N(1 + \varepsilon)^2 + 2N^2(\varepsilon(2 + \varepsilon))^2 \sum_{j \in J} |\gamma_j|^2.$$

Since $\varepsilon(2 + \varepsilon) \leq (2N)^{-1}$ by assumption (H2), it follows that

$$\sum_{j \in J} |\gamma_j|^2 \leq 4N(1 + \varepsilon)^2 \leq 2 + 4N. \quad \blacksquare$$

The following proposition states a comparison of seminorms. In the applications of this thesis, the seminorms from this proposition will be error estimators. Recall that all eigenvalues in the cluster as well as their approximations are contained in the compact interval $[A, B]$ and that $N = \text{card}(J)$.

Proposition 3.12 (comparison of seminorms). *Suppose (H1) from page 22 and (H2) from page 25. For any $\ell \in I$, any seminorm ρ_ℓ on V_ℓ satisfies*

$$N^{-1} \sum_{j \in J} \rho_\ell(\lambda_j P_\ell u_j)^2 \leq (B/A)^2 \sum_{j \in J} \rho_\ell(\lambda_{\ell, j} u_{\ell, j})^2 \leq (B/A)^4 (2N + 4N^2) \sum_{j \in J} \rho_\ell(\lambda_j P_\ell u_j)^2 \quad (3.7)$$

and

$$N^{-1} \sum_{j \in J} \rho_\ell(\Lambda_\ell u_j)^2 \leq (B/A)^2 \sum_{j \in J} \rho_\ell(u_{\ell, j})^2 \leq (B/A)^4 (2N + 4N^2) \sum_{j \in J} \rho_\ell(\Lambda_\ell u_j)^2. \quad (3.8)$$

Proof. For the proof of the first inequality of (3.7), let $k \in J$. The expansion

$$P_\ell u_k = \sum_{j \in J} \alpha_j u_{\ell, j}$$

with respect to the orthonormal basis $(u_{\ell, j} \mid j \in J)$ leads to

$$\sum_{j \in J} \alpha_j^2 = \|P_\ell u_k\|_{b, \text{NC}}^2 \leq 1.$$

Thus, the triangle inequality followed by the Cauchy inequality and (3.3) proves

$$\begin{aligned} \rho_\ell(\lambda_k P_\ell u_k)^2 &\leq \left(\sum_{j \in J} \lambda_k |\alpha_j| \rho_\ell(u_{\ell, j}) \right)^2 \\ &\leq \lambda_k^2 \left(\sum_{j \in J} \alpha_j^2 \right) \sum_{j \in J} \rho_\ell(u_{\ell, j})^2 \leq (B/A)^2 \sum_{j \in J} \rho_\ell(\lambda_{\ell, j} u_{\ell, j})^2. \end{aligned}$$

For the second inequality of (3.7), let $k \in J$. According to Lemma 3.9, $(P_\ell u_j)_{j \in J}$ is a basis of W_ℓ and $u_{\ell,k} = \sum_{j \in J} \beta_j P_\ell u_j$ for real coefficients $(\beta_j \mid j \in J)$. The triangle and Cauchy inequalities and (3.3) prove

$$\rho_\ell(\lambda_{\ell,k} u_{\ell,k})^2 = \rho_\ell(\lambda_{\ell,k} \sum_{j \in J} \beta_j P_\ell u_j)^2 \leq (B/A)^2 \left(\sum_{j \in J} \beta_j^2 \right) \sum_{j \in J} \rho_\ell(\lambda_j P_\ell u_j)^2.$$

As proven in Lemma 3.9 it holds that $\sum_{j \in J} \beta_j^2 \leq (2 + 4N)$. This proves the second inequality in (3.7).

For the proof of (3.8), let $k \in J$. An expansion of $\Lambda_\ell u_k = \sum_{j \in J} \gamma_j u_{\ell,j}$ with coefficients

$$\gamma_j = b_{\text{NC}}(\Lambda_\ell u_k, u_{\ell,j}) = b_{\text{NC}}(R_\ell u_k, u_{\ell,j}) = \lambda_{\ell,j}^{-1} \lambda_k b_{\text{NC}}(u_k, u_{\ell,j})$$

results in $\sum_{j \in J} \gamma_j^2 \leq (B/A)^2$. Thus,

$$\rho_\ell(\Lambda_\ell u_k)^2 \leq (B/A)^2 \sum_{j \in J} \rho_\ell(u_{\ell,j})^2.$$

This proves the first inequality of (3.8).

Lemma 3.9 shows that there exist real coefficients $(\delta_j \mid j \in J)$ such that

$$u_{\ell,k} = \sum_{j \in J} \delta_j \Lambda_\ell u_j \quad \text{and} \quad \sum_{j \in J} \delta_j^2 \leq 2 + 4N.$$

The triangle and Cauchy inequalities lead to

$$\rho_\ell(u_{\ell,k})^2 \leq \left(\sum_{j \in J} \delta_j^2 \right) \sum_{j \in J} \rho_\ell(\Lambda_\ell u_j)^2 \leq (2 + 4N) \sum_{j \in J} \rho_\ell(\Lambda_\ell u_j)^2.$$

This and $(B/A)^2 \geq 1$ conclude the proof. ■

3.3. Upper and Lower Spectral Bounds

This section discusses the computation of upper and lower bounds for eigenvalues. The Rayleigh-Ritz principle (also known as the Courant-Fischer min-max principle) [Weinstein and Stenger, 1972] states that the j -th eigenvalue λ_j of (3.1) satisfies

$$\lambda_j = \min_{\dim \tilde{V} = j} \max_{v \in \tilde{V} \setminus \{0\}} \frac{\|v\|_a^2}{\|v\|_b^2}, \quad (3.9)$$

where the minimum runs over all subspaces $\tilde{V} \subseteq V$ with dimension (smaller than or) equal to j . The j -th discrete eigenvalue $\lambda_{\ell,j}$ of (3.2) equals

$$\lambda_{\ell,j} = \min_{\dim \tilde{V}_\ell = j} \max_{v_\ell \in \tilde{V}_\ell \setminus \{0\}} \frac{\|v_\ell\|_{a,\text{NC}}^2}{\|v_\ell\|_{b,\text{NC}}^2}, \quad (3.10)$$

where the minimum runs over all subspaces $\tilde{V}_\ell \subseteq V_\ell$ with dimension (smaller than or) equal to j . Hence, any conforming discretisation (i.e., $V_\ell \subseteq V$) will lead to an upper bound

$$\lambda_j \leq \lambda_{\ell,j}.$$

3. Eigenvalue Clusters

The task of computing lower bounds for λ_j turns out to be more involved. The computation of lower eigenvalue bounds is a classical problem and various approaches have been developed, see [Kuznetsov and Repin, 2013] for an overview.

The recent works of Carstensen and Gedicke [2014], Carstensen and Gallistl [2014], Liu and Oishi [2013] develop a new methodology for lower eigenvalue bounds that relies on projection operators. This approach can be unified in the following abstract lemma.

Lemma 3.13 (lower eigenvalue bounds). *Suppose that there exists a linear operator $\Phi_\ell : V \rightarrow V_\ell$ with the projection property*

$$a_{\text{NC}}(v - \Phi_\ell v, \Phi_\ell v) = 0 \quad \text{for all } v \in V \quad (3.11)$$

and the $\|\cdot\|_{b,\text{NC}}$ norm estimate for some $\varepsilon_\ell > 0$

$$\|v - \Phi_\ell v\|_{b,\text{NC}} \leq \varepsilon_\ell \|v - \Phi_\ell v\|_{a,\text{NC}} \quad \text{for all } v \in V. \quad (3.12)$$

Then,

$$\frac{\lambda_{\ell,1}}{1 + \varepsilon_\ell^2 \lambda_{\ell,1}} \leq \lambda_1.$$

If, in addition, $\varepsilon_\ell < (\sqrt{1 + K^{-1}} - 1) / \sqrt{\lambda_K}$ holds for some $K \in \mathbb{N}$, then

$$\frac{\lambda_{\ell,K}}{1 + \varepsilon_\ell^2 \lambda_{\ell,K}} \leq \lambda_K.$$

Proof. The projection property (3.11) and the min-max principle (3.10) for $\lambda_{\ell,1}$ prove that

$$\|u_1 - \Phi_\ell u_1\|_{a,\text{NC}}^2 + \lambda_{\ell,1} \|\Phi_\ell u_1\|_{b,\text{NC}}^2 \leq \|u_1 - \Phi_\ell u_1\|_{a,\text{NC}}^2 + \|\Phi_\ell u_1\|_{a,\text{NC}}^2 = \|u_1\|_a^2 = \lambda_1. \quad (3.13)$$

The Young (Proposition 2.30) and Cauchy inequalities prove for any $0 < \delta \leq 1$ that

$$(1 - \delta) + (1 - \delta^{-1}) \|u_1 - \Phi_\ell u_1\|_{b,\text{NC}}^2 \leq 1 + \|u_1 - \Phi_\ell u_1\|_{b,\text{NC}}^2 - 2 \|u_1 - \Phi_\ell u_1\|_{b,\text{NC}} \leq \|\Phi_\ell u_1\|_{b,\text{NC}}^2.$$

The combination of the foregoing two displayed inequalities with the $\|\cdot\|_{b,\text{NC}}$ norm estimate (3.12) and the choice of

$$\delta := \varepsilon_\ell^2 \lambda_{\ell,1} / (1 + \varepsilon_\ell^2 \lambda_{\ell,1})$$

proves the lower bound for λ_1 .

The assumptions (3.11)–(3.12) on Φ_ℓ show, for any $j \in \{1, \dots, K\}$, that

$$\|u_j - \Phi_\ell u_j\|_{b,\text{NC}} \leq \varepsilon_\ell \|u_j - \Phi_\ell u_j\|_{a,\text{NC}} \leq \varepsilon_\ell \|u_j\|_{a,\text{NC}} \leq \varepsilon_\ell \sqrt{\lambda_K}.$$

The assumption on ε_ℓ and an argument with the Gershgorin theorem as in the proof of Lemma 3.9 shows that all the eigenvalues of the matrix

$$(b_{\text{NC}}(\Phi_\ell u_j, \Phi_\ell u_k))_{j,k \in \{1, \dots, K\}^2}$$

are positive and, hence, the functions $\Phi_\ell u_1, \dots, \Phi_\ell u_K$ are linearly independent. Hence, there exist real coefficients ξ_1, \dots, ξ_K with $\sum_{j=1}^K \xi_j^2 = 1$ such that the maximiser of the

Rayleigh quotient in $\text{span}\{\Phi_\ell u_1, \dots, \Phi_\ell u_K\}$ is equal to $\sum_{j=1}^K \xi_j \Phi_\ell u_j$. Therefore, the function $v := \sum_{j=1}^K \xi_j u_j$ satisfies $\Phi_\ell v \neq 0$ and

$$\lambda_{\ell,K} \leq \frac{\|\Phi_\ell v\|_{a,\text{NC}}^2}{\|\Phi_\ell v\|_{b,\text{NC}}^2}. \quad (3.14)$$

The projection property of Φ_ℓ and the orthogonality of the eigenfunctions prove

$$\|v - \Phi_\ell v\|_{a,\text{NC}}^2 + \|\Phi_\ell v\|_{a,\text{NC}}^2 = \|v\|_a^2 = \sum_{j=1}^K \xi_j^2 \lambda_j \leq \lambda_K.$$

This and (3.14) yield

$$\|v - \Phi_\ell v\|_{a,\text{NC}}^2 + \lambda_{\ell,K} \|\Phi_\ell v\|_{b,\text{NC}}^2 \leq \lambda_K.$$

This estimate replaces (3.13) in the case of the first eigenvalue. The remaining parts of the proof are identical to the proof for the first eigenvalue. \blacksquare

Remark 3.14. The proof shows that the mesh-size restriction of [Liu and Oishi, 2013, Theorem 5.1] can be dropped. On the other hand it points out that, for higher eigenvalues, an additional condition $\varepsilon_\ell < \left(\sqrt{1+K^{-1}} - 1\right) / \sqrt{\lambda_K}$ is needed also in their analysis. \blacklozenge

3.4. Adaptive Algorithms

The main aspect of this thesis is the adaptive finite element computation of eigenvalues. Suppose the space V_ℓ is defined by means of a regular triangulation $\mathcal{T}_\ell \in \mathbb{T}$ and that there exists a computable refinement indicator $(\eta_\ell^2(T) \mid T \in \mathcal{T}_\ell)$ based on the discrete eigenpairs $(\lambda_{\ell,j}, u_{\ell,j})_{j \in J}$. Examples can be found in Sections 4.2, 5.6, 6.3, and 7.6. The adaptive algorithm is driven by this computable error estimator and runs the following loop.

Algorithm 3.15 (abstract AFEM for eigenvalue clusters).

Input: Initial triangulation \mathcal{T}_0 , bulk parameter $0 < \theta \leq 1$.

for $\ell = 0, 1, 2, \dots$ **do**

Solve. Compute discrete eigenpairs $(\lambda_{\ell,j}, u_{\ell,j})_{j \in J}$ of (3.2) with respect to \mathcal{T}_ℓ .

Estimate. Compute local contributions of the error estimator $(\eta_\ell^2(T))_{T \in \mathcal{T}_\ell}$.

Mark. The Dörfler marking chooses a minimal subset $\mathcal{M}_\ell \subseteq \mathcal{T}_\ell$ such that

$$\theta \eta_\ell^2(\mathcal{T}_\ell) \leq \eta_\ell^2(\mathcal{M}_\ell) := \sum_{T \in \mathcal{M}_\ell} \eta_\ell^2(T).$$

Refine. Generate the smallest admissible refinement $\mathcal{T}_{\ell+1} := \text{refine}(\mathcal{T}_\ell, \mathcal{M}_\ell)$ of \mathcal{T}_ℓ with $\mathcal{M}_\ell \cap \mathcal{T}_{\ell+1} = \emptyset$ with Algorithm 2.15.

end for

Output: Triangulations $(\mathcal{T}_\ell)_{\ell \in \mathbb{N}_0}$ and discrete eigenpairs $((\lambda_{\ell,j}, u_{\ell,j})_{j \in J})_{\ell \in \mathbb{N}_0}$. \blacklozenge

For the convergence analysis of this kind of adaptive algorithms, a theoretical, non-computable error estimator $(\mu_\ell^2(T, \lambda_j, u_j) \mid T \in \mathcal{T}_\ell)$ will be employed. Suppose that, for any $T \in \mathcal{T}$, there exist seminorms $\rho_{1,T}, \rho_{2,T}$ such that

$$\eta_\ell^2(T) = \sum_{j \in J} (\rho_{1,T}(\lambda_{\ell,j} u_{\ell,j})^2 + \rho_{2,T}(u_{\ell,j})^2) \quad \text{and}$$

$$\mu_\ell^2(T, \lambda_j, u_j) = (\rho_{1,T}(\lambda_j P_\ell u_j)^2 + \rho_{2,T}(\Lambda_\ell u_j)^2) \quad \text{for all } j \in J.$$

The next proposition states that these contributions are equivalent.

3. Eigenvalue Clusters

Proposition 3.16 (bulk criterion). *Suppose (H1) and (H2). Then, for any $T \in \mathcal{T}_\ell$, the error estimator contributions can be compared as follows*

$$N^{-1} \sum_{j \in J} \mu_\ell^2(T, \lambda_j, u_j) \leq (B/A)^2 \eta_\ell^2(T) \leq (B/A)^4 (2N + 4N^2) \sum_{j \in J} \mu_\ell^2(T, \lambda_j, u_j). \quad (3.15)$$

Therefore, $\mu_\ell(\mathcal{M}_\ell) := \sum_{T \in \mathcal{M}_\ell} \sum_{j \in J} \mu_\ell^2(T, \lambda_j, u_j)$ satisfies the bulk criterion

$$\tilde{\theta} \mu_\ell(\mathcal{T}_\ell) \leq \mu_\ell(\mathcal{M}_\ell)$$

for the modified bulk parameter

$$\tilde{\theta} := ((B/A)^4 (2N^2 + 4N^3))^{-1} \theta < 1. \quad (3.16)$$

Proof. The claimed inequalities in (3.15) are an immediate consequence of Proposition 3.12. The bulk criterion then follows from elementary calculations. \blacksquare

Throughout the mathematical analysis of this thesis, it is assumed that the algebraic eigenvalue problems are solved exactly. This assumption is not realistic in practice and a practical adaptive algorithm has to involve an iterative solve with a controlled termination criterion. The optimal convergence rates of algorithms of this type was analysed in [Becker and Mao, 2008, 2009] for linear problems and in [Carstensen and Gedicke, 2012, Carstensen, Gallistl, and Schedensack, 2014c] for eigenvalue problems.

Recall Remark 2.35 and let, for finite-dimensional subspaces $X_\ell \subseteq V_\ell$ and $Y_\ell \subseteq V_\ell$, the largest principal angle from X_ℓ to Y_ℓ (measured in the a_{NC} scalar product) be indicated by

$$\sin_{a_{\text{NC}}}^2 \angle(X_\ell, Y_\ell) := \sup_{\substack{x_\ell \in X_\ell \\ \|x_\ell\|_{a_{\text{NC}}}=1}} \inf_{y_\ell \in Y_\ell} \|x_\ell - y_\ell\|_{a_{\text{NC}}}^2.$$

Algorithm 3.17 (AFEM with inexact solution of the algebraic eigenvalue problem).

Input: Initial triangulation \mathcal{T}_0 , bulk parameter $0 < \theta \leq 1$ and parameter $0 < \varkappa < \infty$.

for $\ell = 0, 1, 2, \dots$ **do**

Inexact Solve and Estimate. Compute approximations $(\tilde{\lambda}_{\ell,j}, \tilde{u}_{\ell,j})_{j \in J}$ to the discrete eigenpairs $(\lambda_{\ell,j}, u_{\ell,j})_{j \in J}$ of (3.2) with respect to \mathcal{T}_ℓ with local contributions of the error estimator $(\eta_\ell^2(T))_{T \in \mathcal{T}_\ell}$ based on the quantities $(\tilde{\lambda}_{\ell,j}, \tilde{u}_{\ell,j})_{j \in J}$ such that (with $\eta_{-1}^2 := \infty$)

$$\sin_{a_{\text{NC}}}^2 \angle(W_\ell, \text{span}\{\tilde{u}_{\ell,j} \mid j \in J\}) \leq \varkappa \min\{\eta_\ell^2, \eta_{\ell-1}^2\}. \quad (3.17)$$

Mark. Choose a minimal subset $\mathcal{M}_\ell \subseteq \mathcal{T}_\ell$ with $\theta \eta_\ell^2(\mathcal{T}_\ell) \leq \eta_\ell^2(\mathcal{M}_\ell) := \sum_{T \in \mathcal{M}_\ell} \eta_\ell^2(T)$.

Refine. Generate $\mathcal{T}_{\ell+1} := \text{refine}(\mathcal{T}_\ell, \mathcal{M}_\ell)$ with Algorithm 2.15.

end for

Output: Sequences of triangulations $(\mathcal{T}_\ell)_\ell$ and discrete eigenpairs $((\lambda_{\ell,j}, u_{\ell,j})_{j \in J})_\ell$. \blacklozenge

The criterion (3.17) requires an additional internal loop as in [Carstensen and Gedicke, 2012]. The optimality analysis of this thesis is carried out for the case $\varkappa = 0$ which means that the discrete eigenvalue problems are solved exactly. The analysis can be extended to the case of inexact solve for sufficiently small $\varkappa \ll 1$ by a perturbation analysis as in [Carstensen and Gedicke, 2012] or [Carstensen, Gallistl, and Schedensack, 2014c].

Remark 3.18 (bounds on the linear-algebraic error). A posteriori bounds for the linear-algebraic approximation error of an invariant subspace as in (3.17) can be found in [Davis and Kahan, 1970]. A recent overview and refinement of this type of results is given in [Ovtchinnikov, 2006a,b]. Guaranteed estimates for (3.17) require information on the spectral gap, that is the separation of the computed eigenvalue cluster to the rest of the spectrum. This motivates the approximation of eigenvalue clusters not only on the level of a finite element approximation but also from the linear-algebraic point of view, see also the discussion in Section 11 of [Parlett, 1998]. \blacklozenge

Remark 3.19 (angle with respect to a_{NC}). The a posteriori error estimators for the finite element discretisation of the elliptic PDEs considered in this thesis are based on estimates in the energy norm. Therefore, the angle with respect to the scalar product a_{NC} is the canonical error measure for the linear-algebraic error if one wants to combine the linear-algebraic error with the a posteriori analysis as in [Miedlar, 2011]. \blacklozenge

Remark 3.20 (normalisation). The eigenvalue problems in this thesis are based on the normalisation $\|\cdot\|_{b,\text{NC}} = 1$ and typically approximation quantities like

$$\sup_{\substack{w \in W \\ \|w\|_{b,\text{NC}}=1}} \inf_{v_\ell \in W_\ell} \|w - v_\ell\|_{a,\text{NC}}^2$$

arise in the analysis. To see that this quantity essentially describes the angle $\sin_{a,\text{NC}}^2 \angle(W, W_\ell)$ up to some scaling, consider the expansion of w in terms of the eigenfunctions of W . Then the eigenvalue problem implies

$$\begin{aligned} \sin_{a,\text{NC}}^2 \angle(W, W_\ell) &= \sup_{w \in W \setminus \{0\}} \frac{\inf_{v_\ell \in W_\ell} \|w - v_\ell\|_{a,\text{NC}}^2}{\|w\|_{b,\text{NC}}^2} \frac{\|w\|_{b,\text{NC}}^2}{\|w\|_{a,\text{NC}}^2} \\ &\leq \frac{1}{\lambda_{n+1}} \sup_{\substack{w \in W \\ \|w\|_{b,\text{NC}}=1}} \inf_{v_\ell \in W_\ell} \|w - v_\ell\|_{a,\text{NC}}^2 \\ &\leq \frac{\lambda_{n+N}}{\lambda_{n+1}} \sin_{a,\text{NC}}^2 \angle(W, W_\ell) \leq \frac{B}{A} \sin_{a,\text{NC}}^2 \angle(W, W_\ell). \end{aligned}$$

This means that the error quantities are comparable up to a factor described by the ratio of the cluster bounds. \blacklozenge

Numerical tests on the interplay of the adaptive mesh-refinement and the linear-algebraic error can be found in [Mehrmann and Miedlar, 2011, Miedlar, 2011] or [Carstensen and Gedicke, 2012] for simple eigenvalues. Section 9.5 of this thesis presents corresponding numerical examples for clustered eigenvalues.

4. Conforming \mathcal{P}_1 FEM for the Eigenvalues of the Laplacian

This chapter enfoldes an optimality analysis of the conforming \mathcal{P}_1 finite element discretisation of the Laplace eigenvalue problem. It extends the optimality results of Dai et al. [2008], Carstensen and Gedicke [2011] and Dai et al. [2013] to the case of eigenvalue clusters and identifies the dependence of the involved constants explicitly. Table 4.1 quantifies the resulting conditions on the initial mesh-size to be sufficiently small. Section 4.1 introduces the Laplace eigenvalue problem and its conforming discretisation. Section 4.2 presents the adaptive algorithm and a suitable approximation class. The theoretical error estimator and its discrete reliability follow in Section 4.3. This and the contraction property of Section 4.4 lead to the proof of optimal convergence rates in Section 4.5.

4.1. Conforming Discretisation

Let $V := H_0^1(\Omega)$ be equipped with the scalar products

$$a(v, w) := (Dv, Dw)_{L^2(\Omega)} \quad \text{and} \quad b(v, w) := (v, w)_{L^2(\Omega)}$$

and induced norms $\|v\| := a(v, v)^{1/2}$ and $\|v\| := b(v, v)^{1/2}$. The Laplace eigenvalue problem seeks eigenpairs $(\lambda, u) \in \mathbb{R} \times V$ with $\|u\| = 1$ such that

$$a(u, v) = \lambda b(u, v) \quad \text{for all } v \in V. \quad (4.1)$$

The finite element discretisation relies on a regular triangulation \mathcal{T}_ℓ and $V_\ell := \mathcal{P}_1(\mathcal{T}_\ell) \cap V$ and seeks discrete eigenpairs $(\lambda_\ell, u_\ell) \in \mathbb{R} \times V_\ell$ with $\|u_\ell\| = 1$ and

$$a(u_\ell, v_\ell) = \lambda_\ell b(u_\ell, v_\ell) \quad \text{for all } v_\ell \in V_\ell. \quad (4.2)$$

Adopt the notation of Section 3.1 with exact and discrete eigenvalues

$$0 < \lambda_1 \leq \lambda_2 \leq \dots \quad \text{and} \quad 0 < \lambda_{\ell,1} \leq \dots \leq \lambda_{\ell, \dim(V_\ell)}$$

and their corresponding b -orthonormal systems of eigenfunctions

$$(u_1, u_2, u_3, \dots) \quad \text{and} \quad (u_{\ell,1}, u_{\ell,2}, \dots, u_{\ell, \dim(V_\ell)}).$$

The eigenvalue cluster is described by the index set $J := \{n+1, \dots, n+N\}$ and the spaces $W := \text{span}\{u_j\}_{j \in J}$ and $W_\ell := \text{span}\{u_{\ell,j}\}_{j \in J}$. In the present case of nested conforming finite element spaces, the interval $[A, B]$ containing the cluster can be chosen as $A := \lambda_{n+1}$, $B := \lambda_{0, n+N}$ with respect to the coarse initial triangulation \mathcal{T}_0 . The min-max principle (3.9)–(3.10) assures that the discrete eigenvalues of the cluster will be contained in $[A, B]$ for all $\mathcal{T}_\ell \in \mathbb{T}$.

4. Conforming \mathcal{P}_1 FEM for the Eigenvalues of the Laplacian

Recall the notation of Section 3.1: Let $R_\ell : V \rightarrow V_\ell$ denote the quasi-Ritz projection of Definition 3.1 (in the present case, R_ℓ is the a -orthogonal projection onto $V_\ell \subseteq V$, i.e., the Ritz-Galerkin projection) and let P_ℓ denote the L^2 projection onto W_ℓ and define

$$\Lambda_\ell := \Lambda_{\mathcal{T}_\ell} := P_\ell \circ R_\ell. \quad (4.3)$$

Let $0 < s \leq 1$ indicate the elliptic regularity index of the Poisson problem [Grisvard, 1985] with homogeneous Dirichlet boundary conditions in the sense that, for given $f \in L^2(\Omega)$,

$$-\Delta u = f \quad \text{and} \quad \|u\|_{H^{1+s}(\Omega)} \leq C(s) \|f\|_{L^2(\Omega)}. \quad (4.4)$$

The following proposition provides an L^2 error estimate for $\Lambda_\ell u$. The proof follows the arguments of Strang and Fix [1973, Theorem 6.2].

Proposition 4.1. *The condition (H1) from page 22 implies that there exists a constant $C_{\text{reg}} \approx 1$ such that any eigenfunction $u \in W$ with $\|u\| = 1$ satisfies*

$$\|u - P_\ell u\| \leq \|u - \Lambda_\ell u\| \leq (1 + M_J) C_{\text{reg}} \|h_0\|_\infty^s \|u - R_\ell u\| \leq (1 + M_J) C_{\text{reg}} \|h_0\|_\infty^s \|u - \Lambda_\ell u\|.$$

Proof. Proposition 3.3 and the Aubin-Nitsche duality technique [Strang and Fix, 1973, Braess, 2007] for the boundary value problem imply for some constant C_{reg} (dependent on s) that

$$\|u - \Lambda_\ell u\| \leq (1 + M_J) \|u - R_\ell u\| \leq (1 + M_J) C_{\text{reg}} \|h_0\|_\infty^s \|u - R_\ell u\|.$$

The last stated inequality of the Lemma follows from the best-approximation property of the Ritz projection R_ℓ with respect to the norm $\|\cdot\|$. ■

The analysis is merely concerned with an approximation of the eigenfunctions. The following proposition is a consequence of Theorem 3.5. Recall that the eigenvalue cluster is contained in the interval $[A, B]$.

Proposition 4.2. *There exists some constant C such that for any $j \in J$ the eigenvalue error is controlled as*

$$|\lambda_{\ell,j} - \lambda_j| \leq \lambda_{\ell,j} (1 + M_J^2 B^2 C) \sup_{\substack{w \in E(\lambda_j) \\ \|w\|=1}} \inf_{v_\ell \in W_\ell} \|w - v_\ell\|^2. \quad \blacksquare$$

The following best-approximation result generalises [Carstensen et al., 2012b, Gudi, 2010] to eigenvalue problems for an arbitrary regular triangulation $\mathcal{T}_\ell \in \mathbb{T}$ in any space dimension.

Proposition 4.3 (best-approximation result). *There exists a constant C_{ba} such that, provided the condition (H1) holds, any eigenpair $(\lambda, u) \in \mathbb{R} \times W$ with $\|u\| = 1$ and the elliptic regularity parameter $0 < s \leq 1$ satisfies*

$$\|u - \Lambda_\ell u\| \leq C_{\text{ba}} (1 + (1 + M_J) \lambda \|h_0\|_\infty^s) (1 + \lambda \|h_0\|_\infty^2) \|(1 - \Pi_\ell^0) Du\|.$$

Proof. Set $v_\ell := R_\ell u - \Lambda_\ell u$. Lemma 3.4 and the eigenvalue problem for u lead to

$$a(R_\ell u - \Lambda_\ell u, v_\ell) = \lambda b(u - P_\ell u, v_\ell) \leq \lambda \|u - P_\ell u\| \|v_\ell\|.$$

Hence, the Friedrichs inequality [Braess, 2007] with constant C_F proves $\|R_\ell u - \Lambda_\ell u\| \leq \lambda C_F \|u - P_\ell u\|$. This and the triangle inequality lead to

$$\|u - \Lambda_\ell u\| \leq \|u - R_\ell u\| + \lambda C_F \|u - P_\ell u\|.$$

This and Proposition 4.1 prove

$$\|u - \Lambda_\ell u\| \leq (1 + \|h_0\|_\infty^s \lambda (1 + M_J) C_{\text{reg}} C_F) \|u - R_\ell u\|.$$

The comparison results of Carstensen et al. [2012b] and Gudi [2010] for the right-hand side $f := \lambda u$ prove the existence of a constant C_{comp} , which only depends on the shape regularity of \mathcal{T}_ℓ , such that

$$\|u - R_\ell u\| \leq C_{\text{comp}} (\|(1 - \Pi_\ell^0) Du\| + \|h_\ell (1 - \Pi_\ell^0) \lambda u\|).$$

(Note that the analysis of [Carstensen et al., 2012b, Gudi, 2010] is carried out for $d = 2$. The generalisation to $d \geq 3$, however, can be proven using Proposition 5.8 on page 54 below.) The remaining part of the proof bounds the oscillation term $\|h_\ell (1 - \Pi_\ell^0) \lambda u\|$. Let $T \in \mathcal{T}_\ell$ and let $\mathbf{b}_T \in H_0^1(\text{int}(T)) \cap \mathcal{P}_{d+1}(T)$ denote the bubble function on T with $\|\mathbf{b}_T\|_{L^\infty(T)} = 1$. Define $\psi_T := \mathbf{b}_T \Pi_\ell^1(\lambda u)$. The arguments of Verfürth [1996] yield

$$\|h_T (1 - \Pi_\ell^0) \lambda u\|_{L^2(T)}^2 \leq \|h_T \lambda u\|_{L^2(T)}^2 \lesssim h_T^2 b(\lambda u, \psi_T) + \|h_T (1 - \Pi_\ell^1)(\lambda u)\|_{L^2(T)}^2. \quad (4.5)$$

Since $\Pi_\ell^0 D\psi = 0$ by the divergence theorem, the eigenvalue problem implies

$$b(\lambda u, \psi_T) = (Du, D\psi_T)_{L^2(\Omega)} = ((1 - \Pi_\ell^0) Du, D\psi_T)_{L^2(\Omega)}.$$

This and an inverse estimate [Brenner and Scott, 2008] $\|D\psi_T\|_{L^2(T)} \lesssim h_T^{-1} \|\psi_T\|_{L^2(T)}$ and $\|\mathbf{b}_T\|_{L^\infty(T)} = 1$ prove

$$b(\lambda u, \psi_T) \lesssim \|(1 - \Pi_\ell^0) Du\|_{L^2(T)} \|h_T^{-1} \Pi_\ell^1(\lambda u)\|_{L^2(T)}.$$

The second term of (4.5) can be bounded as

$$\|h_T (1 - \Pi_\ell^1)(\lambda u)\|_{L^2(T)} \leq \|h_T (1 - \mathcal{I}_\ell^{\text{en}})(\lambda u)\|_{L^2(T)} \leq \kappa h_T^2 \lambda \|(1 - \Pi_\ell^0) Du\|_{L^2(T)}$$

for the nonconforming \mathcal{P}_1 interpolation operator $\mathcal{I}_\ell^{\text{en}}$ from Section 5.1 and the constant κ from the error estimate (5.2). \blacksquare

4.2. Adaptive Algorithm

This section introduces the adaptive algorithm AFEM and states the optimality result based on the concept of approximation classes.

For any simplex $T \in \mathcal{T}_\ell$, the explicit residual-based error estimator based on [Durán et al., 2003] consists of the sum of the residuals of the computed discrete eigenfunctions $(u_{\ell,j})_{j \in J}$,

$$\eta_\ell^2(T) := \sum_{j \in J} \left(h_T^2 \|\lambda_{\ell,j} u_{\ell,j}\|_{L^2(T)}^2 + \sum_{F \in \mathcal{F}(T) \cap \mathcal{F}_\ell(\Omega)} h_T \| [Du_{\ell,j}]_F \mathbf{v}_F \|_{L^2(F)}^2 \right).$$

4. Conforming \mathcal{P}_1 FEM for the Eigenvalues of the Laplacian

(H1)	$M_J := \sup_{\mathcal{T}_\ell \in \mathbb{T}} \max_{j \in \{1, \dots, \dim(V_\ell)\} \setminus J} \max_{k \in J} \frac{\lambda_k}{ \lambda_{\ell,j} - \lambda_k } < \infty$	p. 22
(H2)	$\varepsilon := \max_{j \in J} \ u_j - \Lambda_\ell u_j\ \leq \sqrt{1 + (2N)^{-1}} - 1$	p. 25
(H3)	$\ h_0\ _\infty^2 B^2 C_{\text{drel}}^2 (1 + M_J)^2 \leq 1$	p. 39
(H4)	$4(1 + M_J)^2 (BC_{\text{qo}} \ h_0\ _\infty^{2s} + 2B^2 C_{\text{reg}}^2 \ h_0\ _\infty^{2+2s}) < \min \left\{ 1, \frac{1-\rho_1}{KC_{\text{drel}}^2} \right\}$	p. 39

Table 4.1.: Overview of assumptions on the initial mesh-size for the conforming \mathcal{P}_1 finite element method and their first occurrence in this thesis. B acts as upper bound for all $(\lambda_j \mid j \in J)$.

Let, for any subset $\mathcal{K} \subseteq \mathcal{T}$,

$$\eta_\ell^2(\mathcal{K}) := \sum_{T \in \mathcal{K}} \eta_\ell^2(T).$$

The adaptive algorithm is driven by this computable error estimator and runs the following loop (cf. Algorithm 3.15).

Algorithm 4.4 (conforming AFEM for the Laplace eigenvalue problem).

Input: Initial triangulation \mathcal{T}_0 , bulk parameter $0 < \theta \leq 1$.

for $\ell = 0, 1, 2, \dots$ **do**

Solve. Compute discrete eigenpairs $(\lambda_{\ell,j}, u_{\ell,j})_{j \in J}$ of (4.2) with respect to \mathcal{T}_ℓ .

Estimate. Compute local contributions of the error estimator $(\eta_\ell^2(T))_{T \in \mathcal{T}_\ell}$.

Mark. Choose a minimal subset $\mathcal{M}_\ell \subseteq \mathcal{T}_\ell$ such that $\theta \eta_\ell^2(\mathcal{T}_\ell) \leq \eta_\ell^2(\mathcal{M}_\ell)$.

Refine. Generate $\mathcal{T}_{\ell+1} := \text{refine}(\mathcal{T}_\ell, \mathcal{M}_\ell)$ with Algorithm 2.15.

end for

Output: Sequences of triangulations $(\mathcal{T}_\ell)_\ell$ and discrete solutions $((\lambda_{\ell,j}, u_{\ell,j})_{j \in J})_\ell$. \blacklozenge

Remark 4.5 (inexact solve). A practical algorithm similar to Algorithm 3.17 which includes the inexact solution of the algebraic eigenvalue problem will be investigated empirically in Section 9.5. The optimality analysis of this thesis carries over to the inexact solve provided the parameter \varkappa from Algorithm 3.17 is sufficiently small. \blacklozenge

The optimality result is stated in terms of nonlinear approximation classes. Define, for any $\sigma > 0$, the seminorm

$$|u|_{\mathfrak{A}_\sigma} := \sup_{m \in \mathbb{N}} m^\sigma \inf_{\mathcal{T} \in \mathbb{T}(m)} \|(1 - \Pi_{\mathcal{T}}^0)Du\|$$

and the approximation class

$$\mathfrak{A}_\sigma := \{v \in V \mid |v|_{\mathfrak{A}_\sigma} < \infty\}.$$

The set \mathfrak{A}_σ is a true approximation class which does not depend on the finite element method and instead concerns the approximability of the derivative by piecewise constant functions. The following alternative set, also referred to as approximation class, will turn out to be more suitable for the analysis

$$\mathfrak{A}'_\sigma := \{u \in V \mid |u|_{\mathfrak{A}'_\sigma} < \infty\}$$

for

$$|u|_{\mathfrak{A}'_\sigma} := \sup_{m \in \mathbb{N}} m^\sigma \inf_{\mathcal{T} \in \mathbb{T}(m)} \|u - \Lambda_{\mathcal{T}} u\|.$$

Proposition 4.3 implies the equivalence of those two approximation classes in the sense that any eigenfunction $u \in W$ satisfies

$$u \in \mathfrak{A}_\sigma \text{ if and only if } u \in \mathfrak{A}'_\sigma \quad (\text{with equivalent seminorms}).$$

The following theorem states the optimality of the adaptive algorithm. It generalises [Carstensen and Gedicke, 2012, Thm. 5.4] and [Dai et al., 2008, Thm 6.7] for simple eigenvalues and [Dai et al., 2013, Thm. 5.1] for multiple eigenvalues to the case of eigenvalue clusters. The proof follows in Section 4.5.

Theorem 4.6 (optimal convergence rates). *Provided the bulk parameter $\theta \ll 1$ is sufficiently small and the initial mesh size $\|h_0\|_\infty$ satisfies the conditions (H1)–(H4) of Table 4.1, Algorithm 4.4 computes triangulations $(\mathcal{T}_\ell)_\ell$ and discrete eigenpairs $((\lambda_{\ell,j}, u_{\ell,j})_{j \in J})_\ell$ with optimal rate of convergence in the sense that, for some constant C_{opt} , it holds that*

$$\sup_{\ell \in \mathbb{N}_0} (\text{card}(\mathcal{T}_\ell) - \text{card}(\mathcal{T}_0))^{2\sigma} \sum_{j \in J} \|u_j - \Lambda_\ell u_j\|^2 \leq C_{\text{opt}}^2 \sum_{j \in J} |u_j|_{\mathfrak{A}'_\sigma}^2.$$

The constant C_{opt} does not depend on the eigenvalue cluster, but is a generic constant that only depends on the domain Ω and the shape-regularity of \mathcal{T}_ℓ .

The following corollary improves the results of [Dai et al., 2008, Carstensen and Gedicke, 2012, Dai et al., 2013] in that the approximation class \mathfrak{A}_σ does not depend on the used scheme but only measures the approximability of the derivatives.

Corollary 4.7. *Under the conditions of Theorem 4.6, the adaptive algorithm computes triangulations $(\mathcal{T}_\ell)_\ell$ and discrete eigenpairs $((\lambda_{\ell,j}, u_{\ell,j})_{j \in J})_\ell$ with optimal rate of convergence in the sense that, for all $k \in J$, it holds that*

$$\begin{aligned} & A^{1/2} (1 + M_J^2 B^2 C)^{-1/2} \left(\frac{|\lambda_k - \lambda_{\ell,k}|}{\lambda_{\ell,k}} \right)^{1/2} + \sup_{j \in J} \sup_{\substack{w \in E(\lambda_j) \\ \|w\|=1}} \inf_{v_\ell \in W_\ell} \|w - v_\ell\| \\ & \leq 2C_{\text{ba}} (1 + (1 + M_J) B \|h_0\|_\infty^s) (1 + B \|h_0\|_\infty^2) C_{\text{opt}} (\text{card}(\mathcal{T}_\ell) - \text{card}(\mathcal{T}_0))^{-\sigma} \left(\sum_{j \in J} |u_j|_{\mathfrak{A}'_\sigma}^2 \right)^{1/2}. \end{aligned}$$

Proof. The proof follows from Proposition 4.2 and 4.3 and the observation that

$$\sup_{j \in J} \sup_{\substack{w \in E(\lambda_j) \\ \|w\|=1}} \inf_{v_\ell \in W_\ell} \|w - v_\ell\|^2 \leq \lambda_{n+1}^{-1} \sup_{j \in J} \sup_{\substack{w \in E(\lambda_j) \\ \|w\|=1}} \inf_{v_\ell \in W_\ell} \|w - v_\ell\|^2$$

where λ_{n+1}^{-1} acts as a Friedrichs-type constant, cf. Remark 3.20. ■

Remark 4.8 (optimality for inexact solve). The optimality results of Theorem 4.6 and Corollary 4.7 carry over to Algorithm 3.17 for sufficiently small $\varkappa \ll 1$ by means of a perturbation analysis as in [Carstensen and Gedicke, 2012] or [Carstensen, Gallistl, and Schedensack, 2014c]. ◆

4.3. Theoretical Error Estimator

In order to compare two finite element solutions on different meshes, the analysis relies on a theoretical, non-computable error estimator that does not depend on the choice of the discrete eigenfunctions. Given an eigenpair (λ, u) , the error estimator includes the elementwise residuals in terms of $P_\ell u$ and $\Lambda_\ell u$. More precisely, define, for any $T \in \mathcal{T}_\ell$,

$$\mu_\ell^2(T, \lambda, u) := h_T^2 \|\lambda P_\ell u\|_{L^2(T)}^2 + \sum_{F \in \mathcal{F}(T) \cap \mathcal{F}_\ell(\Omega)} h_T \| [D\Lambda_\ell u]_F \mathbf{v}_F \|_{L^2(F)}^2.$$

For any subset $\mathcal{K} \subseteq \mathcal{T}_\ell$, set

$$\mu_\ell^2(\mathcal{K}, \lambda_j, u_j) := \sum_{T \in \mathcal{K}} \mu_\ell^2(T, \lambda_j, u_j) \quad \text{and} \quad \mu_\ell^2(\mathcal{K}) := \sum_{j \in J} \mu_\ell^2(\mathcal{K}, \lambda_j, u_j).$$

The theoretical error estimator satisfies the following discrete reliability.

Proposition 4.9 (discrete reliability). *Under the assumption (H1) of page 22 there exists C_{drel} solely dependent on \mathcal{T}_0 such that any discrete eigenpair $(\lambda, u) \in \mathbb{R} \times W$ with $\|u\| = 1$ satisfies*

$$2C_{\text{drel}}^{-2} \|\Lambda_{\ell+m} u - \Lambda_\ell u\|^2 \leq \mu_\ell^2(\mathcal{T}_\ell \setminus \mathcal{T}_{\ell+m}, \lambda, u) + \|h_0\|_\infty^2 \lambda^2 (1 + M_J)^2 \|u - \Lambda_\ell u\|^2.$$

Proof. Let $\varphi_{\ell+m} := \Lambda_{\ell+m} u - \Lambda_\ell u \in V_{\ell+m}$. It is well-established [Scott and Zhang, 1990] that there exists a quasi-interpolant $\varphi_\ell \in V_\ell$ with quasi-local approximation and stability properties

$$h_T^{-1} \|\varphi_{\ell+m} - \varphi_\ell\|_{L^2(T)} + \|D\varphi_\ell\|_{L^2(T)} \leq C_{\text{stab}} \|D\varphi_{\ell+m}\|_{L^2(\omega_T)}$$

for any $T \in \mathcal{T}_\ell$ and its patch ω_T from Definition 2.25. The function φ_ℓ can be chosen in such a way that $\varphi_\ell = \varphi_{\ell+m}$ holds along all $(d-1)$ -dimensional hyper-faces in the set $\mathcal{F}_\ell \cap \mathcal{F}_{\ell+m}$. Elementary algebraic manipulations lead to

$$a((\Lambda_{\ell+m} - \Lambda_\ell)u, \varphi_{\ell+m}) = a(\Lambda_{\ell+m} u, \varphi_{\ell+m}) - a(\Lambda_\ell u, \varphi_\ell) + a(\Lambda_\ell u, \varphi_\ell - \varphi_{\ell+m}).$$

The arguments of [Stevenson, 2007, Theorem 4.1] and the aforementioned properties of φ_ℓ lead to some mesh-size independent constant C_1 such that

$$a(\Lambda_\ell u, \varphi_\ell - \varphi_{\ell+m}) \leq C_1 \left(\sum_{T \in \mathcal{T}_\ell \setminus \mathcal{T}_{\ell+m}} \sum_{F \in \mathcal{F}(T) \cap \mathcal{F}_\ell(\Omega)} h_T \| [D\Lambda_\ell u]_F \mathbf{v}_F \|_{L^2(F)}^2 \right) \|\varphi_{\ell+m}\|.$$

Lemma 3.4 and the approximation and stability properties of the quasi-interpolation imply for the constant C_F of the Friedrichs inequality [Braess, 2007] that

$$\begin{aligned} & a(\Lambda_{\ell+m} u, \varphi_{\ell+m}) - a(\Lambda_\ell u, \varphi_\ell) \\ &= \lambda (b(P_{\ell+m} u, \varphi_{\ell+m}) - b(P_\ell u, \varphi_\ell)) \\ &= \lambda (b(P_{\ell+m} u - P_\ell u, \varphi_{\ell+m}) + b(P_\ell u, \varphi_{\ell+m} - \varphi_\ell)) \\ &\leq \max\{C_F, C_{\text{stab}}\} \left(\lambda \|P_{\ell+m} u - P_\ell u\| + \|h_\ell \lambda P_\ell u\|_{L^2(\cup \mathcal{T}_\ell \setminus \mathcal{T}_{\ell+m})} \right) \|\varphi_{\ell+m}\|. \end{aligned}$$

The triangle inequality reveals

$$\|P_{\ell+m} u - P_\ell u\| \leq \|u - P_{\ell+m} u\| + \|u - P_\ell u\|. \quad (4.6)$$

Proposition 4.1 proves that

$$\|u - P_{\ell+m}u\| \leq (1 + M_J)C_{\text{reg}}\|h_0\|_\infty^s \|u - R_{\ell+m}u\|.$$

An analogous argument for the second term of (4.6) with $\ell + m$ replaced by m and the relation $V_\ell \subseteq V_{\ell+m}$ conclude the proof. \blacksquare

The discrete reliability implies the following corollary.

Corollary 4.10 (reliability and efficiency). *Assume (H1) from page 22. Provided the initial mesh is sufficiently fine in the sense that*

$$\|h_0\|_\infty^{2s} \lambda^2 C_{\text{drel}}^2 (1 + M_J)^2 \leq 1, \quad (\text{H3})$$

any discrete eigenpair $(\lambda, u) \in \mathbb{R} \times W$ with $\|u\| = 1$ satisfies

$$\|u - \Lambda_\ell u\|^2 \leq C_{\text{drel}}^2 \mu_\ell^2(\mathcal{T}_\ell, \lambda, u). \quad (\text{4.7})$$

Provided the initial mesh-size satisfies

$$4(1 + M_J)^2 (\lambda C_{\text{qo}} \|h_0\|_\infty^{2s} + 2\lambda^2 C_{\text{reg}}^2 \|h_0\|_\infty^{2+2s}) < \min \left\{ 1, \frac{1 - \rho_1}{KC_{\text{drel}}^2} \right\} \quad (\text{H4})$$

for the constant C_{qo} from Proposition 4.14 on page 41 below, the efficiency reads

$$\mu_\ell(\mathcal{T}_\ell, \lambda, u) \leq C_{\text{eff}} \|u - \Lambda_\ell u\|. \quad (\text{4.8})$$

Remark 4.11. Assumption (H4) is stronger than required for the proof of efficiency. This mesh-size restriction will be needed later in the analysis of the contraction property. \blacklozenge

Proof of Corollary 4.10. Proposition 4.3 shows that $\Lambda_{\ell+m}u \rightarrow u$ with respect to $\|\cdot\|$ on a sequence of regular triangulations such that $\|h_{\ell+m}\|_{L^\infty(\Omega)} \rightarrow 0$ for $m \rightarrow \infty$. Hence, Proposition 4.9 proves the reliability estimate

$$2C_{\text{drel}}^{-2} \|u - \Lambda_\ell u\|^2 \leq \mu_\ell^2(\mathcal{T}_\ell, \lambda, u) + \|h_0\|_\infty^{2s} \lambda^2 (1 + M_J)^2 \|u - \Lambda_\ell u\|^2.$$

Hence, assumption (H3) implies the reliability (4.7). The efficiency

$$2\mu_\ell(\mathcal{T}_\ell, \lambda, u) \leq C_{\text{eff}} (1 + \lambda \|h_0\|_\infty^{1+s} (1 + M_J) C_{\text{reg}}) \|u - \Lambda_\ell u\|$$

follows from the standard arguments of Verfürth [1996] (cf. the proof of Proposition 4.3) combined with the L^2 error control of Proposition 4.1. The assumption (H4) implies the claimed efficiency estimate (with the precise constants). \blacksquare

Remark 4.12 (comparison with Dai et al. [2013]). Some explanations shall clarify the difference of the reliability proof in Dai et al. [2013] and the mathematical arguments in this thesis. We focus on the conforming \mathcal{P}_1 FEM of the Laplace eigenvalue problem. In [Dai et al., 2013], the authors consider one multiple eigenvalue $\lambda := \lambda_{n+1} = \lambda_{n+2} = \dots = \lambda_{n+N}$ with discrete approximations $\lambda_{\ell, n+1} \leq \lambda_{\ell, n+2} \leq \dots \leq \lambda_{\ell, n+N}$. For a suitable closed curve $\Gamma \subseteq \mathbb{C}$ around $(\lambda_{\ell, j} \mid j \in J)$ in the complex plane and the solution operator to the discrete linear problem $K_\ell := R_\ell \circ \Delta^{-1}$, the discrete spectral projection [Chatelin, 1983] reads as

$$E_\ell := \frac{1}{2\pi i} \int_\Gamma (z - K_\ell)^{-1} dz.$$

4. Conforming \mathcal{P}_1 FEM for the Eigenvalues of the Laplacian

The projection E_ℓ maps V to the linear hull W_ℓ of discrete eigenfunctions. For any eigenpair $(\lambda, u) \in \mathbb{R} \times W$, the authors define $\lambda^{(\ell)} := \|E_\ell u\|^2 / \|E_\ell u\|^2$ via the Rayleigh quotient and the error estimator

$$\tilde{\eta}_\ell(E_\ell u) := \sqrt{\|h_\ell \lambda^{(\ell)} E_\ell u\|_{L^2(\Omega)}^2 + \sum_{F \in \mathcal{F}_\ell(\Omega)} h_F \| [DE_\ell u]_F \nu_F \|_{L^2(F)}^2}.$$

For real coefficients $(\alpha_{\ell,j} \mid j \in J)$ of $E_\ell u = \sum_{j \in J} \alpha_{\ell,j} u_{\ell,j}$, the authors define

$$w^{(\ell)} := - \sum_{j \in J} \alpha_{\ell,j} \lambda_{\ell,j} \Delta^{-1} u_{\ell,j}$$

and prove the identity $E_\ell u = R_\ell w^{(\ell)}$. For sufficiently small initial mesh-size (dependent on λ), Theorem 3.1 of [Dai et al., 2013] states

$$\|u - E_h u\| \lesssim \|w^{(\ell)} - R_\ell w^{(\ell)}\|.$$

Let \tilde{C}_1 denote the reliability constant of the explicit residual-based a posteriori error estimator for the discretisation of the linear Laplace boundary value problem [see, e.g., Verfürth, 1996]. Inequality (3.17) of [Dai et al., 2013] claims the reliability in the form

$$\|w^{(\ell)} - R_\ell w^{(\ell)}\| \leq \tilde{C}_1 \tilde{\eta}_\ell(E_\ell u). \quad (4.9)$$

This inequality (4.9), however, is unclear because it assumes $-\Delta w^{(\ell)} = \lambda^{(\ell)} E_\ell u$. But, obviously, $-\Delta w^{(\ell)} = \sum_{j \in J} \alpha_{\ell,j} \lambda_{\ell,j} u_{\ell,j}$. \blacklozenge

Remark 4.13. A possible alternative a posteriori error analysis of the left-hand side in (4.9) with the standard techniques of Verfürth [1996] replaces the volume term of $\tilde{\eta}_\ell(E_\ell u)$ by $\|h_\ell \sum_{j \in J} \alpha_{\ell,j} \lambda_{\ell,j} u_{\ell,j}\|_{L^2(\Omega)}^2$. The triangle inequality leads to

$$\|h_\ell \sum_{j \in J} \alpha_{\ell,j} \lambda_{\ell,j} u_{\ell,j}\|_{L^2(\Omega)} \leq \|h_\ell \lambda^{(\ell)} E_\ell u\|_{L^2(\Omega)} + \|h_\ell \sum_{j \in J} \alpha_{\ell,j} (\lambda_{\ell,j} - \lambda^{(\ell)}) u_{\ell,j}\|_{L^2(\Omega)}.$$

The second term on the right-hand side can be estimated (recall that $N = \text{card}(J)$) via

$$\|h_\ell \sum_{j \in J} \alpha_{\ell,j} (\lambda_{\ell,j} - \lambda^{(\ell)}) u_{\ell,j}\|_{L^2(\Omega)} \leq N \|E_\ell u\| \|h_\ell\|_{L^\infty(\Omega)} \sup_{j \in J} |\lambda_{\ell,j} - \lambda^{(\ell)}|.$$

In the case of one multiple eigenvalue, this term may be expected to be of higher order and the analysis of [Dai et al., 2013] is applicable with this modification. For an eigenvalue cluster, however, this yields a non-efficient additive term in the error estimator. That term has the same order of magnitude as the cluster-width $(B - A)$. Therefore, the author of this thesis questions the conclusion in [Dai et al., 2013, Sect. 7.1] that the extension to the case of clustered eigenvalues is a “simple deduction”. In the analysis of this thesis, the cluster-width $(B - A)$ does *not* enter the estimates of Proposition 4.9 and Corollary 4.10 as an additive constant. Lemma 3.4 is the technical tool that allows the ‘cluster-robust’ (discrete) reliability. \blacklozenge

4.4. Contraction Property

This section presents the contraction property for a linear combination of error and error estimator under the conditions (H1)–(H4) of Table 4.1.

The following quasi-orthogonality replaces the Galerkin orthogonality. The concept of ‘quasi-orthogonality’ was first introduced by Carstensen and Hoppe [2006] in the context of nonconforming finite element methods.

Proposition 4.14 (quasi-orthogonality). *Let $(\lambda, u) \in \mathbb{R} \times W$ with $\|u\| = 1$ be an eigenpair of (4.1). Under hypothesis (H1) there exists a constant C_{qo} such that any admissible refinement $\mathcal{T}_{\ell+m} \in \mathbb{T}(\mathcal{T}_\ell)$ of $\mathcal{T}_\ell \in \mathbb{T}$ satisfies*

$$|2a(u - \Lambda_{\ell+m}u, \Lambda_{\ell+m}u - \Lambda_\ell u)| \leq \lambda C_{qo}(1 + M_J)^2 \|h_0\|_\infty^{2s} \|u - \Lambda_\ell u\|^2.$$

Proof. The eigenvalue problem (4.1) and Lemma 3.4 followed by the Cauchy and Young inequalities show

$$\begin{aligned} a(u - \Lambda_{\ell+m}u, \Lambda_{\ell+m}u - \Lambda_\ell u) &= \lambda b(u - P_{\ell+m}u, \Lambda_{\ell+m}u - \Lambda_\ell u) \\ &\leq \lambda (\|u - P_{\ell+m}u\|^2 + \|\Lambda_{\ell+m}u - \Lambda_\ell u\|^2)/2. \end{aligned}$$

The triangle inequality, Proposition 4.1 and $V_{\ell+m} \subseteq V_\ell$ prove the result. \blacksquare

The error estimator reduction [Cascon et al., 2008] is a standard tool in the convergence analysis of adaptive algorithms.

Proposition 4.15 (error estimator reduction for μ_ℓ). *Provided the initial mesh-size $\|h_0\|_\infty$ satisfies (H1)–(H2), there exist constants $0 < \rho_1 < 1$ and $0 < K < \infty$ such that $\mathcal{T}_\ell \in \mathbb{T}$ and its one-level refinement $\mathcal{T}_{\ell+1}$ generated by Algorithm 4.4 and any eigenfunction $u \in W$ with $\|u\| = 1$ and eigenvalue λ satisfy*

$$\mu_{\ell+1}^2(\mathcal{T}_{\ell+1}, \lambda, u) \leq \rho_1 \mu_\ell^2(\mathcal{T}_\ell, \lambda, u) + K (\|\Lambda_{\ell+1}u - \Lambda_\ell u\|^2 + \|h_{\ell+1} \lambda (P_{\ell+1}u - P_\ell u)\|^2).$$

Proof. The design of the error estimator $\mu_\ell^2(\mathcal{T}_\ell, \lambda, u)$ and the bulk criterion from Proposition 3.16 allow the use of the standard arguments of [Cascon et al., 2008, Stevenson, 2007] to prove the result. \blacksquare

The foregoing two results allow the proof of the contraction property. It states the contraction of a linear combination of error and error estimator. For simple or multiple eigenvalues, the contraction property was established in [Dai et al., 2008, Carstensen and Gedicke, 2012, Dai et al., 2013]. The proof in this thesis applies to the case of clustered eigenvalues.

Proposition 4.16 (contraction property). *Under the conditions (H1)–(H4) of Table 4.1 there exist $0 < \rho_2 < 1$ and $0 < \beta < \infty$ such that, for any eigenpair $(\lambda, u) \in \mathbb{R} \times W$ with $\|u\| = 1$, the term $\xi_\ell^2 := \mu_\ell^2(\mathcal{T}_\ell, \lambda, u) + \beta \|u - \Lambda_\ell u\|^2$ satisfies*

$$\xi_{\ell+1}^2 \leq \rho_2 \xi_\ell^2 \quad \text{for all } \ell \in \mathbb{N}_0.$$

4. Conforming \mathcal{P}_1 FEM for the Eigenvalues of the Laplacian

Proof. Throughout the proof, the following shorthand notation is employed

$$\begin{aligned} e_\ell &:= u - \Lambda_\ell u, & e_{\ell+1} &:= u - \Lambda_{\ell+1} u, \\ \mu_\ell^2 &:= \mu_\ell^2(\mathcal{T}_\ell, \lambda, u), & \mu_{\ell+1}^2 &:= \mu_{\ell+1}^2(\mathcal{T}_{\ell+1}, \lambda, u). \end{aligned}$$

The error estimator reduction from Proposition 4.15 and elementary algebraic manipulations lead to

$$\begin{aligned} &\mu_{\ell+1}^2 + K \|e_{\ell+1}\|^2 \\ &\leq \rho_1 \mu_\ell^2 + K \left(\|e_\ell\|^2 + 2a(e_{\ell+1}, (\Lambda_\ell - \Lambda_{\ell+1})u) + \|h_0\|_\infty^2 \|\lambda(P_{\ell+1} - P_\ell)u\|^2 \right). \end{aligned} \quad (4.10)$$

The quasi-orthogonality of Proposition 4.14 reads as

$$|2a(e_{\ell+1}, (\Lambda_{\ell+1} - \Lambda_\ell)u)| \leq \lambda C_{\text{qo}} (1 + M_J)^2 \|h_0\|_\infty^{2s} \|e_\ell\|^2.$$

The triangle inequality and Proposition 4.1 lead to

$$\|h_0\|_\infty^2 \|\lambda(P_{\ell+1} - P_\ell)u\|^2 \leq 2(1 + M_J)^2 \lambda^2 C_{\text{reg}}^2 \|h_0\|_\infty^{2+2s} (\|e_{\ell+1}\|^2 + \|e_\ell\|^2).$$

The combination of the preceding two displayed formulas with (4.10) leads to

$$\begin{aligned} &\mu_{\ell+1}^2 + K \left(1 - (1 + M_J)^2 2\lambda^2 C_{\text{reg}}^2 \|h_0\|_\infty^{2+2s} \right) \|e_{\ell+1}\|^2 \\ &\leq \rho_1 \mu_\ell^2 + K \left(1 + (1 + M_J)^2 (\lambda C_{\text{qo}} \|h_0\|_\infty^{2s} + 2\lambda^2 C_{\text{reg}}^2 \|h_0\|_\infty^{2+2s}) \right) \|e_\ell\|^2. \end{aligned} \quad (4.11)$$

For any $0 < \delta < 1$, the reliability (4.7) bounds the right-hand side of (4.11) by

$$\begin{aligned} &\left(\rho_1 + \delta C_{\text{drel}}^2 K (1 + (1 + M_J)^2 (\lambda C_{\text{qo}} \|h_0\|_\infty^{2s} + 2\lambda^2 C_{\text{reg}}^2 \|h_0\|_\infty^{2+2s})) \right) \mu_\ell^2 \\ &\quad + K (1 + (1 + M_J)^2 (\lambda C_{\text{qo}} \|h_0\|_\infty^{2s} + 2\lambda^2 C_{\text{reg}}^2 \|h_0\|_\infty^{2+2s})) (1 - \delta) \|e_\ell\|^2 \\ &\leq \rho_2 (\mu_\ell^2(\lambda, u, \mathcal{T}_\ell) + \beta \|u - \Lambda_\ell u\|^2) \end{aligned}$$

for

$$\begin{aligned} \beta &:= K(1 - (1 + M_J)^2 2\lambda^2 C_{\text{reg}}^2 \|h_0\|_\infty^{2+2s}) \quad \text{and} \\ \rho_2 &:= \max \left\{ \rho_1 + \delta C_{\text{drel}}^2 K (1 + (1 + M_J)^2 (\lambda C_{\text{qo}} \|h_0\|_\infty^{2s} + 2\lambda^2 C_{\text{reg}}^2 \|h_0\|_\infty^{2+2s})), \right. \\ &\quad \left. \frac{1 + (1 + M_J)^2 (\lambda C_{\text{qo}} \|h_0\|_\infty^{2s} + 2\lambda^2 C_{\text{reg}}^2 \|h_0\|_\infty^{2+2s})}{1 - (1 + M_J)^2 2\lambda^2 C_{\text{reg}}^2 \|h_0\|_\infty^{2+2s}} (1 - \delta) \right\}. \end{aligned}$$

Assumption (H4) from page 39 and the choice of

$$\delta := 2(1 + M_J)^2 (\lambda C_{\text{qo}} \|h_0\|_\infty^{2s} + 2\lambda^2 C_{\text{reg}}^2 \|h_0\|_\infty^{2+2s}) < 1/2$$

lead to $\rho_2 < 1$ and $0 < \beta < K$. ■

4.5. Optimal Convergence Rates

This section is devoted to the proof of Theorem 4.6. While the results of the preceding sections were stated for each eigenfunction $u_j \in W$ separately, the optimality proof of this section is concerned with the simultaneous error of all eigenfunction approximations. Consider

$$\Xi_\ell^2 := \mu_\ell^2(\mathcal{T}_\ell) + \beta \sum_{j \in J} \|u_j - \Lambda_\ell u_j\|^2 \quad \text{for all } \ell \in \mathbb{N}_0$$

for the parameter β from Proposition 4.16. The contraction property of Proposition 4.16 implies that also the sum Ξ_ℓ^2 contracts with the factor $0 < \rho_2 < 1$. The proof may therefore exclude the pathological case $\Xi_0 = 0$. Choose $0 < \tau \leq \sum_{j \in J} |u_j|_{\mathfrak{H}_\sigma}^2 / \Xi_0^2$, and set $\varepsilon(\ell) := \sqrt{\tau} \Xi_\ell$. Let $N(\ell) \in \mathbb{N}$ be minimal with the property

$$\sum_{j \in J} |u_j|_{\mathfrak{H}_\sigma}^2 \leq \varepsilon(\ell)^2 N(\ell)^{2\sigma}.$$

If $N(\ell) \geq 2$, the minimality of $N(\ell)$ and $N(\ell) \leq 2(N(\ell) - 1)$ imply

$$N(\ell) \leq 2 \left(\sum_{j \in J} |u_j|_{\mathfrak{H}_\sigma}^2 \right)^{1/(2\sigma)} \varepsilon(\ell)^{-1/\sigma} \quad \text{for all } \ell \in \mathbb{N}_0. \quad (4.12)$$

The definition of $\varepsilon(\ell)$ and the contraction property from Proposition 4.16 (applied to Ξ_ℓ with contraction $0 < \rho_2 < 1$) show that (4.12) is also true for $N(\ell) = 1$.

Let $\tilde{\mathcal{T}}_\ell \in \mathbb{T}$ denote the optimal triangulation of cardinality

$$\text{card}(\tilde{\mathcal{T}}_\ell) \leq \text{card}(\mathcal{T}_0) + N(\ell)$$

in the sense that the projection $\tilde{\Lambda} := \Lambda_{\tilde{\mathcal{T}}_\ell}$ from (4.3) with respect to $\tilde{\mathcal{T}}_\ell$ satisfies

$$\sum_{j \in J} \|u_j - \tilde{\Lambda} u_j\|^2 \leq N(\ell)^{-2\sigma} \sum_{j \in J} |u_j|_{\mathfrak{H}_\sigma}^2 \leq \varepsilon(\ell)^2. \quad (4.13)$$

The overlay $\hat{\mathcal{T}}_\ell$ is the smallest common refinement of \mathcal{T}_ℓ and $\tilde{\mathcal{T}}_\ell$ (see Definition 2.11). Lemma 2.12 implies

$$\text{card}(\hat{\mathcal{T}}_\ell) - \text{card}(\mathcal{T}_\ell) \leq \text{card}(\tilde{\mathcal{T}}_\ell) - \text{card}(\mathcal{T}_0) \leq N(\ell). \quad (4.14)$$

Since $\hat{\mathcal{T}}_\ell$ is a refinement of \mathcal{T}_ℓ , it holds that $\text{card}(\mathcal{T}_\ell \setminus \hat{\mathcal{T}}_\ell) \leq \text{card}(\hat{\mathcal{T}}_\ell) - \text{card}(\mathcal{T}_\ell)$. This and (4.12)–(4.14) lead to

$$\text{card}(\mathcal{T}_\ell \setminus \hat{\mathcal{T}}_\ell) \leq N(\ell) \leq 2 \left(\sum_{j \in J} |u_j|_{\mathfrak{H}_\sigma}^2 \right)^{1/(2\sigma)} \varepsilon(\ell)^{-1/\sigma}. \quad (4.15)$$

Let $\hat{\Lambda} := \Lambda_{\hat{\mathcal{T}}_\ell}$ denote the projection from (4.3) with respect to $\hat{\mathcal{T}}_\ell$.

Lemma 4.17. *The assumptions (H1)–(H4) of Table 4.1 imply*

$$\sum_{j \in J} \|u_j - \hat{\Lambda} u_j\|^2 \leq 2\varepsilon(\ell)^2. \quad (4.16)$$

4. Conforming \mathcal{P}_1 FEM for the Eigenvalues of the Laplacian

Proof. Elementary manipulations and the quasi-orthogonality of Proposition 4.14 reveal, for any $j \in J$, that

$$\begin{aligned} \|u_j - \widehat{\Lambda}u_j\|^2 &= \|u_j - \widetilde{\Lambda}u_j\|^2 - \|\widetilde{\Lambda}u_j - \widehat{\Lambda}u_j\|^2 - 2a(u_j - \widehat{\Lambda}u_j, \widehat{\Lambda}u_j - \widetilde{\Lambda}u_j) \\ &\leq (1 + \lambda_j C_{\text{qo}}(1 + M_J)^2 \|h_0\|_\infty^{2s}) \|u_j - \widetilde{\Lambda}u_j\|^2 - \|\widetilde{\Lambda}u_j - \widehat{\Lambda}u_j\|^2. \end{aligned}$$

This, the assumption (H4) and (4.13) lead to

$$\sum_{j \in J} \|u_j - \widehat{\Lambda}u_j\|^2 \leq 2 \sum_{j \in J} \|u_j - \widetilde{\Lambda}u_j\|^2 \leq 2\varepsilon(\ell)^2. \quad \blacksquare$$

Remark 4.18. Alternatively, one can prove Lemma 4.17 by employing the best-approximation result of Proposition 4.3, which leads to a shorter proof but more restrictions on the initial mesh size $\|h_0\|_\infty$. \blacklozenge

Lemma 4.19 (key argument). *There exists $C_2 \approx 1$ with*

$$\mu_\ell^2(\mathcal{T}_\ell) \leq C_2 \mu_\ell^2(\mathcal{T}_\ell \setminus \widehat{\mathcal{T}}_\ell).$$

Proof. The quasi-orthogonality from Proposition 4.14 and the discrete reliability from Proposition 4.9 plus (H3)–(H4) yield, for any $j \in J$, that

$$\begin{aligned} \|u_j - \Lambda_\ell u_j\|^2 &= 2a(u_j - \widehat{\Lambda}_\ell u_j, \widehat{\Lambda}_\ell u_j - \Lambda_\ell u_j) + \|u_j - \widehat{\Lambda}_\ell u_j\|^2 + \|\widehat{\Lambda}_\ell u_j - \Lambda_\ell u_j\|^2 \\ &\leq \|u_j - \widehat{\Lambda}_\ell u_j\|^2 + \lambda_j^2(1 + M_J)^2 \|h_0\|_\infty^{2s} (C_{\text{qo}} + 2^{-1} C_{\text{drel}}^2) \|u_j - \Lambda_\ell u_j\|^2 \\ &\quad + 2^{-1} C_{\text{drel}}^2 \mu_\ell^2(\mathcal{T}_\ell \setminus \widehat{\mathcal{T}}_\ell, \lambda_j, u_j) \\ &\leq \|u_j - \widehat{\Lambda}_\ell u_j\|^2 + \frac{1}{2} \|u_j - \Lambda_\ell u_j\|^2 + 2^{-1} C_{\text{drel}}^2 \mu_\ell^2(\mathcal{T}_\ell \setminus \widehat{\mathcal{T}}_\ell, \lambda_j, u_j). \end{aligned}$$

Therefore, (4.16) implies

$$\frac{1}{2} \sum_{j \in J} \|u_j - \Lambda_\ell u_j\|^2 \leq 2\varepsilon(\ell)^2 + 2^{-1} C_{\text{drel}}^2 \mu_\ell^2(\mathcal{T}_\ell \setminus \widehat{\mathcal{T}}_\ell).$$

Let C_{eq} denote the constant of $2\varepsilon_\ell^2 \leq C_{\text{eq}} \mu_\ell^2(\mathcal{T}_\ell)$ (which exists by reliability). The efficiency (4.8), the definition of $\varepsilon(\ell)$ and the preceding estimates prove

$$\begin{aligned} \frac{1}{2} C_{\text{eff}}^{-2} \mu_\ell^2(\mathcal{T}_\ell) &\leq 2\varepsilon(\ell)^2 + C_{\text{drel}}^2 \mu_\ell^2(\mathcal{T}_\ell \setminus \widehat{\mathcal{T}}_\ell) \\ &\leq \tau C_{\text{eq}} \mu_\ell^2(\mathcal{T}_\ell) + C_{\text{drel}}^2 \mu_\ell^2(\mathcal{T}_\ell \setminus \widehat{\mathcal{T}}_\ell). \end{aligned}$$

The constant $C_2 := (2^{-1} C_{\text{eff}}^{-2} - \tau C_{\text{eq}})^{-1} C_{\text{drel}}^2 / 2$ is positive for some sufficiently small choice of τ . \blacksquare

The finish of the optimality proof follows the arguments of [Cascon et al., 2008, Stevenson, 2007]. The constant C_2 stems from Lemma 4.19.

Lemma 4.20 (finish of the optimality proof). *The choice*

$$0 < \theta \leq 1 / (C_2 (B/A)^4 (2N^2 + 4N^3)) \quad (4.17)$$

implies that there exists some constant $C(\sigma) \approx 1$ such that

$$\sup_{\ell \in \mathbb{N}_0} (\text{card}(\mathcal{T}_\ell) - \text{card}(\mathcal{T}_0))^\sigma \left(\sum_{j \in J} \|u_j - \Lambda_\ell u_j\|^2 \right)^{1/2} \leq C(\sigma) \left(\sum_{j \in J} |u_j|_{\mathcal{U}_\sigma}^2 \right)^{1/2}.$$

Proof. The marking step in the adaptive algorithm selects $\mathcal{M}_\ell \subseteq \mathcal{T}_\ell$ with minimal cardinality such that $\theta \eta_\ell^2(\mathcal{T}_\ell) \leq \eta_\ell^2(\mathcal{M}_\ell)$. Lemma 4.19 and the comparison (3.15) from Proposition 3.16 lead to

$$\eta_\ell^2(\mathcal{T}_\ell) \leq C_2(B/A)^4(2N^2 + 4N^3)\eta_\ell^2(\mathcal{T}_\ell \setminus \widehat{\mathcal{T}}_\ell).$$

The choice of θ in (4.17) implies that also $\mathcal{T}_\ell \setminus \widehat{\mathcal{T}}_\ell$ satisfies the bulk criterion. The minimality of \mathcal{M}_ℓ and (4.15) show

$$\text{card}(\mathcal{M}_\ell) \leq \text{card}(\mathcal{T}_\ell \setminus \widehat{\mathcal{T}}_\ell) \leq 2 \left(\sum_{j \in J} |u_j|_{\mathfrak{H}_\sigma}^2 \right)^{1/(2\sigma)} \tau^{-1/(2\sigma)} \Xi_\ell^{-1/\sigma}.$$

By Theorem 2.17 there exists a constant C_{BDV} such that

$$\begin{aligned} \text{card}(\mathcal{T}_\ell) - \text{card}(\mathcal{T}_0) &\leq C_{\text{BDV}} \sum_{k=0}^{\ell-1} \text{card}(\mathcal{M}_k) \\ &\leq 2C_{\text{BDV}} \left(\sum_{j \in J} |u_j|_{\mathfrak{H}_\sigma}^2 \right)^{1/(2\sigma)} \tau^{-1/(2\sigma)} \sum_{k=0}^{\ell-1} \Xi_k^{-1/\sigma}. \end{aligned}$$

The contraction property from Proposition 4.16 implies $\Xi_\ell^2 \leq \rho_2^{\ell-m} \Xi_m^2$ for $0 \leq m \leq \ell$. Since $\rho_2 < 1$, a geometric series argument leads to

$$\sum_{j=0}^{\ell-1} \Xi_j^{-1/\sigma} \leq \Xi_\ell^{-1/\sigma} \sum_{j=0}^{\ell-1} \rho_2^{(j-\ell)/(2\sigma)} \leq \Xi_\ell^{-1/\sigma} \rho_2^{1/(2\sigma)} / (1 - \rho_2^{1/(2\sigma)}).$$

The combination of the above estimates results in

$$\begin{aligned} \text{card}(\mathcal{T}_\ell) - \text{card}(\mathcal{T}_0) &\leq 2C_{\text{BDV}} \left(\sum_{j \in J} |u_j|_{\mathfrak{H}_\sigma}^2 \right)^{1/(2\sigma)} \tau^{-1/(2\sigma)} \Xi_\ell^{-1/\sigma} \rho_2^{1/(2\sigma)} / (1 - \rho_2^{1/(2\sigma)}). \end{aligned}$$

The equivalence of Ξ_ℓ^2 with the error $\sum_{j \in J} \|u_j - \Lambda_\ell u_j\|^2$ concludes the proof. \blacksquare

Remark 4.21 (higher-order FEM). The extension of the present analysis to higher-order methods based on \mathcal{P}_k polynomials with $k \geq 2$ remains as an open question. For higher-order methods, the volume contribution of the error estimator on a simplex T reads as $\|\lambda_{\ell,j} u_{\ell,j} + \Delta u_{\ell,j}\|_{L^2(T)}$. The proof of equivalence of this term to theoretical quantities of the form

$$\|\lambda P_\ell u + \Delta \Lambda_\ell u\|_{L^2(T)} \quad \text{or} \quad \|\lambda \Lambda_\ell u + \Delta \Lambda_\ell u\|_{L^2(T)}$$

with the methodology of Proposition 3.12 seems problematic unless only one multiple eigenvalue is considered. Let $k \in J$ and let, in analogy to the proof of Proposition 3.12, $\Lambda_\ell u_k = \sum_{j \in J} \alpha_j u_{\ell,j}$. The Cauchy and triangle inequalities show

$$\begin{aligned} &\|\lambda_k \Lambda_\ell u_k + \Delta \Lambda_\ell u_k\|_{L^2(T)}^2 \\ &\leq \|\Lambda_\ell u_k\|_{L^2(T)} \sum_{j \in J} \|\lambda_k u_{\ell,j} + \Delta u_{\ell,j}\|_{L^2(T)}^2 \\ &\leq \|\Lambda_\ell u_k\|_{L^2(T)} \sum_{j \in J} \left(\|\lambda_{\ell,j} u_{\ell,j} + \Delta u_{\ell,j}\|_{L^2(T)} + \|u_{\ell,j}\|_{L^2(T)} |\lambda_{\ell,j} - \lambda_k| \right)^2. \end{aligned}$$

Only in the case that all $(\lambda_{\ell,j} \mid j \in J)$ converge to one multiple eigenvalue λ the additional term $|\lambda_{\ell,j} - \lambda_k|$ is an appropriate error measure. In case of an eigenvalue cluster, this term describes the cluster width $(B - A)$ and, thus, is not efficient. \blacklozenge

5. Nonconforming \mathcal{P}_1 FEM for the Eigenvalues of the Laplacian

This chapter is devoted to the adaptive nonconforming \mathcal{P}_1 finite element method for the eigenvalues of the Laplacian. The first proof of optimal convergence rates for this method was obtained by Carstensen, Gallistl, and Schedensack [2014c] for simple eigenvalues on simply-connected two-dimensional domains. This chapter introduces the nonconforming \mathcal{P}_1 finite element space in Section 5.1. Section 5.2 introduces conforming companion operators. Section 5.3 outlines the proof of the discrete distance control from [Carstensen, Gallistl, and Schedensack, 2013a]. Section 5.4 revisits the linear Poisson problem and its nonconforming finite element discretisation and generalises the best-approximation property from [Gudi, 2010] to arbitrary space dimensions with a refined oscillation term. The nonconforming discretisation of the Laplace eigenvalue problem in Section 5.5 involves L^2 error estimates and a best-approximation property. Section 5.6 presents the error estimator and the adaptive algorithm and states the optimality result in terms of nonlinear approximation classes. The theoretical error estimator and its (discrete) reliability are introduced in Section 5.7. Sections 5.8 and 5.9 prove the contraction property and optimal convergence rates.

Throughout this section, let $V := H_0^1(\Omega)$.

5.1. The Nonconforming \mathcal{P}_1 Finite Element Space

This section introduces the nonconforming \mathcal{P}_1 FEM and the nonconforming interpolation operator.

Definition 5.1 (nonconforming \mathcal{P}_1 finite element space). The nonconforming \mathcal{P}_1 finite element space, sometimes referred to as Crouzeix-Raviart finite element space [Crouzeix and Raviart, 1973], reads as

$$\mathfrak{C}\mathfrak{R}_0^1(\mathcal{T}_\ell) := \left\{ v_\ell \in \mathcal{P}_1(\mathcal{T}_\ell) \left| \begin{array}{l} v_\ell \text{ is continuous in the interior hyper-faces'} \\ \text{midpoints and vanishes in the midpoints} \\ \text{of hyper-faces on the boundary} \end{array} \right. \right\}.$$

◆

Throughout this section, let $V_\ell := V(\mathcal{T}_\ell) := \mathfrak{C}\mathfrak{R}_0^1(\mathcal{T}_\ell)$. This finite element space is accompanied with the following interpolation operator.

Definition 5.2 (nonconforming \mathcal{P}_1 interpolation). Given an admissible refinement $\mathcal{T}_{\ell+m} \in \mathbb{T}(\mathcal{T}_\ell)$ of \mathcal{T}_ℓ , define the operator $\mathcal{I}_\ell^{\mathfrak{C}\mathfrak{R}} : V + V_{\ell+m} \rightarrow V_\ell$ by

$$\int_F (v - \mathcal{I}_\ell^{\mathfrak{C}\mathfrak{R}} v) ds = 0 \quad \text{for all } F \in \mathcal{F}_\ell \text{ and all } v \in V + V_{\ell+m}.$$

◆

5. Nonconforming \mathcal{P}_1 FEM for the Eigenvalues of the Laplacian

Note that $\mathcal{J}_\ell^{\mathfrak{C}\mathfrak{R}}$ is indeed well-defined for functions in $\mathfrak{C}\mathfrak{R}_0^1(\mathcal{T}_{\ell+m})$. A (piecewise) integration by parts proves the projection property $D_{\text{NC}}\mathcal{J}_\ell^{\mathfrak{C}\mathfrak{R}} = \Pi_\ell^0 D$, i.e.,

$$\int_T D_{\text{NC}}\mathcal{J}_\ell^{\mathfrak{C}\mathfrak{R}} v dx = \int_T Dv dx \quad \text{for all } T \in \mathcal{T}_\ell \text{ and all } v \in V + V_{\ell+m}. \quad (5.1)$$

The proof of the approximation and stability property

$$\|h_T^{-1}(v - \mathcal{J}_\ell^{\mathfrak{C}\mathfrak{R}} v)\|_{L^2(T)} + \|D_{\text{NC}}(v - \mathcal{J}_\ell^{\mathfrak{C}\mathfrak{R}} v)\|_{L^2(T)} \lesssim \|(1 - \Pi_\ell^0)D_{\text{NC}}v\|_{L^2(T)} \quad (5.2)$$

for any $v \in V + V_{\ell+m}$ and any $T \in \mathcal{T}_\ell$ follows from the discrete Friedrichs inequality (Proposition 2.32).

The following estimate gives an explicit value for the constant for $\mathcal{J}_\ell^{\mathfrak{C}\mathfrak{R}} : V \rightarrow V_\ell$ in the case of a planar domain ($d = 2$). It is a refined version of a result of Carstensen and Gedicke [2014]. Let $j_{1,1} = 3.8317059702$ denote the first positive root of the Bessel function of the first kind [Laugesen and Siudeja, 2010] and set

$$\kappa_{\mathfrak{C}\mathfrak{R}} := \sqrt{1/48 + j_{1,1}^{-2}} = 0.298234942888.$$

Proposition 5.3 (explicit error estimate for $\mathcal{J}_\ell^{\mathfrak{C}\mathfrak{R}}$ for $d = 2$). *In the case $d = 2$, the nonconforming interpolation operator $\mathcal{J}_\ell^{\mathfrak{C}\mathfrak{R}}$ satisfies, for any triangle $T \in \mathcal{T}_\ell$ and any function $v \in H^1(\text{int}(T))$, the error estimate*

$$\|v - \mathcal{J}_\ell^{\mathfrak{C}\mathfrak{R}} v\|_{L^2(T)} \leq \kappa_{\mathfrak{C}\mathfrak{R}} \text{diam}(T) \|D(v - \mathcal{J}_\ell^{\mathfrak{C}\mathfrak{R}} v)\|_{L^2(T)}.$$

Proof. The proof can be found in [Carstensen and Gallistl, 2014]. It is a refined version of the original proof of [Carstensen and Gedicke, 2014]. \blacksquare

5.2. Conforming Companion Operators

This section presents conforming companion operators. The idea behind these operators is to design for a nonconforming finite element function v_ℓ some conforming companion $J_{d+1}v_\ell \in V$ with certain conservation properties. For $d = 2$ these kind of operators have been constructed by Carstensen, Gallistl, and Schedensack [2014c] and independently by Mao and Shi [2010]. The following result extends [Carstensen, Gallistl, and Schedensack, 2014c] to any dimension $d \geq 2$.

Proposition 5.4 (companion operator in any space dimension). *For any $v_\ell \in V_\ell$ there exists some $J_{d+1}v_\ell \in \mathcal{P}_{d+1}(\mathcal{T}_\ell) \cap V$ such that $v_\ell - J_{d+1}v_\ell$ is L^2 orthogonal onto the space $\mathcal{P}_0(\mathcal{T}_\ell)$ of piecewise constants, it enjoys the integral mean property*

$$\Pi_\ell^0(D_{\text{NC}}(v_\ell - J_{d+1}v_\ell)) = 0, \quad (5.3)$$

and it satisfies the approximation and stability property

$$\|h_\ell^{-1}(v_\ell - J_{d+1}v_\ell)\|_{L^2(\Omega)} + \|D_{\text{NC}}(v_\ell - J_{d+1}v_\ell)\|_{L^2(\Omega)} \lesssim \min_{v \in V} \|D_{\text{NC}}(v_\ell - v)\|_{L^2(\Omega)}. \quad (5.4)$$

Proof. The design follows in three steps.

Step 1. The operator $J_1 : V_\ell \rightarrow P_1(\mathcal{T}_\ell) \cap V$ acts on any function $v_\ell \in V_\ell$ by averaging the function values at each interior vertex z , i.e.,

$$J_1 v_\ell(z) = \text{card}(\mathcal{T}_\ell(z))^{-1} \sum_{T \in \mathcal{T}_\ell(z)} v_\ell|_T(z) \quad \text{for all } z \in \mathcal{N}_\ell(\Omega).$$

This operator is also known as enriching operator in the context of fast solvers [Brenner, 1996]. The proof of the approximation property

$$\|h_\ell^{-1}(v_\ell - J_1 v_\ell)\|_{L^2(\Omega)} \lesssim \min_{v \in V} \|D_{\text{NC}}(v_\ell - v)\|_{L^2(\Omega)} \quad (5.5)$$

is included in [Carstensen et al., 2012a, Thm. 5.1] for $d = 2$. A generalisation to higher dimensions is outlined in the proof of [Carstensen, Gallistl, and Schedensack, 2013a, Thm. 4.9]. This and an inverse estimate [Brenner and Scott, 2008] imply the stability property

$$\|D_{\text{NC}}(v_\ell - J_1 v_\ell)\|_{L^2(\Omega)} \lesssim \min_{v \in V} \|D_{\text{NC}}(v_\ell - v)\|_{L^2(\Omega)}. \quad (5.6)$$

Step 2. Given any hyper-face $F = \text{conv}\{z_1, \dots, z_d\}$ with nodal \mathcal{P}_1 conforming basis functions $\varphi_1, \dots, \varphi_d \in \mathcal{P}_1(\mathcal{T}_\ell) \cap V$, the quadratic edge-bubble function

$$\mathbf{b}_F := \frac{(2d-1)!}{(d-1)!} \prod_{j=1}^d \varphi_j$$

is supported on $\overline{\omega_F}$ and satisfies $\int_F \mathbf{b}_F ds = 1$. For any function $v_\ell \in V_\ell$ the operator $J_d : V_\ell \rightarrow \mathcal{P}_d(\mathcal{T}_\ell) \cap V$ acts as

$$J_d v_\ell := J_1 v_\ell + \sum_{F \in \mathcal{F}_\ell(\Omega)} \left(\int_F (v_\ell - J_1 v_\ell) ds \right) \mathbf{b}_F.$$

An immediate consequence of this choice reads as

$$\int_F J_d v_\ell ds = \int_F v_\ell ds \quad \text{for all } F \in \mathcal{F}_\ell.$$

An integration by parts shows the integral mean property of the gradients $\Pi_\ell^0 D J_d = D_{\text{NC}}$, i.e.,

$$\int_T D J_d v_\ell dx = \int_T D_{\text{NC}} v_\ell dx \quad \text{for all } T \in \mathcal{T}_\ell.$$

Let $T \in \mathcal{T}_\ell$ with $F \in \mathcal{F}(T)$. The scaling $\|\mathbf{b}_F\|_{L^2(\Omega)} \lesssim h_T^{d/2}$ and the Hölder and trace inequalities (Proposition 2.31) show

$$\begin{aligned} h_T^{-1} \left\| \sum_{F \in \mathcal{F}(T)} \left(\int_F (v_\ell - J_1 v_\ell) ds \right) \mathbf{b}_F \right\|_{L^2(T)} &\lesssim h_T^{(d-2)/2} \sum_{F \in \mathcal{F}(T)} \left| \int_F (v_\ell - J_1 v_\ell) ds \right| \\ &\lesssim h_T^{-1/2} \sum_{F \in \mathcal{F}(T)} \|v_\ell - J_1 v_\ell\|_{L^2(F)} \\ &\lesssim h_T^{-1} \|v_\ell - J_1 v_\ell\|_{L^2(T)} + \|D_{\text{NC}}(v_\ell - J_1 v_\ell)\|_{L^2(T)}. \end{aligned}$$

5. Nonconforming \mathcal{P}_1 FEM for the Eigenvalues of the Laplacian

This, the triangle inequality and the properties (5.5)–(5.6) yield

$$\|h_\ell^{-1}(v_\ell - J_d v_\ell)\|_{L^2(\Omega)} \lesssim \min_{v \in V} \|D_{\text{NC}}(v_\ell - v)\|_{L^2(\Omega)}. \quad (5.7)$$

The stability property of J_d follows with an inverse estimate [Brenner and Scott, 2008]

$$\|D_{\text{NC}}(v_\ell - J_d v_\ell)\|_{L^2(\Omega)} \lesssim \|h_\ell^{-1}(v_\ell - J_d v_\ell)\|_{L^2(\Omega)} \lesssim \min_{v \in V} \|D_{\text{NC}}(v_\ell - v)\|_{L^2(\Omega)}.$$

Step 3. On any simplex $T = \text{conv}\{z_1, \dots, z_{d+1}\}$ with nodal basis functions $\varphi_1, \dots, \varphi_{d+1}$, the volume bubble function is defined by

$$\mathbf{b}_T := \frac{(2d+1)!}{d!} \prod_{j=1}^{d+1} \varphi_j \in H_0^1(\text{int}(T)) \quad (5.8)$$

and satisfies $\int_T \mathbf{b}_T dx = 1$. Define

$$J_{d+1} v_\ell := J_d v_\ell + \sum_{T \in \mathcal{T}_\ell} \left(\int_T (v_\ell - J_d v_\ell) dx \right) \mathbf{b}_T.$$

The difference $v_\ell - J_{d+1} v_\ell$ is L^2 -orthogonal to all piecewise constant functions. Since \mathbf{b}_T vanishes on all $F \in \mathcal{F}_\ell$, J_{d+1} enjoys the integral mean property $\Pi_\ell^0 D J_{d+1} = D_{\text{NC}}$. The Hölder inequality and (5.7) imply

$$\left| \int_T (v_\ell - J_d v_\ell) dx \right| \lesssim h_T^{-d/2} \|v_\ell - J_d v_\ell\|_{L^2(T)} \lesssim h_T^{-(d-2)/2} \min_{v \in V} \|D_{\text{NC}}(v_\ell - v)\|_{L^2(\Omega)}.$$

The scaling $\|D \mathbf{b}_T\|_{L^2(\Omega)} \approx h_T^{(d-2)/2}$ and the triangle inequality prove the stability property

$$\|D_{\text{NC}}(v_\ell - J_{d+1} v_\ell)\|_{L^2(\Omega)} \lesssim \min_{v \in V} \|D_{\text{NC}}(v_\ell - v)\|_{L^2(\Omega)}.$$

A piecewise Poincaré inequality proves the approximation property

$$\|h_\ell^{-1}(v_\ell - J_{d+1} v_\ell)\|_{L^2(\Omega)} \lesssim \min_{v \in V} \|D_{\text{NC}}(v_\ell - v)\|_{L^2(\Omega)}. \quad \blacksquare$$

5.3. Discrete Distance Control

The nonconforming finite element spaces are, in general, not nested. Hence, the distance of a given discrete function $v_\ell \in \mathfrak{C}\mathfrak{R}_0^1(\mathcal{T}_\ell)$ to the finite element space $\mathfrak{C}\mathfrak{R}_0^1(\mathcal{T}_{\ell+m})$ (with respect to some refinement $\mathcal{T}_{\ell+m}$) is relevant. For simply-connected domains in \mathbb{R}^2 , Becker et al. [2010] employed the discrete Helmholtz decomposition of Arnold and Falk [1989] for some distance control. The construction of upper bounds for this distance by an averaging operator as in [Becker and Mao, 2011] is problematic because their constant may depend on the number m of refinement steps. Hu and Xu [2013a,b] suggested a refined analysis by means of an averaging operator based on different layers. This section presents the discrete distance control for multiply-connected domains for $d \geq 2$ and outlines its proof by Carstensen, Gallistl, and Schedensack [2013a].

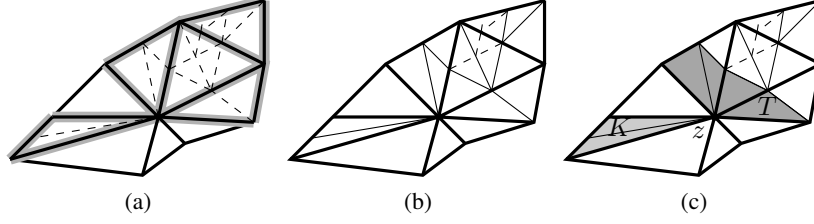


Figure 5.1.: Triangulation \mathcal{T}_ℓ (thick) and refinement $\mathcal{T}_{\ell+m}$ (dashed). (a) Highlighted edges appear in the sum in (5.9). (b) Intermediate triangulation $\widehat{\mathcal{T}}_\ell$ (solid). (c) Sets $\mathcal{Z}(z, K)$ (light grey) and $\mathcal{Z}(z, T)$ (dark grey).

Theorem 5.5 (discrete distance control). *There exists a constant $C_{\text{ddc}} \approx 1$ such that any refinement $\mathcal{T}_{\ell+m} \in \mathbb{T}(\mathcal{T}_\ell)$ of \mathcal{T}_ℓ and any function $u_\ell \in \mathfrak{C}\mathfrak{R}_0^1(\mathcal{T}_\ell)$ satisfy*

$$\min_{v_{\ell+m} \in \mathfrak{C}\mathfrak{R}_0^1(\mathcal{T}_{\ell+m})} \|D_{\text{NC}}(u_\ell - v_{\ell+m})\|_{L^2(\Omega)}^2 \leq C_{\text{ddc}} \sum_{T \in \mathcal{T}_\ell \setminus \mathcal{T}_{\ell+m}} \sum_{F \in \mathcal{F}(T)} h_F^{-1} \| [u_\ell]_F \|_{L^2(F)}^2. \quad (5.9)$$

Figure 5.1a illustrates possible triangulations $\mathcal{T}_\ell \in \mathbb{T}$ and $\mathcal{T}_{\ell+m} \in \mathbb{T}(\mathcal{T}_\ell)$ and emphasises the hyper-faces which appear in the sum in the right-hand side in (5.9). The point is that hyper-faces $F \in \mathcal{F}_\ell$ for which all adjacent simplices $T \in \mathcal{T}_\ell$ with $F \in \mathcal{F}(T)$ are not refined can be neglected. The proof of discrete distance control is an immediate consequence of the following result from [Carstensen, Gallistl, and Schedensack, 2013a, Thm. 3.2]. An outline of the proof is given for completeness and convenient reading.

Theorem 5.6 (transfer operator). *Given $\mathcal{T}_\ell \in \mathbb{T}$ and some refinement $\mathcal{T}_{\ell+m} \in \mathbb{T}(\mathcal{T}_\ell)$, there exists an operator $\mathcal{J} : \mathfrak{C}\mathfrak{R}_0^1(\mathcal{T}_\ell) \rightarrow \mathfrak{C}\mathfrak{R}_0^1(\mathcal{T}_{\ell+m})$ such that, for any $u_\ell \in \mathfrak{C}\mathfrak{R}_0^1(\mathcal{T}_\ell)$, $\mathcal{J}u_\ell|_T = u_\ell|_T$ for all $T \in \mathcal{T}_\ell \cap \mathcal{T}_{\ell+m}$ and*

$$\|D_{\text{NC}}(u_\ell - \mathcal{J}u_\ell)\|_{L^2(\Omega)}^2 \lesssim \sum_{T \in \mathcal{T}_\ell \setminus \mathcal{T}_{\ell+m}} \sum_{F \in \mathcal{F}(T)} h_F^{-1} \| [u_\ell]_F \|_{L^2(F)}^2.$$

Proof. The design of the operator \mathcal{J} is based on an intermediate triangulation $\widehat{\mathcal{T}}_\ell$.

Step 1 (intermediate triangulation). Let $\widehat{\mathcal{T}}_\ell$ denote the coarsest refinement of \mathcal{T}_ℓ such that $(\mathcal{F}_\ell \setminus \mathcal{F}_{\ell+m}) \cap \mathcal{F}(\widehat{\mathcal{T}}_\ell) = \emptyset$. This triangulation satisfies $\mathcal{T}_\ell \cap \mathcal{T}_{\ell+m} = \mathcal{T}_\ell \cap \widehat{\mathcal{T}}_\ell$. Figure 5.1b illustrates the definition of the intermediate triangulation $\widehat{\mathcal{T}}_\ell$ with $\mathbb{T}(\mathcal{T}_{\ell+m}) \subsetneq \mathbb{T}(\widehat{\mathcal{T}}_\ell) \subsetneq \mathbb{T}(\mathcal{T}_\ell)$. It follows from Proposition 2.8 that $\widehat{\mathcal{T}}_\ell$ can be created by two calls of `refine` from Algorithm 2.15. Proposition 2.21 implies that any two simplices $K \in \mathcal{T}_\ell$ and $T \in \widehat{\mathcal{T}}_\ell$ with $T \subseteq K$ have comparable sizes $h_K \approx h_T$.

Step 2 (averaging operator). Consider the vertex $z \in \mathcal{N}(T)$ of a simplex $T \in \widehat{\mathcal{T}}_\ell$ in the intermediate triangulation $\widehat{\mathcal{T}}_\ell$ and define the set of the hyper-face-connected refined simplices at z by $\mathcal{Z}(z; T) := \{T\}$ for $T \in \widehat{\mathcal{T}}_\ell \cap \mathcal{T}_\ell$ and otherwise (i.e. for $T \in \widehat{\mathcal{T}}_\ell \setminus \mathcal{T}_\ell$) set

$$\mathcal{Z}(z; T) := \left\{ K \in \widehat{\mathcal{T}}_\ell \setminus \mathcal{T}_\ell \left| \begin{array}{l} \text{there exist } n \in \mathbb{N} \text{ and } (T_1, \dots, T_n) \in (\widehat{\mathcal{T}}_\ell \setminus \mathcal{T}_\ell)^n \text{ such that} \\ T = T_1 \text{ and } K = T_n \text{ and} \\ z \in (T_{j-1} \cap T_j) \in \mathcal{F}(\widehat{\mathcal{T}}_\ell) \text{ for all } j \in \{2, \dots, n\} \end{array} \right. \right\}.$$

This set contains those simplices that can be reached from T by a chain of elements in $T \in \widehat{\mathcal{T}}_\ell \setminus \mathcal{T}_\ell$ that share z and are connected through hyper-faces in $\mathcal{F}(\widehat{\mathcal{T}}_\ell)$. Figure 5.1c

5. Nonconforming \mathcal{P}_1 FEM for the Eigenvalues of the Laplacian

illustrates this definition of $\mathcal{Z}(z; T)$ and its dependence on $T \in \widehat{\mathcal{T}}_\ell$. Define the averaging operator $J^* : \mathfrak{C}\mathfrak{N}_0^1(\mathcal{T}_\ell) \rightarrow \mathcal{P}_1(\widehat{\mathcal{T}}_\ell)$ for $z \in \mathcal{N}(\widehat{\mathcal{T}}_\ell) \cap \Omega$ and $T \in \widehat{\mathcal{T}}_\ell(z)$ by

$$J^*u_\ell|_T(z) := \text{card}(\mathcal{Z}(z; T))^{-1} \sum_{K \in \mathcal{Z}(z; T)} u_\ell|_K(z),$$

while $J^*u_\ell(z) := 0$ for $z \in \mathcal{N}(\widehat{\mathcal{T}}_\ell) \cap \partial\Omega$. The difference to Step 1 in the proof of Proposition 5.4 is that the averaging only considers the set $\mathcal{Z}(z; T)$. Thus, the resulting function may be discontinuous. The crucial point is that the definition of $\mathcal{Z}(z; T)$ implies for $T \in \mathcal{T}_\ell \setminus \widehat{\mathcal{T}}_\ell$ that $J^*u_\ell|_T(z)$ does not depend on the values of u_ℓ on the simplices of $T \in \mathcal{T}_\ell \cap \widehat{\mathcal{T}}_\ell$.

Step 3 (transfer operator). Given $u_\ell \in \mathfrak{C}\mathfrak{N}_0^1(\mathcal{T}_\ell)$, define $\mathcal{J}u_\ell \in \mathcal{P}_1(\widehat{\mathcal{T}}_\ell)$ as a combination of the averaging operator J^* and the identity for simplices $T \in \mathcal{T}_\ell \cap \widehat{\mathcal{T}}_\ell$, i.e., for $T \in \widehat{\mathcal{T}}_\ell$ and $F \in \mathcal{F}(T)$, set

$$\mathcal{J}u_\ell|_T(\text{mid}(F)) := \begin{cases} u_\ell(\text{mid}(F)) & \text{if } F \in \mathcal{F}_\ell \cap \mathcal{F}(\widehat{\mathcal{T}}_\ell), \\ J^*u_\ell|_T(\text{mid}(F)) & \text{if } F \in \mathcal{F}(\widehat{\mathcal{T}}_\ell) \setminus \mathcal{F}_\ell. \end{cases}$$

This definition leads to

$$\mathcal{J}u_\ell \in \mathfrak{C}\mathfrak{N}_0^1(\mathcal{T}_{\ell+m}) \cap \mathfrak{C}\mathfrak{N}_0^1(\widehat{\mathcal{T}}_\ell) \quad \text{and} \quad \mathcal{J}u_\ell|_T = u_\ell|_T \text{ for all } T \in \mathcal{T}_\ell \cap \mathcal{T}_{\ell+m}.$$

A detailed proof can be found in [Carstensen, Gallistl, and Schedensack, 2013a].

Step 4 (error estimate). For any $T \in \widehat{\mathcal{T}}_\ell$ and $z \in \mathcal{N}(T)$, the set of hyper-surfaces of $\mathcal{F}(\widehat{\mathcal{T}}_\ell)$ that contain z and belong to $\mathcal{Z}(z; T)$ is defined as

$$\widehat{\mathcal{F}}_\ell(z, T) := \{F \in \mathcal{F}(\widehat{\mathcal{T}}_\ell) \mid z \in F \text{ and there exists } K \in \mathcal{Z}(z; T) \text{ with } F \in \mathcal{F}(K)\}.$$

With arguments similar to those of Step 1 in the proof of Proposition 5.4 in this thesis, Theorem 4.9 of [Carstensen, Gallistl, and Schedensack, 2013a] proves the following error estimate for any $T \in \widehat{\mathcal{T}}_\ell \setminus \mathcal{T}_\ell$,

$$\|D_{\text{NC}}(u_\ell - \mathcal{J}u_\ell)\|_{L^2(T)}^2 \lesssim \sum_{z \in \mathcal{N}(T)} \sum_{F \in \widehat{\mathcal{F}}_\ell(z, T)} h_F^{-1} \| [u_\ell]_F \|_{L^2(F)}^2.$$

Hence, the property $u_\ell = \mathcal{J}u_\ell$ on $\mathcal{T}_\ell \cap \widehat{\mathcal{T}}_\ell$ implies

$$\|D_{\text{NC}}(u_\ell - \mathcal{J}u_\ell)\|_{L^2(\Omega)} \lesssim \sum_{T \in \mathcal{T}_\ell \setminus \mathcal{T}_{\ell+m}} \sum_{z \in \mathcal{N}(T)} \sum_{F \in \widehat{\mathcal{F}}_\ell(z, T)} h_F^{-1} \| [u_\ell]_F \|_{L^2(F)}^2.$$

Since $h_G \lesssim h_F$ for $G \in \mathcal{F}_\ell$, $F \in \mathcal{F}(\widehat{\mathcal{T}}_\ell)$ with $F \subseteq G$, the finite overlap of the nodal patches in $\widehat{\mathcal{T}}_\ell$ implies

$$\|D_{\text{NC}}(u_\ell - \mathcal{J}u_\ell)\|_{L^2(\Omega)}^2 \lesssim \sum_{T \in \mathcal{T}_\ell \setminus \mathcal{T}_{\ell+m}} \sum_{F \in \mathcal{F}(T)} h_F^{-1} \| [u_\ell]_F \|_{L^2(F)}^2. \quad \blacksquare$$

5.4. Nonconforming FEM for the Poisson Model Problem

This section proves some nonstandard results for the nonconforming \mathcal{P}_1 discretisation of the linear Poisson equation. Let $V := H_0^1(\Omega)$ be equipped with the scalar products

$$a(v, w) := (Dv, Dw)_{L^2(\Omega)} \quad \text{and} \quad b(v, w) := (v, w)_{L^2(\Omega)}$$

and induced norms $\|v\| := a(v, v)^{1/2}$ and $\|v\| := b(v, v)^{1/2}$. Given $f \in L^2(\Omega)$, the weak formulation of the Poisson problem $-\Delta u = f$ under homogeneous Dirichlet boundary conditions reads as

$$a(u, v) = b(f, v) \quad \text{for all } v \in V. \quad (5.10)$$

The nonconforming finite element discretisation is based on the space $V_\ell := \mathfrak{C}\mathfrak{R}_0^1(\mathcal{T}_\ell)$ and the scalar product

$$a_{\text{NC}}(v_\ell, w_\ell) := (D_{\text{NC}}v_\ell, D_{\text{NC}}w_\ell)_{L^2(\Omega)} \quad \text{for all } (v_\ell, w_\ell) \in V_\ell^2$$

with norm $\|\cdot\|_{\text{NC}} := a_{\text{NC}}(\cdot, \cdot)$ and seeks $u_\ell \in V_\ell$ such that

$$a_{\text{NC}}(u_\ell, v_\ell) = b(f, v_\ell) \quad \text{for all } v_\ell \in V_\ell. \quad (5.11)$$

It is well known [Brenner and Scott, 2008] that these continuous and discrete problems are uniquely solvable. A posteriori and a priori error estimates as well as best-approximation properties for this problem are well-studied in the literature (at least in the case $d = 2$) [see, e.g., Braess, 2007, Dari et al., 1996, Gudi, 2010, Carstensen et al., 2012b]. Error estimates in the L^2 norm require a modification of the usual duality argument for conforming finite element methods. The following proposition establishes an L^2 error estimate. The main ingredient is the use of the companion operator from Section 5.2. For $d = 2$, this result was first obtained by [Carstensen, Gallistl, and Schedensack, 2014c] and [Carstensen and Park, 2013]. A similar approach has independently been developed by Mao and Shi [2010] for $d = 2$. The result presented here compares the L^2 error directly with the energy error and therefore uses no a priori results of the eigenfunction approximation. This is important as the L^2 control will usually lead to higher-order terms which can be absorbed for $\|h_0\|_\infty \ll 1$.

Let $0 < s \leq 1$ indicate the elliptic regularity index of the Poisson problem $-\Delta u = f$ with homogeneous Dirichlet boundary conditions in the sense that $\|u\|_{H^{1+s}(\Omega)} \leq C(s)\|f\|_{L^2(\Omega)}$, cf. (4.4).

Proposition 5.7 (L^2 error estimate for the linear problem). *The exact solution u to (5.10) and the discrete solution u_ℓ to (5.11) satisfy*

$$\|u - u_\ell\| \lesssim \|h_0\|_\infty^s \|u - u_\ell\|_{\text{NC}}.$$

Proof. Let $e := u - u_\ell$ and let $z \in V$ denote the solution of

$$a(z, v) = b(e, v) \quad \text{for all } v \in V.$$

Recall the companion operator J_{d+1} from Proposition 5.4. Since $\Pi_\ell^0(u_\ell - J_{d+1}u_\ell) = 0$, it holds that

$$\begin{aligned} \|e\|^2 &= b(J_{d+1}u_\ell - u_\ell, e) + b(e, u - J_{d+1}u_\ell) \\ &= b(J_{d+1}u_\ell - u_\ell, (1 - \Pi_\ell^0)e) + a(z, u - J_{d+1}u_\ell). \end{aligned} \quad (5.12)$$

5. Nonconforming \mathcal{P}_1 FEM for the Eigenvalues of the Laplacian

Piecewise Poincaré inequalities and (5.4) lead to

$$b(J_{d+1}u_\ell - u_\ell, (1 - \Pi_\ell^0)e) \lesssim \|h_0\|_\infty^2 \|e\|_{\text{NC}}^2.$$

Since e is perpendicular to the conforming finite element functions in $\mathcal{P}_1(\mathcal{T}) \cap V$ and since $\Pi_\ell^0 D_{\text{NC}}(u_\ell - J_{d+1}u_\ell) = 0$, the Scott-Zhang quasi-interpolation $z_C \in \mathcal{P}_1(\mathcal{T}) \cap V$ of z [Scott and Zhang, 1990] satisfies

$$\begin{aligned} a(z, u - J_{d+1}u_\ell) &= a_{\text{NC}}(e, z) + a_{\text{NC}}(u_\ell - J_{d+1}u_\ell, z) \\ &= a_{\text{NC}}(e, z - z_C) + a_{\text{NC}}(u_\ell - J_{d+1}u_\ell, z - z_C). \end{aligned}$$

The Cauchy inequality and (5.4) imply

$$a_{\text{NC}}(e, z - z_C) + a_{\text{NC}}(u_\ell - J_{d+1}u_\ell, z - z_C) \lesssim \|e\|_{\text{NC}} \|z - z_C\|_{\text{NC}}.$$

Standard a priori error estimates [Brenner and Scott, 2008] and the elliptic regularity (4.4) imply

$$\|z - z_C\| \lesssim \|h_0\|_\infty^s \|z\|_{H^{1+s}(\Omega)} \lesssim \|h_0\|_\infty^s \|e\|.$$

The combination of the above estimates proves

$$\|e\| \lesssim \|h_0\|_\infty^s \|e\|_{\text{NC}}. \quad \blacksquare$$

The next result states a best-approximation property in any space dimension. It generalises some recent results of the medius analysis [Braess, 2009, Gudi, 2010, Carstensen et al., 2012b] to arbitrary space dimensions. The result is stated with a refined oscillation term $\text{osc}_{1,1}(f, \mathcal{T}_\ell)$ (see Definition 2.29). This will be important for the analysis of eigenvalue problems.

Proposition 5.8 (best-approximation property). *The solution $u \in V$ to (5.10) with right-hand side $f \in L^2(\Omega)$ and the discrete solution $u_\ell \in V_\ell$ to (5.11) satisfy*

$$\|u - u_\ell\|_{\text{NC}} \lesssim \|(1 - \Pi_\ell^0)Du\| + \text{osc}_{1,1}(f, \mathcal{T}_\ell).$$

Proof. The projection property (5.1) of the nonconforming interpolation operator $\mathcal{J}_\ell^{\text{CR}}$ and the Pythagoras theorem show that

$$\|u - u_\ell\|_{\text{NC}}^2 = \|u_\ell - \mathcal{J}_\ell^{\text{CR}}u\|_{\text{NC}}^2 + \|u - \mathcal{J}_\ell^{\text{CR}}u\|_{\text{NC}}^2.$$

Since $\|u - \mathcal{J}_\ell^{\text{CR}}u\|_{\text{NC}} = \|(1 - \Pi_\ell^0)Du\|$, it remains to estimate the first term on the right-hand side. Set $\varphi_\ell := u_\ell - \mathcal{J}_\ell^{\text{CR}}u$. The properties of the companion operator from Proposition 5.4 show that

$$\|u_\ell - \mathcal{J}_\ell^{\text{CR}}u\|_{\text{NC}}^2 = a_{\text{NC}}(u_\ell - u, \varphi_\ell) = b(f, \varphi_\ell - J_{d+1}\varphi_\ell) + ((1 - \Pi_\ell^0)Du, D_{\text{NC}}(J_{d+1} - 1)\varphi_\ell)_{L^2(\Omega)}.$$

The approximation and stability properties (5.4) show that this is bounded by

$$(\|h_\ell f\| + \|(1 - \Pi_\ell^0)Du\|) \|\varphi_\ell\|_{\text{NC}}.$$

The efficiency $\|h_\ell f\| \lesssim \|(1 - \Pi_\ell^0)Du\| + \text{osc}_{1,1}(f, \mathcal{T}_\ell)$ follows from arguments similar to those of Proposition 4.3. This concludes the proof. \blacksquare

5.5. Discretisation of the Laplace Eigenvalue Problem

The Laplace eigenvalue problem seeks eigenpairs $(\lambda, u) \in \mathbb{R} \times V$ with $\|u\| = 1$ such that

$$a(u, v) = \lambda b(u, v) \quad \text{for all } v \in V. \quad (5.13)$$

The finite element discretisation based on a regular triangulation \mathcal{T}_ℓ seeks discrete eigenpairs $(\lambda_\ell, u_\ell) \in \mathbb{R} \times V_\ell$ with $\|u_\ell\| = 1$ and

$$a_{\text{NC}}(u_\ell, v_\ell) = \lambda_\ell b(u_\ell, v_\ell) \quad \text{for all } v_\ell \in V_\ell. \quad (5.14)$$

Adopt the notation of Section 3.1 with exact and discrete eigenvalues

$$0 < \lambda_1 \leq \lambda_2 \leq \dots \quad \text{and} \quad 0 < \lambda_{\ell,1} \leq \dots \leq \lambda_{\ell, \dim(V_\ell)}$$

and their corresponding b -orthonormal systems of eigenfunctions

$$(u_1, u_2, u_3, \dots) \quad \text{and} \quad (u_{\ell,1}, u_{\ell,2}, \dots, u_{\ell, \dim(V_\ell)}).$$

Recall the definitions of Section 3.1: The set $J = \{n+1, \dots, n+N\}$ describes the eigenvalue cluster of interest and $W := \text{span}\{u_j \mid j \in J\}$ and $W_\ell := \text{span}\{u_{\ell,j} \mid j \in J\}$ are the exact and discrete invariant subspaces (not necessarily eigenspaces) related to the cluster. In the present situation, the quasi-Ritz projection R_ℓ from Definition 3.1 maps the solution $u \in V$ of the linear problem (5.10) to the solution $R_\ell u$ of the discrete linear problem (5.11). With the L^2 projection $P_{\mathcal{T}_\ell} := P_\ell$ onto W_ℓ let $\Lambda_{\mathcal{T}_\ell} := \Lambda_\ell := P_\ell \circ R_\ell$.

The remaining parts of this section prove an L^2 error estimate as well as a best-approximation result and discuss lower eigenvalue bounds.

Proposition 5.9 (L^2 error control). *Provided $\|h_0\|_\infty \ll 1$, any eigenpair $(\lambda, u) \in \mathbb{R} \times W$ with $\|u\| = 1$ satisfies for some constant C_{L^2} and the separation constant M_J from (H1) (page 22) that*

$$\|u - P_\ell u\| \leq \|u - \Lambda_\ell u\| \lesssim (1 + M_J) \|u - R_\ell u\| \leq C_{L^2} (1 + M_J) \|h_0\|_\infty^s \|u - \Lambda_\ell u\|_{\text{NC}}.$$

Proof. Note that $R_\ell u$ solves (5.11) with right-hand side $f := \lambda u$. The combination of Proposition 3.3 with Proposition 5.7 and Proposition 5.8 yields

$$\|u - P_\ell u\| \leq \|u - \Lambda_\ell u\| \lesssim (1 + M_J) \|h_0\|_\infty^s (\|u - \Lambda_\ell u\|_{\text{NC}} + \text{osc}_{1,1}(\lambda u, \mathcal{T}_\ell)).$$

Provided $\|h_0\|_\infty \ll 1$, the oscillation term can be absorbed. ■

Proposition 5.10 (best-approximation property). *Provided $\|h_0\|_\infty \ll 1$, any eigenpair $(\lambda, u) \in \mathbb{R} \times W$ of (5.13) with $\|u\| = 1$ satisfies*

$$\|u - \Lambda_\ell u\|_{\text{NC}} \lesssim \|(1 - \Pi_\ell^0)Du\|_{L^2(\Omega)}.$$

Proof. The triangle inequality proves for the quasi-Ritz projection $R_\ell u$ that

$$\|u - \Lambda_\ell u\|_{\text{NC}} \leq \|u - R_\ell u\|_{\text{NC}} + \|R_\ell u - \Lambda_\ell u\|_{\text{NC}}.$$

Set $\varphi_\ell := R_\ell u - \Lambda_\ell u$. The definition of R_ℓ and the discrete problem (cf. Lemma 3.4) prove that

$$\|R_\ell u - \Lambda_\ell u\|_{\text{NC}}^2 = a_{\text{NC}}(R_\ell u - \Lambda_\ell u, \varphi_\ell) = \lambda b(u - P_\ell u, \varphi_\ell).$$

5. Nonconforming \mathcal{P}_1 FEM for the Eigenvalues of the Laplacian

Hence, the Cauchy and discrete Friedrichs inequalities (Proposition 2.32) and the L^2 control from Proposition 5.9 prove that

$$\|R_\ell u - \Lambda_\ell u\|_{\text{NC}} \lesssim \lambda(1 + M_J) \|h_0\|_\infty^s \|u - \Lambda_\ell u\|_{\text{NC}}.$$

The combination of the foregoing estimates with Proposition 5.8 results in

$$\|u - \Lambda_\ell u\|_{\text{NC}} \lesssim \|(1 - \Pi_\ell^0)Du\|_{L^2(\Omega)} + \lambda(1 + M_J) \|h_0\|_\infty^s \|u - \Lambda_\ell u\|_{\text{NC}} + \text{osc}_{1,1}(\lambda u, \mathcal{T}_\ell).$$

If $\|h_0\|_\infty \ll 1$ is sufficiently small, the higher-order terms on the right-hand side can be absorbed. \blacksquare

Proposition 5.10 and Proposition 4.3 show that the conforming and the nonconforming \mathcal{P}_1 methods yield comparable results for the eigenvalues of the Laplacian. One advantage of the nonconforming discretisation is that it leads to guaranteed lower eigenvalue bounds provided the constant in the L^2 error estimate (5.2) for functions $v \in V$ is known explicitly. The proof is a consequence of the abstract result in Lemma 3.13. For the constant C (cf. (5.2)) that satisfies

$$\|v - \mathcal{J}_\ell^{\mathfrak{CR}} v\|_{L^2(T)} \leq Ch_T \|D_{\text{NC}}(v - \mathcal{J}_\ell^{\mathfrak{CR}} v)\|_{L^2(T)} \quad \text{for all } v \in V \text{ and all } T \in \mathcal{T}_\ell,$$

the lower bound for the eigenvalue λ_j reads as

$$\lambda_{\ell,j} / (1 + C^2 \|h_\ell\|_\infty^2 \lambda_{\ell,j}) \leq \lambda_j. \quad (5.15)$$

For the case $d = 2$, the explicit error estimate of Proposition 5.3 results in the lower bound of Carstensen and Gedicke [2014] with the constant $\kappa_{\mathfrak{CR}}$ from Proposition 5.3 and

$$\lambda_{\ell,j} / (1 + \kappa_{\mathfrak{CR}}^2 \max_{T \in \mathcal{T}_\ell} \text{diam}(T)^2 \lambda_{\ell,j}) \leq \lambda_j.$$

5.6. Adaptive Algorithm and Approximation Classes

This section presents the computable residual-based error estimator and the adaptive algorithm and states the optimality result.

For any simplex $T \in \mathcal{T}_\ell$, the explicit residual-based error estimator consists of the sum of the residuals of the computed discrete eigenfunctions $(u_{\ell,j})_{j \in J}$,

$$\eta_\ell^2(T) := \sum_{j \in J} \left(h_T^2 \|\lambda_{\ell,j} u_{\ell,j}\|_{L^2(T)}^2 + \sum_{F \in \mathcal{F}(T)} h_T^{-1} \|[u_{\ell,j}]_F\|_{L^2(F)}^2 \right).$$

Let, for any subset $\mathcal{K} \subseteq \mathcal{T}$,

$$\eta_\ell^2(\mathcal{K}) := \sum_{T \in \mathcal{K}} \eta_\ell^2(T).$$

For simple eigenvalues this type of error estimator was introduced by Dari et al. [2012]. The adaptive algorithm is driven by this computable error estimator and runs the following loop.

Algorithm 5.11 (nonconforming AFEM for the Laplace eigenvalue problem).

Input: Initial triangulation \mathcal{T}_0 , bulk parameter $0 < \theta \leq 1$.

for $\ell = 0, 1, 2, \dots$ **do**

Solve. Compute discrete eigenpairs $(\lambda_{\ell,j}, u_{\ell,j})_{j \in J}$ of (5.14) with respect to \mathcal{T}_ℓ .

Estimate. Compute local contributions of the error estimator $(\eta_\ell^2(T))_{T \in \mathcal{T}_\ell}$.

Mark. Choose a minimal subset $\mathcal{M}_\ell \subseteq \mathcal{T}_\ell$ such that $\theta \eta_\ell^2(\mathcal{T}_\ell) \leq \eta_\ell^2(\mathcal{M}_\ell)$.

Refine. Generate $\mathcal{T}_{\ell+1} := \text{refine}(\mathcal{T}_\ell, \mathcal{M}_\ell)$ with Algorithm 2.15.

end for

Output: Sequences of triangulations $(\mathcal{T}_\ell)_\ell$ and discrete solutions $((\lambda_{\ell,j}, u_{\ell,j})_{j \in J})_\ell$. \blacklozenge

Remark 5.12. It is assumed that all algebraic eigenvalue problems are solved exactly. A more practical approach is based on Algorithm 3.17 and the analysis of this chapter carries over to the practical algorithm by means of a perturbation analysis as in [Carstensen, Gallistl, and Schedensack, 2014c]. \blacklozenge

Recall the approximation class \mathfrak{A}_σ from Section 4.2 and define the following alternative set, also referred to as approximation class

$$\mathfrak{A}_\sigma^{\text{NC}, \Delta} := \left\{ u \in V \mid |u|_{\mathfrak{A}_\sigma^{\text{NC}, \Delta}} < \infty \right\}$$

for

$$|u|_{\mathfrak{A}_\sigma^{\text{NC}, \Delta}} := \sup_{m \in \mathbb{N}} m^\sigma \inf_{\mathcal{T} \in \mathbb{T}(m)} \|u - \Lambda_{\mathcal{T}} u\|_{\text{NC}}$$

for the eigenfunction approximation $\Lambda_{\mathcal{T}} u$ from page 55 with respect to a triangulation \mathcal{T} . Proposition 5.10 proves that these two approximation classes are equivalent in the sense that any eigenfunction $u \in W$ belongs to \mathfrak{A}_σ if and only if it belongs to $\mathfrak{A}_\sigma^{\text{NC}, \Delta}$. The following theorem states optimality of Algorithm 5.11. The proof follows in the remaining parts of this chapter.

Theorem 5.13 (optimal convergence rates). *Provided the bulk parameter $\theta \ll 1$ and the initial mesh-size $\|h_0\|_\infty \ll 1$ are sufficiently small, Algorithm 5.11 computes triangulations $(\mathcal{T}_\ell)_\ell$ and discrete eigenpairs $((\lambda_{\ell,j}, u_{\ell,j})_{j \in J})_\ell$ with optimal rate of convergence in the sense that, for some constant C_{opt} ,*

$$\sup_{\ell \in \mathbb{N}} (\text{card}(\mathcal{T}_\ell) - \text{card}(\mathcal{T}_0))^\sigma \left(\sum_{j \in J} \|u_j - \Lambda_{\mathcal{T}_\ell} u_j\|_{\text{NC}}^2 \right)^{1/2} \leq C_{\text{opt}} \left(\sum_{j \in J} |u_j|_{\mathfrak{A}_\sigma^{\text{NC}, \Delta}}^2 \right)^{1/2}.$$

Proposition 5.10 implies the following immediate consequence.

Corollary 5.14. *Provided the bulk parameter $\theta \ll 1$ and the initial mesh-size $\|h_0\|_\infty \ll 1$ are sufficiently small, Algorithm 5.11 computes triangulations $(\mathcal{T}_\ell)_\ell$ and discrete eigenpairs $((\lambda_{\ell,j}, u_{\ell,j})_{j \in J})_\ell$ with optimal rate of convergence in the sense that*

$$\sup_{\ell \in \mathbb{N}} (\text{card}(\mathcal{T}_\ell) - \text{card}(\mathcal{T}_0))^\sigma \sup_{\substack{w \in W \\ \|w\|=1}} \inf_{v_\ell \in W_\ell} \|w - v_\ell\|_{\text{NC}} \lesssim \left(\sum_{j \in J} |u_j|_{\mathfrak{A}_\sigma}^2 \right)^{1/2}. \quad \blacksquare$$

The optimal decay rate of the eigenvalue error will be proven in Chapter 8, see Corollary 8.13.

Remark 5.15 (optimality for inexact solve). The optimality results of Theorem 5.13 and Corollary 5.14 carry over to Algorithm 3.17 for sufficiently small $\varkappa \ll 1$ by means of a perturbation analysis as in [Carstensen and Gedicke, 2012] or [Carstensen, Gallistl, and Schedensack, 2014c]. \blacklozenge

5.7. Theoretical Error Estimator and Discrete Reliability

The analysis relies on a theoretical, non-computable error estimator that does not depend on the choice of the discrete eigenfunctions. Given an eigenpair (λ, u) , the error estimator includes the elementwise residuals in terms of $P_\ell u$ and $\Lambda_\ell u$. More precisely, define, for any $T \in \mathcal{T}_\ell$,

$$\mu_\ell^2(T, \lambda, u) := h_T^2 \|\lambda P_\ell u\|_{L^2(T)}^2 + \sum_{F \in \mathcal{F}(T)} h_T^{-1} \|[\Lambda_\ell u]_F\|_{L^2(F)}^2$$

and, for any subset $\mathcal{K} \subseteq \mathcal{T}_\ell$,

$$\mu_\ell^2(\mathcal{K}, \lambda_j, u_j) := \sum_{T \in \mathcal{K}} \mu_\ell^2(T, \lambda_j, u_j) \quad \text{and} \quad \mu_\ell^2(\mathcal{K}) := \sum_{j \in J} \mu_\ell^2(\mathcal{K}, \lambda_j, u_j).$$

The following shorthand notation for higher-order terms will be frequently used in the remaining parts of this chapter. For $(\ell, m) \in \mathbb{N}_0^2$ define (with the constant C_{L^2} from Proposition 5.9)

$$\mathbf{r}_{\ell, m} := \|h_0\|_\infty^s \lambda (1 + M_J) C_{L^2} \sqrt{\|u - \Lambda_\ell u\|^2 + \|u - \Lambda_{\ell+m} u\|^2}. \quad (5.16)$$

The theoretical error estimator satisfies the following discrete reliability.

Proposition 5.16 (discrete reliability). *There exists a constant $C_{\text{drel}} \approx 1$ solely dependent on \mathcal{T}_0 with $\|h_0\|_\infty \ll 1$ such that any eigenpair $(\lambda, u) \in \mathbb{R} \times W$ of (5.13) with $\|u\| = 1$ satisfies*

$$2\|\Lambda_{\ell+m} u - \Lambda_\ell u\|^2 \leq C_{\text{drel}}^2 (\mu_\ell^2(\mathcal{T}_\ell \setminus \mathcal{T}_{\ell+m}, \lambda, u) + \mathbf{r}_{\ell, m}^2).$$

Proof. Let $v_{\ell+m}$ denote the best-approximation (with respect to the norm $\|\cdot\|_{\text{NC}}$) of $\Lambda_\ell u$ in $V_{\ell+m}$. The Pythagoras theorem reads as

$$\|(\Lambda_{\ell+m} - \Lambda_\ell)u\|_{\text{NC}}^2 = \|\Lambda_{\ell+m} u - v_{\ell+m}\|_{\text{NC}}^2 + \min_{w_{\ell+m} \in V_{\ell+m}} \|w_{\ell+m} - \Lambda_\ell u\|_{\text{NC}}^2.$$

The second term has been estimated in the discrete distance control (Theorem 5.5) by means of the jumps of $\Lambda_\ell u$. For the analysis of the first term, let $\varphi_{\ell+m} := \Lambda_{\ell+m} u - v_{\ell+m}$. The projection property (5.1) of the nonconforming interpolation and the discrete eigenvalue problems (cf. Lemma 3.4) reveal that

$$\begin{aligned} \|\Lambda_{\ell+m} u - v_{\ell+m}\|_{\text{NC}}^2 &= a_{\text{NC}}((\Lambda_{\ell+m} - \Lambda_\ell)u, \varphi_{\ell+m}) \\ &= \lambda b((P_{\ell+m} - P_\ell)u, \varphi_{\ell+m}) + \lambda b(P_\ell u, (1 - \mathcal{I}_\ell^{\text{CR}})\varphi_{\ell+m}). \end{aligned}$$

The L^2 error estimate from Proposition 5.9 and the approximation and stability property (5.2) conclude the proof. \blacksquare

The reliability of the error estimator is an immediate consequence.

Proposition 5.17 (reliability and efficiency). *Provided $\|h_0\|_\infty \ll 1$, any eigenpair $(\lambda, u) \in \mathbb{R} \times W$ of (5.13) with $\|u\| = 1$ satisfies*

$$\|u - \Lambda_\ell u\|_{\text{NC}}^2 \leq C_{\text{drel}}^2 \mu_\ell^2(\mathcal{T}_\ell, \lambda, u). \quad (5.17)$$

For some constant $C_{\text{eff}} \approx 1$, it holds that

$$\mu_\ell(\mathcal{T}_\ell, \lambda, u)^2 \leq C_{\text{eff}}^2 \|u - \Lambda_\ell u\|_{\text{NC}}^2. \quad (5.18)$$

Proof. The reliability

$$2\|u - \Lambda_\ell u\|_{\text{NC}}^2 \leq C_{\text{drel}}^2 (\mu_\ell^2(\mathcal{T}_\ell, \lambda, u) + \|h_0\|_\infty^{2s} \lambda^2 (1 + M_J)^2 \|u - \Lambda_\ell u\|_{\text{NC}}^2)$$

follows from the discrete reliability on a sequence of meshes $\mathcal{T}_{\ell+m}$ with $\|h_{\ell+m}\|_\infty \rightarrow 0$ and the a priori convergence result of Proposition 5.10. Provided the initial mesh is sufficiently fine, the higher-order terms on the right-hand side can be absorbed. The efficiency

$$2\mu_\ell^2(\mathcal{T}_\ell, \lambda, u) \leq C_{\text{eff}}^2 (1 + \lambda \|h_0\|_\infty^{1+s} (1 + M_J) C_{L^2})^2 \|u - \Lambda_\ell u\|_{\text{NC}}^2$$

follows from the triangle inequality and the L^2 error control from Proposition 5.9 combined with the standard arguments of Verfürth [1996]. The assumption $\|h_0\|_\infty \ll 1$ implies

$$\mu_\ell^2(\mathcal{T}_\ell, \lambda, u) \leq C_{\text{eff}}^2 \|u - \Lambda_\ell u\|_{\text{NC}}^2. \quad \blacksquare$$

5.8. Contraction Property

This section is devoted to the proof of the contraction property. The first proposition states the error estimator reduction property.

Proposition 5.18 (error estimator reduction for μ_ℓ). *Provided (H1)–(H2), there exist constants $0 < \rho_1 < 1$ and $0 < K < \infty$ such that \mathcal{T}_ℓ and its one-level refinement $\mathcal{T}_{\ell+1}$ generated by Algorithm 5.11 and any eigenfunction $u \in W$ with $\|u\| = 1$ and eigenvalue λ satisfy (with $\mathbf{r}_{\ell,1}$ from (5.16)) that*

$$\mu_{\ell+1}^2(\mathcal{T}_{\ell+1}, \lambda, u) \leq \rho_1 \mu_\ell^2(\mathcal{T}_\ell, \lambda, u) + K (\|\Lambda_{\ell+1} u - \Lambda_\ell u\|_{\text{NC}}^2 + \|h_0\|_\infty^2 \mathbf{r}_{\ell,1}^2).$$

Proof. The standard techniques of [Cascon et al., 2008, Stevenson, 2007] and the bulk criterion (3.16) lead to a constant \tilde{K} such that

$$\mu_{\ell+1}^2(\mathcal{T}_{\ell+1}, \lambda, u) \leq \rho_1 \mu_\ell^2(\mathcal{T}_\ell, \lambda, u) + \tilde{K} (\|\Lambda_{\ell+1} u - \Lambda_\ell u\|_{\text{NC}}^2 + \|h_{\ell+1} \lambda (P_{\ell+1} - P_\ell) u\|^2).$$

The triangle inequality for the term $\|h_{\ell+1} \lambda (P_{\ell+1} - P_\ell) u\|$ and the L^2 error control from Proposition 5.9 prove the result. \blacksquare

The next technical result is needed for the reduction of the volume contribution of the error estimator. Inequalities of this type were previously utilised in [Rabus, 2010] for $d = 2$ for the linear Poisson problem and in [Carstensen, Gallistl, and Schedensack, 2013a] for boundary value problems for $d \geq 2$.

Lemma 5.19 (control of the volume contribution). *Provided $\|h_0\|_\infty \ll 1$, any triangulation $\mathcal{T}_\ell \in \mathbb{T}$ and any admissible refinement $\mathcal{T}_{\ell+m} \in \mathbb{T}(\mathcal{T}_\ell)$ satisfy for any $0 < \delta < \infty$ and any eigenpair $(\lambda, u) \in \mathbb{R} \times W$ of (5.13) with $\|u\| = 1$ that*

$$\begin{aligned} \|h_{\ell+m} \lambda P_{\ell+m} u\|_{L^2(\Omega)}^2 + (1 + \delta^{-1})(1 - 2^{-2/d}) \|h_\ell \lambda P_\ell u\|_{L^2(\cup(\mathcal{T}_\ell \setminus \mathcal{T}_{\ell+m}))}^2 \\ \leq 2(1 + \delta) \|h_0\|_\infty^2 \mathbf{r}_{\ell,m}^2 + (1 + \delta^{-1}) \|h_\ell \lambda P_\ell u\|_{L^2(\Omega)}^2. \end{aligned}$$

5. Nonconforming \mathcal{P}_1 FEM for the Eigenvalues of the Laplacian

Proof. The triangle and Young inequalities (Proposition 2.30) prove for any $0 < \delta < \infty$ that

$$\|h_{\ell+m}\lambda P_{\ell+m}u\|_{L^2(\Omega)}^2 \leq (1+\delta)\|h_{\ell+m}\lambda(P_{\ell+m}u - P_\ell u)\|_{L^2(\Omega)}^2 + (1+\delta^{-1})\|h_{\ell+m}\lambda P_\ell u\|_{L^2(\Omega)}^2.$$

The relation $h_{\ell+m}^d \leq h_\ell^d/2$ on $\mathcal{T}_\ell \setminus \mathcal{T}_{\ell+m}$ proves

$$\|h_\ell\lambda P_\ell u\|_{L^2(\cup(\mathcal{T}_\ell \setminus \mathcal{T}_{\ell+m}))}^2 \leq (1-2^{-2/d})^{-1}(\|h_\ell\lambda P_\ell u\|_{L^2(\Omega)}^2 - \|h_{\ell+m}\lambda P_\ell u\|_{L^2(\Omega)}^2).$$

The preceding two displayed formulas together with Proposition 5.9 prove the result. \blacksquare

Remark 5.20 (failure of Galerkin orthogonality). In the case of nonconforming discretisations of eigenvalue problems, the Galerkin orthogonality is violated at two points. As in Proposition 4.14, the nonlinearity leads to a perturbation of the right-hand side. Furthermore, the nonconforming finite element functions are not admissible test functions in the continuous problem and, thus, additional techniques enter the analysis. The first result of this type for linear problems as well as the notion of quasi-orthogonality trace back to Carstensen and Hoppe [2006]. \blacklozenge

Proposition 5.21 (quasi-orthogonality). *Under the hypothesis $\|h_0\|_\infty \ll 1$ there exists a constant C_{qo} such that any eigenpair $(\lambda, u) \in \mathbb{R} \times W$ of (5.13) with $\|u\| = 1$, any $\mathcal{T}_\ell \in \mathbb{T}$, and any admissible refinement $\mathcal{T}_{\ell+m} \in \mathbb{T}(\mathcal{T}_\ell)$ satisfy*

$$\begin{aligned} & |2a_{\text{NC}}(u - \Lambda_{\ell+m}u, \Lambda_{\ell+m}u - \Lambda_\ell u)| \\ & \leq C_{\text{qo}}(\|h_\ell\lambda P_\ell u\|_{L^2(\cup(\mathcal{T}_\ell \setminus \mathcal{T}_{\ell+m}))} + \mathbf{r}_{\ell,m})\|u - \Lambda_{\ell+m}u\|_{\text{NC}}. \end{aligned}$$

Proof. Some algebraic manipulations with the projection property (5.1) of the nonconforming interpolation and the discrete eigenvalue problems (cf. Lemma 3.4) reveal

$$\begin{aligned} & a_{\text{NC}}((1 - \Lambda_{\ell+m})u, (\Lambda_{\ell+m} - \Lambda_\ell)u) \\ & = a_{\text{NC}}(\Lambda_{\ell+m}u, \mathcal{J}_{\ell+m}^{\mathfrak{R}}(1 - \Lambda_{\ell+m})u) - a_{\text{NC}}(\Lambda_\ell u, \mathcal{J}_\ell^{\mathfrak{R}}(1 - \Lambda_{\ell+m})u) \\ & = \lambda b(P_{\ell+m}u, \mathcal{J}_{\ell+m}^{\mathfrak{R}}(1 - \Lambda_{\ell+m})u) - \lambda b(P_\ell u, \mathcal{J}_\ell^{\mathfrak{R}}(1 - \Lambda_{\ell+m})u) \\ & = \lambda b(P_\ell u, (\mathcal{J}_{\ell+m}^{\mathfrak{R}} - \mathcal{J}_\ell^{\mathfrak{R}})(1 - \Lambda_{\ell+m})u) + \lambda b((P_{\ell+m} - P_\ell)u, \mathcal{J}_{\ell+m}^{\mathfrak{R}}(1 - \Lambda_{\ell+m})u). \end{aligned}$$

Since $\mathcal{J}_{\ell+m}^{\mathfrak{R}}v|_T = \mathcal{J}_\ell^{\mathfrak{R}}v|_T$ for all $T \in \mathcal{T}_\ell \cap \mathcal{T}_{\ell+m}$, the first term of the right-hand side can be controlled with (5.2) as

$$\begin{aligned} & \lambda b(P_\ell u, (\mathcal{J}_{\ell+m}^{\mathfrak{R}} - \mathcal{J}_\ell^{\mathfrak{R}})(1 - \Lambda_{\ell+m})u) \\ & \lesssim \|h_\ell\lambda P_\ell u\|_{L^2(\cup(\mathcal{T}_\ell \setminus \mathcal{T}_{\ell+m}))} \|D_{\text{NC}}(1 - \Lambda_{\ell+m})u\|_{L^2(\cup(\mathcal{T}_\ell \setminus \mathcal{T}_{\ell+m}))}. \end{aligned}$$

For the second term, the discrete Friedrichs inequality (Proposition 2.32) and the stability of $\mathcal{J}_\ell^{\mathfrak{R}}$ reveal

$$\lambda b((P_{\ell+m} - P_\ell)u, \mathcal{J}_{\ell+m}^{\mathfrak{R}}(1 - \Lambda_{\ell+m})u) \lesssim \lambda \|(P_{\ell+m} - P_\ell)u\| \|u - \Lambda_{\ell+m}u\|_{\text{NC}}.$$

The triangle inequality and Proposition 5.9 control the term $\lambda \|(P_{\ell+m} - P_\ell)u\|$ by $\mathbf{r}_{\ell,m}$ from (5.16). This concludes the proof. \blacksquare

The following contraction property implies the convergence of the adaptive algorithm.

Proposition 5.22 (contraction property). *Under the condition $\|h_0\|_\infty \ll 1$, there exist $0 < \rho_2 < 1$ and $0 < \beta, \gamma < \infty$ such that, for any eigenpair $(\lambda, u) \in \mathbb{R} \times W$ with $\|u\| = 1$, the term $\xi_\ell^2 := \mu_\ell^2(\mathcal{T}_\ell, \lambda, u) + \beta \|u - \Lambda_\ell u\|_{\text{NC}}^2 + \gamma \|h_\ell P_\ell u\|^2$ satisfies*

$$\xi_{\ell+1}^2 \leq \rho_2 \xi_\ell^2 \quad \text{for all } \ell \in \mathbb{N}_0.$$

Proof. Throughout the proof, the following shorthand notation applies

$$\begin{aligned} \mathbf{e}_\ell &:= \|u - \Lambda_\ell u\|_{\text{NC}}, & \mathbf{e}_{\ell+1} &:= \|u - \Lambda_{\ell+1} u\|_{\text{NC}}, \\ \mu_\ell^2 &:= \mu_\ell^2(\mathcal{T}_\ell, \lambda, u), & \mu_{\ell+1}^2 &:= \mu_{\ell+1}^2(\mathcal{T}_{\ell+1}, \lambda, u). \end{aligned}$$

The error estimator reduction from Proposition 5.18 and elementary algebraic manipulations plus the quasi-orthogonality (Proposition 5.21) lead to

$$\begin{aligned} \mu_{\ell+1}^2 + K \mathbf{e}_{\ell+1}^2 &\leq \rho_1 \mu_\ell^2 + K \left(\mathbf{e}_\ell^2 + 2a(u - \Lambda_{\ell+1} u, (\Lambda_\ell - \Lambda_{\ell+1})u) + \|h_0\|_\infty^2 \mathbf{r}_{\ell,1}^2 \right) \\ &\leq \rho_1 \mu_\ell^2 + K \left(\mathbf{e}_\ell^2 + C_{\text{qo}} (\|h_\ell \lambda P_\ell u\|_{L^2(\cup \mathcal{T}_\ell \setminus \mathcal{T}_{\ell+1})} + \mathbf{r}_{\ell,1}) \mathbf{e}_{\ell+1} + \|h_0\|_\infty^2 \mathbf{r}_{\ell,1}^2 \right). \end{aligned}$$

This and the Young inequality (Proposition 2.30) for any $0 < \varepsilon < 1$ lead to

$$\begin{aligned} \mu_{\ell+1}^2 + K(1 - C_{\text{qo}}\varepsilon/2) \mathbf{e}_{\ell+1}^2 \\ \leq \rho_1 \mu_\ell^2 + K \left(\mathbf{e}_\ell^2 + C_{\text{qo}}/\varepsilon (\|h_\ell \lambda P_\ell u\|_{L^2(\cup \mathcal{T}_\ell \setminus \mathcal{T}_{\ell+m})}^2 + \mathbf{r}_{\ell,1}^2) + \|h_0\|_\infty^2 \mathbf{r}_{\ell,1}^2 \right). \end{aligned}$$

The reliability (5.17) proves for any $0 < \zeta < \infty$ that this is bounded by

$$(\rho_1 + K\zeta C_{\text{drel}}^2) \mu_\ell^2 + K \left((1 - \zeta) \mathbf{e}_\ell^2 + C_{\text{qo}}/\varepsilon (\|h_\ell \lambda P_\ell u\|_{L^2(\cup \mathcal{T}_\ell \setminus \mathcal{T}_{\ell+m})}^2 + \mathbf{r}_{\ell,1}^2) + \|h_0\|_\infty^2 \mathbf{r}_{\ell,1}^2 \right).$$

Lemma 5.19 states for any $0 < \delta < \infty$ and $c_d := (1 - 2^{-2/d})$ that

$$\|h_\ell \lambda P_\ell u\|_{L^2(\cup \mathcal{T}_\ell \setminus \mathcal{T}_{\ell+1})}^2 \leq \frac{2\delta \|h_0\|_\infty^2 \mathbf{r}_{\ell,1}^2}{c_d} + \frac{\|h_\ell \lambda P_\ell u\|^2}{c_d} - \frac{\|h_{\ell+1} \lambda P_{\ell+1} u\|^2}{(1 + \delta^{-1})c_d}.$$

Altogether,

$$\begin{aligned} \mu_{\ell+1}^2 + K \left((1 - C_{\text{qo}}\varepsilon/2) \mathbf{e}_{\ell+1}^2 + \frac{C_{\text{qo}} \|h_{\ell+1} \lambda P_{\ell+1} u\|^2}{\varepsilon(1 + \delta^{-1})c_d} \right) \\ \leq (\rho_1 + K\zeta C_{\text{drel}}^2) \mu_\ell^2 \\ + K \left((1 - \zeta) \mathbf{e}_\ell^2 + \left(\varepsilon^{-1} C_{\text{qo}} (1 + 2\delta \|h_0\|_\infty^2 / c_d) + \|h_0\|_\infty^2 \right) \mathbf{r}_{\ell,1}^2 + \frac{C_{\text{qo}} \|h_\ell \lambda P_\ell u\|^2}{\varepsilon c_d} \right). \end{aligned}$$

Define

$$t(\|h_0\|_\infty, \varepsilon, \delta) := C_{\text{drel}}^2 \|h_0\|_\infty^{2s} \lambda^2 (1 + M_J)^2 C_{L^2}^2 K (\varepsilon^{-1} C_{\text{qo}} (1 + 2\delta \|h_0\|_\infty^2 / c_d) + \|h_0\|_\infty^2).$$

Recall the definition (5.16) of $\mathbf{r}_{\ell,1}$. The reliability (5.17) implies

$$K \left(\varepsilon^{-1} C_{\text{qo}} (1 + 2\delta \|h_0\|_\infty^2 / c_d) + \|h_0\|_\infty^2 \right) \mathbf{r}_{\ell,1}^2 \leq t(\|h_0\|_\infty, \varepsilon, \delta) (\mu_\ell^2 + \mu_{\ell+1}^2).$$

5. Nonconforming \mathcal{P}_1 FEM for the Eigenvalues of the Laplacian

This and the fact that $\|h_\ell \lambda P_\ell u\|^2 \leq \mu_\ell^2$ together with the foregoing estimates prove

$$\begin{aligned} & (1 - t(\|h_0\|_\infty, \varepsilon, \delta)) \mu_{\ell+1}^2 + K \left((1 - C_{\text{qo}} \varepsilon / 2) \mathbf{e}_{\ell+1}^2 + \frac{C_{\text{qo}} \|h_{\ell+1} \lambda P_{\ell+1} u\|^2}{\varepsilon (1 + \delta^{-1}) c_d} \right) \\ & \leq (\rho_1 + K \zeta C_{\text{drel}}^2 + t(\|h_0\|_\infty, \varepsilon, \delta) + K \varepsilon) \mu_\ell^2 + K \left((1 - \zeta) \mathbf{e}_\ell^2 + \left(\frac{C_{\text{qo}}}{\varepsilon c_d} - \varepsilon \right) \|h_\ell \lambda P_\ell u\|^2 \right). \end{aligned}$$

Hence, for

$$\beta := \frac{K(1 - C_{\text{qo}} \varepsilon / 2)}{1 - t(\|h_0\|_\infty, \varepsilon, \delta)}, \quad \gamma := \frac{K C_{\text{qo}}}{\varepsilon (1 + \delta^{-1}) c_d (1 - t(\|h_0\|_\infty, \varepsilon, \delta))},$$

and

$$\rho_2 := \max \left\{ \frac{\rho_1 + K \zeta C_{\text{drel}}^2 + t(\|h_0\|_\infty, \varepsilon, \delta) + K \varepsilon}{1 - t(\|h_0\|_\infty, \varepsilon, \delta)}, \frac{1 - \zeta}{1 - C_{\text{qo}} \varepsilon / 2}, (1 + \delta^{-1}) (C_{\text{qo}} - \varepsilon^2 c_d) / C_{\text{qo}} \right\},$$

it follows that

$$\mu_{\ell+1} + \beta \mathbf{e}_{\ell+1}^2 + \gamma \|h_{\ell+1} \lambda P_{\ell+1} u\|^2 \leq \rho_2 (\mu_\ell + \beta \mathbf{e}_\ell^2 + \gamma \|h_\ell \lambda P_\ell u\|^2).$$

Choose $\delta := C_{\text{qo}} / (\varepsilon^2 c_d)$ and $\varepsilon < 2 \zeta C_{\text{qo}}^{-1}$. The choice of sufficiently small ζ , ε and $\|h_0\|_\infty$ yields $\rho_2 < 1$. \blacksquare

5.9. Optimal Convergence Rates

This section is devoted to the proof of Theorem 5.13 which follows the steps of Section 4.5. The optimality proof of this section is concerned with the simultaneous error of all eigenfunction approximations. Consider

$$\Xi_\ell^2 := \mu_\ell^2(\mathcal{T}_\ell) + \beta \sum_{j \in J} \|u_j - \Lambda_\ell u_j\|_{\text{NC}}^2 + \gamma \sum_{j \in J} \|h_\ell \lambda_j P_\ell u_j\|^2 \quad \text{for all } \ell \in \mathbb{N}_0$$

for the parameters β and γ from Proposition 5.22. The proof excludes the pathological case $\Xi_0 = 0$. Choose $0 < \tau \leq \sum_{j \in J} |u_j|_{\mathfrak{A}_\sigma^{\text{NC}, \Delta}}^2 / \Xi_0^2$, and set $\varepsilon(\ell) := \sqrt{\tau} \Xi_\ell$. Let $N(\ell) \in \mathbb{N}$ be minimal with the property

$$\sum_{j \in J} |u_j|_{\mathfrak{A}_\sigma^{\text{NC}, \Delta}}^2 \leq \varepsilon(\ell)^2 N(\ell)^{2\sigma}.$$

Let for a fixed $\ell \in \mathbb{N}$, $\tilde{\mathcal{T}}_\ell \in \mathbb{T}$ denote the optimal triangulation of cardinality

$$\text{card}(\tilde{\mathcal{T}}_\ell) \leq \text{card}(\mathcal{T}_0) + N(\ell)$$

in the sense that the projection $\tilde{\Lambda} := \Lambda_{\tilde{\mathcal{T}}_\ell}$ with respect to $\tilde{\mathcal{T}}_\ell$ satisfies

$$\sum_{j \in J} \|u_j - \tilde{\Lambda} u_j\|_{\text{NC}}^2 \leq N(\ell)^{-2\sigma} \sum_{j \in J} |u_j|_{\mathfrak{A}_\sigma^{\text{NC}, \Delta}}^2 \leq \varepsilon(\ell)^2 \quad (5.19)$$

and define $\hat{\mathcal{T}}_\ell := \mathcal{T}_\ell \otimes \tilde{\mathcal{T}}_\ell$ as the overlay of Definition 2.11. The arguments of Section 4.5 lead to

$$\text{card}(\mathcal{T}_\ell \setminus \hat{\mathcal{T}}_\ell) \leq N(\ell) \leq 2 \left(\sum_{j \in J} |u_j|_{\mathfrak{A}_\sigma^{\text{NC}, \Delta}}^2 \right)^{1/(2\sigma)} \varepsilon(\ell)^{-1/\sigma}. \quad (5.20)$$

Let $\hat{\Lambda} := \Lambda_{\hat{\mathcal{T}}_\ell}$ denote the projection with respect to $\hat{\mathcal{T}}_\ell$.

Lemma 5.23. *Provided $\|h_0\|_\infty \ll 1$, it holds that*

$$\sum_{j \in J} \|u_j - \widehat{\Lambda} u_j\|_{\text{NC}}^2 \lesssim \varepsilon(\ell)^2.$$

Proof. Recall that by definition of the overlay (Definition 2.11) the triangulations $\widehat{\mathcal{T}}_\ell \in \mathbb{T}(\widetilde{\mathcal{T}}_\ell)$ and $\widetilde{\mathcal{T}}_\ell$ are nested. Hence, the best-approximation result of Proposition 5.10 and (5.19) prove

$$\sum_{j \in J} \|u_j - \widehat{\Lambda} u_j\|_{\text{NC}}^2 \lesssim \sum_{j \in J} \|u_j - \widetilde{\Lambda} u_j\|_{\text{NC}}^2 \leq \varepsilon(\ell)^2. \quad \blacksquare$$

Lemma 5.24 (key argument). *Provided $\|h_0\|_\infty \ll 1$, there exists $C_2 \approx 1$ such that*

$$\mu_\ell^2(\mathcal{T}_\ell) \leq C_2 \mu_\ell^2(\mathcal{T}_\ell \setminus \widehat{\mathcal{T}}_\ell).$$

Proof. The triangle inequality and the Young inequality from Proposition 2.30 imply for any $j \in J$, that

$$\|u_j - \Lambda_\ell u_j\|_{\text{NC}}^2 \leq 2\|u_j - \widehat{\Lambda} u_j\|_{\text{NC}}^2 + 2\|\widehat{\Lambda} u_j - \Lambda_\ell u_j\|_{\text{NC}}^2.$$

Hence, the discrete reliability from Proposition 5.16 leads to

$$\begin{aligned} \|u_j - \Lambda_\ell u_j\|_{\text{NC}}^2 &\leq (2 + C_{\text{drel}}^2 \lambda_j^2 \|h_0\|_\infty^{2s} (1 + M_J)^2 C_{L^2}^2) \|u_j - \widehat{\Lambda} u_j\|_{\text{NC}}^2 \\ &\quad + C_{\text{drel}}^2 \lambda_j^2 \|h_0\|_\infty^{2s} (1 + M_J)^2 C_{L^2}^2 \|u_j - \Lambda_\ell u_j\|_{\text{NC}}^2 \\ &\quad + C_{\text{drel}}^2 \mu_\ell^2(\mathcal{T}_\ell \setminus \widehat{\mathcal{T}}_\ell, \lambda_j, u_j). \end{aligned}$$

The term with $\|u_j - \Lambda_\ell u_j\|_{\text{NC}}^2$ can be absorbed for sufficiently small $\|h_0\|_\infty \ll 1$. Therefore, Lemma 5.23 implies for constants $C_3 \approx 1 \approx C_4$ and $\|h_0\|_\infty \ll 1$ that

$$\sum_{j \in J} \|u_j - \Lambda_\ell u_j\|_{\text{NC}}^2 \leq C_3 \varepsilon(\ell)^2 + C_4 \mu_\ell^2(\mathcal{T}_\ell \setminus \widehat{\mathcal{T}}_\ell).$$

Let C_{eq} denote the constant of $C_3 \Xi_\ell^2 \leq C_{\text{eq}} \mu_\ell^2(\mathcal{T}_\ell)$ (which exists by reliability). The efficiency (5.18), the definition of $\varepsilon(\ell)$ and the preceding estimates prove

$$\begin{aligned} C_{\text{eff}}^{-2} \mu_\ell^2(\mathcal{T}_\ell) &\leq C_3 \varepsilon(\ell)^2 + C_4 \mu_\ell^2(\mathcal{T}_\ell \setminus \widehat{\mathcal{T}}_\ell) \\ &\leq \tau C_{\text{eq}} \mu_\ell^2(\mathcal{T}_\ell) + C_4 \mu_\ell^2(\mathcal{T}_\ell \setminus \widehat{\mathcal{T}}_\ell). \end{aligned}$$

For a sufficiently small choice of τ , the constant $C_2 := (C_{\text{eff}}^{-2} - \tau C_{\text{eq}})^{-1} C_4$ is positive. \blacksquare

The finish of the optimality proof follows the arguments of [Cascon et al., 2008, Stevenson, 2007]. The proof is identical to that of Lemma 4.20 and therefore omitted.

Lemma 5.25 (finish of the optimality proof). *The choice*

$$0 < \theta \leq 1 / (C_2 (B/A)^4 (2N^2 + 4N^3))$$

implies the existence of a constant $C(\sigma)$ such that

$$(\text{card}(\mathcal{T}_\ell) - \text{card}(\mathcal{T}_0))^\sigma \left(\sum_{j \in J} \|u_j - \Lambda_\ell u_j\|_{\text{NC}}^2 \right)^{1/2} \leq C(\sigma) \left(\sum_{j \in J} |u_j|_{\mathfrak{H}_\sigma^{\text{NC}, \Delta}}^2 \right)^{1/2}. \quad \blacksquare$$

6. Eigenvalues of the Stokes System

One important advantage of the nonconforming \mathcal{P}_1 finite element method is that it provides a stable low-order discretisation of the Stokes equations [Crouzeix and Raviart, 1973]. The strong form of the linear Stokes equations for a given force f seeks the velocity field u and the pressure p such that

$$-\Delta u + (Dp)^\top = f \text{ and } \operatorname{div} u = 0 \text{ in } \Omega, \quad u|_{\partial\Omega} = 0.$$

Conforming finite elements satisfying the constraint $\operatorname{div} u = 0$ pointwise a.e. are rather complicated [see Scott and Vogelius, 1985, Guzmán and Neilan, 2014]. The nonconforming \mathcal{P}_1 finite element satisfies the favourable local mass-conservation property for the piecewise divergence.

6.1. Nonconforming Discretisation of the Stokes Equations

Let $V := H_0^1(\Omega; \mathbb{R}^d)$ and $M := L_0^2(\Omega)$ and define the bilinear form

$$a(v, w) := (Dv, Dw)_{L^2(\Omega)} \quad \text{for all } (v, w) \in V^2$$

with induced norm $\|\cdot\|$. Furthermore define

$$b(v, q) := -(\operatorname{div} v, q)_{L^2(\Omega)} \quad \text{for all } (v, q) \in V \times M$$

and set $c(\cdot, \cdot) := (\cdot, \cdot)_{L^2(\Omega)}$ with $\|\cdot\| := \|\cdot\|_{L^2(\Omega)}$.

Given $f \in L^2(\Omega; \mathbb{R}^d)$, the linear Stokes problem seeks $(u, p) \in V \times M$ such that

$$\begin{aligned} a(u, v) + b(v, p) &= c(f, v) & \text{for all } v \in V, \\ b(u, q) &= 0 & \text{for all } q \in M. \end{aligned} \tag{6.1}$$

This mixed system can be reformulated as an elliptic problem. Let $Z := \{v \in V \mid \operatorname{div} v = 0\}$ denote the space of divergence-free vector fields. Problem (6.1) is equivalent to

$$a(u, v) = c(f, v) \quad \text{for all } v \in Z \tag{6.2}$$

and the pressure variable p plays the role of a Lagrange multiplier. The equivalence with (6.1) follows from the Ladyzhenskaya lemma [Brenner and Scott, 2008, Acosta et al., 2006] which states that the divergence operator $\operatorname{div} : V \rightarrow M$ has a continuous right-inverse. Note that (6.1) carries more information than (6.2) in the sense that the pressure variable p extracts information from $f \in L^2(\Omega; \mathbb{R}^d)$ even if f is zero as an element of the dual space Z^* .

The nonconforming \mathcal{P}_1 finite element discretisation of the linear Stokes equations is based on the nonconforming finite element space $V_\ell := [\mathcal{CR}_0^1(\mathcal{T}_\ell)]^d$ from Definition 5.1 and $M_\ell := \mathcal{P}_0(\mathcal{T}_\ell) \cap L_0^2(\Omega)$ and the bilinear forms

$$a_{\text{NC}}(v_\ell, w_\ell) := (D_{\text{NC}} v_\ell, D_{\text{NC}} w_\ell)_{L^2(\Omega)} \quad \text{for all } (v_\ell, w_\ell) \in V_\ell^2$$

6. Eigenvalues of the Stokes System

with induced norm $\|\cdot\|_{\text{NC}}$ and

$$b_{\text{NC}}(v_\ell, q_\ell) := -(\text{div}_{\text{NC}} v_\ell, q_\ell)_{L^2(\Omega)} \quad \text{for all } (v_\ell, q_\ell) \in V_\ell \times M_\ell.$$

The nonconforming FEM seeks $(u_\ell, p_\ell) \in V_\ell \times M_\ell$ such that

$$\begin{aligned} a_{\text{NC}}(u_\ell, v_\ell) + b_{\text{NC}}(v_\ell, p_\ell) &= c(f, v_\ell) & \text{for all } v_\ell \in V_\ell, \\ b_{\text{NC}}(u_\ell, q_\ell) &= 0 & \text{for all } q_\ell \in M_\ell. \end{aligned} \quad (6.3)$$

The well-posedness of this problem follows from the discrete inf-sup condition [Boffi et al., 2013]

$$0 < \beta \leq \inf_{q_\ell \in M_\ell \setminus \{0\}} \sup_{v_\ell \in V_\ell \setminus \{0\}} \frac{b_{\text{NC}}(v_\ell, q_\ell)}{\|v_\ell\|_{\text{NC}} \|q_\ell\|}. \quad (6.4)$$

It is well known [Boffi et al., 2013] that this condition is not satisfied when V_ℓ is the space of H_0^1 -conforming $\mathcal{P}_1(\mathcal{T}_\ell)$ vector fields. The nonconforming \mathcal{P}_1 finite element space is “richer” in the sense that the piecewise divergence div_{NC} is a surjective mapping onto M_ℓ .

Obviously, the discrete solution u_ℓ of (6.3) is piecewise divergence-free, $\text{div}_{\text{NC}} u_\ell = 0$. The equivalent formulation based on the space $Z_\ell := \{v_\ell \in V_\ell \mid \text{div}_{\text{NC}} v_\ell = 0\}$ reads as

$$a_{\text{NC}}(u_\ell, v_\ell) = b(f, v_\ell) \quad \text{for all } v_\ell \in Z_\ell. \quad (6.5)$$

For a construction of a basis of Z_ℓ in two space dimensions see, e.g., [Boffi et al., 2013, Braess, 2007]. In two space dimensions, problem (6.5) can be directly implemented via the streamfunction-vorticity formulation [Girault and Raviart, 1986] as described in Section 7.8. This leads to a positive definite system and (in 2D) to a diagonal mass matrix.

Note that the nonconforming interpolation operator $\mathcal{J}_\ell^{\text{CN}}$ maps the space Z onto Z_ℓ . This follows from the projection property (5.1).

It is well-established in the literature [Dari et al., 1995] and follows from the discrete inf-sup condition (6.4) of the system (6.3) that the error in the pressure variable can be controlled as

$$\|p - p_\ell\| \lesssim \|h_\ell f\| + \|u - u_\ell\|_{\text{NC}}. \quad (6.6)$$

The main difference to the analysis of the Laplace operator from Chapter 5 is that the pressure variable enters the analysis even if one considers the elliptic formulations (6.2) and (6.5). One reason is that the companion operator J_{d+1} from Proposition 5.4 does not map the space Z_ℓ on Z only. Also the efficiency error estimate of the volume term $\|h_\ell f\|$ leads to a pressure term on the right-hand side.

The following best-approximation result has been proved by Carstensen et al. [2014e] with techniques from the medius analysis [Gudi, 2010] for the case $d = 2$,

$$\|p - p_\ell\| + \|u - u_\ell\|_{\text{NC}} \lesssim \|(1 - \Pi_\ell^0)p\| + \|(1 - \Pi_\ell^0)Du\| + \text{osc}_{1,0}(f, \mathcal{T}_\ell).$$

The following result gives a generalisation to $d \geq 2$ space dimensions with a refined oscillation term.

Proposition 6.1 (best-approximation result). *Let $f \in L^2(\Omega; \mathbb{R}^d)$. Then, the solution $(u, p) \in V \times M$ of (6.1) and the discrete solution $(u_\ell, p_\ell) \in V_\ell \times M_\ell$ of (6.3) satisfy*

$$\|u - u_\ell\|_{\text{NC}} + \|p - p_\ell\| \lesssim \|(1 - \Pi_\ell^0)Du\|_{L^2(\Omega)} + \|(1 - \Pi_\ell^0)p\| + \text{osc}_{1,1}(f, \mathcal{T}_\ell).$$

Proof. The projection property (5.1) of the nonconforming interpolation operator $\mathcal{J}_\ell^{\mathfrak{C}\mathfrak{R}}$ and the Pythagoras theorem show that

$$\|u - u_\ell\|_{\text{NC}}^2 = \|u_\ell - \mathcal{J}_\ell^{\mathfrak{C}\mathfrak{R}} u\|_{\text{NC}}^2 + \|u - \mathcal{J}_\ell^{\mathfrak{C}\mathfrak{R}} u\|_{\text{NC}}^2.$$

Since $\|u - \mathcal{J}_\ell^{\mathfrak{C}\mathfrak{R}} u\|_{\text{NC}} = \|(1 - \Pi_\ell^0)Du\|$, it remains to estimate the first term on the right-hand side. Set $\varphi_\ell := u_\ell - \mathcal{J}_\ell^{\mathfrak{C}\mathfrak{R}} u$. The properties of the companion operator from Proposition 5.4 and $\text{div}_{\text{NC}} u_\ell = 0 = \text{div}_{\text{NC}} \mathcal{J}_\ell^{\mathfrak{C}\mathfrak{R}} u$ show that

$$\begin{aligned} \|u_\ell - \mathcal{J}_\ell^{\mathfrak{C}\mathfrak{R}} u\|_{\text{NC}}^2 &= a_{\text{NC}}(u_\ell - u, \varphi_\ell) \\ &= c(f, \varphi_\ell - J_{d+1} \varphi_\ell) - b_{\text{NC}}(\varphi_\ell - J_{d+1} \varphi_\ell, (1 - \Pi_\ell^0)p) + ((1 - \Pi_\ell^0)Du, D_{\text{NC}}(J_{d+1} - 1)\varphi_\ell)_{L^2(\Omega)}. \end{aligned}$$

The approximation and stability properties (5.4) show that this is bounded by

$$(\|h_\ell f\| + \|(1 - \Pi_\ell^0)p\| + \|u_\ell - \mathcal{J}_\ell^{\mathfrak{C}\mathfrak{R}} u\|_{\text{NC}}) \|\varphi_\ell\|_{\text{NC}}.$$

The efficiency $\|h_\ell f\| \lesssim \|(1 - \Pi_\ell^0)Du\| + \|(1 - \Pi_\ell^0)p\| + \text{osc}_{1,1}(f, \mathcal{T}_\ell)$ follows from arguments similar to those of Proposition 4.3. This and (6.6) conclude the proof. \blacksquare

Remark 6.2. One may ask whether possibly an estimate of the type

$$\|u - u_\ell\|_{\text{NC}} \lesssim \|(1 - \Pi_\ell^0)Du\| + \text{oscillations}$$

may be valid. To see that the estimate is indeed untrue consider the case of a simply-connected domain Ω for $d = 2$ and the constant right-hand side $f = (1, 1)$. Clearly, f is an irrotational vector field which implies that there is a function $\psi \in H^1(\Omega)$ such that $f = D\psi$. The integration by parts therefore shows that

$$c(f, v) = 0 \quad \text{for all } v \in Z.$$

Hence, $u = 0$ and the right-hand side of the estimate equals zero, while the left-hand side equals $\|u_\ell\|_{\text{NC}}$. The latter, however, is not zero because f does not represent the zero functional in the dual space Z_ℓ^* , although it is zero in Z^* . This is due to the fact that the integration by parts with functions $v_\ell \in Z_\ell$ leads to additional jump terms. \blacklozenge

The next result is an L^2 error estimate for arbitrary regularity of the solution. Let $0 < s \leq 1$ indicate the elliptic regularity of the problem (6.1) in the sense that [Fabes et al., 1988, Savaré, 1998]

$$\|u\|_{H^{1+s}(\Omega)} + \|p\|_{H^s(\Omega)} \leq C(s) \|f\|_{L^2(\Omega)}. \quad (6.7)$$

Proposition 6.3 (L^2 error control for the linear Stokes problem). *The exact solution $(u, p) \in V \times M$ of the linear problem (6.1) and its nonconforming finite element approximation $(u_\ell, p_\ell) \in V_\ell \times M_\ell$ from (6.3) satisfy*

$$\|u - u_\ell\| \lesssim \|h_\ell\|_\infty^s (\|u - u_\ell\|_{\text{NC}} + \|p - p_\ell\| + \text{osc}_{1,1}(f, \mathcal{T}_\ell)).$$

Proof. Let $(z, q) \in V \times M$ denote the solution of problem (6.1) with right-hand side $e := u - u_\ell$ and set $v := u - J_{d+1} u_\ell$ for the companion operator J_{d+1} from Proposition 5.4. Since $\Pi_\ell^0(u_\ell - J_{d+1} u_\ell) = 0$, it holds that

$$\begin{aligned} \|e\|^2 &= c(J_{d+1} u_\ell - u_\ell, e) + c(e, v) \\ &= (J_{d+1} u_\ell - u_\ell, (1 - \Pi_\ell^0)e)_{L^2(\Omega)} + a(z, v) + b(v, q). \end{aligned} \quad (6.8)$$

6. Eigenvalues of the Stokes System

Piecewise Poincaré inequalities and (5.4) lead to

$$(J_{d+1}u_\ell - u_\ell, (1 - \Pi_\ell^0)e)_{L^2(\Omega)} \lesssim \|h_0\|_\infty^2 \|e\|_{\text{NC}}^2.$$

The definition of v and $\text{div } u = 0 = \text{div}_{\text{NC}} u_\ell$ prove

$$a(z, v) + b(v, q) = a_{\text{NC}}(e, z) + a_{\text{NC}}((1 - J_{d+1})u_\ell, z) + b_{\text{NC}}(u_\ell - J_{d+1}u_\ell, q). \quad (6.9)$$

The projection property (5.1) of $\mathcal{J}_\ell^{\text{CR}}$ and the continuous and discrete problems (6.1) and (6.3) followed by the approximation and stability properties (5.2) of $\mathcal{J}_\ell^{\text{CR}}$ show for the first term on the right-hand side of (6.9) that

$$a_{\text{NC}}(e, z) = a(u, z) - a_{\text{NC}}(u_\ell, \mathcal{J}_\ell^{\text{CR}} z) = (f, z - \mathcal{J}_\ell^{\text{CR}} z)_{L^2(\Omega)} \lesssim \|h_\ell f\| \|(1 - \Pi_\ell^0)Dz\|.$$

Recall that $\text{div}_{\text{NC}} \mathcal{J}_\ell^{\text{CR}} z = \text{div } z = 0$. The projection property (5.3) and the stability (5.4) of J_{d+1} show for the second term on the right-hand side of (6.9) that

$$a_{\text{NC}}((1 - J_{d+1})u_\ell, z) = (D_{\text{NC}}(1 - J_{d+1})u_\ell, (1 - \Pi_\ell^0)Dz)_{L^2(\Omega)} \leq \|u - u_\ell\|_{\text{NC}} \|(1 - \Pi_\ell^0)Dz\|.$$

Since $\Pi_\ell^0 \text{div}(u_\ell - J_{d+1}u_\ell) = 0$, the third contribution of (6.9) satisfies

$$b_{\text{NC}}((u_\ell - J_{d+1}u_\ell), q) = b_{\text{NC}}(u_\ell - J_{d+1}u_\ell, (1 - \Pi_\ell^0)q) \leq \|u_\ell - J_{d+1}u_\ell\|_{\text{NC}} \|(1 - \Pi_\ell^0)q\|.$$

The best-approximation property (5.4) of J_{d+1} proves that $\|u_\ell - J_{d+1}u_\ell\|_{\text{NC}} \lesssim \|e\|_{\text{NC}}$. Altogether,

$$\|e\|_{L^2(\Omega)}^2 \lesssim \|h_0\|_\infty^2 \|e\|_{\text{NC}}^2 + \|h_\ell f\| \|(1 - \Pi_\ell^0)Dz\| + \|e\|_{\text{NC}} (\|(1 - \Pi_\ell^0)q\| + \|(1 - \Pi_\ell^0)Dz\|).$$

Standard a priori estimates [Brenner and Scott, 2008] and the elliptic regularity (6.7) imply

$$\|(1 - \Pi_\ell^0)Dz\| + \|(1 - \Pi_\ell^0)q\| \lesssim \|h_0\|_\infty^s \|e\|.$$

The combination of the above estimates proves

$$\|e\| \lesssim \|h_0\|_\infty^s (\|e\|_{\text{NC}} + \|h_\ell f\|).$$

An efficiency estimate similar to that of Proposition 4.3 proves

$$\|h_\ell f\| \lesssim \|(1 - \Pi_\ell^0)Du\| + \|(1 - \Pi_\ell^0)p\| + \text{osc}_{1,1}(f, \mathcal{T}_\ell).$$

This concludes the proof. ■

Remark 6.4. The right-hand side in Proposition 6.3 is also an upper bound for $p - p_\ell$ in the H^{-1} norm. Although the proof is not difficult, it is not given here because the H^{-1} error control is not required in the analysis of this thesis. ◆

6.2. Discretisation of the Stokes Eigenvalue Problem

The Stokes eigenvalue problem seeks $(\lambda, u, p) \in \mathbb{R} \times V \times M$ with $\|u\| = 1$ such that

$$\begin{aligned} a(u, v) + b(v, p) &= \lambda c(u, v) & \text{for all } v \in V, \\ b(u, q) &= 0 & \text{for all } q \in M. \end{aligned} \quad (6.10)$$

Although (λ, u, p) is rather a triple than a pair it is referred to as eigenpair and identified with the pair $(\lambda, (u, p))$. As in the foregoing section, an equivalent formulation reads as

$$a(u, v) = \lambda c(u, v) \quad \text{for all } v \in Z. \quad (6.11)$$

The nonconforming FEM seeks $(u_\ell, p_\ell) \in V_\ell \times M_\ell$ with $\|u_\ell\| = 1$ such that

$$\begin{aligned} a_{\text{NC}}(u_\ell, v_\ell) + b_{\text{NC}}(v_\ell, p_\ell) &= \lambda_\ell c(u_\ell, v_\ell) & \text{for all } v_\ell \in V_\ell, \\ b_{\text{NC}}(u_\ell, q_\ell) &= 0 & \text{for all } q_\ell \in M_\ell. \end{aligned} \quad (6.12)$$

An equivalent formulation reads as

$$a_{\text{NC}}(u_\ell, v_\ell) = \lambda_\ell c(u_\ell, v_\ell) \quad \text{for all } v_\ell \in Z_\ell. \quad (6.13)$$

The elliptic formulation on the spaces Z and Z_ℓ shows that this problem fits in the framework of Section 3.1 (where b from Section 3.1 is replaced by c) with exact and discrete eigenvalues

$$0 < \lambda_1 \leq \lambda_2 \leq \dots \quad \text{and} \quad 0 < \lambda_{\ell,1} \leq \dots \leq \lambda_{\ell, \dim(Z_\ell)}$$

and their corresponding c -orthonormal systems of eigenfunctions

$$(u_1, u_2, u_3, \dots) \in Z^\mathbb{N} \quad \text{and} \quad (u_{\ell,1}, u_{\ell,2}, \dots, u_{\ell, \dim(Z_\ell)}) \in Z_\ell^{\dim(Z_\ell)}.$$

The corresponding pressures are denoted by p_1, p_2, \dots and $p_{\ell,1}, \dots, p_{\ell, \dim(Z_\ell)}$, respectively. Recall the definitions of Section 3.1: The set $J = \{n+1, \dots, n+N\}$ describes the eigenvalue cluster of interest and $W := \text{span}\{u_j \mid j \in J\} \subseteq Z$ and $W_\ell := \text{span}\{u_{\ell,j} \mid j \in J\} \subseteq Z_\ell$ are the exact and discrete invariant subspaces (not necessarily eigenspaces) related to the cluster. In the present situation, the quasi-Ritz projection R_ℓ from Definition 3.1 maps the solution $u \in Z$ of the linear problem (6.2) to the solution $R_\ell u \in Z_\ell$ of the discrete linear problem (6.5). The L^2 projection onto W_ℓ is denoted by $P_{\mathcal{T}_\ell} := P_\ell$. Furthermore $\Lambda_{\mathcal{T}_\ell} := \Lambda_\ell := P_\ell \circ R_\ell$. In view of Lemma 3.4, the discrete pressure $p(\Lambda_\ell u) \in M_\ell$ corresponding to $\Lambda_\ell u$ is defined via

$$a_{\text{NC}}(\Lambda_\ell u, v_\ell) + b_{\text{NC}}(v_\ell, p(\Lambda_\ell u)) = \lambda c(P_\ell u, v_\ell) \quad \text{for all } v_\ell \in V_\ell. \quad (6.14)$$

It is not difficult to see that $p(\Lambda_\ell u)$ is well-defined: Lemma 3.4 shows that $\Lambda_\ell u$ solves the discrete source problem (6.5) with right-hand side $f = P_\ell u$. Hence, $p(\Lambda_\ell u)$ is the discrete pressure (or Lagrange multiplier) of (6.3).

The following result gives an L^2 error estimate for the eigenfunctions.

Proposition 6.5 (L^2 error estimate). *Provided $\|h_0\|_\infty \ll 1$, there exists a constant C_{L^2} such that any eigenpair $(\lambda, u, p) \in \mathbb{R} \times W \times M$ of (6.10) with $\|u\| = 1$ satisfies*

$$\|u - P_\ell u\| \leq \|u - \Lambda_\ell u\| \leq C_{L^2}(1 + M_J) \|h_0\|_\infty^s (\|(1 - \Pi_\ell^0)Du\|_{L^2(\Omega)} + \|(1 - \Pi_\ell^0)p\|).$$

6. Eigenvalues of the Stokes System

Proof. Proposition 3.3 and the L^2 error estimate from Proposition 6.3 result in the following inequality for the solution $(R_\ell u, p(R_\ell u))$ of (6.3) to the right-hand side $f := \lambda u$,

$$\|u - P_\ell u\| \leq \|u - \Lambda_\ell u\| \lesssim (1 + M_J) \|h_\ell\|_\infty^s (\|u - R_\ell u\|_{\text{NC}} + \|p - p(R_\ell u)\| + \text{osc}_{1,1}(\lambda u, \mathcal{T}_\ell)).$$

The best-approximation result for the linear Stokes problem (Proposition 6.1) therefore yields

$$\|u - \Lambda_\ell u\| \lesssim (1 + M_J) \|h_\ell\|_\infty^s (\|(1 - \Pi_\ell^0)Du\| + \|(1 - \Pi_\ell^0)p\| + \text{osc}_{1,1}(\lambda u, \mathcal{T}_\ell)).$$

If the initial mesh-size is sufficiently small, the discrete Friedrichs inequality (Proposition 2.32) allows to absorb the oscillation terms on the right-hand side. \blacksquare

The L^2 error control and the best-approximation of the quasi-Ritz projection from Proposition 6.1 result in the following best-approximation property for the eigenfunction approximation.

Proposition 6.6 (best-approximation property). *Provided the initial mesh-size is sufficiently fine $\|h_0\|_\infty \ll 1$, any eigenpair $(\lambda, u, p) \in \mathbb{R} \times W \times M$ of (6.12) with $\|u\| = 1$ satisfies*

$$\|u - \Lambda_\ell u\|_{\text{NC}} + \|p - p(\Lambda_\ell u)\| \lesssim \|(1 - \Pi_\ell^0)Du\|_{L^2(\Omega)} + \|(1 - \Pi_\ell^0)p\|_{L^2(\Omega)}.$$

Proof. The L^2 control of Proposition 6.5 and the best-approximation result for the linear case of Proposition 6.1 enable the arguments from the proof of Proposition 5.10. The details are omitted for brevity. \blacksquare

The fact that the nonconforming interpolation operator $\mathcal{J}_\ell^{\text{CN}}$ maps divergence-free functions to the space Z_ℓ of piecewise divergence-free discrete functions leads to guaranteed lower bounds as in Section 5.5. For the constant C that satisfies (see (5.2))

$$\|v - \mathcal{J}_\ell^{\text{CN}} v\|_{L^2(\Omega)} \leq Ch_T \|D_{\text{NC}}(v - \mathcal{J}_\ell^{\text{CN}} v)\|_{L^2(\Omega)} \quad \text{for all } v \in V \text{ and all } T \in \mathcal{T}_\ell,$$

the lower bound for the eigenvalue λ_j reads as

$$\lambda_{\ell,j} / (1 + C^2 \|h_\ell\|_\infty^2 \lambda_{\ell,j}) \leq \lambda_j. \quad (6.15)$$

For the case $d = 2$, the explicit error estimate of Proposition 5.3 results in the lower bound

$$\lambda_{\ell,j} / (1 + \kappa_{\text{CN}}^2 \max_{T \in \mathcal{T}_\ell} \text{diam}(T)^2 \lambda_{\ell,j}) \leq \lambda_j.$$

This is essentially the idea of Carstensen and Gedicke [2014] and Carstensen and Gallistl [2014] applied to the eigenvalues of the Stokes system.

6.3. Adaptive Algorithm

This section presents the adaptive algorithm and the optimality results.

The computable error estimator that acts as refinement indicator is essentially that of Chapter 5. For the linear Stokes problem this type of error estimator without pressure contribution was introduced by Dari et al. [1995].

For any simplex $T \in \mathcal{T}_\ell$, the explicit residual-based error estimator consists of the sum of the residuals of the computed discrete eigenfunctions $(u_{\ell,j})_{j \in J}$,

$$\eta_\ell^2(T) := \sum_{j \in J} \left(h_T^2 \|\lambda_{\ell,j} u_{\ell,j}\|_{L^2(T)}^2 + \sum_{F \in \mathcal{F}(T)} h_T^{-1} \|[u_{\ell,j}]_F\|_{L^2(F)}^2 \right).$$

Let, for any subset $\mathcal{K} \subseteq \mathcal{T}$,

$$\eta_\ell^2(\mathcal{K}) := \sum_{T \in \mathcal{K}} \eta_\ell^2(T).$$

The adaptive algorithm is driven by this computable error estimator and runs the following loop.

Algorithm 6.7 (AFEM for the Stokes eigenvalue problem).

Input: Initial triangulation \mathcal{T}_0 , bulk parameter $0 < \theta \leq 1$.

for $\ell = 0, 1, 2, \dots$ **do**

Solve. Compute discrete eigenpairs $(\lambda_{\ell,j}, u_{\ell,j}, p_{\ell,j})_{j \in J}$ of (6.13) with respect to \mathcal{T}_ℓ .

Estimate. Compute local contributions of the error estimator $(\eta_\ell^2(T))_{T \in \mathcal{T}_\ell}$.

Mark. Choose a minimal subset $\mathcal{M}_\ell \subseteq \mathcal{T}_\ell$ such that $\theta \eta_\ell^2(\mathcal{T}_\ell) \leq \eta_\ell^2(\mathcal{M}_\ell)$.

Refine. Generate $\mathcal{T}_{\ell+1} := \text{refine}(\mathcal{T}_\ell, \mathcal{M}_\ell)$ with Algorithm 2.15.

end for

Output: Sequences of triangulations $(\mathcal{T}_\ell)_\ell$ and discrete solutions $((\lambda_{\ell,j}, u_{\ell,j}, p_{\ell,j})_{j \in J})_\ell$. \blacklozenge

Remark 6.8. As in the foregoing chapters, all algebraic eigenvalue problems are assumed to be solved exactly. The analysis of this chapter carries over to practical algorithms as Algorithm 3.17 by perturbation arguments as in [Carstensen, Gallistl, and Schedensack, 2014c]. \blacklozenge

Define the seminorm

$$|(u, p)|_{\mathfrak{A}_\sigma^{\text{Stokes}}} := \sup_{m \in \mathbb{N}} m^\sigma \inf_{\mathcal{T} \in \mathbb{T}(m)} (\|(1 - \Pi_\mathcal{T}^0)Du\| + \|(1 - \Pi_\mathcal{T}^0)p\|)$$

and the approximation class

$$\mathfrak{A}_\sigma^{\text{Stokes}} := \left\{ (v, q) \in V \times M \mid |(v, q)|_{\mathfrak{A}_\sigma^{\text{Stokes}}} < \infty \right\}.$$

The set $\mathfrak{A}_\sigma^{\text{Stokes}}$ does not depend on the finite element method and instead concerns the approximability of the derivative and the pressure variable by piecewise constant functions. As in Chapters 4 and 5, an alternative set, also referred to as approximation class, is used for proving optimal convergence rates

$$\mathfrak{A}_\sigma^{\text{NC,Stokes}} := \left\{ (u, p) \in V \times M \mid |u|_{\mathfrak{A}_\sigma^{\text{NC,Stokes}}} < \infty \right\}$$

for

$$|(u, p)|_{\mathfrak{A}_\sigma^{\text{NC,Stokes}}} := \sup_{m \in \mathbb{N}} m^\sigma \inf_{\mathcal{T} \in \mathbb{T}(m)} (\|u - \Lambda_\mathcal{T} u\|_{\text{NC}} + \|p - p(\Lambda_\mathcal{T} u)\|).$$

Proposition 6.6 establishes the equivalence of those two approximation classes in the sense that any eigenfunction $(u, p) \in W \times M$ satisfies $(u, p) \in \mathfrak{A}_\sigma^{\text{Stokes}}$ if and only if $(u, p) \in \mathfrak{A}_\sigma^{\text{NC,Stokes}}$. The following theorem states optimality of Algorithm 6.7. The proof will be given in the remaining sections of this chapter.

6. Eigenvalues of the Stokes System

Theorem 6.9 (optimal convergence rates). *Provided the bulk parameter $\theta \ll 1$ and the initial mesh-size $\|h_0\|_\infty \ll 1$ are sufficiently small, Algorithm 6.7 computes triangulations $(\mathcal{T}_\ell)_\ell$ and discrete eigenpairs $((\lambda_{\ell,j}, u_{\ell,j}, p_{\ell,j}))_{j \in J}_\ell$ with optimal rate of convergence in the sense that, for some constant C_{opt} , it holds that*

$$\begin{aligned} \sup_{\ell \in \mathbb{N}} (\text{card}(\mathcal{T}_\ell) - \text{card}(\mathcal{T}_0))^\sigma \left(\sum_{j \in J} (\|u_j - \Lambda_\ell u_j\|_{\text{NC}}^2 + \|p_j - p(\Lambda_\ell u_j)\|^2) \right)^{1/2} \\ \leq C_{\text{opt}} \left(\sum_{j \in J} |(u_j, p_j)|_{\mathfrak{A}_\sigma^{\text{NC}, \text{Stokes}}}^2 \right)^{1/2}. \end{aligned}$$

Let for any $w \in W$ with the representation $w = \sum_{j \in J} \alpha_j u_j$ the corresponding pressure be defined as $p(w) := \sum_{j \in J} \alpha_j p_j$. For any $v_\ell \in W_\ell$ with representation $v_\ell = \sum_{j \in J} \beta_j \Lambda_\ell u_j$ define $p(v_\ell) := \sum_{j \in J} \beta_j p(\Lambda_\ell u_j)$. Proposition 6.6 implies the following immediate consequence.

Corollary 6.10. *Provided the bulk parameter $\theta \ll 1$ and the initial mesh-size $\|h_0\|_\infty \ll 1$ are sufficiently small, Algorithm 6.7 computes triangulations $(\mathcal{T}_\ell)_\ell$ and discrete eigenpairs $((\lambda_{\ell,j}, u_{\ell,j}, p_{\ell,j}))_{j \in J}_\ell$ with optimal rate of convergence in the sense that*

$$\begin{aligned} \sup_{\ell \in \mathbb{N}} (\text{card}(\mathcal{T}_\ell) - \text{card}(\mathcal{T}_0))^\sigma \sup_{\substack{w \in W \\ \|w\|=1}} \inf_{v_\ell \in W_\ell} (\|w - v_\ell\|_{\text{NC}}^2 + \|p(w) - p(v_\ell)\|^2)^{1/2} \\ \lesssim \left(\sum_{j \in J} |(u_j, p_j)|_{\mathfrak{A}_\sigma^{\text{Stokes}}}^2 \right)^{1/2}. \quad \blacksquare \end{aligned}$$

The optimal convergence rate for the error of the eigenvalues will be given in Corollary 8.19.

Remark 6.11 (optimality for inexact solve). The optimality results of Theorem 6.9 and Corollary 6.10 carry over to Algorithm 3.17 for sufficiently small $\varkappa \ll 1$ by means of a perturbation analysis as in [Carstensen and Gedicke, 2012] or [Carstensen, Gallistl, and Schedensack, 2014c]. \blacklozenge

6.4. Theoretical Error Estimator and Discrete Reliability

The analysis relies on a theoretical, non-computable error estimator that does not depend on the choice of the discrete eigenfunctions. Given an eigenpair (λ, u) , the theoretical error estimator includes the elementwise residuals in terms of $P_\ell u$ and $\Lambda_\ell u$. More precisely, define, for any $T \in \mathcal{T}_\ell$,

$$\mu_\ell^2(T, \lambda, u) := h_T^2 \|\lambda P_\ell u\|_{L^2(T)}^2 + \sum_{F \in \mathcal{F}(T)} h_T^{-1} \|\Lambda_\ell u\|_{L^2(F)}^2$$

and, for any subset $\mathcal{K} \subseteq \mathcal{T}_\ell$,

$$\mu_\ell^2(\mathcal{K}, \lambda_j, u_j) := \sum_{T \in \mathcal{K}} \mu_\ell^2(T, \lambda_j, u_j) \quad \text{and} \quad \mu_\ell^2(\mathcal{K}) := \sum_{j \in J} \mu_\ell^2(\mathcal{K}, \lambda_j, u_j).$$

Note that the pressure variable does not contribute to the error estimator.

The following shorthand notation for higher-order terms will be frequently used in the remaining parts of this chapter. For $(\ell, m) \in \mathbb{N}_0^2$ define

$$\begin{aligned} \mathbf{r}_{\ell,m} := & \|h_0\|_\infty^s (1 + M_J) C_{L^2} \left(\|p - p(\Lambda_\ell u)\|^2 + \|p - p(\Lambda_{\ell+m} u)\|^2 \right. \\ & \left. + \|u - u_\ell\|_{\text{NC}}^2 + \|u - u_{\ell+m}\|_{\text{NC}}^2 \right)^{1/2}. \end{aligned} \quad (6.16)$$

The following result states the discrete reliability for the theoretical error estimator. The discrete reliability for the linear Stokes problem was first established by Hu and Xu [2013a]. The proof presented here is valid for the eigenvalue problem and any space dimension.

Proposition 6.12 (discrete reliability). *There exists a constant $C_{\text{drel}} \approx 1$ such that, for any eigenpair $(\lambda, u, p) \in \mathbb{R} \times W \times M$ of (6.10) with $\|u\| = 1$, any admissible refinement $\mathcal{T}_{\ell+m} \in \mathbb{T}(\mathcal{T}_\ell)$ of $\mathcal{T}_\ell \in \mathbb{T}$ and the respective discrete eigenfunction approximations $\Lambda_\ell u \in V_\ell$ and $\Lambda_{\ell+m} u \in V_{\ell+m}$ satisfy*

$$\|p(\Lambda_{\ell+m} u) - p(\Lambda_\ell u)\|^2 \lesssim \|(\Lambda_{\ell+m} - \Lambda_\ell)u\|_{\text{NC}}^2 + \|h_\ell \lambda P_\ell u\|_{L^2(\cup \mathcal{T}_\ell \setminus \mathcal{T}_{\ell+m})}^2 + \mathbf{r}_{\ell,m}^2, \quad (6.17)$$

$$2(\|(\Lambda_{\ell+m} - \Lambda_\ell)u\|_{\text{NC}}^2 + \|p(\Lambda_{\ell+m} u) - p(\Lambda_\ell u)\|^2) \leq C_{\text{drel}}^2 (\mu_\ell^2(\mathcal{T}_\ell \setminus \mathcal{T}_{\ell+m}) + \mathbf{r}_{\ell,m}^2). \quad (6.18)$$

Proof. The discrete inf-sup condition (6.4) shows that there exists some $\varphi_{\ell+m} \in V_{\ell+m}$ with $\|\varphi_{\ell+m}\|_{\text{NC}} = 1$ such that

$$\|p(\Lambda_{\ell+m} u) - p(\Lambda_\ell u)\| \lesssim b_{\text{NC}}(\varphi_{\ell+m}, p(\Lambda_{\ell+m} u) - p(\Lambda_\ell u)).$$

The discrete eigenvalue problems on the levels $\ell + m$ and ℓ (recall Lemma 3.4 and (6.14)), some algebra and the integral mean property (5.1) of the nonconforming interpolation operator $\mathcal{J}_\ell^{\text{CN}}$ show that

$$\begin{aligned} b(\varphi_{\ell+m}, p(\Lambda_{\ell+m} u) - p(\Lambda_\ell u)) &= c(\lambda(P_{\ell+m} - P_\ell)u, \varphi_{\ell+m}) + c(\lambda P_\ell u, (1 - \mathcal{J}_\ell^{\text{CN}})\varphi_{\ell+m}) \\ &\quad - a_{\text{NC}}((\Lambda_{\ell+m} - \Lambda_\ell)u, \varphi_{\ell+m}). \end{aligned}$$

Proposition 6.5 and the discrete Friedrichs inequality from Proposition 2.32 control the first term on the right-hand side as

$$c(\lambda(P_{\ell+m} - P_\ell)u, \varphi_{\ell+m}) \lesssim \mathbf{r}_{\ell,m}.$$

This, the approximation and stability properties (5.2) and the discrete Friedrichs inequality (Proposition 2.32) for $\varphi_{\ell+m}$ prove (6.17).

Let $v_{\ell+m}$ denote the best-approximation with respect to the norm $\|\cdot\|_{\text{NC}}$ of $\Lambda_\ell u$ in $V_{\ell+m}$. The Pythagoras theorem

$$\|(\Lambda_{\ell+m} - \Lambda_\ell)u\|_{\text{NC}}^2 = \|\Lambda_{\ell+m} u - v_{\ell+m}\|_{\text{NC}}^2 + \|v_{\ell+m} - \Lambda_\ell u\|_{\text{NC}}^2 \quad (6.19)$$

proves together with (6.17) that

$$\begin{aligned} & \|p(\Lambda_{\ell+m} u) - p(\Lambda_\ell u)\|^2 + \|(\Lambda_{\ell+m} - \Lambda_\ell)u\|_{\text{NC}}^2 \\ & \lesssim \|\Lambda_{\ell+m} u - v_{\ell+m}\|_{\text{NC}}^2 + \|v_{\ell+m} - \Lambda_\ell u\|_{\text{NC}}^2 + \|h_\ell \lambda P_\ell u\|_{L^2(\cup \mathcal{T}_\ell \setminus \mathcal{T}_{\ell+m})}^2 + \mathbf{r}_{\ell,m}^2. \end{aligned} \quad (6.20)$$

6. Eigenvalues of the Stokes System

Set $\phi_{\ell+m} := \Lambda_{\ell+m}u - v_{\ell+m}$. Elementary algebra and the projection property (5.1) show

$$\|\Lambda_{\ell+m}u - v_{\ell+m}\|_{\text{NC}}^2 = a_{\text{NC}}(\Lambda_{\ell+m}u - v_{\ell+m}, \phi_{\ell+m}) = a_{\text{NC}}(\Lambda_{\ell+m}u, \phi_{\ell+m}) - a_{\text{NC}}(\Lambda_{\ell}u, \mathcal{J}_{\ell}^{\mathfrak{C}\mathfrak{R}}\phi_{\ell+m}).$$

The discrete eigenvalue problem (6.12) and the identity (6.14) show that this equals

$$\begin{aligned} & a_{\text{NC}}(\Lambda_{\ell+m}u, \phi_{\ell+m}) - a_{\text{NC}}(\Lambda_{\ell}u, \mathcal{J}_{\ell}^{\mathfrak{C}\mathfrak{R}}\phi_{\ell+m}) \\ &= c(\lambda P_{\ell+m}u, \phi_{\ell+m}) - c(\lambda P_{\ell}u, \mathcal{J}_{\ell}^{\mathfrak{C}\mathfrak{R}}\phi_{\ell+m}) - b_{\text{NC}}(\phi_{\ell+m}, p(\Lambda_{\ell+m}u)) + b_{\text{NC}}(\mathcal{J}_{\ell}^{\mathfrak{C}\mathfrak{R}}\phi_{\ell+m}, p(\Lambda_{\ell}u)). \end{aligned}$$

Since the velocity approximations $\Lambda_{\ell}u \in W_{\ell}$ and $\Lambda_{\ell+m}u \in W_{\ell+m}$ are piecewise divergence-free, the projection property of $\mathcal{J}_{\ell}^{\mathfrak{C}\mathfrak{R}}$ shows that

$$b_{\text{NC}}(\phi_{\ell+m}, p(\Lambda_{\ell+m}u)) - b_{\text{NC}}(\mathcal{J}_{\ell}^{\mathfrak{C}\mathfrak{R}}\phi_{\ell+m}, p(\Lambda_{\ell}u)) = b_{\text{NC}}(v_{\ell+m} - \Lambda_{\ell}u, p(\Lambda_{\ell}u) - p(\Lambda_{\ell+m}u)).$$

The combination of the foregoing three displayed formulae yields

$$\begin{aligned} \|\Lambda_{\ell+m}u - v_{\ell+m}\|_{\text{NC}}^2 &= \lambda c(P_{\ell+m}u - P_{\ell}u, \phi_{\ell+m}) + \lambda c(P_{\ell}u, \phi_{\ell+m} - \mathcal{J}_{\ell}^{\mathfrak{C}\mathfrak{R}}\phi_{\ell+m}) \\ &\quad + b_{\text{NC}}(v_{\ell+m} - \Lambda_{\ell}u, p(\Lambda_{\ell+m}u) - p(\Lambda_{\ell}u)). \end{aligned} \quad (6.21)$$

As above, Proposition 6.5 and the discrete Friedrichs inequality (Proposition 2.32) control the first contribution as

$$\lambda c(P_{\ell+m} - P_{\ell}u, \phi_{\ell+m}) \lesssim \mathbf{r}_{\ell,m} \|\phi_{\ell+m}\|_{\text{NC}}.$$

The approximation and stability properties of $\mathcal{J}_{\ell}^{\mathfrak{C}\mathfrak{R}}$ and the fact that $\mathcal{J}_{\ell}^{\mathfrak{C}\mathfrak{R}}\phi_{\ell+m}|_T = \phi_{\ell+m}|_T$ for all $T \in \mathcal{T}_{\ell} \setminus \mathcal{T}_{\ell+m}$ prove for the second term of (6.21) that

$$c(\lambda P_{\ell}u, \phi_{\ell+m} - \mathcal{J}_{\ell}^{\mathfrak{C}\mathfrak{R}}\phi_{\ell+m}) \lesssim \|h_{\ell}\lambda P_{\ell}u\|_{L^2(\cup \mathcal{T}_{\ell} \setminus \mathcal{T}_{\ell+m})} \|\phi_{\ell+m}\|_{\text{NC}}.$$

Therefore, the combination of (6.20)–(6.21) and the Young inequality from Proposition 2.30 prove for some constant $C \approx 1$ that

$$\begin{aligned} & \|p(\Lambda_{\ell+m}u) - p(\Lambda_{\ell}u)\|^2 + \|\Lambda_{\ell+m}u - \Lambda_{\ell}u\|_{\text{NC}}^2 \\ & \leq C \left(\|h_{\ell}\lambda P_{\ell}u\|_{L^2(\cup \mathcal{T}_{\ell} \setminus \mathcal{T}_{\ell+m})}^2 + \mathbf{r}_{\ell,m}^2 + \|v_{\ell+m} - \Lambda_{\ell}u\|_{\text{NC}}^2 \right) \\ & \quad + \frac{1}{2} \|\phi_{\ell+m}\|_{\text{NC}}^2 + \frac{1}{2} \|p(\Lambda_{\ell+m}u) - p(\Lambda_{\ell}u)\|^2. \end{aligned}$$

The Pythagoras theorem implies the stability $\|\phi_{\ell+m}\|_{\text{NC}} \leq \|(\Lambda_{\ell+m} - \Lambda_{\ell})u\|_{\text{NC}}$. Hence, the terms on the right-hand side with the prefactor 1/2 can be absorbed. The estimate

$$\|v_{\ell+m} - \Lambda_{\ell}u\|_{\text{NC}}^2 \lesssim \sum_{T \in \mathcal{T}_{\ell} \setminus \mathcal{T}_{\ell+m}} \sum_{F \in \mathcal{F}(T)} h_T^{-1} \|[\Lambda_{\ell}u]_F\|_{L^2(F)}^2$$

is proven in Theorem 5.5 and bounds the second contribution on the right-hand side of (6.19). \blacksquare

As in Section 5.7, the following reliability and efficiency are an immediate consequence of the discrete reliability.

Corollary 6.13 (reliability and efficiency). *Provided $\|h_0\|_\infty \ll 1$, any eigenpair $(\lambda, u, p) \in \mathbb{R} \times W \times M$ of (6.10) with $\|u\| = 1$ satisfies*

$$\|u - \Lambda_\ell u\|_{\text{NC}}^2 + \|p - p(\Lambda_\ell u)\|^2 \leq C_{\text{drel}}^2 \mu_\ell^2(\mathcal{T}_\ell, \lambda, u) \quad (6.22)$$

and, for some constant $C_{\text{eff}} \approx 1$,

$$\mu_\ell(\mathcal{T}_\ell, \lambda, u)^2 \leq C_{\text{eff}}^2 (\|u - \Lambda_\ell u\|_{\text{NC}}^2 + \|p - p(\Lambda_\ell u)\|^2). \quad (6.23)$$

Proof. Let $(\mathcal{T}_{\ell+m} \mid m \in \mathbb{N})$ be a sequence of nested refinements of \mathcal{T}_ℓ with $\|h_{\ell+m}\|_\infty \rightarrow 0$ as $m \rightarrow \infty$. The a priori convergence results (for instance Proposition 6.6) and the discrete reliability prove the reliability. The efficiency follows from the standard techniques of Verfürth [1996]. Higher-order terms are absorbed for $\|h_0\|_\infty \ll 1$. ■

6.5. Contraction Property and Optimal Convergence Rates

This section establishes optimal convergence rates of Algorithm 6.7. For the linear Stokes problem, the optimal convergence of AFEMs has been proven in [Becker and Mao, 2011, Hu and Xu, 2013a, Carstensen et al., 2013b].

The proof of optimal convergence rates follows in a similar way as for the eigenvalues of the Laplacian. The error estimator reduction is identical to that of Proposition 5.18.

Proposition 6.14 (quasi-orthogonality). *Under the hypothesis $\|h_0\|_\infty \ll 1$ there exists a constant C_{qo} such that any eigenpair $(\lambda, u, p) \in \mathbb{R} \times W \times M$ of (6.10) with $\|u\| = 1$, any $\mathcal{T}_\ell \in \mathbb{T}$ and any admissible refinement $\mathcal{T}_{\ell+m} \in \mathbb{T}(\mathcal{T}_\ell)$ satisfy*

$$|2a_{\text{NC}}(u - \Lambda_{\ell+m} u, \Lambda_{\ell+m} u - \Lambda_\ell u)| \leq C_{\text{qo}} (\|h_\ell \lambda P_\ell u\|_{L^2(\cup \mathcal{T}_\ell \setminus \mathcal{T}_{\ell+m})} + \mathbf{r}_{\ell+m}) \|u - \Lambda_{\ell+m} u\|_{\text{NC}}.$$

Proof. The nonconforming interpolation operator $\mathcal{I}_\ell^{\text{nc}}$ maps functions from Z as well as functions from $Z_{\ell+m}$ to the space Z_ℓ , i.e., it preserves the (piecewise) divergence-free property. Hence, the proof of Proposition 5.21 applies almost verbatim. The details are omitted. ■

Note that the quasi-orthogonality is stated for the velocity approximations only. A quasi-orthogonality of the pressure as in [Hu and Xu, 2013a] is not needed in this analysis.

Proposition 6.15 (contraction property). *Under the condition $\|h_0\|_\infty \ll 1$, there exist $0 < \rho_2 < 1$ and $0 < \beta, \gamma < \infty$ such that, for any eigenpair $(\lambda, u, P) \in \mathbb{R} \times W \times M$ of (6.10) with $\|u\| = 1$, the term $\xi_\ell^2 := \mu_\ell^2(\mathcal{T}_\ell, \lambda, u) + \beta \|u - \Lambda_\ell u\|^2 + \gamma \|h_\ell P_\ell u\|^2$ satisfies*

$$\xi_{\ell+1}^2 \leq \rho_2 \xi_\ell^2 \quad \text{for all } \ell \in \mathbb{N}_0.$$

Proof. The proof essentially follows the steps from Proposition 5.22. The pressure variable only arises in higher-order terms that are controlled by the error estimator. The details are omitted for brevity. ■

The proof of optimal convergence rates is almost identical to that presented in Section 5.9. The only difference is that the pressure term appears in certain estimates. The modifications are sketched in the remaining part of this section.

6. Eigenvalues of the Stokes System

Consider

$$\Xi_\ell^2 := \mu_\ell^2(\mathcal{T}_\ell) + \beta \sum_{j \in J} \|u_j - \Lambda_\ell u_j\|_{\text{NC}}^2 + \gamma \sum_{j \in J} \|h_\ell \lambda_j P_\ell u_j\|^2 \quad \text{for all } \ell \in \mathbb{N}_0$$

for the parameters β and γ from Proposition 6.15. Choose

$$0 < \tau \leq \sum_{j \in J} |(u_j, p_j)|_{\mathfrak{A}_\sigma^{\text{NC, Stokes}}}^2 / \Xi_0^2$$

and set $\varepsilon(\ell) := \sqrt{\tau} \Xi_\ell$. Let $N(\ell) \in \mathbb{N}$ be minimal with the property

$$\sum_{j \in J} |(u_j, p_j)|_{\mathfrak{A}_\sigma^{\text{NC, Stokes}}}^2 \leq \varepsilon(\ell)^2 N(\ell)^{2\sigma}.$$

Let $\tilde{\mathcal{T}}_\ell \in \mathbb{T}$ denote the optimal triangulation of cardinality

$$\text{card}(\tilde{\mathcal{T}}_\ell) \leq \text{card}(\mathcal{T}_0) + N(\ell)$$

in the sense that the projection $\tilde{\Lambda} := \Lambda_{\tilde{\mathcal{T}}_\ell}$ with respect to $\tilde{\mathcal{T}}_\ell$ satisfies

$$\sum_{j \in J} \left(\|u_j - \tilde{\Lambda} u_j\|_{\text{NC}}^2 + \|p_j - p(\tilde{\Lambda} u_j)\|^2 \right) \leq N(\ell)^{-2\sigma} \sum_{j \in J} |u_j|_{\mathfrak{A}_\sigma^{\text{NC, Stokes}}}^2 \leq \varepsilon(\ell)^2 \quad (6.24)$$

and define $\hat{\mathcal{T}}_\ell := \mathcal{T}_\ell \otimes \tilde{\mathcal{T}}_\ell$ as the overlay. The arguments of Section 4.5 lead to

$$\text{card}(\mathcal{T}_\ell \setminus \hat{\mathcal{T}}_\ell) \leq N(\ell) \leq 2 \left(\sum_{j \in J} |u_j|_{\mathfrak{A}_\sigma^{\text{NC, Stokes}}}^2 \right)^{1/(2\sigma)} \varepsilon(\ell)^{-1/\sigma}.$$

Let $\hat{\Lambda} := \Lambda_{\hat{\mathcal{T}}_\ell}$ denote the projection with respect to $\hat{\mathcal{T}}_\ell$.

Lemma 6.16. *Provided $\|h_0\|_\infty \ll 1$, it holds that*

$$\sum_{j \in J} \left(\|u_j - \hat{\Lambda} u_j\|_{\text{NC}}^2 + \|p_j - p(\hat{\Lambda} u_j)\|^2 \right) \lesssim \varepsilon(\ell)^2.$$

Proof. As in the proof of Lemma 5.23, recall that by definition of the overlay (Definition 2.11) the triangulations $\hat{\mathcal{T}}_\ell \in \mathbb{T}(\tilde{\mathcal{T}}_\ell)$ and $\tilde{\mathcal{T}}_\ell$ are nested. Hence, the best-approximation result of Proposition 6.6 and (6.24) prove

$$\sum_{j \in J} \left(\|u_j - \hat{\Lambda} u_j\|_{\text{NC}}^2 + \|p_j - p(\hat{\Lambda} u_j)\|^2 \right) \lesssim \sum_{j \in J} \left(\|u_j - \tilde{\Lambda} u_j\|_{\text{NC}}^2 + \|p_j - p(\tilde{\Lambda} u_j)\|^2 \right) \leq \varepsilon(\ell)^2. \quad \blacksquare$$

Lemma 6.17 (key argument). *Provided $\|h_0\|_\infty \ll 1$, there exists $C_2 \approx 1$ such that*

$$\mu_\ell^2(\mathcal{T}_\ell) \leq C_2 \mu_\ell^2(\mathcal{T}_\ell \setminus \hat{\mathcal{T}}_\ell).$$

Proof. The discrete reliability from Proposition 6.12, the efficiency from Corollary 6.13 and the arguments of Lemma 5.24 lead to the desired estimate. The details are omitted for brevity. \blacksquare

The finish of the optimality proof is identical to that of Lemma 4.20.

Lemma 6.18 (finish of the optimality proof). *The choice*

$$0 < \theta \leq 1 / (C_2(B/A)^4(2N^2 + 4N^3))$$

implies the existence of some constant $C(\sigma)$ such that

$$\begin{aligned} \sup_{\ell \in N} (\text{card}(\mathcal{T}_\ell) - \text{card}(\mathcal{T}_0))^\sigma \left(\sum_{j \in J} (\|u_j - \Lambda_\ell u_j\|_{\text{NC}}^2 + \|p_j - p(\Lambda_\ell u_j)\|^2) \right)^{1/2} \\ \leq C(\sigma) \left(\sum_{j \in J} |(u_j, p_j)|_{\mathfrak{H}_\sigma^{\text{NC, Stokes}}}^2 \right)^{1/2}. \quad \blacksquare \end{aligned}$$

7. Biharmonic Eigenvalue Problem

This chapter is devoted to the analysis of the Morley finite element method for the eigenvalues of the biharmonic operator. This finite element dates back to Morley [1968] and was first analysed for eigenvalue problems by Rannacher [1979]. Section 7.1 recalls the Morley FEM and proves some new error estimates for the related interpolation operator. Section 7.2 introduces a novel conforming companion operator. The discrete Helmholtz decomposition of Section 7.3 will be the main tool for the proof of discrete reliability. Section 7.4 revisits the linear biharmonic equation and employs the companion operator for the proof of an L^2 error estimate. Section 7.5 introduces the discretisation of the eigenvalue problem and presents error estimates for the eigenfunctions in the energy and L^2 norms. The optimality result is stated in Section 7.6 and proven in Section 7.7. Section 7.8 discusses the extension to buckling problems.

7.1. Morley Finite Element Method

This section introduces the setting which is needed for the statement of fourth-order problems. It introduces the Morley finite element space and provides novel proofs of error estimates for the Morley interpolation operator.

Let throughout this chapter the space dimension be $d = 2$ and let Ω be simply-connected. The boundary is decomposed into mutually disjoint clamped (Γ_C), simply supported (Γ_S), and free (Γ_F) parts

$$\partial\Omega = \Gamma_C \cup \Gamma_S \cup \Gamma_F$$

such that Γ_C and $\Gamma_C \cup \Gamma_S$ are closed sets. For all regular triangulations $\mathcal{T}_\ell \in \mathbb{T}$ of Ω it is assumed that the relative interior of each boundary edge is contained in one of the parts Γ_C , Γ_S , or Γ_F (in fact, this is only a condition on \mathcal{T}_0).

The vector space of admissible functions reads as

$$V := \{v \in H^2(\Omega) \mid v|_{\Gamma_C \cup \Gamma_S} = 0 \text{ and } (\partial v / \partial \nu)|_{\Gamma_C} = 0\}.$$

Throughout this chapter it is assumed that the only affine function in V is zero, i.e., $V \cap \mathcal{P}_1(\Omega) = \{0\}$.

Let for any edge $F \in \mathcal{F}_\ell$ with normal vector $\mathbf{v}_F = (\mathbf{v}_F(1); \mathbf{v}_F(2))$ the tangent vector be defined as $\boldsymbol{\tau}_F := (-\mathbf{v}_F(2); \mathbf{v}_F(1))$ and denote by $\boldsymbol{\tau} := (-\mathbf{v}(2); \mathbf{v}(1))$ the tangent vector of $\partial\Omega$.

Definition 7.1 (Morley finite element). The Morley finite element space reads as

$$\mathfrak{M}_\ell := \mathfrak{M}(\mathcal{T}_\ell) := \left\{ v \in \mathcal{P}_2(\mathcal{T}_\ell) \left| \begin{array}{l} v \text{ is continuous at } \mathcal{N}_\ell(\Omega) \text{ and vanishes at } \mathcal{N}_\ell(\Gamma_C \cup \Gamma_S); \\ D_{\text{NC}} v \text{ is continuous at the interior edges' midpoints} \\ \text{and vanishes at the midpoints of the edges of } \Gamma_C \end{array} \right. \right\}.$$

7. Biharmonic Eigenvalue Problem

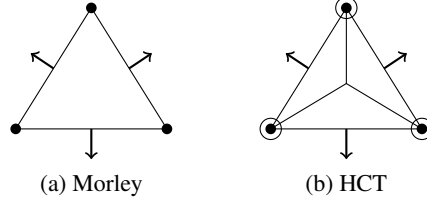


Figure 7.1.: Mnemonic diagrams of two finite elements for the biharmonic equation.

On each triangle the local degrees of freedom are the evaluation of the function at each vertex and the evaluation of the normal derivative at the edges' midpoints. See Figure 7.1a for an illustration. \blacklozenge

Definition 7.2 (Morley interpolation). Let $\mathcal{T}_{\ell+m} \in \mathbb{T}(\mathcal{T}_\ell)$ be any admissible refinement of \mathcal{T}_ℓ . The Morley interpolation operator $\mathcal{J}_\ell^{\mathfrak{M}} : V + \mathfrak{M}(\mathcal{T}_{\ell+m}) \rightarrow \mathfrak{M}(\mathcal{T}_\ell)$ is defined via

$$\begin{aligned} (\mathcal{J}_\ell^{\mathfrak{M}} v)(z) &= v(z) && \text{for any } z \in \mathcal{N}_\ell \text{ and any } v \in V + \mathfrak{M}(\mathcal{T}_{\ell+m}), \\ \int_F \frac{\partial \mathcal{J}_\ell^{\mathfrak{M}} v}{\partial \mathbf{v}_F} ds &= \int_F \frac{\partial v}{\partial \mathbf{v}_F} ds && \text{for any } F \in \mathcal{F}_\ell \text{ and any } v \in V + \mathfrak{M}(\mathcal{T}_{\ell+m}). \end{aligned}$$

\blacklozenge

A piecewise integration by parts proves the projection property for the Hessian

$$\Pi_\ell^0 D_{\text{NC}}^2 = D_{\text{NC}}^2 \mathcal{J}_\ell^{\mathfrak{M}}. \quad (7.1)$$

A direct calculation reveals the following connection to the nonconforming \mathcal{P}_1 interpolation operator

$$D_{\text{NC}} \mathcal{J}_\ell^{\mathfrak{M}} = \mathcal{J}_\ell^{\mathfrak{M}} D. \quad (7.2)$$

The following generalisation of the trace inequality (Proposition 2.31) is necessary for proving error estimates for the Morley interpolation operator.

Proposition 7.3 (discrete trace inequality). *Let $T \in \mathcal{T}_\ell$ be a triangle and \mathcal{K} be a regular triangulation of T and let $G \in \mathcal{F}(T)$ be an edge of T . Any piecewise (with respect to \mathcal{K}) smooth function f satisfies the discrete trace inequality*

$$\|f\|_{L^2(G)} \lesssim h_T^{-1/2} \|f\|_{L^2(T)} + h_T^{1/2} \|D_{\text{NC}} f\|_{L^2(T)} + h_T^{1/2} \sqrt{\sum_{\substack{F \in \mathcal{F}(\mathcal{K}) \\ F \not\subseteq \partial T}} h_F^{-1} \|[f]_F\|_{L^2(F)}^2}.$$

Proof. Denote by P_G the vertex of T opposite to G . A piecewise integration by parts proves the discrete trace identity

$$\frac{1}{2} \int_T (\bullet - P_G) \cdot D_{\text{NC}} f \, dx = - \int_T f \, dx + \text{dist}(P_G, G) \int_G f \, ds + \sum_{\substack{F \in \mathcal{F}(\mathcal{K}) \\ F \not\subseteq \partial T}} \int_F (\bullet - P_G) \cdot \mathbf{v}_F [f]_F \, ds.$$

The application of this identity to the function f^2 together with elementary algebraic manipulations and $\text{dist}(P_G, G) \leq \text{diam}(T) \lesssim h_T$ result in

$$\|f\|_{L^2(G)}^2 \lesssim \left| \int_T D_{\text{NC}}(f^2) dx \right| + h_T^{-1} \|f\|_{L^2(T)}^2 + h_T^{-1} \sum_{\substack{F \in \mathcal{F}(\mathcal{K}) \\ F \not\subseteq \partial T}} \int_F (\bullet - P_G) \cdot \mathbf{v}_F [f^2]_F ds. \quad (7.3)$$

The Young inequality from Proposition 2.30 shows that the first term on the right-hand side can be controlled as

$$\begin{aligned} \left| \int_T D_{\text{NC}}(f^2) dx \right| &= \left| \int_T 2f D_{\text{NC}} f dx \right| \leq 2h_T^{-1/2} \|f\|_{L^2(T)} h_T^{1/2} \|D_{\text{NC}} f\|_{L^2(T)} \\ &\leq h_T^{-1} \|f\|_{L^2(T)}^2 + h_T \|D_{\text{NC}} f\|_{L^2(T)}^2. \end{aligned}$$

It remains to bound the third term on the right-hand side of (7.3). Let $F \in \mathcal{F}(\mathcal{K})$ be an interior edge shared by two triangles K_+ and K_- such that $F = K_+ \cap K_-$. Denote $f_+ := f|_{K_+}$ and $f_- := f|_{K_-}$. A direct calculation proves for the jump of f^2 across F that

$$[f^2]_F = [f]_F (f_+ + f_-).$$

Thus, the Cauchy and triangle inequalities followed by the Young inequality from Proposition 2.30 prove

$$\begin{aligned} \int_F (\bullet - P_G) \cdot \mathbf{v}_F [f^2]_F ds &\leq \text{diam}(T) h_F^{-1/2} h_T^{1/2} \|[f]_F\|_{L^2(F)} h_F^{1/2} h_T^{-1/2} (\|f_+\|_{L^2(F)} + \|f_-\|_{L^2(F)}) \\ &\leq \text{diam}(T) \left(h_F^{-1} h_T \|[f]_F\|_{L^2(F)}^2 + h_F h_T^{-1} (\|f_+\|_{L^2(F)} + \|f_-\|_{L^2(F)})^2 \right). \end{aligned}$$

The trace inequality from Proposition 2.31 and an inverse estimate [Brenner and Scott, 2008] applied to the edge patch ω_F prove that

$$h_F h_T^{-1} (\|f_+\|_{L^2(F)} + \|f_-\|_{L^2(F)})^2 \lesssim h_T^{-1} \|f\|_{L^2(\omega_F)}^2.$$

The foregoing two displayed inequalities, the finite overlap of the edge patches and the shape regularity prove

$$h_T^{-1} \sum_{\substack{F \in \mathcal{F}(\mathcal{K}) \\ F \not\subseteq \partial T}} \int_F (\bullet - P_G) \cdot \mathbf{v}_F [f^2]_F ds \lesssim h_T^{-1} \|f\|_{L^2(T)}^2 + h_T \sum_{\substack{F \in \mathcal{F}(\mathcal{K}) \\ F \not\subseteq \partial T}} h_F^{-1} \|[f]_F\|_{L^2(F)}^2.$$

The combination of the above estimates concludes the proof. \blacksquare

Remark 7.4. In the proof of Proposition 7.3, the ratio h_T/h_F is not required to be uniformly bounded. \blacklozenge

The next proposition provides an error estimate for the Morley interpolation operator.

Proposition 7.5 (error estimate for the Morley interpolation). *Let $T \in \mathcal{T}_\ell$ be a triangle, and let $\mathcal{T}_{\ell+m}$ be a regular triangulation of T . Any $v_{\ell+m} \in H^2(\text{int}(T)) + \mathfrak{M}(\mathcal{T}_{\ell+m})$ and its interpolation $\mathcal{J}_\ell^{\mathfrak{M}} v_{\ell+m}$ of Definition 7.2 satisfy*

$$\begin{aligned} \|h_T^{-2} (1 - \mathcal{J}_\ell^{\mathfrak{M}}) v_{\ell+m}\|_{L^2(T)} + \|h_T^{-1} D_{\text{NC}} (1 - \mathcal{J}_\ell^{\mathfrak{M}}) v_{\ell+m}\|_{L^2(T)} \\ \lesssim \|D_{\text{NC}}^2 (1 - \mathcal{J}_\ell^{\mathfrak{M}}) v_{\ell+m}\|_{L^2(T)}. \end{aligned} \quad (7.4)$$

7. Biharmonic Eigenvalue Problem

Remark 7.6. Error estimates of this type are stated and utilised in [Hu et al., 2012], but their proof employs a compactness argument. Proofs based on equivalence of norms in finite-dimensional spaces lead to constants that may depend on the space dimensions (dependent on m in this case). To make the constant in the estimate more transparent, a new proof is given in this thesis. It shall be pointed out that the constant in the assertion of Proposition 7.5 does not depend on the (possibly very large) cardinality of the triangulation $\mathcal{T}_{\ell+m}$. \blacklozenge

Proof of Proposition 7.5. Let, without loss of generality, $v_{\ell+m} \in H^4(\text{int}(T)) + \mathfrak{M}(\mathcal{T}_{\ell+m})$ (the general case then follows with a density argument). The discrete Friedrichs inequality of Proposition 2.32 and the fact that $\mathcal{J}_\ell^{\mathfrak{M}} v_{\ell+m}$ is continuous on T yield that

$$\begin{aligned} \|(1 - \mathcal{J}_\ell^{\mathfrak{M}})v_{\ell+m}\|_{L^2(T)}^2 &\lesssim \left| \int_{\partial T} (1 - \mathcal{J}_\ell^{\mathfrak{M}})v_{\ell+m} ds \right|^2 + h_T^2 \sum_{\substack{F \in \mathcal{F}(\mathcal{T}_{\ell+m}) \\ F \not\subseteq \partial T}} h_F^{-1} \|[v_{\ell+m}]_F\|_{L^2(F)}^2 \\ &\quad + \|h_T D_{\text{NC}}(1 - \mathcal{J}_\ell^{\mathfrak{M}})v_{\ell+m}\|_{L^2(T)}^2. \end{aligned}$$

For any edge $G \in \mathcal{F}(T)$, the Hölder and Friedrichs inequalities prove that

$$\begin{aligned} \left| \int_G (1 - \mathcal{J}_\ell^{\mathfrak{M}})v_{\ell+m} ds \right| &\lesssim h_G^{1/2} \|(1 - \mathcal{J}_\ell^{\mathfrak{M}})v_{\ell+m}\|_{L^2(G)} \\ &\lesssim h_G^{3/2} \|\partial(1 - \mathcal{J}_\ell^{\mathfrak{M}})v_{\ell+m}/\partial \tau_G\|_{L^2(G)}. \end{aligned}$$

(Note that $v_{\ell+m}$ is differentiable along G .) The discrete trace inequality from Proposition 7.3 proves that this is controlled by some constant times

$$\begin{aligned} h_T \|D_{\text{NC}}(1 - \mathcal{J}_\ell^{\mathfrak{M}})v_{\ell+m}\|_{L^2(T)} + h_T^2 \|D_{\text{NC}}^2(1 - \mathcal{J}_\ell^{\mathfrak{M}})v_{\ell+m}\|_{L^2(T)} \\ + h_T^2 \sqrt{\sum_{\substack{F \in \mathcal{F}(\mathcal{T}_{\ell+m}) \\ F \not\subseteq \partial T}} h_F^{-1} \|[D_{\text{NC}} v_{\ell+m}]_F\|_{L^2(F)}^2}. \end{aligned}$$

For any face $F \in \mathcal{F}(\mathcal{T}_{\ell+m})$ with $F \not\subseteq \partial T$, the Friedrichs and Poincaré inequality prove that

$$h_F^{-1} \|[v_{\ell+m}]_F\|_{L^2(F)}^2 \lesssim h_F \|[D_{\text{NC}} v_{\ell+m}]_F \tau_F\|_{L^2(F)}^2 \lesssim h_F^3 \|[D_{\text{NC}}^2 v_{\ell+m}]_F \tau_F\|_{L^2(F)}^2.$$

Altogether,

$$\begin{aligned} \|(1 - \mathcal{J}_\ell^{\mathfrak{M}})v_{\ell+m}\|_{L^2(T)} &\lesssim h_T \|D_{\text{NC}}(1 - \mathcal{J}_\ell^{\mathfrak{M}})v_{\ell+m}\|_{L^2(T)} + h_T^2 \|D_{\text{NC}}^2(1 - \mathcal{J}_\ell^{\mathfrak{M}})v_{\ell+m}\|_{L^2(T)} \\ &\quad + h_T^2 \sqrt{\sum_{\substack{F \in \mathcal{F}(\mathcal{T}_{\ell+m}) \\ F \not\subseteq \partial T}} h_F \|[D_{\text{NC}}^2 v_{\ell+m}]_F \tau_F\|_{L^2(F)}^2}. \end{aligned}$$

The identity (7.2) and the estimate (5.2) imply

$$h_T \|D_{\text{NC}}(1 - \mathcal{J}_\ell^{\mathfrak{M}})v_{\ell+m}\|_{L^2(T)} \lesssim h_T^2 \|D_{\text{NC}}^2(1 - \mathcal{J}_\ell^{\mathfrak{M}})v_{\ell+m}\|_{L^2(T)}.$$

For the estimate of the jump terms let $F = \text{conv}\{z_1, z_2\} \in \mathcal{F}(\mathcal{T}_{\ell+m})$ be the convex hull of the vertices z_1, z_2 such that F is an interior edge and denote, for $j \in \{1, 2\}$, by $\varphi_j \in$

$\mathcal{P}_1(\mathcal{T}_{\ell+m})$ the piecewise affine function with $\varphi_j(z_j) = 1$ and $\varphi_j(y) = 0$ for all $y \in \mathcal{N}(\mathcal{T}_{\ell+m}) \setminus \{z_j\}$. The piecewise quadratic edge-bubble function $\mathbf{b}_F := 6\varphi_1\varphi_2 \in H_0^1(\omega_F)$ satisfies

$$\|\mathbf{b}_F\|_{L^\infty(T)} = 3/2 \quad \text{and} \quad \int_F \mathbf{b}_F ds = h_F.$$

Define $\psi_F := (\mathbf{b}_F [D_{\text{NC}}^2 v_{\ell+m}]_F \tau_F) \in H_0^1(\omega_F; \mathbb{R}^2)$. Since $[D_{\text{NC}}^2 v_{\ell+m}]_F$ is constant along F , it follows that

$$\|[D_{\text{NC}}^2 v_{\ell+m}]_F \tau_F\|_{L^2(F)}^2 = \|\mathbf{b}_F^{1/2} [D_{\text{NC}}^2 v_{\ell+m}]_F \tau_F\|_{L^2(F)}^2.$$

For any $v \in H^2(\omega_F)$, an integration by parts and the L^2 -orthogonality of $\text{Curl } \psi_F$ on $D^2 v$ reveal that

$$\|\mathbf{b}_F^{1/2} [D_{\text{NC}}^2 v_{\ell+m}]_F \tau_F\|_{L^2(F)}^2 = \int_F ([D_{\text{NC}}^2 v_{\ell+m}]_F \tau_F) \cdot \psi_F ds = (D_{\text{NC}}^2(v_{\ell+m} - v), \text{Curl } \psi_F)_{L^2(\omega_F)}.$$

The Cauchy and inverse inequalities prove that this is bounded by

$$\|D_{\text{NC}}^2(v_{\ell+m} - v)\|_{L^2(\omega_F)} \|\text{Curl } \psi_F\|_{L^2(\omega_F)} \lesssim \|D_{\text{NC}}^2(v_{\ell+m} - v)\|_{L^2(\omega_F)} \|[D_{\text{NC}}^2 v_{\ell+m}]_F \tau_F\|.$$

This implies

$$h_F \|[D_{\text{NC}}^2 v_{\ell+m}]_F \tau_F\|_{L^2(F)}^2 \lesssim \min_{v \in H^2(\text{int}(T))} \|D_{\text{NC}}^2(v_{\ell+m} - v)\|_{L^2(\omega_F)}^2.$$

The sum over all interior edges of $\mathcal{F}(\mathcal{T}_{\ell+m})$ and the finite overlap of edge-patches prove the result. \blacksquare

The following result gives an explicit constant for the L^2 error estimate of the Morley interpolation when applied to a H^2 function (and not, as in Proposition 7.5, a more general piecewise smooth function). This estimate has been published in [Carstensen and Gallistl, 2014]. Recall the constant $\kappa_{\mathcal{E}\mathfrak{R}}$ from Proposition 5.3 and define

$$\kappa_{\mathfrak{M}} := \left(\sqrt{(\kappa_{\mathcal{E}\mathfrak{R}}^2 + \kappa_{\mathcal{E}\mathfrak{R}})/12} + \kappa_{\mathcal{E}\mathfrak{R}}/j_{1,1} \right) \leq 0.25745784466,$$

where $j_{1,1}$ is the first positive root of the Bessel function of the first type [Laugesen and Siudeja, 2010].

Proposition 7.7 (explicit error estimate for $\mathcal{J}_\ell^{\mathfrak{M}}$ for $d = 2$). *The Morley interpolation operator $\mathcal{J}_\ell^{\mathfrak{M}}$ satisfies for any triangle $T \in \mathcal{T}_\ell$ and any function $v \in H^2(\text{int}(T))$ the error estimate*

$$\begin{aligned} \|v - \mathcal{J}_\ell^{\mathfrak{M}} v\|_{L^2(T)} &\leq \kappa_{\mathfrak{M}} \text{diam}(T)^2 \|D^2(v - \mathcal{J}_\ell^{\mathfrak{M}} v)\|_{L^2(T)}, \\ \|D(v - \mathcal{J}_\ell^{\mathfrak{M}} v)\|_{L^2(T)} &\leq \kappa_{\mathcal{E}\mathfrak{R}} \text{diam}(T) \|D^2(v - \mathcal{J}_\ell^{\mathfrak{M}} v)\|_{L^2(T)}. \end{aligned}$$

Proof. See Theorem 3 of [Carstensen and Gallistl, 2014]. \blacksquare

7.2. Conforming Companion Operator

This section is devoted to the design of a new conforming companion operator. In contrast to the operator from Section 5.2, H^2 conformity is required. Compared to certain averaging operators that can be found in the literature [e.g., Brenner et al., 2010, Gudi, 2010], the proposed companion operator has additional conservation properties for the integral mean and the integral mean of the Hessian. These properties will be exploited in the proof of L^2 error estimates for eigenfunction approximations.

The Hsieh-Clough-Tocher finite element [Ciarlet, 1978] enters the design of a conforming companion operator.

Definition 7.8 (HCT finite element). Let any $T \in \mathcal{T}_\ell$ be decomposed into three sub-triangles as depicted in Figure 7.1b, where the vertex shared by the three sub-triangles is the midpoint $\text{mid}(T)$. Given this triangulation $\mathcal{K}_\ell(T)$ of T , let

$$V_{\text{HCT}}(\mathcal{T}_\ell) := \{v \in V \mid v|_T \in \mathcal{P}_3(\mathcal{K}_\ell(T)) \text{ for all } T \in \mathcal{T}_\ell\}.$$

The local degrees of freedom on each triangle T are the nodal values of the function and its derivative and the value of the normal derivative at the midpoints of the edges of T in Figure 7.1b. \blacklozenge

The HCT finite element is one of the simplest conforming finite elements for the biharmonic problem, but it is still much more difficult to implement than nonconforming methods, see, e.g., [Meyer, 2012] for an outline of the assembly of local stiffness matrices for a simplified version of this finite element. Nevertheless, such conforming finite elements turn out to be useful for the theoretical analysis. The following proposition presents a simple averaging operator, similar to that of [Brenner et al., 2010, Gudi, 2010], for the case of more general boundary conditions.

Proposition 7.9 (HCT enrichment). *There exists an operator $\mathcal{A} : \mathfrak{M}(\mathcal{T}_\ell) \rightarrow V_{\text{HCT}}(\mathcal{T}_\ell)$ such that any $v_\ell \in \mathfrak{M}(\mathcal{T}_\ell)$ satisfies*

$$\begin{aligned} \|h_\ell^{-2}(v_\ell - \mathcal{A}v_\ell)\|_{L^2(\Omega)}^2 &\lesssim \sum_{F \in \mathcal{F}_\ell(\Omega \cup \Gamma_C)} h_F \| [D^2 v_\ell]_F \boldsymbol{\tau}_F \|_{L^2(F)}^2 + \sum_{F \in \mathcal{F}_\ell(\Gamma_S)} h_F \| \boldsymbol{\tau}_F \cdot [D^2 v_\ell]_F \boldsymbol{\tau}_F \|_{L^2(F)}^2 \\ &\lesssim \min_{v \in V} \|D_{\text{NC}}^2(v_\ell - v)\|_{L^2(\Omega)}. \end{aligned}$$

Proof. Given $v_\ell \in \mathfrak{M}(\mathcal{T}_\ell)$, define $\mathcal{A}v_\ell \in V_{\text{HCT}}(\mathcal{T}_\ell)$ by setting the degrees of freedom as follows

$$\begin{aligned} (v_\ell - \mathcal{A}v_\ell)(z) &= 0 && \text{for all } z \in \mathcal{N}_\ell, \\ \frac{\partial(v_\ell - \mathcal{A}v_\ell)}{\partial \mathbf{v}_F}(\text{mid}(F)) &= 0 && \text{for all } F \in \mathcal{F}_\ell, \\ D(\mathcal{A}v_\ell)(z) &= \text{card}(\mathcal{T}_\ell(z))^{-1} \sum_{T \in \mathcal{T}_\ell(z)} (Dv_\ell|_T)(z) && \text{for all } z \in \mathcal{N}_\ell(\Omega \cup \Gamma_F). \end{aligned}$$

In other words, the degrees of freedom are defined by averaging. For the remaining vertices on the boundary, set

$$D(\mathcal{A}v_\ell)(z) = 0 \quad \text{for all } z \in \mathcal{N}_\ell(\Gamma_S) \text{ with angle } \neq \pi \text{ and all } z \in \mathcal{N}_\ell(\Gamma_C)$$

and, for all $z \in \mathcal{N}_\ell(\Gamma_S)$ with angle $= \pi$,

$$\frac{\partial \mathcal{A}v_\ell}{\partial \tau}(z) = 0 \quad \text{and} \quad \frac{\partial \mathcal{A}v_\ell}{\partial \mathbf{v}}(z) = (\text{card}(\mathcal{T}_\ell(z)))^{-1} \sum_{F \in \{F_+, F_-\}} \frac{\partial v_\ell}{\partial \mathbf{v}(z)} \Big|_F(z)$$

where $(F_+, F_-) \in \mathcal{T}_\ell(\Gamma_S)^2$ are the two boundary edges sharing z . Note that, for corners of the domain Ω with angle $\neq \pi$, the simply supported boundary condition implies that the full derivative vanishes at z .

The remaining part of the proof is devoted to the error estimate for \mathcal{A} . For a multi-index α of length $|\alpha| = 1$ and any vertex $z \in \mathcal{N}_\ell$, let $\psi_{z,\alpha}$ denote the nodal basis function of $V_{\text{HCT}}(\mathcal{T}_\ell)$ with $(\partial \psi_{z,\alpha} / \partial x^\alpha)(z) = 1$ that vanishes for the remaining degrees of freedom described in Definition 7.8. Since the Hsieh-Clough-Tocher finite element is a finite element in the sense of Ciarlet [1978], for any $T \in \mathcal{T}_\ell$ the function $v_\ell|_T \in \mathcal{P}_2(T)$ can be represented by means of the local HCT basis functions. By definition of \mathcal{A} , the difference $v_\ell - \mathcal{A}v_\ell$ can be represented as follows

$$\|h_\ell^{-2}(v_\ell - \mathcal{A}v_\ell)\|_{L^2(\Omega)}^2 = \sum_{T \in \mathcal{T}_\ell} \left\| h_T^{-2} \sum_{z \in \mathcal{N}(T)} \sum_{|\alpha|=1} \frac{\partial^{|\alpha|}(v_\ell|_T - \mathcal{A}v_\ell)}{\partial x^\alpha}(z) \psi_{z,\alpha} \right\|_{L^2(T)}^2.$$

For any $T \in \mathcal{T}_\ell$, the scaling of the basis functions [Ciarlet, 1978, Thm. 6.3.1, p. 344] reads as

$$\|h_T^{-2} \psi_{z,\alpha}\|_{L^2(T)} \lesssim 1 \text{ for } |\alpha| = 1$$

(note that this estimate cannot be obtained by a simple transformation to some reference triangle because the Hsieh-Clough-Tocher finite element is not affine-equivalent). Thus, the triangle inequality implies that

$$\|h_\ell^{-2}(v_\ell - \mathcal{A}v_\ell)\|_{L^2(\Omega)}^2 \lesssim \sum_{T \in \mathcal{T}_\ell} \sum_{z \in \mathcal{N}(T)} |D(v_\ell|_T - \mathcal{A}v_\ell)(z)|^2.$$

The triangle inequality and equivalence of seminorms prove, for any vertex $z \in \mathcal{N}_\ell(\Omega \cup \Gamma_F)$, that

$$|D(v_\ell|_T - \mathcal{A}v_\ell)(z)|^2 \lesssim \sum_{F \in \mathcal{F}_\ell(z) \cap \mathcal{F}_\ell(\Omega)} [D_{\text{NC}} v_\ell(z)]_F^2 \lesssim \sum_{F \in \mathcal{F}_\ell(z) \cap \mathcal{F}_\ell(\Omega)} h_F^{-1} \|[D_{\text{NC}} v_\ell]_F\|_{L^2(F)}^2. \quad (7.5)$$

For any vertex $z \in \mathcal{N}_\ell(\Gamma_C)$ and any triangle T with $z \in T$ the definition of \mathcal{A} implies

$$|(D_{\text{NC}} v_\ell|_T - \mathcal{A}v_\ell)(z)| = |Dv_\ell|_T(z)|.$$

Any vertex $z \in \mathcal{N}_\ell(\Gamma_S)$ and any triangle T with $z \in T$ satisfy

$$|(\partial(v_\ell|_T - \mathcal{A}v_\ell) / \partial \tau)(z)| = |(\partial v_\ell|_T / \partial \tau)(z)|$$

and, as in (7.5), it follows in the case that the angle at z equals π , that

$$|(\partial(v_\ell|_T - \mathcal{A}v_\ell) / \partial \mathbf{v})(z)| \lesssim \sum_{F \in \mathcal{F}_\ell(z) \cap \mathcal{F}_\ell(\Omega)} |[\partial v_\ell / \partial \mathbf{v}_F]_F(z)|.$$

Equivalence of norms and Poincaré inequalities along $F \in \mathcal{F}_\ell$ prove

$$\begin{aligned} |[\partial v_\ell / \partial \tau_F]_F(z)| &\lesssim h_F^{-1/2} \|[\partial v_\ell / \partial \tau_F]_F\|_{L^2(F)} \lesssim h_F^{1/2} \|\tau_F \cdot [D_{\text{NC}}^2 v_\ell]_F\|_{L^2(F)}, \\ |[\partial v_\ell / \partial \mathbf{v}_E]_E(z)| &\lesssim h_F^{-1/2} \|[\partial v_\ell / \partial \mathbf{v}_F]_F\|_{L^2(F)} \lesssim h_F^{1/2} \|\mathbf{v}_F \cdot [D_{\text{NC}}^2 v_\ell]_F\|_{L^2(F)}. \end{aligned}$$

7. Biharmonic Eigenvalue Problem

This proves the first inequality of the proposition.

The proof of the efficiency estimate can be carried out by using the bubble function technique from the proof of Proposition 7.5. \blacksquare

Proposition 7.10 (companion operator). *For any $v_\ell \in \mathfrak{M}(\mathcal{T}_\ell)$ there exists some $\mathbb{C}v_\ell \in V$ such that $v_\ell - \mathbb{C}v_\ell$ and its second-order partial derivatives are L^2 -orthogonal on the space $\mathcal{P}_0(\mathcal{T}_\ell)$ of piecewise constants,*

$$\Pi_\ell^0(v_\ell - \mathbb{C}v_\ell) = 0 \quad \text{and} \quad \Pi_\ell^0(D_{\text{NC}}^2(v_\ell - \mathbb{C}v_\ell)) = 0. \quad (7.6)$$

It satisfies the approximation and stability property

$$\begin{aligned} \|h_\ell^{-2}(v_\ell - \mathbb{C}v_\ell)\|_{L^2(\Omega)} + \|h_\ell^{-1}D_{\text{NC}}(v_\ell - \mathbb{C}v_\ell)\|_{L^2(\Omega)} + \|D_{\text{NC}}^2(v_\ell - \mathbb{C}v_\ell)\|_{L^2(\Omega)} \\ \lesssim \min_{v \in V} \|D_{\text{NC}}^2(v_\ell - v)\|_{L^2(\Omega)}. \end{aligned} \quad (7.7)$$

Proof. The design follows in three steps.

Step 1. Proposition 7.9 and inverse estimates [Brenner and Scott, 2008] prove for the operator \mathcal{A} that

$$\begin{aligned} \|h_\ell^{-2}(v_\ell - \mathcal{A}v_\ell)\|_{L^2(\Omega)} + \|h_\ell^{-1}D_{\text{NC}}(v_\ell - \mathcal{A}v_\ell)\|_{L^2(\Omega)} + \|D_{\text{NC}}^2(v_\ell - \mathcal{A}v_\ell)\|_{L^2(\Omega)} \\ \lesssim \min_{v \in V} \|D_{\text{NC}}^2(v_\ell - v)\|_{L^2(\Omega)}. \end{aligned}$$

Step 2. Let $T = \text{conv}\{z_1, z_2, z_3\}$ be a triangle of \mathcal{T}_ℓ and let $F \in \mathcal{F}(T)$ with $F = \text{conv}\{z_1, z_2\}$ and denote the continuous nodal \mathcal{P}_1 basis functions by $\varphi_1, \varphi_2, \varphi_3 \in \mathcal{P}_1(\mathcal{T}_\ell) \cap H^1(\Omega)$. Let \mathbf{v}_T denote the outward pointing unit normal of T and define the function $\zeta_{F,T}$ by

$$\zeta_{F,T} := 30(\mathbf{v}_T \cdot \mathbf{v}_F) \text{dist}(z_3, F) \varphi_1^2 \varphi_2^2 \varphi_3.$$

For any $F \in \mathcal{F}_\ell$, the function

$$\zeta_F := \begin{cases} \zeta_{F,K} & \text{on triangles } K \in \mathcal{T}_\ell \text{ with } F \in \mathcal{F}(K), \\ 0 & \text{otherwise} \end{cases}$$

satisfies $\zeta_F \in H^2(\Omega)$ and $\text{supp}(\zeta_F) = \overline{\omega_F}$ as well as $\int_F \partial \zeta_F / \partial \mathbf{v}_F dx = 1$. For the proof that ζ_F is continuously differentiable across interior edges F , note that any adjacent triangle T satisfies $D\varphi_3|_T = (\text{dist}(z_3, F))^{-1} \mathbf{v}_T$ as well as

$$(D\zeta_{F,T})|_F \mathbf{v}_F = 30(\mathbf{v}_T \cdot \mathbf{v}_F) \text{dist}(z_3, F) \varphi_1^2 \varphi_2^2 (D\varphi_3 \mathbf{v}_F) = 30\varphi_1^2 \varphi_2^2.$$

Hence, $\zeta_F \in H^2(\Omega)$.

If $F \in \mathcal{F}_\ell(\Omega)$, it holds that $\zeta_F \in H_0^2(\omega_F)$. Define the operator $\tilde{\mathcal{A}} : V_\ell \rightarrow V$ which acts as

$$\tilde{\mathcal{A}}v_\ell := \mathcal{A}v_\ell + \sum_{F \in \mathcal{F}(\Omega \cup \Gamma_S \cup \Gamma_F)} \left(\int_F \frac{\partial(v_\ell - \mathcal{A}v_\ell)}{\partial \mathbf{v}_F} ds \right) \zeta_F.$$

An immediate consequence of this choice reads as

$$\int_F \partial \tilde{\mathcal{A}}v_\ell / \partial \mathbf{v}_F ds = \int_F \partial v_\ell / \partial \mathbf{v}_F ds \quad \text{for all } F \in \mathcal{F}_\ell.$$

An integration by parts shows the integral mean property of the Hessian $\Pi_\ell^0 D^2 \tilde{\mathcal{A}} = D_{\text{NC}}^2$. The scaling $\|\zeta_F\|_{L^2(T)} \lesssim h_T^2$ and the trace inequality (Proposition 2.31) prove, for any $T \in \mathcal{T}_\ell$, that

$$\begin{aligned} h_T^{-2} \left\| \sum_{F \in \mathcal{F}(T)} \left(\oint_F \frac{\partial(v_\ell - \mathcal{A}v_\ell)}{\partial \mathbf{v}_F} ds \right) \zeta_F \right\|_{L^2(T)} \\ \lesssim \sum_{F \in \mathcal{F}(T)} \left| \oint_F \frac{\partial(v_\ell - \mathcal{A}v_\ell)}{\partial \mathbf{v}_F} ds \right| \\ \lesssim h_T^{-1} \|D_{\text{NC}}(v_\ell - \mathcal{A}v_\ell)\|_{L^2(T)} + \|D_{\text{NC}}^2(v_\ell - \mathcal{A}v_\ell)\|_{L^2(T)}. \end{aligned}$$

This together with the first step of the proof and inverse estimates [Brenner and Scott, 2008] show that

$$\begin{aligned} \|h_\ell^{-2}(v_\ell - \tilde{\mathcal{A}}v_\ell)\|_{L^2(\Omega)} + \|h_\ell^{-1}D_{\text{NC}}(v_\ell - \tilde{\mathcal{A}}v_\ell)\|_{L^2(\Omega)} + \|D_{\text{NC}}^2(v_\ell - \tilde{\mathcal{A}}v_\ell)\|_{L^2(\Omega)} \\ \lesssim \min_{v \in V} \|D_{\text{NC}}^2(v_\ell - v)\|_{L^2(\Omega)}. \end{aligned} \quad (7.8)$$

Step 3. On any triangle $T = \text{conv}\{z_1, z_2, z_3\}$ with nodal basis functions $\varphi_1, \varphi_2, \varphi_3$, the volume bubble function is defined as

$$\tilde{\mathbf{b}}_T := 2520 \varphi_1^2 \varphi_2^2 \varphi_3^2 \in H_0^2(\text{int}(T))$$

and satisfies $\oint_T \tilde{\mathbf{b}}_T dx = 1$. Define

$$\mathcal{C}v_\ell := \tilde{\mathcal{A}}v_\ell + \sum_{T \in \mathcal{T}_\ell} \left(\oint_T (v_\ell - \tilde{\mathcal{A}}v_\ell) dx \right) \tilde{\mathbf{b}}_T.$$

The difference $v_\ell - \mathcal{C}v_\ell$ is L^2 orthogonal to all piecewise constant functions. Since $\tilde{\mathbf{b}}_T$ vanishes on $F \in \mathcal{F}_\ell$, \mathcal{C} enjoys the integral mean property $\Pi_\ell^0 D^2 \mathcal{C} = D_{\text{NC}}^2$. The fact that $\|\tilde{\mathbf{b}}_T\|_{L^\infty(T)} \lesssim 1$ and the Hölder inequality prove

$$\left\| \oint_T (v_\ell - \tilde{\mathcal{A}}v_\ell) dx \tilde{\mathbf{b}}_T \right\|_{L^2(T)} \lesssim \|v_\ell - \tilde{\mathcal{A}}v_\ell\|_{L^2(T)}.$$

Hence, the triangle inequality, (7.8) and inverse estimates prove the claimed error estimate for \mathcal{C} . ■

Remark 7.11. The operator \mathcal{C} maps into a discrete space, namely the sum of $V_{\text{HCT}}(\mathcal{T}_\ell)$ and $\mathcal{P}_6(\mathcal{T}_\ell)$. ◆

7.3. Discrete Helmholtz Decompositions

This section is devoted to the proof of a discrete Helmholtz-type decomposition which will be employed for the proof of discrete reliability in Section 7.7. The concept of a discrete Helmholtz decomposition dates back at least to Arnold and Falk [1989] who proved discrete decompositions of piecewise constant vector fields in 2D by means of the nonconforming and conforming \mathcal{P}_1 finite element spaces. This section proves a decomposition which is useful in the context of the Morley finite element method. It can be viewed as

7. Biharmonic Eigenvalue Problem

a discrete analogue of the Helmholtz decomposition obtained by Beirão da Veiga et al. [2010]. For clamped boundary conditions, this discrete Helmholtz decomposition was introduced by Carstensen, Gallistl, and Hu [2014b]. This thesis extends the result to general boundary conditions. The new result will be employed for the proof of discrete reliability in Section 7.7 for the case of simply supported and free boundary conditions.

Define

$$\hat{H}^1(\Omega; \mathbb{R}^2) := \{v \in H^1(\Omega; \mathbb{R}^2) \mid \int_{\Omega} v \, dx = 0 \text{ and } \int_{\Omega} \operatorname{div} v \, dx = 0\} \quad (7.9)$$

and

$$\mathfrak{X}(\mathcal{T}_{\ell}) := \left\{ v \in \mathcal{P}_1(\mathcal{T}_{\ell}; \mathbb{R}^2) \cap \hat{H}^1(\Omega; \mathbb{R}^2) \left| \begin{array}{l} 1. \text{ for all } F = \operatorname{conv}\{z_1, z_2\} \in \mathcal{F}_{\ell}(\Gamma_S \cup \Gamma_F) \\ \quad (v(z_2) - v(z_1)) \cdot \mathbf{v}_F = 0, \\ 2. \text{ for all } (F_-, F_+) \in \mathcal{F}_{\ell}(\Gamma_F)^2 \\ \quad \text{with } F_- = \operatorname{conv}\{z_-, z\}, F_+ = \operatorname{conv}\{z, z_+\} \\ \quad h_{F_-}^{-1}(v(z) - v(z_-)) \cdot \boldsymbol{\tau}_{F_-} = h_{F_+}^{-1}(v(z_+) - v(z)) \cdot \boldsymbol{\tau}_{F_+} \end{array} \right. \right\}.$$

Remark 7.12. In other words, the functions of $\mathfrak{X}(\mathcal{T}_{\ell})$ satisfy that $\partial(\boldsymbol{\psi} \cdot \mathbf{v})/\partial \boldsymbol{\tau} = 0$ on $\Gamma_S \cup \Gamma_F$ and $(D\boldsymbol{\psi}\boldsymbol{\tau}) \cdot \boldsymbol{\tau}$ is constant on each connectivity component of Γ_F . The definition of $\mathfrak{X}(\mathcal{T}_{\ell})$ above is stated in such a way that one can see that this defines $\operatorname{card}(\mathcal{F}_{\ell}(\Gamma_S \cup \Gamma_F)) + \operatorname{card}(\mathcal{N}_{\ell}(\Gamma_F))$ linear independent constraints on $\mathcal{P}_1(\mathcal{T}_{\ell}; \mathbb{R}^2) \cap \hat{H}^1(\Omega; \mathbb{R}^2)$. Recall that Γ_C and $\Gamma_C \cup \Gamma_S$ are assumed to be closed sets and, thus, $\mathcal{N}_{\ell}(\Gamma_F)$ contains exactly those vertices that are shared by two edges of Γ_F . \blacklozenge

Theorem 7.13 (discrete Helmholtz decomposition for piecewise constant symmetric tensor fields). *Let Ω be simply-connected. Given any piecewise constant symmetric tensor field $\boldsymbol{\sigma}_{\ell} \in \mathcal{P}_0(\mathcal{T}_{\ell}; \mathbb{S})$, there exist unique $\boldsymbol{\phi}_{\ell} \in \mathfrak{M}(\mathcal{T}_{\ell})$ and $\boldsymbol{\psi}_{\ell} \in \mathfrak{X}(\mathcal{T}_{\ell})$ such that*

$$\boldsymbol{\sigma}_{\ell} = D_{\text{NC}}^2 \boldsymbol{\phi}_{\ell} + \operatorname{sym} \operatorname{Curl} \boldsymbol{\psi}_{\ell}. \quad (7.10)$$

The decomposition is L^2 orthogonal and the functions $\boldsymbol{\phi}_{\ell}$, $\boldsymbol{\psi}_{\ell}$, $\boldsymbol{\sigma}_{\ell}$ from (7.10) satisfy, with the constant C_{trdevdiv} from Lemma 7.15 below, that

$$\|D_{\text{NC}}^2 \boldsymbol{\phi}_{\ell}\|_{L^2(\Omega)} + \|\operatorname{Curl} \boldsymbol{\psi}_{\ell}\|_{L^2(\Omega)} \leq \max\{1, 3C_{\text{trdevdiv}}\} \|\boldsymbol{\sigma}_{\ell}\|_{L^2(\Omega)}. \quad (7.11)$$

The proof is based on an analogue of Korn's inequality. Recall the following well-known result, which is some straightforward modification of [Boffi et al., 2013, Prop. 9.1.1]. It states that the L^2 norm of a tensor field $\boldsymbol{\rho} \in L^2(\Omega; \mathbb{R}^{2 \times 2})$ can be controlled by the sum of the L^2 norm of its deviatoric part $\operatorname{dev} \boldsymbol{\rho} := \boldsymbol{\rho} - 1/2 \operatorname{tr}(\boldsymbol{\rho}) \mathbf{1}_{2 \times 2}$ and the H^{-1} norm of its divergence.

Lemma 7.14 (tr-dev-div Lemma). *There exists a constant $0 \leq C_{\text{trdevdiv}} < \infty$ such that any $\boldsymbol{\rho} \in L^2(\Omega; \mathbb{R}^{2 \times 2})$ with $\int_{\Omega} \operatorname{tr}(\boldsymbol{\rho}) \, dx = 0$ satisfies*

$$\|\boldsymbol{\rho}\|_{L^2(\Omega)} \leq C_{\text{trdevdiv}} (\|\operatorname{dev} \boldsymbol{\rho}\|_{L^2(\Omega)} + \|\operatorname{div} \boldsymbol{\rho}\|_{H^{-1}(\Omega)}). \quad \blacksquare$$

The following stability result is proven in Lemma 3.3 of [Carstensen, Gallistl, and Hu, 2014b]. Recall the space $\hat{H}^1(\Omega; \mathbb{R}^2)$ from (7.9).

Lemma 7.15 (Korn-type inequality). *Any $v \in \hat{H}^1(\Omega; \mathbb{R}^2)$ satisfies*

$$\|\operatorname{Curl} v\|_{L^2(\Omega)} \leq 3C_{\text{trdevdiv}} \|\operatorname{sym} \operatorname{Curl} v\|_{L^2(\Omega)}.$$

Proof. The proof of [Carstensen, Gallistl, and Hu, 2014b] is replicated here for convenient reading.

Direct calculations reveal

$$\|\operatorname{Curl} v\|_{L^2(\Omega)} = \|Dv\|_{L^2(\Omega)} \quad \text{and} \quad \|\operatorname{sym} \operatorname{Curl} v\|_{L^2(\Omega)} = \|\operatorname{dev} Dv\|_{L^2(\Omega)}. \quad (7.12)$$

Since $\int_{\Omega} \operatorname{div} v \, dx = 0$, $\rho := Dv$ in Lemma 7.14 leads to

$$\|Dv\|_{L^2(\Omega)} \leq C_{\operatorname{trdevdiv}} (\|\operatorname{dev} Dv\|_{L^2(\Omega)} + \|\Delta v\|_{H^{-1}(\Omega)}). \quad (7.13)$$

For the estimate of $\|\Delta v\|_{H^{-1}(\Omega)}$, let $\varphi = (\varphi_1; \varphi_2) \in H_0^1(\Omega; \mathbb{R}^2)$ with $\|D\varphi\|_{L^2(\Omega)} = 1$. A direct calculation proves

$$D\varphi + \operatorname{Curl} \begin{pmatrix} \varphi_2 \\ -\varphi_1 \end{pmatrix} = 2 \operatorname{dev} \operatorname{sym} D\varphi.$$

This and the orthogonality of Dv and $\operatorname{Curl}(\varphi_2; -\varphi_1)$ lead to

$$(Dv, D\varphi)_{L^2(\Omega)} = (Dv, D\varphi + \operatorname{Curl} \begin{pmatrix} \varphi_2 \\ -\varphi_1 \end{pmatrix})_{L^2(\Omega)} = 2(Dv, \operatorname{dev} \operatorname{sym} D\varphi)_{L^2(\Omega)}.$$

Elementary algebraic manipulations show that this equals

$$2(\operatorname{dev} Dv, \operatorname{sym} D\varphi)_{L^2(\Omega)} \leq 2\|\operatorname{dev} Dv\|_{L^2(\Omega)}. \quad (7.14)$$

Altogether, this shows

$$\|\Delta v\|_{H^{-1}(\Omega)} \leq 2\|\operatorname{dev} Dv\|_{L^2(\Omega)}.$$

The combination with (7.12)–(7.13) concludes the proof. \blacksquare

Proof of Theorem 7.13. The first step of the proof shows the L^2 -orthogonality of the decomposition. Let $\phi_{\ell} \in \mathfrak{M}(\mathcal{T}_{\ell})$ and $\psi_{\ell} \in \mathfrak{X}(\mathcal{T}_{\ell})$. The integration by parts shows that

$$(D_{\operatorname{NC}}^2 \phi_{\ell}, \operatorname{Curl} \psi_{\ell})_{L^2(\Omega)} = \sum_{F \in \mathcal{F}_{\ell}(\Gamma_S \cup \Gamma_F)} \int_F D\phi_{\ell}(D\psi_{\ell}\tau) \, ds.$$

For any edge $F \in \mathcal{F}_{\ell}(\Gamma_S \cup \Gamma_F)$ it follows from the first condition imposed on the space $\mathfrak{X}(\mathcal{T}_{\ell})$ that $\partial(\psi_{\ell} \cdot \nu)|_F / \partial \tau = 0$ and thus

$$\int_F D\phi_{\ell}(D\psi_{\ell}\tau) \, ds = \int_F (D\phi_{\ell}\tau) \cdot (D\psi_{\ell}\tau) \, ds.$$

If $F \in \mathcal{F}_{\ell}(\Gamma_S)$ belongs to the simply supported part of the boundary, then $\int_F D\phi_{\ell}\tau \, ds = 0$ and, hence, $\int_F D\phi_{\ell}(D\psi_{\ell}\tau) \, ds = 0$. Let $\gamma \subseteq \Gamma_F$ denote a connectivity component of the free boundary Γ_F with vertices $(z_0, \dots, z_k) \in \mathcal{N}_{\ell}^{k+1}$ and edges $(F_1, \dots, F_k) \in \mathcal{F}_{\ell}^k$ with $F_j = \operatorname{conv}\{z_{j-1}, z_j\}$ such that the closure of γ equals $\cup\{F_j \mid j \in \{1, \dots, k\}\}$. Then, by the main theorem of calculus and the fact that $\phi_{\ell}(z_0) = \phi_{\ell}(z_k) = 0$, it follows that

$$\begin{aligned} & \sum_{j=1}^k \int_{F_j} (D\phi_{\ell}\tau_{F_j}) \tau_{F_j} \cdot (D\psi_{\ell}\tau_{F_j}) \, ds \\ &= \sum_{j=1}^k h_{F_j}^{-1} (\phi_{\ell}(z_j) - \phi_{\ell}(z_{j-1})) \tau_{F_j} \cdot (\psi_{\ell}(z_j) - \psi_{\ell}(z_{j-1})) \\ &= \sum_{j=1}^{k-1} \left(h_{F_j}^{-1} (\psi_{\ell}(z_j) - \psi_{\ell}(z_{j-1})) \tau_{F_j} - h_{F_{j+1}}^{-1} (\psi_{\ell}(z_{j+1}) - \psi_{\ell}(z_j)) \tau_{F_{j+1}} \right) \cdot \phi_{\ell}(z_j). \end{aligned}$$

7. Biharmonic Eigenvalue Problem

The conditions imposed on $\mathfrak{X}(\mathcal{T}_\ell)$ make these summands equal zero. Hence, ϕ_ℓ and ψ_ℓ are L^2 -orthogonal.

Since the contributions on the right-hand side of (7.10) are L^2 -orthogonal and since

$$D_{\text{NC}}^2(\mathfrak{M}(\mathcal{T}_\ell)) + \text{sym Curl}(\mathfrak{X}(\mathcal{T}_\ell)) \subseteq \mathcal{P}_0(\mathcal{T}_\ell; \mathbb{S}),$$

it suffices to prove

$$\dim(\mathcal{P}_0(\mathcal{T}_\ell; \mathbb{S})) = \dim(D_{\text{NC}}^2(\mathfrak{M}(\mathcal{T}_\ell))) + \dim(\text{sym Curl}(\mathfrak{X}(\mathcal{T}_\ell))). \quad (7.15)$$

Obviously, the dimension of the Morley finite element space satisfies

$$\dim(\mathfrak{M}(\mathcal{T}_\ell)) = \text{card}(\mathcal{N}_\ell(\Omega \cup \Gamma_F)) + \text{card}(\mathcal{F}_\ell(\Omega \cup \Gamma_S \cup \Gamma_F)).$$

Lemma 7.15 implies that the kernel spaces of Curl and sym Curl coincide,

$$\dim(\text{sym Curl}(\mathfrak{X}(\mathcal{T}_\ell))) = \dim(\text{Curl}(\mathfrak{X}(\mathcal{T}_\ell))) = \dim(D(\mathfrak{X}(\mathcal{T}_\ell))).$$

Since the constraints on the space \mathfrak{X}_ℓ are linearly independent, it follows that

$$\dim(\mathfrak{X}(\mathcal{T}_\ell)) = 2 \text{card}(\mathcal{N}_\ell) - \text{card}(\mathcal{F}_\ell(\Gamma_S \cup \Gamma_F)) - \text{card}(\mathcal{N}_\ell(\Gamma_F)) - 3$$

and therefore

$$\dim(\mathfrak{M}(\mathcal{T}_\ell)) + \dim(\mathfrak{X}(\mathcal{T}_\ell)) = \text{card}(\mathcal{N}_\ell(\Omega)) + \text{card}(\mathcal{F}_\ell(\Omega)) + 2 \text{card}(\mathcal{N}_\ell) - 3.$$

Hence, the proof of (7.15) follows from the well-known Euler formulae (for two space dimensions and simply-connected domains; the proof follows from mathematical induction)

$$\text{card}(\mathcal{N}_\ell) + \text{card}(\mathcal{T}_\ell) = 1 + \text{card}(\mathcal{F}_\ell) \quad \text{and} \quad 2 \text{card}(\mathcal{T}_\ell) + 1 = \text{card}(\mathcal{N}_\ell) + \text{card}(\mathcal{F}_\ell(\Omega)).$$

Indeed, the first formula implies that

$$\begin{aligned} & \text{card}(\mathcal{N}_\ell(\Omega)) + \text{card}(\mathcal{F}_\ell(\Omega)) + 2 \text{card}(\mathcal{N}_\ell) - 3 \\ &= \text{card}(\mathcal{N}_\ell(\Omega)) + \text{card}(\mathcal{F}_\ell(\Omega)) + \text{card}(\mathcal{N}_\ell) + \text{card}(\mathcal{F}_\ell) - \text{card}(\mathcal{T}_\ell) - 2 \\ &= 2(\text{card}(\mathcal{N}_\ell) + \text{card}(\mathcal{F}_\ell(\Omega)) - 1) - \text{card}(\mathcal{T}_\ell). \end{aligned}$$

The second formula shows that this equals $3 \text{card}(\mathcal{T}_\ell)$.

The proof of the stability (7.11) follows from the orthogonality of the decomposition and Lemma 7.15. \blacksquare

Note that this discrete Helmholtz decomposition allows an alternative proof of the following result of Beirão da Veiga et al. [2010].

Theorem 7.16 (Lemma 1 and Corollary 1 of [Beirão da Veiga et al., 2010]). *Given any $\sigma \in L^2(\Omega; \mathbb{R}^{2 \times 2})$ on the simply-connected domain Ω , there exist $\phi \in V$, $\psi \in H^1(\Omega; \mathbb{R}^2) \cap L_0^2(\Omega; \mathbb{R}^2)$ and $\rho \in L_0^2(\Omega)$ such that*

$$\sigma = D^2 \phi + \text{Curl } \psi + \begin{pmatrix} 0 & \rho \\ -\rho & 0 \end{pmatrix}$$

and

$$\|D^2 \phi\|_{L^2(\Omega)} + \|\text{Curl } \psi\|_{L^2(\Omega)} + \|\rho\|_{L^2(\Omega)} \lesssim \|\sigma\|_{L^2(\Omega)}.$$

Moreover, $\partial(\psi \cdot \nu)/\partial \tau = 0$ on $\Gamma_S \cup \Gamma_F$ and $(D\psi \tau) \cdot \tau$ is constant on each connectivity component of Γ_F .

Proof. The result can be proven with the methodology of [Carstensen, Gallistl, and Hu, 2014b]. Since the theorem will not be utilised in this thesis, the proof is omitted. \blacksquare

7.4. Morley FEM for the Linear Biharmonic Equation

This section presents L^2 and best-approximation error estimates for the Morley finite element discretisation of the linear biharmonic equation. The companion operator from Section 7.2 allows the proof of an L^2 error estimate for possibly singular solutions of the biharmonic equation.

Given $f \in L^2(\Omega)$, the biharmonic problem seeks $u \in H^2(\Omega)$ with

$$\Delta^2 u = f \quad \text{in } \Omega, \quad u = 0 \quad \text{on } \Gamma_C \cup \Gamma_S, \quad \frac{\partial u}{\partial \nu} = 0 \quad \text{on } \Gamma_C.$$

Its weak form utilises the bilinear form

$$a(v, w) := (D^2 v, D^2 w)_{L^2(\Omega)} \quad \text{for all } (v, w) \in V^2$$

with induced norm $\|\cdot\| := a(\cdot, \cdot)^{1/2}$ and $b(\cdot, \cdot) := (\cdot, \cdot)_{L^2(\Omega)}$ with induced norm $\|\cdot\|$. The weak formulation seeks $u \in V$ such that

$$a(u, v) = b(f, v) \quad \text{for all } v \in V. \quad (7.16)$$

Existence and uniqueness of the solution follow from the assumption that the only affine function in V is zero $V \cap \mathcal{P}_1(\Omega) = \{0\}$ (see Section 7.1) which guarantees that $(V, a(\cdot, \cdot))$ is a Hilbert space. Throughout this chapter, $0 < s \leq 1$ indicates the elliptic regularity of the solution to (7.16) in the sense that $\|u\|_{H^{2+s}(\Omega)} \leq C(s)\|f\|_{L^2(\Omega)}$.

Let $V_\ell := V_{\mathcal{T}_\ell} := \mathfrak{M}(\mathcal{T}_\ell)$ denote the Morley finite element space from Definition 7.1. The discrete version of the energy scalar product reads as

$$a_{\text{NC}}(v, w) := (D_{\text{NC}}^2 v, D_{\text{NC}}^2 w)_{L^2(\Omega)} \quad \text{for all } (v, w) \in (V + V_\ell)^2$$

with induced discrete energy norm $\|\cdot\|_{\text{NC}} := a_{\text{NC}}(\cdot, \cdot)^{1/2}$. The Morley finite element discretisation of (7.16) seeks $u_\ell \in V_\ell$ such that

$$a_{\text{NC}}(u_\ell, v_\ell) = b(f, v_\ell) \quad \text{for all } v_\ell \in V_\ell. \quad (7.17)$$

The assumption $V \cap \mathcal{P}_1(\Omega) = \{0\}$ implies $V_\ell \cap \mathcal{P}_1(\Omega) = \{0\}$. Hence, $a_{\text{NC}}(\cdot, \cdot)$ defines a scalar product on V_ℓ and there is a unique solution u_ℓ [Ciarlet, 1978].

The following best-approximation is a refined version of a result of Gudi [2010].

Proposition 7.17 (best-approximation result). *The exact solution u of (7.16) and the discrete solution u_ℓ of (7.17) satisfy*

$$\|u - u_\ell\|_{\text{NC}} \lesssim \|(1 - \Pi_\ell^0)D^2 u\|_{L^2(\Omega)} + \text{osc}_{2,2}(f, \mathcal{T}_\ell).$$

Proof. Gudi [2010] proved the inequality

$$\|u - u_\ell\|_{\text{NC}} \lesssim \|(1 - \Pi_\ell^0)D^2 u\|_{L^2(\Omega)} + \text{osc}_{0,2}(f, \mathcal{T}_\ell).$$

A refined efficiency analysis of the oscillation term as in the proof of Proposition 4.3 leads to the claimed best-approximation result. ■

7. Biharmonic Eigenvalue Problem

Error estimates for the Morley FEM in the L^2 norm are well-established [Lascaux and Lesaint, 1975] for the case of a smooth solution $u \in V \cap H^3(\Omega)$. The smoothness enters the classical proofs in that traces of certain second-order derivatives are assumed to exist. This smoothness assumption is satisfied for the purely clamped case $\partial\Omega = \Gamma_C$ where it is known [Blum and Rannacher, 1980, Melzer and Rannacher, 1980] that $u \in H^{5/2+\varepsilon}$ for some $\varepsilon > 0$. For the more general boundary conditions considered in this thesis, this smoothness assumption is generally not satisfied. The new companion operator \mathcal{C} from Section 7.2 allows the proof of an L^2 error estimate for any $u \in V$.

Proposition 7.18 (L^2 control for the linear problem). *The exact solution u of (7.16) and the discrete solution u_ℓ of (7.17) satisfy*

$$\|u - u_\ell\| \lesssim \|h_0\|_\infty^s (\|u - u_\ell\|_{\text{NC}} + \text{osc}_{2,2}(f, \mathcal{T}_\ell)).$$

Proof. Let $e := u - u_\ell$ and let $z \in V$ denote the solution of

$$a(z, v) = b(e, v) \quad \text{for all } v \in V.$$

Since $\Pi_\ell^0(u_\ell - \mathcal{C}u_\ell) = 0$ by Proposition 7.10, it holds that

$$\begin{aligned} \|e\|^2 &= b(\mathcal{C}u_\ell - u_\ell, e) + b(e, u - \mathcal{C}u_\ell) \\ &= b(\mathcal{C}u_\ell - u_\ell, (1 - \Pi_\ell^0)e) + a(z, u - \mathcal{C}u_\ell). \end{aligned} \tag{7.18}$$

Piecewise Poincaré inequalities, the discrete Friedrichs inequality from Proposition 2.32, and (7.7) lead to

$$b(\mathcal{C}u_\ell - u_\ell, (1 - \Pi_\ell^0)e) \lesssim \|h_0\|_\infty^3 \|e\|_{\text{NC}}^2.$$

The second term of the right-hand side in (7.18) satisfies

$$a(z, u - \mathcal{C}u_\ell) = a_{\text{NC}}(z, u - u_\ell) + a_{\text{NC}}(z, u_\ell - \mathcal{C}u_\ell). \tag{7.19}$$

The projection property (7.1) of $\mathcal{J}_\ell^{\mathfrak{M}}$, the problems (7.16) and (7.17), the Cauchy inequality and the approximation and stability properties (7.4) prove for the first term of the right-hand side in (7.19) that

$$a_{\text{NC}}(z, u - u_\ell) = b(f, z - \mathcal{J}_\ell^{\mathfrak{M}}z) \lesssim \|h_\ell^2 f\|_{L^2(\Omega)} \|(1 - \Pi_\ell^0)D^2 z\|_{L^2(\Omega)}.$$

The integral mean property (7.6) of \mathcal{C} and the approximation and stability properties (7.7) prove for the second term of (7.19) that

$$a_{\text{NC}}(z, u_\ell - \mathcal{C}u_\ell) = a_{\text{NC}}(z - \mathcal{J}_\ell^{\mathfrak{M}}z, u_\ell - \mathcal{C}u_\ell) \lesssim \|u - u_\ell\|_{\text{NC}} \|(1 - \Pi_\ell^0)D^2 z\|_{L^2(\Omega)}.$$

The regularity estimates of [Blum and Rannacher, 1980, Grisvard, 1985] and the stability of the problem (7.16) prove that

$$\|(1 - \Pi_\ell^0)D^2 z\|_{L^2(\Omega)} \lesssim \|h_0\|_\infty^s \|z\|_{H^{2+s}(\Omega)} \lesssim \|h_0\|_\infty^s \|e\|_{L^2(\Omega)}.$$

Efficiency estimates similar to those in the proof of Proposition 4.3 shows that

$$\|h_\ell^2 f\|_{L^2(\Omega)} \lesssim \|u - u_\ell\|_{\text{NC}} + \text{osc}_{2,2}(f, \mathcal{T}_\ell).$$

The combination of the foregoing estimates concludes the proof. ■

7.5. Biharmonic Eigenvalue Problem

The weak form of the biharmonic eigenvalue problem seeks eigenpairs $(\lambda, u) \in \mathbb{R} \times V$ with $\|u\| = 1$ such that

$$a(u, v) = \lambda b(u, v) \quad \text{for all } v \in V. \quad (7.20)$$

Its Morley finite element discretisation seeks $(\lambda_\ell, u_\ell) \in \mathbb{R} \times V_\ell$ with $\|u_\ell\| = 1$ such that

$$a_{\text{NC}}(u_\ell, v_\ell) = \lambda_\ell b(u_\ell, v_\ell) \quad \text{for all } v_\ell \in V_\ell. \quad (7.21)$$

Recall the notation from Section 3.1 for the exact and discrete eigenvalues

$$0 < \lambda_1 \leq \lambda_2 \leq \dots \quad \text{and} \quad 0 < \lambda_{\ell,1} \leq \dots \leq \lambda_{\ell, \dim(V_\ell)}$$

and their corresponding b -orthonormal systems of eigenfunctions

$$(u_1, u_2, u_3, \dots) \quad \text{and} \quad (u_{\ell,1}, u_{\ell,2}, \dots, u_{\ell, \dim(V_\ell)}).$$

The eigenvalue cluster is described by the index set $J := \{n+1, \dots, n+N\}$ and the spaces $W := \text{span}\{u_j \mid j \in J\}$ and $W_\ell := \text{span}\{u_{\ell,j} \mid j \in J\}$. The cluster is contained in the interval $[A, B]$.

Remark 7.19 (guaranteed lower eigenvalue bound). The following guaranteed lower eigenvalue bound of Carstensen and Gallistl [2014] is an immediate consequence of the abstract Lemma 3.13 and the explicit L^2 error estimate for the Morley interpolation operator from Proposition 7.7,

$$\lambda_{\ell,j} / (1 + \kappa_{\mathcal{M}}^2 \max_{T \in \mathcal{T}_\ell} \text{diam}(T)^4 \lambda_{\ell,j}) \leq \lambda_j. \quad \blacklozenge$$

Proposition 7.20 (L^2 control). *Provided $\|h_0\|_\infty \ll 1$, any eigenpair $(\lambda, u) \in \mathbb{R} \times W$ of (7.20) with $\|u\| = 1$ satisfies for some constant C_{L^2} that*

$$\|u - P_\ell u\| \leq \|u - \Lambda_\ell u\| \leq C_{L^2} (1 + M_J) \|h_0\|_\infty^s \|u - \Lambda_\ell u\|_{\text{NC}}.$$

Proof. The combination of Proposition 3.3 with Proposition 7.18 and Proposition 7.17 leads to

$$\|u - \Lambda_\ell u\| \lesssim (1 + M_J) \|h_0\|_\infty^s (\|u - \Lambda_\ell u\|_{\text{NC}} + \text{osc}_{2,2}(\lambda u, \mathcal{T}_\ell)).$$

Provided $\|h_0\|_\infty \ll 1$, the oscillation term can be absorbed. \blacksquare

The following proposition is based on the comparison result from Proposition 7.17 and states a best-approximation property for $\Lambda_\ell u$.

Proposition 7.21 (best-approximation result). *Provided $\|h_0\|_\infty \ll 1$, any eigenfunction $u \in W$ of (7.20) with $\|u\| = 1$ satisfies*

$$\|u - \Lambda_\ell u\|_{\text{NC}} \lesssim \|(1 - \Pi_\ell^0) D^2 u\|_{L^2(\Omega)}.$$

Proof. The L^2 control of Proposition 7.20 and the best-approximation result from Proposition 7.17 enable the arguments from the proof of Proposition 5.10. The details are omitted for brevity. \blacksquare

7.6. Error Estimator and Adaptive Algorithm

This section introduces the adaptive algorithm and states the optimality result.

For any triangle $T \in \mathcal{T}_\ell$, the explicit residual-based error estimator consists of the sum of the residuals of the computed discrete eigenfunctions $(u_{\ell,j})_{j \in J}$,

$$\begin{aligned} \eta_\ell^2(T) := & \sum_{j \in J} \left(h_T^4 \|\lambda_{\ell,j} u_{\ell,j}\|_{L^2(T)}^2 + \sum_{F \in \mathcal{F}(T) \cap \mathcal{F}_\ell(\Omega \cup \Gamma_C)} h_T \| [D_{\text{NC}}^2 u_{\ell,j}]_F \tau_F \|_{L^2(F)}^2 \right. \\ & \left. + \sum_{F \in \mathcal{F}(T) \cap \mathcal{F}_\ell(\Gamma_S)} h_T \| ([D_{\text{NC}}^2 u_{\ell,j}]_F \tau_F) \cdot \tau_F \|_{L^2(F)}^2 \right). \end{aligned}$$

Let, for any subset $\mathcal{K} \subseteq \mathcal{T}$,

$$\eta_\ell^2(\mathcal{K}) := \sum_{T \in \mathcal{K}} \eta_\ell^2(T).$$

This type of error estimator was introduced by Beirão da Veiga et al. [2007, 2010] and Hu and Shi [2009] for linear problems.

The adaptive algorithm is driven by this computable error estimator and runs the following loop.

Algorithm 7.22 (AFEM for the biharmonic eigenvalue problem).

Input: Initial triangulation \mathcal{T}_0 , bulk parameter $0 < \theta \leq 1$.

for $\ell = 0, 1, 2, \dots$ **do**

Solve. Compute discrete eigenpairs $(\lambda_{\ell,j}, u_{\ell,j})_{j \in J}$ of (7.21) with respect to \mathcal{T}_ℓ .

Estimate. Compute local contributions of the error estimator $(\eta_\ell^2(T))_{T \in \mathcal{T}_\ell}$.

Mark. Choose a minimal subset $\mathcal{M}_\ell \subseteq \mathcal{T}_\ell$ such that $\theta \eta_\ell^2(\mathcal{T}_\ell) \leq \eta_\ell^2(\mathcal{M}_\ell)$.

Refine. Generate $\mathcal{T}_{\ell+1} := \text{refine}(\mathcal{T}_\ell, \mathcal{M}_\ell)$ with Algorithm 2.15.

end for

Output: Sequences of triangulations $(\mathcal{T}_\ell)_\ell$ and discrete solutions $((\lambda_{\ell,j}, u_{\ell,j})_{j \in J})_\ell$. \blacklozenge

Remark 7.23. As in the foregoing chapters, all algebraic eigenvalue problems are assumed to be solved exactly. A more practical approach is based on Algorithm 3.17 and the analysis of this chapter carries over to the practical algorithm by means of a perturbation analysis as in [Carstensen, Gallistl, and Schedensack, 2014c]. \blacklozenge

Define the seminorm

$$|u|_{\mathfrak{A}_\sigma^{\Delta\Delta}} := \sup_{m \in \mathbb{N}} m^\sigma \inf_{\mathcal{T} \in \mathbb{T}(m)} \|(1 - \Pi_{\mathcal{T}}^0) D^2 u\|$$

and the approximation class

$$\mathfrak{A}_\sigma^{\Delta\Delta} := \left\{ v \in V \mid |v|_{\mathfrak{A}_\sigma^{\Delta\Delta}} < \infty \right\}.$$

The set $\mathfrak{A}_\sigma^{\Delta\Delta}$ does not depend on the finite element method and instead concerns the approximability of the Hessian by piecewise constant functions. As in Chapters 4, 5, and 6, the following alternative set, also referred to as approximation class, is employed in the analysis of the optimal convergence rates

$$\mathfrak{A}_\sigma^{\text{Morley}} := \left\{ u \in V \mid |u|_{\mathfrak{A}_\sigma^{\text{Morley}}} < \infty \right\}$$

for

$$|u|_{\mathfrak{A}_\sigma^{\text{Morley}}} := \sup_{m \in \mathbb{N}} m^\sigma \inf_{\mathcal{T} \in \mathbb{T}(m)} \|u - \Lambda_{\mathcal{T}} u\|.$$

Proposition 7.21 establishes the equivalence of those two approximation classes in the sense that any eigenfunction $u \in W$ satisfies $u \in \mathfrak{A}_\sigma^{\Delta\Delta}$ if and only if $u \in \mathfrak{A}_\sigma^{\text{Morley}}$. The following theorem states optimality of Algorithm 7.22. The proof will be given in the remaining parts of this chapter.

Theorem 7.24 (optimal convergence rates). *Provided the bulk parameter $\theta \ll 1$ and the initial mesh-size $\|h_0\|_\infty \ll 1$ are sufficiently small, Algorithm 7.22 computes triangulations $(\mathcal{T}_\ell)_\ell$ and discrete eigenpairs $((\lambda_{\ell,j}, u_{\ell,j})_{j \in J})_\ell$ with optimal rate of convergence in the sense that, for some constant C_{opt} ,*

$$\sup_{\ell \in \mathbb{N}} (\text{card}(\mathcal{T}_\ell) - \text{card}(\mathcal{T}_0))^\sigma \left(\sum_{j \in J} \|u_j - \Lambda_\ell u_j\|_{\text{NC}}^2 \right)^{1/2} \leq C_{\text{opt}} \left(\sum_{j \in J} |u_j|_{\mathfrak{A}_\sigma^{\text{Morley}}}^2 \right)^{1/2}.$$

Proposition 7.21 immediately implies the following consequence.

Corollary 7.25. *Provided the bulk parameter $\theta \ll 1$ and the initial mesh-size $\|h_0\|_\infty \ll 1$ are sufficiently small, Algorithm 7.22 computes triangulations $(\mathcal{T}_\ell)_\ell$ and discrete eigenpairs $((\lambda_{\ell,j}, u_{\ell,j})_{j \in J})_\ell$ with optimal rate of convergence in the sense that*

$$\sup_{\ell \in \mathbb{N}} (\text{card}(\mathcal{T}_\ell) - \text{card}(\mathcal{T}_0))^\sigma \sup_{\substack{w \in W \\ \|w\|=1}} \inf_{\substack{v_\ell \in W_\ell \\ \|v_\ell\|=1}} \|w - v_\ell\|_{\text{NC}} \lesssim \left(\sum_{j \in J} |u_j|_{\mathfrak{A}_\sigma^{\Delta\Delta}}^2 \right)^{1/2}. \quad \blacksquare$$

A convergence result for the error of the eigenvalues will be given in Corollary 8.24.

Remark 7.26 (optimality for inexact solve). The optimality results of Theorem 7.24 and Corollary 7.25 carry over to Algorithm 3.17 for sufficiently small $\varkappa \ll 1$ by means of a perturbation analysis as in [Carstensen and Gedicke, 2012] or [Carstensen, Gallistl, and Schedensack, 2014c]. \blacklozenge

7.7. Discrete Reliability and Optimal Convergence Rates

This section proves the discrete reliability for a theoretical error estimator. The proof of discrete reliability is one of the main difficulties in the optimality analysis of the biharmonic eigenvalue problem. The results presented in this section seem to be the first a posteriori results in the literature for the biharmonic eigenvalue problem.

The theoretical error estimator does not depend on the choice of the discrete eigenfunctions. Given an eigenpair (λ, u) , the error estimator is defined, for any $T \in \mathcal{T}_\ell$, as

$$\begin{aligned} \mu_\ell^2(T, \lambda, u) := & \sum_{j \in J} \left(h_T^4 \|\lambda P_\ell u\|_{L^2(T)}^2 + \sum_{F \in \mathcal{F}(T) \cap \mathcal{F}_\ell(\Omega \cup \Gamma_C)} h_T \| [D_{\text{NC}}^2 \Lambda_\ell u]_F \tau_F \|_{L^2(F)}^2 \right. \\ & \left. + \sum_{F \in \mathcal{F}(T) \cap \mathcal{F}_\ell(\Gamma_S)} h_T \| ([D_{\text{NC}}^2 \Lambda_\ell u]_F \tau_F) \cdot \tau_F \|_{L^2(F)}^2 \right). \end{aligned}$$

7. Biharmonic Eigenvalue Problem

Define, for any subset $\mathcal{K} \subseteq \mathcal{T}_\ell$,

$$\mu_\ell^2(\mathcal{K}, \lambda_j, u_j) := \sum_{T \in \mathcal{K}} \mu_\ell^2(T, \lambda_j, u_j) \quad \text{and} \quad \mu_\ell^2(\mathcal{K}) := \sum_{j \in J} \mu_\ell^2(T, \lambda_j, u_j).$$

The following shorthand notation for higher-order terms with respect to an eigenpair $(\lambda, u) \in \mathbb{R} \times W$ of (7.20) is employed throughout this section

$$\mathbf{r}_{\ell,m} := \|h_0\|_\infty^s \lambda (1 + M_J) C_{L^2} \sqrt{\|u - \Lambda_\ell u\|^2 + \|u - \Lambda_{\ell+m} u\|^2}. \quad (7.22)$$

The discrete reliability serves as a key tool for optimality. The first proof of discrete reliability for the Morley element in the context of the linear biharmonic problem was given by Hu et al. [2012]. The proof given here utilises the discrete Helmholtz decomposition of Section 7.3 and thereby circumvents the difficulties that arise from the use of the averaging operator of Hu et al. [2012] (cf. the comments in [Hu et al., 2013]). This new approach applies to the general boundary conditions considered in this thesis and avoids an additional layer of elements that arises in [Hu et al., 2013]. The following Lemma carefully explores the properties of the quasi-interpolation after Scott and Zhang [1990].

Lemma 7.27 (Scott-Zhang quasi-interpolation). *Let $\mathcal{T}_{\ell+m} \in \mathbb{T}(\mathcal{T}_\ell)$ be a refinement of \mathcal{T}_ℓ and let $\psi_{\ell+m} \in \mathcal{P}_1(\mathcal{T}_{\ell+m}; \mathbb{R}^2) \cap H^1(\Omega; \mathbb{R}^2)$ be such that $(D\psi_{\ell+m}\tau) \cdot \nu = 0$ on $\Gamma_S \cup \Gamma_F$ and $(D\psi_{\ell+m}\tau) \cdot \tau$ is constant on each connectivity component of Γ_F . Then there exists $\psi_\ell \in \mathcal{P}_1(\mathcal{T}_\ell; \mathbb{R}^2) \cap H^1(\Omega; \mathbb{R}^2)$ with the property that $\psi_\ell|_F = \psi_{\ell+m}|_F$ for all edges $F \in \mathcal{F}_\ell \cap \mathcal{F}_{\ell+m}$. Moreover, the function ψ_ℓ can be chosen in such a way that it preserves the boundary conditions in the sense that $(D\psi_\ell\tau) \cdot \nu = 0$ on $\Gamma_S \cup \Gamma_F$ and $(D\psi_\ell\tau) \cdot \tau$ is constant on each connectivity component of Γ_F . This quasi-interpolation satisfies the approximation and stability estimate*

$$\|h_\ell^{-1}(\psi_{\ell+m} - \psi_\ell)\|_{L^2(\Omega)} + \|D(\psi_{\ell+m} - \psi_\ell)\|_{L^2(\Omega)} \lesssim \|D\psi_{\ell+m}\|_{L^2(\Omega)}.$$

Remark 7.28. The quasi-interpolation of Lemma 7.27 preserves the boundary conditions imposed on the space $\mathfrak{X}(\mathcal{T}_{\ell+m})$ from Section 7.3 for any refinement $\mathcal{T}_{\ell+m} \in \mathbb{T}(\mathcal{T}_\ell)$. \blacklozenge

Proof of Lemma 7.27. The methodology of Scott and Zhang [1990] assigns to each vertex $z \in \mathcal{N}_\ell$ some edge $F_z \in \mathcal{F}_\ell$. The choice assigns, whenever possible, to a vertex $z \in \mathcal{N}_\ell$ an edge $F_z \in \mathcal{F}_\ell \cap \mathcal{F}_{\ell+m}$. For vertices $z \in \bar{\Gamma}_F$ that touch the free boundary, choose $F_z \in \mathcal{F}_\ell(\Gamma_F)$ if this does not contradict a possible choice of $F_z \in \mathcal{F}_\ell \cap \mathcal{F}_{\ell+m}$. Let, for any edge $F_z \in \mathcal{F}_\ell$, $\Phi_z \in L^2(F_z)$ denote the Riesz representation of the point evaluation δ_z at z in the space $\mathcal{P}_1(F)$.

For vertices that touch the simply supported part of the boundary but not the free part $z \in \bar{\Gamma}_S \setminus \bar{\Gamma}_F$ and that do not belong to any edge of $\mathcal{F}_\ell \cap \mathcal{F}_{\ell+m}$, denote the adjacent boundary edges by $(F_1, F_2) \in \mathcal{F}_\ell^2$ and define

$$\mathbf{v}_{F_1} \cdot \psi_\ell(z) = \int_{F_1} \Phi_z \mathbf{v}_{F_1} \cdot \psi_{\ell+m} ds \quad \text{and} \quad \mathbf{v}_{F_2} \cdot \psi_\ell(z) = \int_{F_2} \Phi_z \mathbf{v}_{F_2} \cdot \psi_{\ell+m} ds.$$

If the angle between F_1 and F_2 equals π , then $\mathbf{v}_{F_1} = \mathbf{v}_{F_2}$ and this definition is consistent. In this case set $\tau_{F_1} \cdot \psi_\ell(z) = \int_{F_1} \Phi_z \tau_{F_1} \cdot \psi_{\ell+m} ds$. For all remaining vertices z of \mathcal{T}_ℓ , define $\psi_\ell(z) \cdot e_j := \int_{F_z} \Phi_z \psi_{\ell+m} \cdot e_j ds$ for the unit vectors $e_j \in \{(1;0), (0;1)\}$.

This definition of ψ_ℓ is an admissible choice in the setting of Scott and Zhang [1990]. In particular, ψ_ℓ coincides with $\psi_{\ell+m}$ on edges of $\mathcal{F}_\ell \cap \mathcal{F}_{\ell+m}$. The error estimate follows from the theory in [Scott and Zhang, 1990].

It remains to show the claimed boundary conditions. Recall that $\psi_{\ell+m}$ satisfies $(D\psi_{\ell+m}\tau) \cdot \nu = 0$ on $\Gamma_S \cup \Gamma_F$ and $(D\psi_{\ell+m}\tau) \cdot \tau$ is constant on each connectivity component of Γ_F . In particular, this implies that $\psi_{\ell+m} \cdot \nu$ is constant along each straight part of $\Gamma_S \cup \Gamma_F$ and that $\psi_{\ell+m} \cdot \tau$ is affine along each straight part of Γ_F . Therefore, the above assignment of the nodal values interpolates $\psi_{\ell+m} \cdot \nu$ along $\overline{\Gamma_S \cup \Gamma_F}$ and $\psi_{\ell+m} \cdot \tau$ along $\overline{\Gamma_F}$ exactly and so these boundary conditions are valid for ψ_ℓ . ■

Proposition 7.29 (discrete reliability). *There exists a constant $C_{\text{drel}} \approx 1$ such that, for $\|h_0\|_\infty \ll 1$, any admissible refinement $\mathcal{T}_{\ell+m} \in \mathbb{T}(\mathcal{T}_\ell)$ of $\mathcal{T}_\ell \in \mathbb{T}$ and any eigenpair $(\lambda, u) \in \mathbb{R} \times W$ of (7.20) with $\|u\| = 1$ and $\mathbf{r}_{\ell,m}$ from (7.22) satisfy*

$$2\|(\Lambda_{\ell+m} - \Lambda_\ell)u\|_{\text{NC}}^2 \leq C_{\text{drel}}^2 (\mu_\ell^2(\mathcal{T}_\ell \setminus \mathcal{T}_{\ell+m}) + \mathbf{r}_{\ell,m}^2).$$

Proof. The discrete Helmholtz decomposition from Theorem 7.13 leads to $\phi_{\ell+m} \in V_{\ell+m}$ and $\psi_{\ell+m} \in \mathfrak{X}(\mathcal{T}_{\ell+m})$ such that

$$D_{\text{NC}}^2((\Lambda_{\ell+m} - \Lambda_\ell)u) = D_{\text{NC}}^2\phi_{\ell+m} + \text{sym Curl } \psi_{\ell+m}.$$

The orthogonality of the decomposition proves

$$\|(\Lambda_{\ell+m} - \Lambda_\ell)u\|_{\text{NC}}^2 = a_{\text{NC}}((\Lambda_{\ell+m} - \Lambda_\ell)u, \phi_{\ell+m}) - (D_{\text{NC}}^2\Lambda_\ell u, \text{Curl } \psi_{\ell+m})_{L^2(\Omega)}. \quad (7.23)$$

The projection property of the Morley interpolation operator (7.1), Lemma 3.4, the L^2 control of Proposition 7.20 and the approximation and stability property (7.4) prove for the first term of (7.23) that

$$\begin{aligned} a_{\text{NC}}((\Lambda_{\ell+m} - \Lambda_\ell)u, \phi_{\ell+m}) &= \lambda b((P_{\ell+m} - P_\ell)u, \phi_{\ell+m}) + \lambda b(P_\ell u, (1 - \mathcal{I}_\ell^{\text{m}})\phi_{\ell+m}) \\ &\lesssim (\mathbf{r}_{\ell,m} + \|h_\ell^2 \lambda P_\ell u\|_{L^2(\cup(\mathcal{T}_\ell \setminus \mathcal{T}_{\ell+m}))}) \|\phi_{\ell+m}\|_{\text{NC}}. \end{aligned}$$

Let $\psi_\ell \in \mathcal{P}_1(\mathcal{T}_\ell; \mathbb{R}^2) \cap H^1(\Omega; \mathbb{R}^2)$ denote the quasi-interpolation from Lemma 7.27. The function ψ_ℓ preserves those boundary conditions of $\psi_{\ell+m}$ that are necessary to guarantee that $\text{Curl } \psi_\ell$ and $D_{\text{NC}}^2\Lambda_\ell u$ are L^2 -orthogonal. Hence, an integration by parts shows for the second term of (7.23) that

$$(D_{\text{NC}}^2\Lambda_\ell u, \text{Curl } \psi_{\ell+m})_{L^2(\Omega)} = \sum_{F \in \mathcal{F}_\ell \setminus \mathcal{F}_{\ell+m}} \int_F ([D_{\text{NC}}^2\Lambda_\ell u]_F \tau_F) \cdot (\psi_{\ell+m} - \psi_\ell) ds.$$

The boundary conditions of $\psi_{\ell+m}$ and ψ_ℓ plus Cauchy and trace inequalities and the approximation and stability properties of the Scott-Zhang quasi-interpolation prove that this is bounded by $\|D\psi_{\ell+m}\|_{L^2(\Omega)}$ times

$$\left(\sum_{T \in \mathcal{T}_\ell \setminus \mathcal{T}_{\ell+m}} \left(\sum_{\substack{F \in \mathcal{F}(T) \\ \cap \mathcal{F}_\ell(\Omega \cup \Gamma_C)}} h_F \| [D_{\text{NC}}^2\Lambda_\ell u]_F \tau_F \|_{L^2(F)}^2 + \sum_{\substack{F \in \mathcal{F}(T) \\ \cap \mathcal{F}_\ell(\Gamma_S)}} h_F \| \tau_F \cdot ([D_{\text{NC}}^2\Lambda_\ell u]_F \tau_F) \|_{L^2(F)}^2 \right) \right)^{1/2}.$$

The combination of the foregoing estimates and the stability (7.11) conclude the proof. ■

7. Biharmonic Eigenvalue Problem

As in Section 5.7, the following reliability and efficiency are an immediate consequence of the discrete reliability and the a priori convergence results (e.g., Proposition 7.21).

Corollary 7.30 (reliability and efficiency). *Provided $\|h_0\|_\infty \ll 1$, it holds that*

$$\|u - \Lambda_\ell u\|_{\text{NC}}^2 \leq C_{\text{drel}}^2 \mu_\ell^2(\mathcal{T}_\ell, \lambda, u). \quad (7.24)$$

For some constant $C_{\text{eff}} \approx 1$, it holds that

$$\mu_\ell^2(\mathcal{T}_\ell, \lambda, u) \leq C_{\text{eff}}^2 \|u - \Lambda_\ell u\|_{\text{NC}}^2. \quad (7.25)$$

■

The proof of the discrete reliability is the main step in proving optimal convergence rates for Algorithm 7.22. The remaining arguments are analogous to those for the nonconforming \mathcal{P}_1 method for the eigenvalues of the Laplacian. The error estimator reduction and the following two results are the remaining ingredients.

The quasi-orthogonality for the Morley FEM was first proven by Hu et al. [2012] in the context of the linear biharmonic problem. The following result is an extension to the case of eigenvalue problems.

Proposition 7.31 (quasi-orthogonality). *Under the hypothesis $\|h_0\|_\infty \ll 1$ there exists a constant C_{qo} such that any eigenpair $(\lambda, u) \in \mathbb{R} \times W$ of (7.20) with $\|u\| = 1$, any $\mathcal{T}_\ell \in \mathbb{T}$ and any admissible refinement $\mathcal{T}_{\ell+m} \in \mathbb{T}(\mathcal{T}_\ell)$ satisfy*

$$\begin{aligned} |2a_{\text{NC}}(u - \Lambda_{\ell+m} u, \Lambda_{\ell+m} u - \Lambda_\ell u)| \\ \leq C_{\text{qo}} \left(\|h_\ell^2 \lambda P_\ell u\|_{L^2(\cup \mathcal{T}_\ell \setminus \mathcal{T}_{\ell+m})} + \mathbf{r}_{\ell,m} \right) \|u - \Lambda_{\ell+m} u\|_{\text{NC}}. \end{aligned}$$

Proof. The properties of the operator $\mathcal{J}_\ell^{\mathfrak{M}}$ of Section 7.1 enable the arguments of Proposition 5.21. In particular the constant of Proposition 7.5 (which is independent of m) enters the analysis. The details are omitted. ■

Proposition 7.32 (contraction property). *Under the condition $\|h_0\|_\infty \ll 1$, there exist $0 < \rho_2 < 1$ and $0 < \beta, \gamma < \infty$ such that, for any eigenpair $(\lambda, u) \in \mathbb{R} \times W$ with $\|u\| = 1$, the term $\xi_\ell^2 := \mu_\ell^2(\mathcal{T}_\ell, \lambda, u) + \beta \|u - \Lambda_\ell u\|_{\text{NC}}^2 + \gamma \|h_\ell^2 P_\ell u\|^2$ satisfies*

$$\xi_{\ell+1}^2 \leq \rho_2 \xi_\ell^2 \quad \text{for all } \ell \in \mathbb{N}_0.$$

Proof. The proof is analogous to that of Proposition 5.22. The details are omitted. ■

The proof of Theorem 7.24 follows the lines of Section 5.9 and is almost identical. Therefore, the details are omitted here.

7.8. Extension to Buckling Problems

This section describes a possible extension of the analysis to buckling problems. The weak form of the buckling problem $\Delta^2 u = \lambda \Delta u$ seeks a parameter λ and the deflection $u \in V$ such that

$$a(u, v) = \lambda b(u, v) \quad \text{for all } v \in V$$

for the bilinear form $b(\cdot, \cdot) := (D\cdot, D\cdot)_{L^2(\Omega)}$. This model describes the critical parameter λ in a stability analysis of a buckling plate [Timoshenko and Gere, 1985]. Its Morley finite element discretisation seeks $(\lambda_\ell, u_\ell) \in \mathbb{R} \times V_\ell$ such that

$$a_{\text{NC}}(u_\ell, v_\ell) = \lambda_\ell b_{\text{NC}}(u_\ell, v_\ell) \quad \text{for all } v_\ell \in V_\ell$$

with the piecewise version $b_{\text{NC}}(\cdot, \cdot) := (D_{\text{NC}}\cdot, D_{\text{NC}}\cdot)_{L^2(\Omega)}$. Assume for simplicity purely clamped boundary conditions $\partial\Omega = \Gamma_C$ and a simple eigenvalue, i.e., $\text{card}J = 1$.

The methodology of this thesis leads to the error estimator of the type

$$\eta_\ell^2 = \|h_\ell \lambda_\ell D_{\text{NC}} u_{\ell,j}\|_{L^2(\Omega)}^2 + \sum_{F \in \mathcal{F}_\ell} h_F \| [D_{\text{NC}}^2 u_{\ell,j}]_F \tau_F \|_{L^2(F)}^2 \quad (7.26)$$

which is reliable up to higher-order terms. The efficiency analysis, however, is unclear. In fact, the volume term $\|h_\ell \lambda_\ell D_{\text{NC}} u_{\ell,j}\|_{L^2(\Omega)}^2$ is not a residual and the techniques of Verfürth [1996] are not applicable. The residual $\|h_\ell^2 \lambda_{\ell,j} \Delta_{\text{NC}} u_{\ell,j}\|_{L^2(\Omega)}^2$ that one would expect in view of the linear problem cannot be obtained by integration by parts without further boundary terms.

It is helpful to consider the related Stokes problem: In two space dimensions, the Stokes eigenvalue problem can be equivalently written as a fourth-order buckling-type problem, the so-called streamfunction-vorticity formulation [Girault and Raviart, 1986]. If $\Omega \subseteq \mathbb{R}^2$ is simply-connected, the Curl operator defines an isomorphism from $H_0^2(\Omega)$ to the space Z of divergence-free $H_0^1(\Omega; \mathbb{R}^2)$ vector fields. Thus, the Stokes eigenproblem (6.11) may be reformulated: Seek $(\lambda, \psi) \in \mathbb{R} \times H_0^2(\Omega)$ such that

$$(D \text{Curl } \psi, D \text{Curl } \varphi) \equiv (D^2 \psi, D^2 \varphi)_{L^2(\Omega)} = \lambda (D \psi, D \varphi)_{L^2(\Omega)} \quad \text{for all } \varphi \in H_0^2(\Omega).$$

The eigenfunction u of (6.13) can be recovered as $u = \text{Curl } \psi$. This describes a fourth-order buckling problem for a clamped plate,

$$\Delta^2 \psi = \lambda \Delta \psi.$$

One possibility of implementing the nonconforming \mathcal{P}_1 FEM for the Stokes problem is to use the Morley finite element from Section 7.1 for this fourth-order problem. It can be easily verified by a dimension argument with the Euler formulae from page 90 that the space Z_ℓ of piecewise divergence-free nonconforming \mathcal{P}_1 vector fields is identical to the piecewise Curls of Morley finite element functions with clamped boundary conditions, details can be found in [Falk and Morley, 1990] or [Brenner, 1995]. Thus, the discrete problem 6.13 can be reformulated as: Seek $(\lambda_\ell, \psi_\ell) \in \mathbb{R} \times V_\ell$ such that

$$(D_{\text{NC}}^2 \psi_\ell, D_{\text{NC}}^2 \varphi_\ell) = \lambda_\ell (D_{\text{NC}} \psi_\ell, D_{\text{NC}} \varphi_\ell) \quad \text{for all } \varphi_\ell \in V_\ell,$$

where V_ℓ is the space of Morley finite element functions from Definition 7.1 with clamped boundary conditions, i.e., $\Gamma_C = \partial\Omega$. The discrete eigenfunction u_ℓ of (6.13) can be recovered as $u_\ell = \text{Curl}_{\text{NC}} \psi_\ell$. (This implementation trick in two dimensions allows to use the Morley finite element for the divergence-free discretisation (6.13).)

It comes out from these considerations that the error estimator (7.26) is exactly that for the nonconforming \mathcal{P}_1 finite element discretisation of the Stokes problem. The discussion in Remark 6.2 shows that one cannot expect this error estimator to be efficient without the error of the pressure approximation on the right-hand side. However, Theorem 6.9 can be applied and shows optimal convergence rates for the adaptive Morley finite element discretisation of the buckling problem with respect to an approximation class that involves the pressure-like variable.

8. Eigenvalue Error Estimates for Nonconforming FEMs

The Chapters 5, 6, and 7 established optimal convergence rates of nonconforming adaptive FEMs in terms of the eigenfunction approximation. This chapter proves that those quantities provide an upper bound for the error of the eigenvalues. The results of Knyazev and Osborn [2006] (Theorem 3.5 of this thesis) do not directly apply in the case of nonconforming FEMs. In this chapter, a novel methodology is employed to prove eigenvalue error estimates which is different from that of Boffi et al. [2014] in that it does not require a conforming subspace. This allows to include the Stokes and the biharmonic eigenproblem in the analysis. The main idea behind this technique is to introduce an auxiliary eigenvalue problem in the sum of the continuous and the discrete spaces. Section 8.1 explains the new functional setting in detail for the nonconforming \mathcal{P}_1 finite element. Section 8.2 establishes error estimates for the eigenvalues of the Laplacian. The eigenvalue error estimate for the Stokes eigenvalues follow in Section 8.3. Section 8.4 is devoted to the eigenvalues of the biharmonic operator.

8.1. A Nonstandard Quasi-Ritz Projection

Throughout this section, let $V := H_0^1(\Omega)$ and let $V_\ell := \mathfrak{C}\mathfrak{R}_0^1(\mathcal{T}_\ell)$ denote the nonconforming \mathcal{P}_1 finite element space from Definition 5.1. As in Chapter 5, define the scalar products

$$a(v, w) := (Dv, Dw)_{L^2(\Omega)} \quad \text{and} \quad b(v, w) := (v, w)_{L^2(\Omega)}$$

and induced norms $\|v\| := a(v, v)^{1/2}$ and $\|v\| := b(v, v)^{1/2}$, as well as the discrete scalar product

$$a_{\text{NC}}(v_\ell, w_\ell) := (D_{\text{NC}}v_\ell, D_{\text{NC}}w_\ell)_{L^2(\Omega)} \quad \text{with} \quad \|v_\ell\|_{\text{NC}} := a_{\text{NC}}(v_\ell, v_\ell)^{1/2}.$$

Define $\widehat{V}_\ell := V + V_\ell$ as the sum of the continuous and the discrete space. Recall that, for any $\mathcal{T}_{\ell+m} \in \mathbb{T}(\mathcal{T}_\ell)$ with $\widehat{V}_{\ell+m} := V + V_{\ell+m}$, the interpolation operator $\mathcal{J}_\ell^{\mathfrak{C}\mathfrak{R}} : \widehat{V}_{\ell+m} \rightarrow V_\ell$ acts as

$$\int_F (\widehat{v}_{\ell+m} - \mathcal{J}_\ell^{\mathfrak{C}\mathfrak{R}} \widehat{v}_{\ell+m}) ds = 0 \quad \text{for all } F \in \mathcal{F}_\ell \text{ and all } \widehat{v}_{\ell+m} \in \widehat{V}_{\ell+m}.$$

Moreover, (5.2) states, for any $T \in \mathcal{T}_\ell$, that

$$\|h_T^{-1}(\widehat{v}_{\ell+m} - \mathcal{J}_\ell^{\mathfrak{C}\mathfrak{R}} \widehat{v}_{\ell+m})\|_{L^2(T)} + \|D_{\text{NC}}(\widehat{v}_{\ell+m} - \mathcal{J}_\ell^{\mathfrak{C}\mathfrak{R}} \widehat{v}_{\ell+m})\|_{L^2(T)} \lesssim \|D_{\text{NC}}(\widehat{v}_{\ell+m} - \mathcal{J}_\ell^{\mathfrak{C}\mathfrak{R}} \widehat{v}_{\ell+m})\|_{L^2(T)}.$$

Definition 8.1 (quasi-Ritz projection in \widehat{V}_ℓ). Given $f \in V$, let $u \in V$ denote the solution to (5.10), namely

$$a(u, v) = b(f, v) \quad \text{for all } v \in V. \tag{8.1}$$

8. Eigenvalue Error Estimates for Nonconforming FEMs

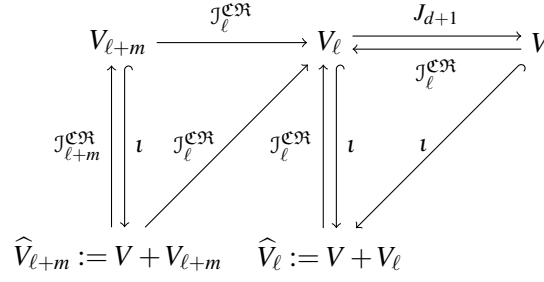


Figure 8.1.: Mappings between the spaces \widehat{V}_{ℓ} , $\widehat{V}_{\ell+m}$, V , V_{ℓ} and $V_{\ell+m}$ for the nonconforming \mathcal{P}_1 FEM; ι is the inclusion.

The quasi-Ritz projection $\widehat{R}_{\ell}u \in \widehat{V}_{\ell}$ is defined as the solution of

$$a_{\text{NC}}(\widehat{R}_{\ell}u, \widehat{v}_{\ell}) = b(f, \widehat{v}_{\ell}) \quad \text{for all } \widehat{v}_{\ell} \in \widehat{V}_{\ell}. \quad \blacklozenge$$

Remark 8.2. This definition is essentially the same as Definition 3.1 with V_{ℓ} replaced by \widehat{V}_{ℓ} . In order to avoid any confusion of V_{ℓ} and \widehat{V}_{ℓ} , it is stated as a separate definition. It should be emphasised that in the present case there is an inclusion $V \subseteq \widehat{V}_{\ell}$. This is an admissible choice in the framework of Section 3.1. \blacklozenge

Definition 8.1 leads to a new view on nonconforming finite element schemes in the following sense: Both V and V_{ℓ} are subspaces of the space \widehat{V}_{ℓ} and the solutions $u \in V$ and $u_{\ell} \in V_{\ell}$ of (5.10) and (5.11) are “conforming approximations” of $R_{\ell}u$. To the best of the author’s knowledge, this is a new approach to nonconforming finite elements that has not been studied in the existing literature.

It is crucial that the nonconforming interpolation operator $\mathcal{J}_{\ell}^{\mathcal{CR}}$ is defined on \widehat{V}_{ℓ} as well as $\widehat{V}_{\ell+m} = V + V_{\ell+m}$ with respect to a refined triangulation $\mathcal{T}_{\ell+m} \in \mathbb{T}(\mathcal{T}_{\ell})$. This operator and the conforming companion operator J_{d+1} from Proposition 5.4 establish suitable connections between the spaces V , V_{ℓ} , \widehat{V}_{ℓ} , $V_{\ell+m}$ and $\widehat{V}_{\ell+m}$. Those two operators displayed in Figure 8.1 are the core of the analysis of \widehat{R}_{ℓ} which is essential to derive eigenvalue error estimates.

The following proposition gives an L^2 error estimate for the quasi-Ritz projection \widehat{R}_{ℓ} from Definition 8.1. Recall the elliptic regularity index s from (4.4) of the Poisson problem.

Proposition 8.3 (L^2 error estimate for \widehat{R}_{ℓ}). *Let $u \in V$ solve the linear problem (8.1) with right-hand side $f \in V$. Then, $\widehat{R}_{\ell}u$ satisfies the following L^2 error estimate*

$$\|u - \widehat{R}_{\ell}u\| \lesssim \|h_0\|_{\infty}^s \|u - \widehat{R}_{\ell}u\|_{\text{NC}}.$$

Remark 8.4. The conformity $V \subseteq \widehat{V}_{\ell}$ shows that u is the a_{NC} -orthogonal projection of $\widehat{R}_{\ell}u$ onto V . Therefore, one may think of using a standard duality argument for the proof of the L^2 error control. Indeed, this procedure can be applied, but it will not immediately lead to a right-hand side that is explicit in the mesh-size $\|h_0\|_{\infty}$. Therefore, the proof of Proposition 8.3 employs a different technique based on the operators $\mathcal{J}_{\ell}^{\mathcal{CR}}$ and J_{d+1} to obtain an estimate in terms of $\|h_0\|_{\infty}$. \blacklozenge

Proof of Proposition 8.3. Set $\widehat{e} := u - \widehat{R}_{\ell}u$ and let $z \in V$ denote the solution to

$$a(z, w) = b(\widehat{e}, w) \quad \text{for all } w \in V.$$

With the companion operator J_{d+1} from Proposition 5.4 and the nonconforming interpolation operator $\mathcal{J}_\ell^{\mathfrak{C}\mathfrak{R}}$, it follows that

$$\|\hat{e}\|^2 = b((1 - J_{d+1})\mathcal{J}_\ell^{\mathfrak{C}\mathfrak{R}}\hat{e}, \hat{e}) + b((1 - \mathcal{J}_\ell^{\mathfrak{C}\mathfrak{R}})\hat{e}, \hat{e}) + b(J_{d+1}\mathcal{J}_\ell^{\mathfrak{C}\mathfrak{R}}\hat{e}, \hat{e}). \quad (8.2)$$

The Cauchy inequality and the error estimates (5.2) and (5.4) bound the first two terms on the right-hand side as

$$b((1 - J_{d+1})\mathcal{J}_\ell^{\mathfrak{C}\mathfrak{R}}\hat{e}, \hat{e}) + b((1 - \mathcal{J}_\ell^{\mathfrak{C}\mathfrak{R}})\hat{e}, \hat{e}) \lesssim \|h_0\|_\infty \|\hat{e}\|_{\text{NC}} \|\hat{e}\|.$$

Since $a(z, \hat{e}) = a(\hat{e}, z) = a(u - \hat{R}_\ell u, z) = 0$ by the definition of \hat{R}_ℓ , the remaining term of (8.2) satisfies

$$\begin{aligned} b(J_{d+1}\mathcal{J}_\ell^{\mathfrak{C}\mathfrak{R}}\hat{e}, \hat{e}) &= a(z, J_{d+1}\mathcal{J}_\ell^{\mathfrak{C}\mathfrak{R}}\hat{e}) \\ &= a_{\text{NC}}(z, (\mathcal{J}_\ell^{\mathfrak{C}\mathfrak{R}} - 1)\hat{e}) + a_{\text{NC}}(z, (J_{d+1} - 1)\mathcal{J}_\ell^{\mathfrak{C}\mathfrak{R}}\hat{e}). \end{aligned}$$

The projection properties (5.1) and (5.3) imply that $D_{\text{NC}}(\mathcal{J}_\ell^{\mathfrak{C}\mathfrak{R}} - 1)\hat{e}$ as well as $D_{\text{NC}}(J_{d+1} - 1)\mathcal{J}_\ell^{\mathfrak{C}\mathfrak{R}}\hat{e}$ are L^2 -orthogonal onto piecewise constants. This and the elliptic regularity (4.4) show that

$$\begin{aligned} &a_{\text{NC}}(z, (\mathcal{J}_\ell^{\mathfrak{C}\mathfrak{R}} - 1)\hat{e}) + a_{\text{NC}}(z, (J_{d+1} - 1)\mathcal{J}_\ell^{\mathfrak{C}\mathfrak{R}}\hat{e}) \\ &= ((1 - \Pi_\ell^0)Dz, D_{\text{NC}}(\mathcal{J}_\ell^{\mathfrak{C}\mathfrak{R}} - 1)\hat{e})_{L^2(\Omega)} + ((1 - \Pi_\ell^0)Dz, D_{\text{NC}}(J_{d+1} - 1)\mathcal{J}_\ell^{\mathfrak{C}\mathfrak{R}}\hat{e})_{L^2(\Omega)} \\ &\lesssim \|h_0\|_\infty^s \|z\|_{H^{1+s}(\Omega)} \|\hat{e}\|_{\text{NC}} \lesssim \|h_0\|_\infty^s \|\hat{e}\| \|\hat{e}\|_{\text{NC}}. \end{aligned}$$

The combination of the above estimates concludes the proof. \blacksquare

The next proposition states that the error $u - \hat{R}_\ell u$ in the energy norm is comparable with the best-approximation of Du by piecewise constants.

Proposition 8.5 (comparison for \hat{R}_ℓ). *Let $u \in V$ solve (5.10) with right-hand side $f \in V$. Then the quasi-Ritz projection $\hat{R}_\ell u$ satisfies*

$$\|u - \hat{R}_\ell u\|_{\text{NC}} \lesssim \|(1 - \Pi_\ell^0)Du\|_{L^2(\Omega)} + \text{osc}_{1,1}(f, \mathcal{T}_\ell).$$

Proof. The triangle inequality shows for the nonconforming interpolation operator $\mathcal{J}_\ell^{\mathfrak{C}\mathfrak{R}}$ that

$$\|u - \hat{R}_\ell u\|_{\text{NC}} \leq \|\hat{R}_\ell u - \mathcal{J}_\ell^{\mathfrak{C}\mathfrak{R}}u\|_{\text{NC}} + \|u - \mathcal{J}_\ell^{\mathfrak{C}\mathfrak{R}}u\|_{\text{NC}}.$$

Since $\|u - \mathcal{J}_\ell^{\mathfrak{C}\mathfrak{R}}u\|_{\text{NC}} = \|(1 - \Pi_\ell^0)Du\|$ by the projection property (5.1), it remains to estimate the first term on the right-hand side. Set $\hat{\phi}_\ell := \hat{R}_\ell u - \mathcal{J}_\ell^{\mathfrak{C}\mathfrak{R}}u$. The definition of \hat{R}_ℓ , the projection property (5.1) and the properties of the companion operator from Proposition 5.4 yield

$$\begin{aligned} \|\hat{R}_\ell u - \mathcal{J}_\ell^{\mathfrak{C}\mathfrak{R}}u\|_{\text{NC}}^2 &= a_{\text{NC}}(\hat{R}_\ell u - \mathcal{J}_\ell^{\mathfrak{C}\mathfrak{R}}u, \hat{\phi}_\ell) \\ &= b(f, \hat{\phi}_\ell) - a_{\text{NC}}(u, \mathcal{J}_\ell^{\mathfrak{C}\mathfrak{R}}\hat{\phi}_\ell) \\ &= b(f, \hat{\phi}_\ell - J_{d+1}\mathcal{J}_\ell^{\mathfrak{C}\mathfrak{R}}\hat{\phi}_\ell) - a_{\text{NC}}(u, (1 - J_{d+1})\mathcal{J}_\ell^{\mathfrak{C}\mathfrak{R}}\hat{\phi}_\ell). \end{aligned}$$

The triangle inequality and the approximation and stability properties (5.2) and (5.4) show for the first term that

$$b(f, \hat{\phi}_\ell - J_{d+1}\mathcal{J}_\ell^{\mathfrak{C}\mathfrak{R}}\hat{\phi}_\ell) \lesssim \|h_\ell f\| \|\hat{\phi}_\ell\|_{\text{NC}}.$$

8. Eigenvalue Error Estimates for Nonconforming FEMs

The known efficiency

$$\|h_\ell f\| \lesssim \|(1 - \Pi_\ell^0)Du\| + \text{osc}_{1,1}(f, \mathcal{T}_\ell)$$

follows from arguments similar to those of Proposition 4.3.

The projection property (5.3) of J_{d+1} and (5.4) reveal

$$a_{\text{NC}}(u, (1 - J_{d+1})\mathcal{J}_\ell^{\text{cgr}}\hat{\phi}_\ell) = ((1 - \Pi_\ell^0)Du, D_{\text{NC}}(1 - J_{d+1})\mathcal{J}_\ell^{\text{cgr}}\hat{\phi}_\ell)_{L^2(\Omega)}.$$

This and the stability properties (5.2) and (5.4) conclude the proof. ■

8.2. Eigenvalues of the Laplacian

This section extends the results of the foregoing Section 8.1 to eigenvalue problems. This leads to eigenvalue error estimates for the nonconforming \mathcal{P}_1 FEM of the Laplace eigenvalue problem.

Recall the notation of Section 8.1 with $\widehat{V}_\ell := V + V_\ell$ and note that \widehat{V}_ℓ equipped with the scalar product a_{NC} is a Hilbert space. The space \widehat{V}_ℓ is a subspace of the finite product $H^1(\mathcal{T}_\ell) := \prod_{T \in \mathcal{T}_\ell} H^1(\text{int}(T))$ and the embedding $(\widehat{V}_\ell, \|\cdot\|_{\text{NC}}) \rightarrow (L^2(\Omega), \|\cdot\|)$ is compact for a fixed triangulation \mathcal{T}_ℓ (for more details on such broken Sobolev spaces see [Buffa and Ortner, 2009]). Hence, the eigenvalue problem

$$a_{\text{NC}}(\hat{u}_\ell, \hat{v}_\ell) = \hat{\lambda}_\ell b(\hat{u}_\ell, \hat{v}_\ell) \quad \text{for all } \hat{v}_\ell \in \widehat{V}_\ell \quad (8.3)$$

has a countable and discrete spectrum

$$0 < \hat{\lambda}_{\ell,1} \leq \hat{\lambda}_{\ell,2} \leq \dots$$

with corresponding b -orthonormal eigenfunctions $(\hat{u}_{\ell,1}, \hat{u}_{\ell,2}, \dots)$. For an eigenvalue cluster described by the index set $J = \{n+1, \dots, n+N\}$, the set $\widehat{W}_\ell := \text{span}\{\hat{u}_{\ell,j} \mid j \in J\}$ describes the corresponding invariant subspace with the L^2 projection \widehat{P}_ℓ onto \widehat{W}_ℓ and let $\widehat{\Lambda}_\ell := \widehat{P}_\ell \circ \widehat{R}_\ell$. Furthermore, adopt the notation on the eigenvalues of the Laplacian and their approximations from Section 5.5.

The eigenvalue problem (8.3) is related to the (inverse of) a compact operator for each triangulation \mathcal{T}_ℓ . The first important observation is that the spectrum is robust under mesh-refinement.

Proposition 8.6. *Let $(\mathcal{T}_\ell)_{\ell \in \mathbb{N}_0}$ be a sequence of triangulations generated by the refinement rules of Section 2.2 with $\|h_0\|_\infty \ll 1$. Then any $j \in \mathbb{N}$ and the constant C from the estimate in (5.2) satisfy*

$$\frac{\lambda_{\ell,j}}{1 + C\|h_\ell\|_\infty^2 \lambda_{\ell,j}} \leq \hat{\lambda}_{\ell,j} \leq \lambda_{\ell,j}. \quad (8.4)$$

In particular, if $\|h_\ell\|_\infty \rightarrow 0$ as $\ell \rightarrow \infty$, one has convergence $\hat{\lambda}_{\ell,j} \rightarrow \lambda_j$.

Proof. The min-max principle (3.9) shows, for any $j \in \mathbb{N}$, that

$$\hat{\lambda}_{\ell,j} \leq \min\{\lambda_j, \lambda_{\ell,j}\}.$$

The properties (5.1) and (5.2) and Lemma 3.13 prove the lower eigenvalue bound in case that $\|h_\ell\|_\infty$ is sufficiently small

$$\frac{\lambda_{\ell,j}}{1 + C\|h_\ell\|_\infty^2 \lambda_{\ell,j}} \leq \hat{\lambda}_{\ell,j}$$

for some constant $C \approx 1$. This proves the two-sided estimate (8.4). This implies the convergence $|\lambda_{\ell,j} - \hat{\lambda}_{\ell,j}| \rightarrow 0$ as $\ell \rightarrow \infty$. The triangle inequality and the a priori estimate (5.15) prove $\hat{\lambda}_{\ell,j} \rightarrow \lambda_j$. ■

The robustness implies the following separation bound.

Corollary 8.7. *Provided $\|h_0\|_\infty \ll 1$, there exists a separation constant for the cluster J in the sense that*

$$\widehat{M}_J := \sup_{\mathcal{T}_\ell \in \mathbb{T}} \max_{j \in \mathbb{N} \setminus J} \max_{k \in J} \max \left\{ \frac{\hat{\lambda}_{k,\ell}}{|\lambda_j - \hat{\lambda}_{k,\ell}|}, \frac{\hat{\lambda}_{k,\ell}}{|\lambda_{\ell,j} - \hat{\lambda}_{k,\ell}|}, \frac{\lambda_k}{|\hat{\lambda}_{\ell,j} - \lambda_k|}, \frac{\lambda_k}{|\lambda_{\ell,j} - \lambda_k|} \right\} < \infty. \quad (\widehat{\text{H1}})$$

This formula uses the convention $\lambda_{\ell,j} := \lambda_{\ell, \dim(V_\ell)}$ for $j > \dim(V_\ell)$.

Remark 8.8. The separation condition $(\widehat{\text{H1}})$ implies (H1) from page 22 with $M_J \leq \widehat{M}_J$. ♦

This separation constant allows the use of the framework of Section 3.1 where the space V is approximated by \widehat{V}_ℓ .

Proposition 8.9 (L^2 error estimate for $\widehat{\Lambda}_\ell$). *Provided $\|h_0\|_\infty \ll 1$, any eigenpair $(\lambda, u) \in \mathbb{R} \times W$ of (5.13) with $\|u\| = 1$ satisfies*

$$\|u - \Lambda_\ell u\| + \|u - \widehat{\Lambda}_\ell u\| \lesssim (1 + \widehat{M}_J) \|h_0\|_\infty^s \|(1 - \Pi_\ell^0)Du\|.$$

Proof. An immediate consequence of Proposition 3.3 (where V_ℓ is replaced by \widehat{V}_ℓ and Λ_ℓ is replaced by $\widehat{\Lambda}_\ell$) and Proposition 8.5 reads

$$\|u - \widehat{\Lambda}_\ell u\| \leq (1 + \widehat{M}_J) \|u - \widehat{R}_\ell u\| \lesssim (1 + \widehat{M}_J) \|h_0\|_\infty^s (\|(1 - \Pi_\ell^0)Du\|_{L^2(\Omega)} + \text{osc}_{1,1}(\lambda u, \mathcal{T}_\ell)).$$

Proposition 5.9, the best approximation result of Proposition 5.10 and $M_J \leq \widehat{M}_J$ imply

$$\|u - \Lambda_\ell u\| \leq C_{L^2} (1 + \widehat{M}_J) \|h_0\|_\infty^s \|(1 - \Pi_\ell^0)Du\|.$$

The sum of the preceding two displayed formulas concludes the proof: Since $\|h_0\|_\infty \ll 1$, the oscillation term $\text{osc}_{1,1}(\lambda u, \mathcal{T}_\ell) \lesssim \|h_0\|_\infty \|u - \Lambda_\ell u\|$ can be absorbed. ■

The next result states that the error of the eigenfunction approximation $\widehat{\Lambda}_\ell u$ in \widehat{V}_ℓ is comparable with the best-approximation of the derivative by piecewise constants.

Proposition 8.10 (comparison result for $\widehat{\Lambda}_\ell$). *Provided $\|h_0\|_\infty \ll 1$, any eigenpair $(\lambda, u) \in \mathbb{R} \times W$ of (5.13) with $\|u\| = 1$ satisfies*

$$\|(1 - \widehat{\Lambda}_\ell)u\|_{\text{nc}} \lesssim \|(1 - \Pi_\ell^0)Du\|.$$

8. Eigenvalue Error Estimates for Nonconforming FEMs

Proof. The triangle inequality gives

$$\|(1 - \widehat{\Lambda}_\ell)u\|_{\text{NC}} \leq \|(1 - \widehat{R}_\ell)u\|_{\text{NC}} + \|(\widehat{R}_\ell - \widehat{\Lambda}_\ell)u\|_{\text{NC}}.$$

Proposition 8.5 implies that the first term on the right-hand side is controlled by $\|(1 - \Pi_0)Du\|$. Set $\widehat{\phi}_\ell := (\widehat{R}_\ell - \widehat{\Lambda}_\ell)u$. The definition of \widehat{R}_ℓ (note that the right-hand side is $f := \lambda u$) and Lemma 3.4 (with V_ℓ replaced by \widehat{V}_ℓ) lead to

$$\|(\widehat{R}_\ell - \widehat{\Lambda}_\ell)u\|_{\text{NC}}^2 = a_{\text{NC}}((\widehat{R}_\ell - \widehat{\Lambda}_\ell)u, \widehat{\phi}_\ell) = \lambda b(u - \widehat{P}_\ell u, \widehat{\phi}_\ell) \leq \lambda \|u - \widehat{P}_\ell u\| \|\widehat{\phi}_\ell\|.$$

The discrete Friedrichs inequality of Proposition 2.32 shows that $\|\widehat{\phi}_\ell\| \lesssim \|\widehat{\phi}_\ell\|_{\text{NC}}$. The L^2 error estimate from Proposition 8.9 concludes the proof. Indeed, the resulting higher-order term $(1 + \widehat{M}_J)\lambda \|h_0\|_\infty^s \|(1 - \widehat{\Lambda}_\ell)u\|_{\text{NC}}$ can be absorbed for $\|h_0\|_\infty \ll 1$. \blacksquare

Recall Remark 2.35 and let, for finite-dimensional subspaces $X \subseteq \widehat{V}_\ell$ and $Y \subseteq \widehat{V}_\ell$ the sine of the largest principal angle from X to Y be denoted by

$$\sin_{a,\text{NC}} \angle(X, Y) = \sup_{\substack{x \in X \\ \|x\|_{\text{NC}}=1}} \inf_{y \in Y} \|x - y\|_{\text{NC}}$$

Provided $\dim(X) = \dim(Y) < \infty$, Corollary 2.34 implies

$$\sin_{a,\text{NC}} \angle(X, Y) = \sin_{a,\text{NC}} \angle(Y, X)$$

as well as

$$\sin_{a,\text{NC}}(X, Y) \leq \sin_{a,\text{NC}} \angle(X, Z) + \sin_{a,\text{NC}} \angle(Z, Y)$$

for any subspace $Z \subseteq \widehat{V}_\ell$ with $\dim(X) = \dim(Y) = \dim(Z) < \infty$.

The tools developed in this section lead to the following eigenvalue error estimate

Theorem 8.11 (eigenvalue error estimates). *Provided $\|h_0\|_\infty \ll 1$, it holds that*

$$\begin{aligned} \max_{j \in J} \frac{|\lambda_j - \lambda_{\ell,j}|}{\max\{\lambda_j, \lambda_{\ell,j}\}} &\lesssim (1 + \widehat{M}_J^2 B^2) \sin_{a,\text{NC}}^2 \angle(W, W_\ell) \\ &\lesssim (1 + \widehat{M}_J^2 B^2) \sup_{\substack{w \in W \\ \|w\|_{\text{NC}}=1}} \|(1 - \Pi_\ell^0)Dw\|_{L^2(\Omega)}^2. \end{aligned}$$

The proof of Theorem 8.11 requires the following Lemma with the constant C_{dF} from the discrete Friedrichs inequality of Proposition 2.32.

Lemma 8.12. *The separation condition $(\widehat{H}1)$ from Corollary 8.7 implies*

$$\max_{j \in J} \frac{|\lambda_j - \lambda_{\ell,j}|}{\max\{\lambda_j, \lambda_{\ell,j}\}} \leq 2(1 + \widehat{M}_J^2 B^2 C_{dF}^4) \left(\sin_{a,\text{NC}}^2 \angle(W, \widehat{W}_\ell) + \sin_{a,\text{NC}}^2 \angle(W, W_\ell) \right).$$

Proof. Notice that, in contrast to the case of conforming finite element methods, the sign of $\lambda_j - \lambda_{\ell,j}$ is not known in the present case of nonconforming methods

The min-max principle and Theorem 3.5 (where V is replaced by \widehat{V}_ℓ and V_ℓ is replaced by V) prove

$$\lambda_j - \lambda_{\ell,j} \leq \lambda_j - \widehat{\lambda}_{\ell,j} \leq \lambda_j (1 + \widehat{M}_J^2 B^2 C_{dF}^4) \sin_{a,\text{NC}}^2 \angle(\widehat{W}_\ell, W). \quad (8.5)$$

Here, Theorem 3.5 has been applied to the case that the eigenvalues in V are Ritz values of the eigenvalues in \widehat{V}_ℓ . Notice carefully that Theorem 3.5 does not require a finite dimension of the “approximating” subspace (in this case V) as pointed out in Remark 3.7.

Since the eigenvalue cluster J is finite and, therefore, the spaces \widehat{W}_ℓ and W have equal finite dimension, Corollary 2.34 implies that

$$\sin_{a,\text{NC}}^2 \angle(\widehat{W}_\ell, W) = \sin_{a,\text{NC}}^2 \angle(W, \widehat{W}_\ell).$$

In order to bound the modulus $|\lambda_j - \lambda_{\ell,j}|$, consider also the reverse sign. Notice that the nonconforming finite element space V_ℓ acts as a conforming subspace of \widehat{V}_ℓ . The min-max principle and Theorem 3.5 (where V is replaced by \widehat{V}_ℓ) then prove

$$\lambda_{\ell,j} - \lambda_j \leq \lambda_{\ell,j} - \hat{\lambda}_{\ell,j} \leq \lambda_{\ell,j} (1 + \widehat{M}_J^2 B^2 C_{dF}^4) \sin_{a,\text{NC}}^2 \angle(\widehat{W}_\ell, W_\ell).$$

Corollary 2.34 implies

$$\begin{aligned} \sin_{a,\text{NC}}^2 \angle(\widehat{W}_\ell, W_\ell) / 2 &\leq \sin_{a,\text{NC}}^2 \angle(\widehat{W}_\ell, W) + \sin_{a,\text{NC}}^2 \angle(W, W_\ell) \\ &= \sin_{a,\text{NC}}^2 \angle(W, \widehat{W}_\ell) + \sin_{a,\text{NC}}^2 \angle(W, W_\ell). \end{aligned} \quad \blacksquare$$

Proof of Theorem 8.11. For any $j \in J$, Lemma 8.12 implies

$$\frac{|\lambda_j - \lambda_{\ell,j}|}{\max\{\lambda_j, \lambda_{\ell,j}\}} \leq 2(1 + \widehat{M}_J^2 B^2 C_{dF}^4) \left(\sin_{a,\text{NC}}^2 \angle(W, \widehat{W}_\ell) + \sin_{a,\text{NC}}^2 \angle(W, W_\ell) \right).$$

Proposition 8.10 shows

$$\sin_{a,\text{NC}}^2 \angle(W, \widehat{W}_\ell) \lesssim \sin_{a,\text{NC}}^2 \angle(W, W_\ell).$$

This proves the first stated inequality. The second inequality follows from Proposition 5.10. \blacksquare

The eigenvalue error estimates of this section and the optimality result of Corollary 5.14 together with Remark 3.20 result in the following optimal convergence rate for the eigenvalue error.

Corollary 8.13. *Provided the bulk parameter $\theta \ll 1$ and the initial mesh-size $\|h_0\|_\infty \ll 1$ are sufficiently small, Algorithm 5.11 computes triangulations $(\mathcal{T}_\ell)_\ell$ and discrete eigenpairs $((\lambda_{\ell,j}, u_{\ell,j})_{j \in J})_\ell$ with optimal rate of convergence in the sense that*

$$\begin{aligned} \max_{k \in J} (1 + \widehat{M}_J^2 B^2)^{-1/2} \left(\frac{|\lambda_k - \lambda_{\ell,k}|}{\max\{\lambda_k, \lambda_{\ell,k}\}} \right)^{1/2} + \sin_{a,\text{NC}} \angle(W, W_\ell) \\ \lesssim A^{-1/2} (\text{card}(\mathcal{T}_\ell) - \text{card}(\mathcal{T}_0))^{-\sigma} \left(\sum_{j \in J} |u_j|_{\mathfrak{A}_\sigma}^2 \right)^{1/2}. \end{aligned} \quad \blacksquare$$

8.3. Stokes System

This section extends the methodology of the previous two sections to the Stokes eigenvalue problem from Chapter 6. The arguments are similar to those for the Laplace operator and therefore not always led out in full detail.

Recall the functional setting from Chapter 6 with $V := H_0^1(\Omega; \mathbb{R}^d)$ and $M := L_0^2(\Omega)$ and the bilinear form

$$a(v, w) := (Dv, Dw)_{L^2(\Omega)} \quad \text{for all } (v, w) \in V^2$$

with induced norm $\|\cdot\|$. Furthermore set

$$b(v, q) := -(\operatorname{div} v, q)_{L^2(\Omega)} \quad \text{for all } (v, q) \in V \times M$$

and the L^2 inner product $c(\cdot, \cdot) := (\cdot, \cdot)_{L^2(\Omega)}$ with $\|\cdot\| := \|\cdot\|_{L^2(\Omega)}$.

The discrete spaces read $V_\ell := [\mathfrak{C}\mathfrak{R}_0^1(\mathcal{T}_\ell)]^d$ and $M_\ell := \mathcal{P}_0(\mathcal{T}_\ell) \cap L_0^2(\Omega)$ with the discrete bilinear forms

$$\begin{aligned} a_{\text{NC}}(v_\ell, w_\ell) &:= (D_{\text{NC}} v_\ell, D_{\text{NC}} w_\ell)_{L^2(\Omega)} \quad \text{for all } (v_\ell, w_\ell) \in V_\ell^2; \\ b_{\text{NC}}(v_\ell, q_\ell) &:= -(\operatorname{div}_{\text{NC}} v_\ell, q_\ell)_{L^2(\Omega)} \quad \text{for all } (v_\ell, q_\ell) \in V_\ell \times M_\ell. \end{aligned}$$

Recall the spaces Z and Z_ℓ of (piecewise) divergence-free functions. Define $\widehat{V}_\ell := V + V_\ell$ and

$$\widehat{Z}_\ell := \{\widehat{v}_\ell \in \widehat{V}_\ell \mid \operatorname{div}_{\text{NC}} \widehat{v}_\ell = 0\}.$$

Note that $Z + Z_\ell \subseteq \widehat{Z}_\ell$, but the reverse inclusion is not true in general. Given $f \in L^2(\Omega; \mathbb{R}^d)$ and the solution $(u, p) \in Z \times M$ of the linear Stokes problem (6.1) with right-hand side $f \in L^2(\Omega; \mathbb{R}^d)$, define the quasi-Ritz projection $\widehat{R}_\ell u \in \widehat{V}_\ell$ and its pressure $p(\widehat{R}_\ell u)$ as the solution to

$$\begin{aligned} a_{\text{NC}}(\widehat{R}_\ell u, \widehat{v}_\ell) + b_{\text{NC}}(\widehat{v}_\ell, p(\widehat{R}_\ell u)) &= c(f, \widehat{v}_\ell) \quad \text{for all } \widehat{v}_\ell \in \widehat{V}_\ell, \\ b_{\text{NC}}(\widehat{R}_\ell u, q) &= 0 \quad \text{for all } q \in M. \end{aligned} \tag{8.6}$$

Since the spaces of Lagrange multipliers $M_\ell \subseteq M$ are nested, this problem is equivalent to an elliptic problem in \widehat{Z}_ℓ . This implies unique solvability with (piecewise) divergence-free $\widehat{R}_\ell u \in \widehat{Z}_\ell$.

Proposition 8.14 (best-approximation result for \widehat{R}_ℓ). *Given $f \in L^2(\Omega; \mathbb{R}^d)$, the solution $(u, p) \in V \times M$ of (6.1) and the quasi-Ritz projection $(\widehat{R}_\ell u, p(\widehat{R}_\ell u)) \in \widehat{V}_\ell \times M$ satisfy*

$$\|u - \widehat{R}_\ell u\|_{\text{NC}} + \|p - p(\widehat{R}_\ell u)\| \lesssim \|(1 - \Pi_\ell^0)u\|_{L^2(\Omega)} + \|(1 - \Pi_\ell^0)p\| + \operatorname{osc}_{1,1}(f, \mathcal{T}_\ell). \tag{8.7}$$

Proof. The proof follows by combining the arguments of Proposition 6.3 and Proposition 8.5. The details are omitted for brevity. ■

Proposition 8.15 (L^2 error control for \widehat{R}_ℓ). *The exact solution $(u, p) \in V \times M$ of the linear problem (6.1) and its quasi-Ritz projection $(\widehat{R}_\ell u, p(\widehat{R}_\ell u)) \in \widehat{V}_\ell \times M$ satisfy*

$$\|u - \widehat{R}_\ell u\| \lesssim \|h_\ell\|_\infty^s (\|u - \widehat{R}_\ell u\|_{\text{NC}} + \|p - p(\widehat{R}_\ell u)\| + \operatorname{osc}_{1,1}(f, \mathcal{T}_\ell)).$$

Proof. The proof follows the arguments of Proposition 6.3 and Proposition 8.3. The details are omitted for brevity. ■

The Stokes-type eigenvalue problem in \widehat{V}_ℓ seeks eigenpairs $(\hat{\lambda}_\ell, \hat{u}_\ell, p(\hat{u}_\ell)) \in \mathbb{R} \times \widehat{V}_\ell \times M$ with $\|\hat{u}_\ell\| = 1$ such that

$$\begin{aligned} a_{\text{NC}}(\hat{u}_\ell, \hat{v}_\ell) + b_{\text{NC}}(\hat{v}_\ell, p(\hat{u}_\ell)) &= \hat{\lambda}_\ell c(\hat{u}_\ell, \hat{v}_\ell) & \text{for all } \hat{v}_\ell \in \widehat{V}_\ell, \\ b_{\text{NC}}(\hat{u}_\ell, q) &= 0 & \text{for all } q \in M. \end{aligned} \quad (8.8)$$

As in Section 8.2 it can be seen from the \widehat{Z}_ℓ ellipticity that this problem has a countable and discrete spectrum

$$0 < \hat{\lambda}_{\ell,1} \leq \hat{\lambda}_{\ell,2} \leq \dots$$

with corresponding c -orthonormal system of eigenfunctions $(\hat{u}_{\ell,1}, \hat{u}_{\ell,2}, \dots)$ with pressures $(p(\hat{u}_{\ell,1}), p(\hat{u}_{\ell,2}), \dots)$. For an eigenvalue cluster described by $J = \{n+1, \dots, n+N\}$, the set $\widehat{W}_\ell := \text{span}\{\hat{u}_{\ell,j} \mid j \in J\}$ describes the corresponding invariant subspace. With the L^2 projection \widehat{P}_ℓ onto \widehat{W}_ℓ set $\widehat{\Lambda}_\ell := \widehat{P}_\ell \circ \widehat{R}_\ell$. Given an eigenfunction $u \in V$ with $\widehat{\Lambda}_\ell u \in \widehat{V}_\ell$, define the pressure $p(\widehat{\Lambda}_\ell u) \in M$ via

$$a_{\text{NC}}(\widehat{\Lambda}_\ell u, \hat{v}_\ell) + b_{\text{NC}}(\hat{v}_\ell, p(\widehat{\Lambda}_\ell u)) = \hat{\lambda}_\ell c(\widehat{P}_\ell u, \hat{v}_\ell) \quad \text{for all } \hat{v}_\ell \in \widehat{V}_\ell.$$

The arguments of Proposition 8.6 show the convergence $\hat{\lambda}_{\ell,j} \rightarrow \lambda_j$ as $\ell \rightarrow \infty$ for all $j \in \mathbb{N}$ provided the maximum mesh-size tends to zero. Furthermore, for $\|h_0\|_\infty \ll 1$, there exists a separation bound

$$\widehat{M}_J := \sup_{\mathcal{T}_\ell \in \mathbb{T}} \max_{j \in \mathbb{N} \setminus J} \max_{k \in J} \left\{ \frac{\hat{\lambda}_{k,\ell}}{|\lambda_j - \hat{\lambda}_{k,\ell}|}, \frac{\hat{\lambda}_{k,\ell}}{|\lambda_{\ell,j} - \hat{\lambda}_{k,\ell}|}, \frac{\lambda_k}{|\hat{\lambda}_{\ell,j} - \lambda_k|}, \frac{\lambda_k}{|\lambda_{\ell,j} - \lambda_k|} \right\} < \infty \quad (\widehat{\text{H1}})$$

with the convention that $\lambda_{\ell,j} := \lambda_{\ell, \dim(Z_\ell)}$ for $j > \dim(Z_\ell)$.

Proposition 8.16 (L^2 error estimate for $\widehat{\Lambda}_\ell$). *Provided $\|h_0\|_\infty \ll 1$, any eigenpair $(\lambda, u, p) \in \mathbb{R} \times W \times M$ of (6.10) with $\|u\| = 1$ satisfies*

$$\|u - \Lambda_\ell u\| + \|u - \widehat{\Lambda}_\ell u\| \lesssim (1 + \widehat{M}_J) \|h_0\|_\infty^s (\|(1 - \Pi_\ell^0)Du\| + \|(1 - \Pi_\ell^0)p\|).$$

Proof. The proof follows with the arguments of Proposition 6.5 and Proposition 8.9. The details are omitted for brevity. \blacksquare

Proposition 8.17 (comparison result for $\widehat{\Lambda}_\ell$). *Provided $\|h_0\|_\infty \ll 1$, any eigenpair $(\lambda, u, p) \in \mathbb{R} \times W \times M$ of (6.10) with $\|u\| = 1$ satisfies*

$$\|(1 - \widehat{\Lambda}_\ell)u\|_{\text{NC}} + \|p - p(\widehat{\Lambda}_\ell u)\| \lesssim (\|(1 - \Pi_\ell^0)Du\| + \|(1 - \Pi_\ell^0)p\|).$$

Proof. The proof follows with the arguments of Proposition 6.6 and Proposition 8.10. The details are omitted for brevity. \blacksquare

The tools developed in this section enable the proof of the following eigenvalue error estimate.

Theorem 8.18 (eigenvalue error estimates). *Provided $\|h_0\|_\infty \ll 1$, it holds that*

$$\begin{aligned} \max_{j \in J} \frac{|\lambda_j - \lambda_{\ell,j}|}{\max\{\lambda_j, \lambda_{\ell,j}\}} &\lesssim (1 + \widehat{M}_J^2 B^2) \sup_{\substack{w \in W \\ \|w\|_{\text{NC}}=1}} \inf_{v_\ell \in W_\ell} (\|w - v_\ell\|_{\text{NC}}^2 + \|p(w) - p(v_\ell)\|^2) \\ &\lesssim (1 + \widehat{M}_J^2 B^2) \sup_{\substack{w \in W \\ \|w\|_{\text{NC}}=1}} \left(\|(1 - \Pi_\ell^0)Dw\|_{L^2(\Omega)}^2 + \|(1 - \Pi_\ell^0)p(w)\|_{L^2(\Omega)}^2 \right). \end{aligned}$$

8. Eigenvalue Error Estimates for Nonconforming FEMs

Proof. The arguments of Lemma 8.12 show

$$\max_{j \in J} \frac{|\lambda_j - \lambda_{\ell,j}|}{\max\{\lambda_j, \lambda_{\ell,j}\}} \lesssim (1 + \widehat{M}_J^2 B^2) \left(\sin_{a,\text{NC}}^2 \angle(W, \widehat{W}_\ell) + \sin_{a,\text{NC}}^2 \angle(W, W_\ell) \right).$$

Note that up to this point the pressure variable has not entered the analysis because W , W_ℓ , and \widehat{W}_ℓ is a subspace of the (piecewise) divergence-free space Z , Z_ℓ , and \widehat{Z}_ℓ , respectively. The proof of the theorem follows with the arguments of Theorem 8.11 by employing the comparison results of Proposition 6.6 and Proposition 8.17. \blacksquare

The eigenvalue error estimate and the optimality result of Corollary 6.10 together with Remark 3.20 result in the following consequence for the convergence of the eigenvalue error.

Corollary 8.19. *Provided the bulk parameter $\theta \ll 1$ and the initial mesh-size $\|h_0\|_\infty \ll 1$ are sufficiently small, Algorithm 6.7 computes triangulations $(\mathcal{T}_\ell)_\ell$ and discrete eigenpairs $((\lambda_{\ell,j}, u_{\ell,j}, p_{\ell,j})_{j \in J})_\ell$ with optimal rate of convergence in the sense that*

$$\begin{aligned} & A^{1/2} \max_{k \in J} (1 + \widehat{M}_J^2 B^2)^{-1/2} \left(\frac{|\lambda_k - \lambda_{\ell,k}|}{\max\{\lambda_k, \lambda_{\ell,k}\}} \right)^{1/2} + \sup_{\substack{w \in W \\ \|w\|=1}} \inf_{v_\ell \in W_\ell} (\|w - v_\ell\|_{\text{NC}} + \|p(w) - p(v_\ell)\|) \\ & \lesssim (\text{card}(\mathcal{T}_\ell) - \text{card}(\mathcal{T}_0))^{-\sigma} \left(\sum_{j \in J} |(u_j, p_j)|_{\mathfrak{A}_\sigma^{\text{Stokes}}}^2 \right)^{1/2}. \end{aligned} \quad \blacksquare$$

8.4. Biharmonic Operator

This section is devoted to eigenvalue error estimates for the Morley finite element discretisation of the biharmonic eigenvalue problem. Adopt the notation of Chapter 7 with the space $V \subseteq H^2$ of H^2 functions satisfying the boundary conditions. The L^2 product of the Hessians is denoted by $a(\cdot, \cdot)$ and the L^2 scalar product is denoted by $b(\cdot, \cdot)$. The discrete counterpart of a reads as $a_{\text{NC}}(\cdot, \cdot) = (D_{\text{NC}}^2 \cdot, D_{\text{NC}}^2 \cdot)_{L^2(\Omega)}$ and V_ℓ denotes the Morley finite element space with respect to the triangulation \mathcal{T}_ℓ . Recall the notation of Section 7.5 on the exact and discrete eigenvalues and the invariant subspaces $W \subseteq V$ and $W_\ell \subseteq V_\ell$ related to the eigenvalue cluster J with the L^2 projection P_ℓ onto W_ℓ and $\Lambda_\ell = P_\ell \circ R_\ell$ where R_ℓ is related to the solution of the linear discrete problem (7.17).

Consider the sum $\widehat{V}_\ell = V + V_\ell$ and the eigenvalue problem

$$a_{\text{NC}}(\hat{u}_\ell, \hat{v}_\ell) = \hat{\lambda}_\ell b(\hat{u}_\ell, \hat{v}_\ell) \quad \text{for all } \hat{v}_\ell \in \widehat{V}_\ell. \quad (8.9)$$

Denote the spectrum by $0 < \hat{\lambda}_{\ell,1} \leq \hat{\lambda}_{\ell,2} \leq \dots$ and the corresponding b -orthonormal eigenfunctions by $(\hat{u}_{\ell,1}, \hat{u}_{\ell,2}, \dots)$. For an eigenvalue cluster described by the index set J , the set $\widehat{W}_\ell := \text{span}\{\hat{u}_{\ell,j} \mid j \in J\}$ describes the corresponding invariant subspace with the L^2 projection \widehat{P}_ℓ onto \widehat{W}_ℓ and $\widehat{\Lambda}_\ell := \widehat{P}_\ell \circ \widehat{R}_\ell$. Here, $\widehat{R}_\ell \in \widehat{V}_\ell$ is the quasi-Ritz projection defined in (8.10) below.

The main achievements in Chapter 7 were the analysis of interpolation and companion operators and the discrete reliability. The technical difficulties therein included the lack of a conforming subspace of the Morley finite element space. Recall the Morley interpolation operator $\mathcal{I}_\ell^{\mathfrak{M}}$ from Definition 7.2 and the companion operator \mathcal{C} from Proposition 7.10. It

turns out that the analysis of the eigenvalue error is very similar to that of Section 8.2. The operators $\mathcal{J}_\ell^{\mathfrak{M}}$ and \mathcal{C} play a similar role as the operators $\mathcal{J}_\ell^{\mathfrak{C}\mathfrak{R}}$ and J_{d+1} in the foregoing sections. The main technical work that tackled the differences in the analysis of the Morley FEM and the nonconforming \mathcal{P}_1 FEM has been done in Chapter 7. The results in this section follow from combining the arguments of the foregoing sections with the properties of the operators from Chapter 7 and are therefore not proven in detail.

Proposition 8.20. *Let $(\mathcal{T}_\ell)_{\ell \in \mathbb{N}_0}$ be a sequence of triangulations generated by the refinement rules of Section 2.2 with $\|h_0\|_\infty \ll 1$. Then any $j \in \mathbb{N}$ and the constant C from the estimate in Proposition 7.5 satisfy*

$$\frac{\lambda_{\ell,j}}{1 + C\|h_\ell\|_\infty^4 \lambda_{\ell,j}} \leq \hat{\lambda}_{\ell,j} \leq \lambda_{\ell,j}.$$

In particular, if $\|h_\ell\|_\infty \rightarrow 0$ as $\ell \rightarrow \infty$, one has convergence $\hat{\lambda}_{\ell,j} \rightarrow \lambda_j$.

Proof. The proof follows the arguments of Proposition 8.6. The projection property (7.1) and Lemma 3.13 lead to the result. \blacksquare

Given $f \in V$, let $u \in V$ denote the solution to the linear problem

$$a(u, v) = b(f, v) \quad \text{for all } v \in V.$$

The quasi-Ritz projection $\hat{R}_\ell u \in \hat{V}_\ell$ is defined as the solution to

$$a_{\text{NC}}(\hat{R}_\ell u, \hat{v}_\ell) = b(f, \hat{v}_\ell) \quad \text{for all } \hat{v}_\ell \in \hat{V}_\ell. \quad (8.10)$$

The following proposition gives an L^2 error estimate and a comparison result for \hat{R}_ℓ .

Proposition 8.21 (properties of \hat{R}_ℓ). *Let $u \in V$ solve the linear problem (7.16) with right-hand side $f \in V$. Then, $\hat{R}_\ell u$ satisfies*

$$\begin{aligned} \|u - \hat{R}_\ell u\| &\lesssim \|h_0\|_\infty^s \|u - \hat{R}_\ell u\|_{\text{NC}}, \\ \text{and } \|u - \hat{R}_\ell u\|_{\text{NC}} &\lesssim \|(1 - \Pi_\ell^0)D^2 u\|_{L^2(\Omega)} + \text{osc}_{2,2}(f, \mathcal{T}_\ell). \end{aligned}$$

Proof. The operators $\mathcal{J}_\ell^{\mathfrak{M}}$ and \mathcal{C} allow to combine the arguments of Propositions 7.17 and 7.18 with those of Proposition 8.3 and 8.5. The details are omitted for brevity. \blacksquare

For $\|h_0\|_\infty \ll 1$, Proposition 8.20 shows that there exists a separation constant for the cluster J in the sense that

$$\hat{M}_J := \sup_{\mathcal{T}_\ell \in \mathbb{T}} \max_{j \in \mathbb{N} \setminus J} \max_{k \in J} \left\{ \frac{\hat{\lambda}_{k,\ell}}{|\lambda_j - \hat{\lambda}_{k,\ell}|}, \frac{\hat{\lambda}_{k,\ell}}{|\lambda_{\ell,j} - \hat{\lambda}_{k,\ell}|}, \frac{\lambda_k}{|\hat{\lambda}_{\ell,j} - \lambda_k|}, \frac{\lambda_k}{|\lambda_{\ell,j} - \lambda_k|} \right\} < \infty \quad (\widehat{\text{H1}})$$

with the convention $\lambda_{\ell,j} = \lambda_{\ell, \dim(V_\ell)}$ for $j > \dim(V_\ell)$.

The next proposition states the L^2 error estimate and the best-approximation property for $\hat{\Lambda}_\ell$.

Proposition 8.22 (properties of $\hat{\Lambda}_\ell$). *Provided $\|h_0\|_\infty \ll 1$, any eigenpair $(\lambda, u) \in \mathbb{R} \times W$ of (7.20) with $\|u\| = 1$ satisfies*

$$\begin{aligned} \|u - \Lambda_\ell u\| + \|u - \hat{\Lambda}_\ell u\| &\lesssim (1 + \hat{M}_J) \|h_0\|_\infty^s \|(1 - \Pi_\ell^0)D^2 u\| \quad \text{and} \\ \|(1 - \hat{\Lambda}_\ell)u\|_{\text{NC}} &\lesssim \|(1 - \Pi_\ell^0)D^2 u\|. \end{aligned}$$

8. Eigenvalue Error Estimates for Nonconforming FEMs

Proof. The proof follows from the combination of the arguments of Propositions 7.20 and 7.21 with those of Propositions 8.9 and 8.10. The details are omitted for brevity. ■

Let $\sin_{a,\text{NC}}(X, Y)$ denote the sine of the largest principal angle of two finite-dimensional subspaces $X \subseteq \widehat{V}_\ell$ and $Y \subseteq \widehat{V}_\ell$ with respect to the scalar product a_{NC} .

Theorem 8.23 (eigenvalue error estimates). *Provided $\|h_0\|_\infty \ll 1$, it holds that*

$$\begin{aligned} \max_{j \in J} \frac{|\lambda_j - \lambda_{\ell,j}|}{\max\{\lambda_j, \lambda_{\ell,j}\}} &\lesssim (1 + \widehat{M}_J^2 B^2) \sin_{a,\text{NC}}^2 \angle(W, W_\ell) \\ &\lesssim (1 + \widehat{M}_J^2 B^2) \sup_{\substack{w \in W \\ \|w\|_{\text{NC}}=1}} \|(1 - \Pi_\ell^0) D^2 w\|_{L^2(\Omega)}^2. \end{aligned}$$

Proof. The proof is similar to that of Theorem 8.11. ■

The eigenvalue error estimates and the optimality result of Corollary 7.25 together with Remark 3.20 lead to the following optimal convergence result for the eigenvalue error.

Corollary 8.24. *Provided the bulk parameter $\theta \ll 1$ and the initial mesh-size $\|h_0\|_\infty \ll 1$ are sufficiently small, Algorithm 7.22 computes triangulations $(\mathcal{T}_\ell)_\ell$ and discrete eigenpairs $((\lambda_{\ell,j}, u_{\ell,j})_{j \in J})_\ell$ with optimal rate of convergence in the sense that*

$$\begin{aligned} \max_{k \in J} (1 + \widehat{M}_J^2 B^2)^{-1/2} \left(\frac{|\lambda_k - \lambda_{\ell,k}|}{\max\{\lambda_k, \lambda_{\ell,k}\}} \right)^{1/2} + \sin_{a,\text{NC}} \angle(W, W_\ell) \\ \lesssim A^{-1/2} (\text{card}(\mathcal{T}_\ell) - \text{card}(\mathcal{T}_0))^{-\sigma} \left(\sum_{j \in J} |u_j|_{\mathfrak{H}_{\frac{\Delta}{\sigma}}}^2 \right)^{1/2}. \end{aligned} \quad \blacksquare$$

9. Numerical Experiments

This chapter presents numerical benchmarks in two space dimensions based on the Matlab software package AFEM [Carstensen et al., 2009] maintained at the Humboldt-Universität. Details on the new routines implemented for this thesis can be found in Appendix B. The complete software is attached in Appendix C. The numerical computations are performed with the Matlab version 7.14.0.739 (R2012a) [The MathWorks, Inc., 2012]. All matrix eigenvalue problems are solved using Matlab's command `eigs`. In Sections 9.2–9.4, the default parameters of `eigs` solve the algebraic eigenvalue problems in high accuracy, while Section 9.5 takes the inexact solution into account with modified parameters of `eigs`.

The convergence history plots are logarithmically scaled and display the absolute error of the eigenvalues with respect to the number of degrees of freedom (ndof).

9.1. Numerical Realisation

Domains and Refinement

Two domains will be considered throughout this chapter. The L-shaped domain is defined as $\Omega := (-1, 1)^2 \setminus ([0, 1] \times [-1, 0])$. The domain and its initial partitions are displayed in Figure 9.1.

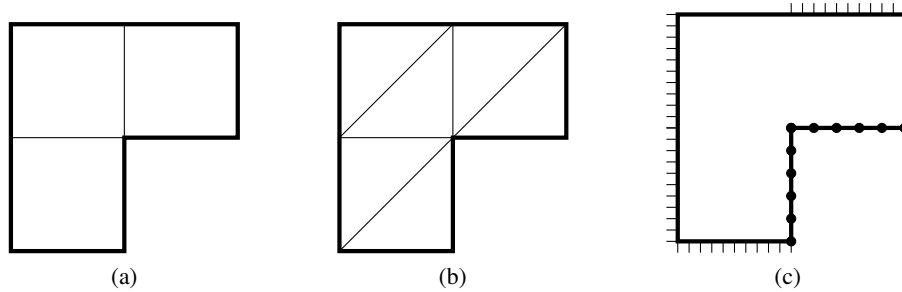


Figure 9.1.: (a)–(b) Coarse initial partitions of the L-shaped domain. (c) Boundary conditions for the example from Section 9.4: clamped |||| , simply supported $\bullet\bullet\bullet$ and free --- boundary conditions.

The perturbed slit domain of Figure 9.2 is defined as

$$\Omega := (-1, 1)^2 \setminus \left(\begin{aligned} &\text{conv}\{(0.5005; 0), (1; 0)\} \cup \text{conv}\{(0; 0.501), (0; 1)\} \\ &\cup \text{conv}\{(-0.499; 0), (-1; 0)\} \cup \text{conv}\{(0; -0.5), (0; -1)\} \end{aligned} \right). \quad (9.1)$$

Besides triangular finite elements, also a rectangular finite element will be used for comparison. Uniform mesh-refinement is performed by the so-called red-refinement. This

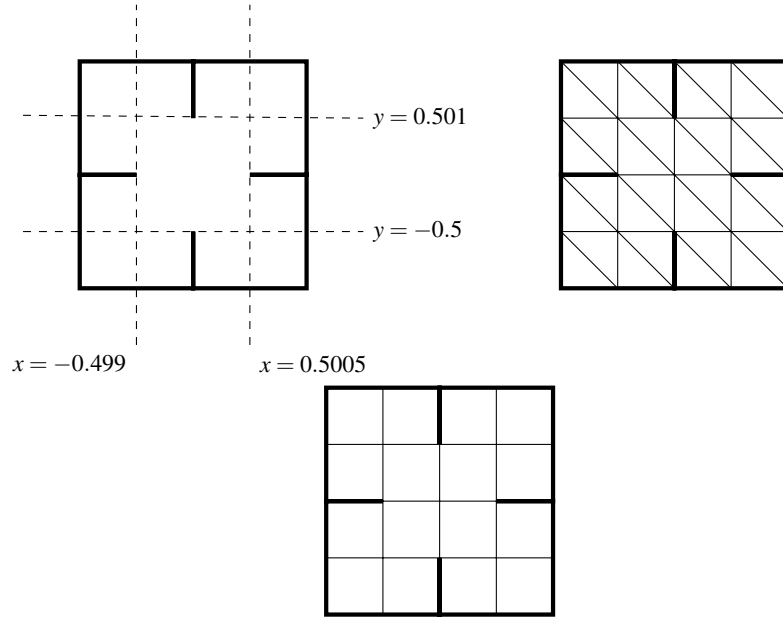


Figure 9.2.: Square domain $(-1, 1)^2$ with perturbed slits and coarse initial partitions with 5 interior vertices.

means that each triangle (resp. rectangle) is subdivided into 4 sub-triangles (resp. sub-rectangles) by connecting the midpoints of the edges. Adaptive mesh-refinement is only performed for triangular partitions and utilises the newest-vertex bisection from Section 2.2. The bulk parameter is set $\theta = 0.1$ in all adaptive computations. This is a typical choice for linear problems.

The Streamfunction-Vorticity Formulation of the Stokes System

Section 7.8 describes the implementation of the Stokes problem with finite elements for fourth-order problems. In particular, the Morley finite element can be employed for a piecewise divergence-free implementation of the nonconforming \mathcal{P}_1 FEM. A second advantage of the streamfunction-vorticity formulation is that it allows a construction of conforming schemes for the Stokes problem in the sense that the discrete solution of the problem is divergence-free whenever a H_0^2 -conforming method is employed. This leads to upper eigenvalue bounds.

The Bogner-Fox-Schmit Finite Element

The computation of the upper bounds for the Stokes and biharmonic eigenproblems is performed with the Bogner-Fox-Schmit FEM [Ciarlet, 1978] of Figure 9.3 on rectangular partitions. Given a partition \mathcal{T}_ℓ of Ω into rectangles, let $\mathcal{Q}_3(\mathcal{T}_\ell)$ denote the space of piecewise polynomials of partial degree 3 (bicubic functions). The Bogner-Fox-Schmit finite

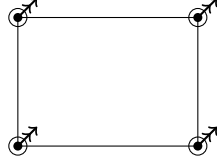


Figure 9.3.: The Bogner-Fox-Schmit bicubic finite element with the values of the function, its first derivative and its mixed second derivative at the free vertices as degrees of freedom.

element space is defined as

$$V_{\text{BFS}}(\mathcal{T}_\ell) := \mathcal{Q}_3(\mathcal{T}_\ell) \cap \{v \in H^2(\Omega) \mid v|_{\Gamma_C \cup \Gamma_S} = 0 \text{ and } (\partial v / \partial \nu)|_{\Gamma_C} = 0\}$$

(for Γ_C, Γ_S as in Chapter 7), see Figure 9.3 for an illustration.

Computation of Reference Eigenvalues

The reference eigenvalues of the test problems are computed as follows. For the eigenvalues of the Laplacian, the eigenvalues of the conforming \mathcal{P}_2 finite element method are computed on a sequence of red-refined triangulations and the reference eigenvalue is extrapolated with the Aitken extrapolation [Stoer and Bulirsch, 2002]. The reference eigenvalues of the Stokes system as well as the eigenvalues of the biharmonic operator are extrapolated from the eigenvalues computed with the Bogner-Fox-Schmit FEM (see Figure 9.3) on a sequence of uniformly refined rectangular partitions.

Outline of the Implementation

The implementation of the AFEM loop as well as the stiffness and mass matrices for the conforming and nonconforming \mathcal{P}_1 methods is provided in large part in the AFEM software package [Carstensen et al., 2009]. Further details can be found in [Alberty et al., 1999, Bahriawati and Carstensen, 2005]. The following lines show the solution of the discrete eigenproblem for the conforming discretisation of the Laplacian.

```
eVect = zeros(nrNodes,nEig);
[V,D] = eigs(A(dof,dof),B(dof,dof),cluster_upper,'sm');
[D,ind] = sort(diag(D));
eVect(dof,:) = V(:,ind(cluster_lower:cluster_upper));
eVal = D(cluster_lower:cluster_upper);
```

Here, A and B are the stiffness matrix and mass matrix and dof is the list of degrees of freedom.

The sum of error estimator contributions in the AFEM loop is implemented as follows.

```
eta4e = zeros(size(n4e,1),1);
% ESTIMATE
for j=1:nEig
    cur_eta4e = estimateP1evpEtaElements(eVal(j),eVect(:,j),...
        c4n,n4e,n4sDb,n4sNb);
    etaList(lvl,j) = sqrt(sum(cur_eta4e));
    eta4e = eta4e + cur_eta4e;
end
etaTotalList(lvl,1) = sqrt(sum(eta4e));
```

9. Numerical Experiments

Since the software for fourth-order problems is not contained in [Carstensen et al., 2009], some details on the implementation are provided here. An overview over the software and explanations how to reproduce the numerical experiments can be found in Appendix B. The complete Matlab programs are provided on the attached data medium (Appendix C). Formulas for the local basis functions of the Morley finite element are given in [Wang and Xu, 2006]. The main program for the Morley finite element method is

```
function [eVect,eVal,ndof,Hess4e,Blocal] = solveMorleyEVPcluster(...  
    cluster_lower,cluster_upper,RHS,c4n,n4e,n4sCb,n4sSb)
```

The assembly of local stiffness matrices is performed in vectorised form. This avoids a for-loop with sparse indexing, see [Funken et al., 2011] for further details.

```
Alocal = zeros(6,6,nelem);  
Blocal = zeros(6,6,nelem);
```

The local stiffness and mass matrices are built up by numerical integration of the basis functions with AFEM's integration routine `integrate`, for instance

```
for j=1:6  
    for k=j:6  
        Blocal(j,k,:) = sum(integrate(c4n,n4e,...  
            @(z,zz,zzz) Basis_functions{j}(zz).*Basis_functions{k}(zz),8),2);  
        Blocal(k,j,:) = Blocal(j,k,:);  
    end  
end  
end
```

The assembly of the global matrices relies on suitable index lists that contain the degrees of freedom in a special ordering.

```
% Assembling global A,B  
dofs_u = [n4e,nrNodes+s4e]';  
I = repmat(dofs_u(:,1),size(dofs_u,1))';  
J = repmat(dofs_u',1,size(dofs_u,1))';  
A = sparse(I(:,J,:),Alocal(:));  
B = sparse(I(:,J,:),Blocal(:));
```

The resulting eigenvalue problem is solved as described above. The implementation of the Bogner-Fox-Schmit finite element is similar. The local basis functions can be determined as tensor products of 1D cubic splines.

9.2. Eigenvalues of the Laplacian

This section presents the numerical results for the eigenvalues of the Laplacian with the conforming and the nonconforming \mathcal{P}_1 finite element methods.

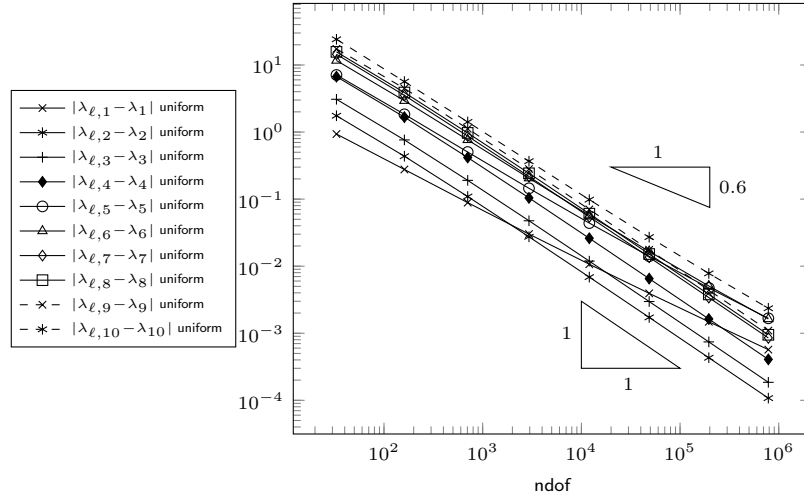
L-Shaped Domain

The following approximations of the first 10 eigenvalues of the Laplacian on the L-shaped domain of Figure 9.1 have been obtained by a \mathcal{P}_2 finite element method on uniformly refined meshes and Aitken extrapolation

$$\begin{array}{ll} \lambda_1 = 9.639723 & \lambda_6 = 41.47450 \\ \lambda_2 = 15.19725 & \lambda_7 = 44.94848 \\ \lambda_3 = 19.73920 & \lambda_8 = 49.34802 \\ \lambda_4 = 29.52148 & \lambda_9 = 49.34802 \\ \lambda_5 = 31.91263 & \lambda_{10} = 56.70961. \end{array}$$

$ndof$	$\lambda_{\ell,10}$ from \mathcal{P}_2 FEM	extrapolation
48 641	56.712670	56.710535
195 585	56.710818	56.709692
784 385	56.710089	56.709615
3 141 633	56.709800	56.709610

Table 9.1.: Aitken extrapolation of the 10th eigenvalue of the Laplacian on the L-shaped domain.

Figure 9.4.: Convergence history for the eigenvalues of the Laplacian on the L-shaped domain for the conforming \mathcal{P}_1 method with uniform mesh-refinement.

The finest mesh in the reference computation has 3 141 633 degrees of freedom. It is plausible that the first six displayed digits are accurate. As an example, the values of the Aitken extrapolation for the 10th eigenvalue are displayed in Table 9.1.

Figure 9.4 shows the convergence history for the first 10 eigenvalues computed by the conforming \mathcal{P}_1 method under uniform refinement. Figure 9.5 displays the convergence history of the simultaneous adaptive refinement of the first 10 eigenvalues (i.e., the cluster is $J = \{1, \dots, 10\}$).

The convergence history of the nonconforming \mathcal{P}_1 method under uniform refinement is displayed in Figure 9.6 and the simultaneous adaptive computation in Figure 9.7. For both methods, the initial mesh is obtained by two red-refinements of the triangular mesh in Figure 9.1. Uniform mesh-refinement leads to suboptimal convergence rates for some of the eigenvalues, whereas the adaptive algorithm leads to the optimal decay rate of the error.

Perturbed Geometry

The second and third eigenvalues of the Laplacian on the slitted unit square (9.1) of Figure 9.2 are approximated by the Aitken extrapolation as

$$\lambda_2 = 17.6557 \quad \lambda_3 = 17.6660.$$

The extrapolated values of Table 9.2 suggest that all displayed digits are accurate.

The convergence history for the conforming \mathcal{P}_1 method is displayed in Figure 9.8. Uniform mesh refinement leads to a suboptimal convergence rate. The adaptive algorithm for

9. Numerical Experiments

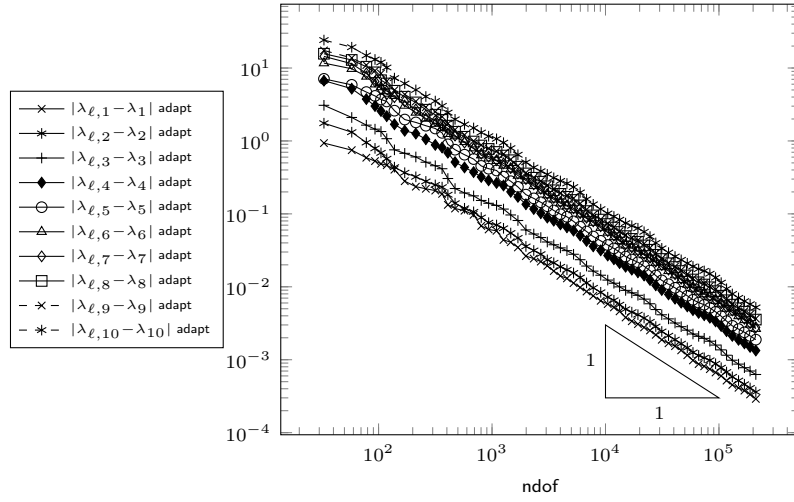


Figure 9.5.: Convergence history for the eigenvalues of the Laplacian on the L-shaped domain for the conforming \mathcal{P}_1 method with adaptive mesh-refinement.

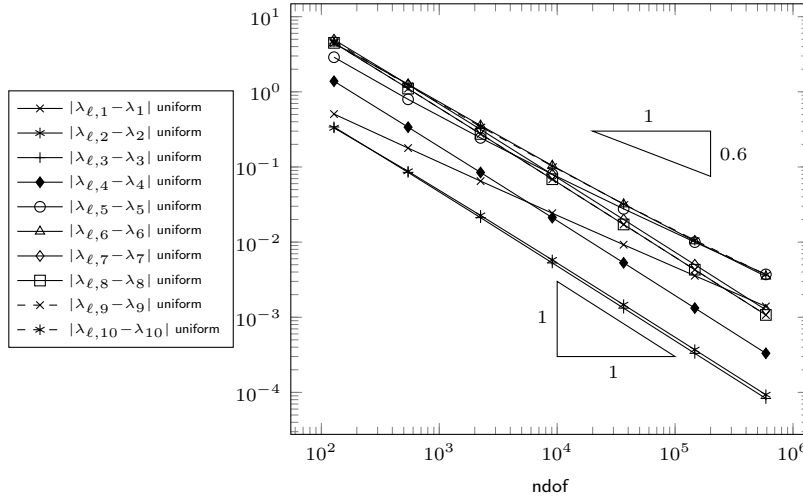


Figure 9.6.: Convergence history for the eigenvalues of the Laplacian on the L-shaped domain for the nonconforming \mathcal{P}_1 method with uniform mesh-refinement.

$ndof$	$\lambda_{\ell,2}$ from \mathcal{P}_2 FEM	extrapolation $\lambda_{\ell,2}$	$\lambda_{\ell,3}$ from \mathcal{P}_2 FEM	extrapolation $\lambda_{\ell,3}$
209	18.051881		18.063794	
929	17.837730		17.847580	
3 905	17.745933	17.677063	17.755968	17.688611
16 001	17.700838	17.657295	17.710971	17.667536
64 769	17.678313	17.655830	17.688494	17.666060
260 609	17.667047	17.655777	17.677253	17.666007
1 045 505	17.661414	17.655779	17.671632	17.666009
4 188 161	17.658597	17.655780	17.668821	17.666010

Table 9.2.: Aitken extrapolation of eigenvalues of the Laplacian on the square with perturbed slits.

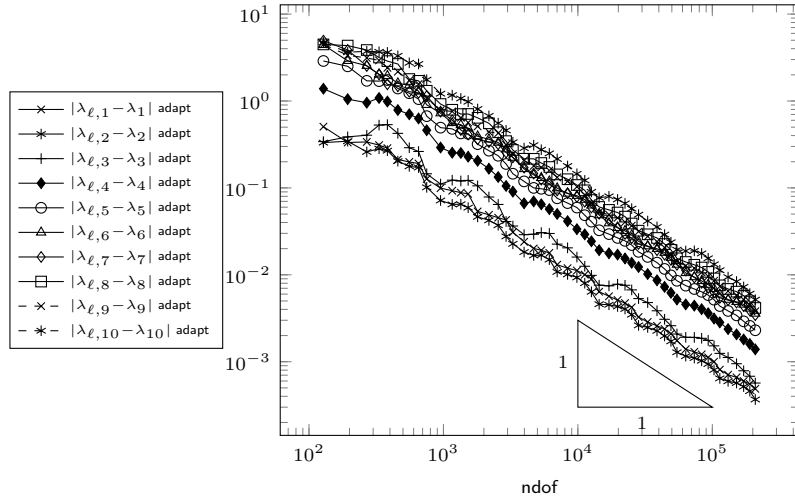


Figure 9.7.: Convergence history for the eigenvalues of the Laplacian on the L-shaped domain for the nonconforming \mathcal{P}_1 method with adaptive mesh-refinement.

the cluster $J = \{2, 3\}$ leads to the optimal convergence rate even for the coarse initial triangulation with 5 degrees of freedom. The choice of $J = \{2\}$, that is marking only with respect to the second computed eigenfunction u_2 , yields a large pre-asymptotic effect up to 4×10^5 degrees of freedom where the adaptive algorithm is not significantly better than uniform refinement. On a finer initial mesh (after one red-refinement) with 41 degrees of freedom, this effect is no more present and the adaptive algorithm appears optimal for any choice of $J \subseteq \{2, 3\}$. This behaviour can –at least on a heuristic level– be explained from the plots of discrete eigenmodes and the adaptive meshes. The second eigenfunction u_2 shows its significant singularities at different slit tips than the third eigenfunction u_3 (this follows from the axial symmetry in the non-perturbed case). Figure 9.10 displays (close approximations to) the eigenmodes u_2 and u_3 . Figure 9.11 displays the eigenmodes computed by the adaptive algorithm for $J = \{2\}$. The initial triangulation does not resolve the eigenvalue cluster and the computed eigenfunction $u_{\ell,2}$ does not capture the shape of u_2 . Accordingly, the AFEM refines near those reentrant corners where the error estimator contributions of $u_{\ell,2}$ are large, but where u_2 is smooth. This can be seen in the adaptive mesh of Figure 9.12 for $J = \{2\}$. This yields only little improvement for the approximation of u_2 . The eigenvalue cluster is only resolved when the global mesh-size is sufficiently small, which requires a large amount of iterations in an adaptive algorithm. In contrast, the adaptive algorithm for $J = \{2, 3\}$ refines at all reentrant corners, even if the eigenvalues in the cluster are not well-separated on the initial mesh. This explains why this algorithm is more robust in the sense that it only requires separation of the cluster from the remaining spectrum, but no resolution within the cluster.

The results for the nonconforming \mathcal{P}_1 approximation are displayed in Figure 9.9. Uniform mesh-refinement leads to a sub-optimal convergence rate. Optimal convergence rates can be observed for any choice of $J \subseteq \{2, 3\}$ even for the coarse initial mesh with 5 degrees of freedom. In this sense, the nonconforming FEM leads to better results than the conforming FEM at least in this example.

9. Numerical Experiments

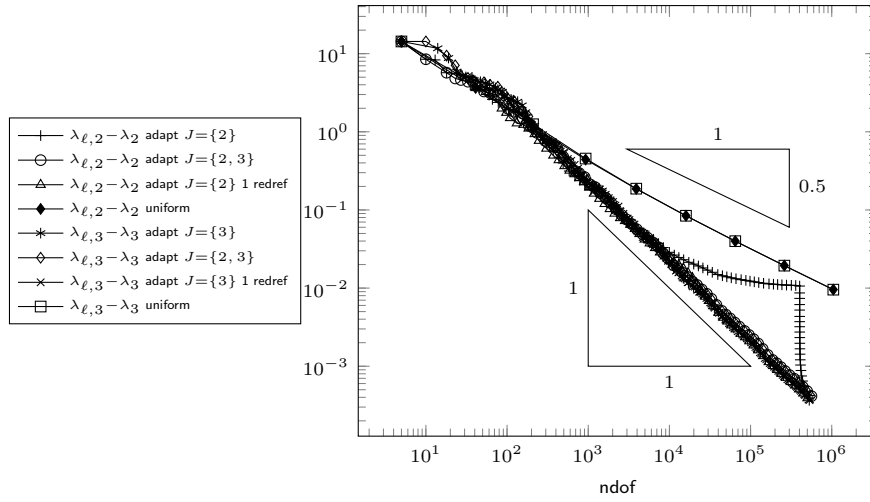


Figure 9.8.: Convergence history of the conforming \mathcal{P}_1 method on the square with perturbed slits. Adaptive mesh-refinement is based on $J \subseteq \{2, 3\}$. The initial triangulation \mathcal{T}_0 has 5 degrees of freedom or (when indicated with “1 redref”) 41 degrees of freedom.

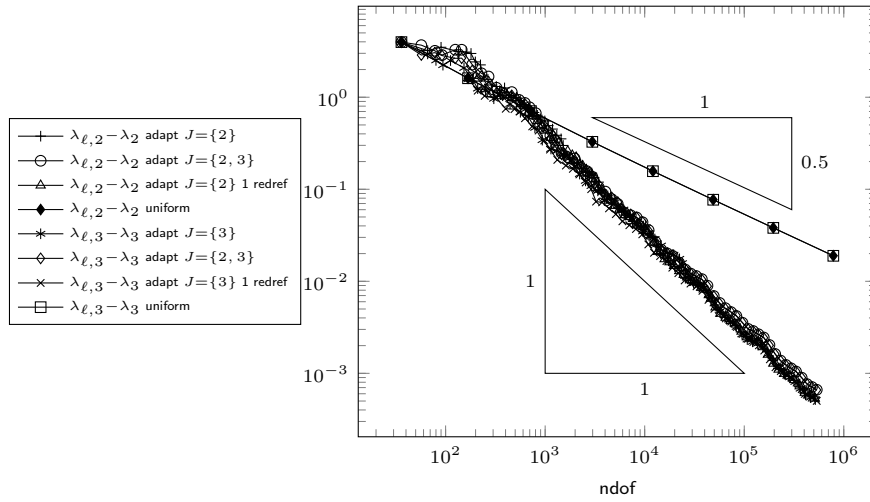


Figure 9.9.: Convergence history of the nonconforming \mathcal{P}_1 method on the square with perturbed slits. Adaptive mesh-refinement is based on $J \subseteq \{2, 3\}$. The initial triangulation \mathcal{T}_0 has 5 degrees of freedom or (when indicated with “1 redref”) 41 degrees of freedom.

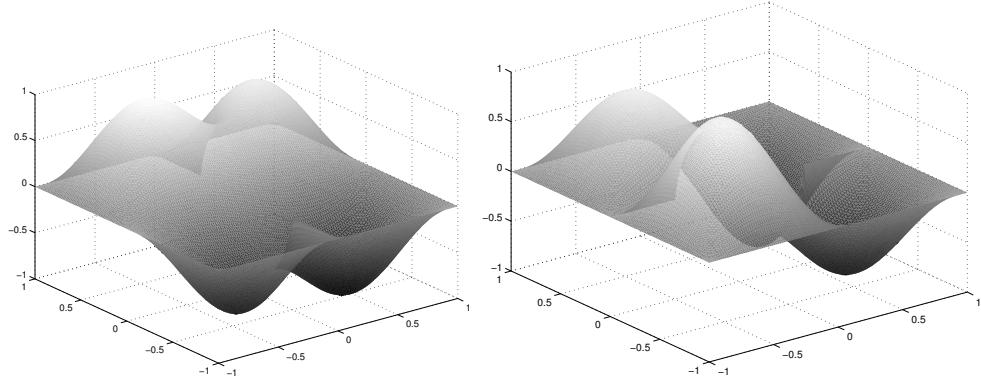


Figure 9.10.: Approximation of the eigenmodes u_2 and u_3 of the Laplacian on the perturbed slit domain, conforming \mathcal{P}_1 method, uniform mesh with 16 001 degrees of freedom.

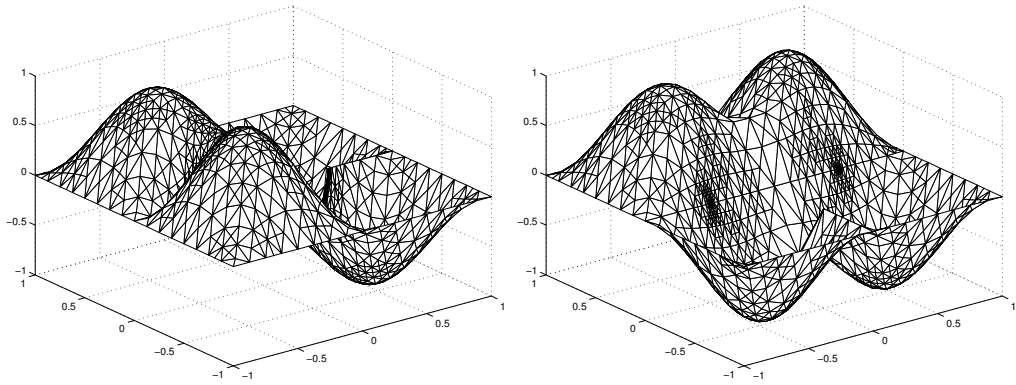


Figure 9.11.: Adaptive approximation of the eigenmodes u_2 and u_3 of the Laplacian on the perturbed slit domain, conforming \mathcal{P}_1 method, $J = \{2\}$, 1 085 degrees of freedom, level 30, from initial triangulation \mathcal{T}_0 with 5 degrees of freedom.

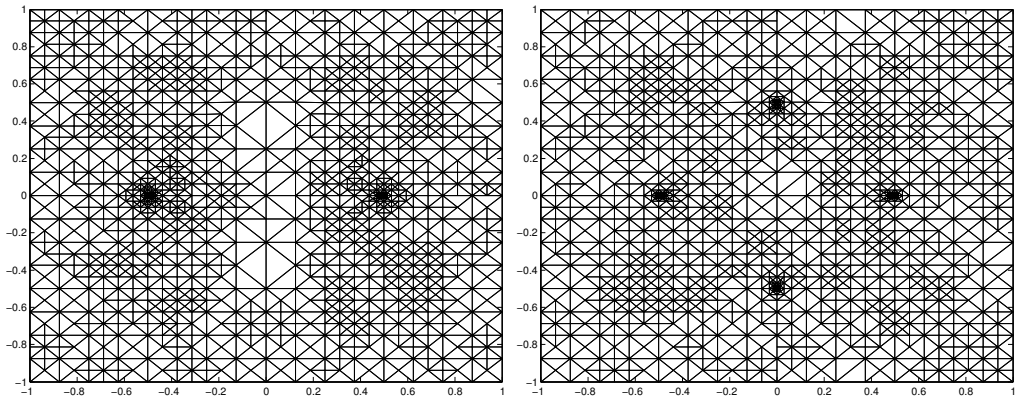


Figure 9.12.: Adaptive meshes ($\theta = 0.1$) for the perturbed slit domain, conforming \mathcal{P}_1 method, from initial triangulation \mathcal{T}_0 with 5 degrees of freedom. Left: $J = \{2\}$, 1 085 degrees of freedom, level 30. Right: $J = \{2, 3\}$, 1 056 degrees of freedom, level 27.

$ndof$	$\lambda_{\ell,10}$ from BFS FEM	extrapolation
48 132	89.259090	89.250984
194 564	89.253207	89.248357
782 340	89.250465	89.248071
3 137 540	89.249183	89.248058

Table 9.3.: Extrapolation of the 10th eigenvalue of the Stokes system on the L-shaped domain.

9.3. Eigenvalues of the Stokes System

This section presents numerical examples for the eigenvalues of the Stokes system and presents one example of lower eigenvalue bounds.

L-shaped Domain

This subsection presents the results of the adaptive nonconforming \mathcal{P}_1 method on the L-shaped domain. The following reference approximations of the first 10 eigenvalues were computed with the Bogner-Fox-Schmit FEM on a sequence of uniformly refined meshes and Aitken extrapolation

$$\begin{array}{ll}
 \lambda_1 = 32.13268 & \lambda_6 = 69.51185 \\
 \lambda_2 = 37.01832 & \lambda_7 = 70.63280 \\
 \lambda_3 = 41.93984 & \lambda_8 = 82.45744 \\
 \lambda_4 = 48.98359 & \lambda_9 = 83.43375 \\
 \lambda_5 = 55.41544 & \lambda_{10} = 89.24805.
 \end{array}$$

To assess the accuracy of those reference values, Table 9.3 displays the extrapolation history for the 10th eigenvalue. The values suggest that at least the first 5 digits are accurate.

Figure 9.13 shows the convergence history for the first 10 eigenvalues under uniform refinement. Some of the eigenvalues do not converge at optimal rate. The convergence history of the simultaneous adaptive refinement of the first 10 eigenvalues (i.e., the cluster is $J = \{1, \dots, 10\}$) is displayed in Figure 9.14 where optimal convergence rates for all eigenvalues can be observed. The initial mesh is obtained by one red-refinement of the triangular mesh in Figure 9.1.

The guaranteed upper and lower bounds for the first eigenvalue (see Section 6.2) under uniform refinement are displayed in Table 9.4.

Perturbed Geometry

The Bogner-Fox-Schmit FEM and Aitken extrapolation suggest that the eigenvalues number 3 and 4 of the Stokes system on the square with perturbed slits are

$$\lambda_3 = 49.7121, \quad \lambda_4 = 49.7214.$$

The last extrapolation steps are displayed in Table 9.5 and suggest that the first four displayed digits are accurate.

Figure 9.15 shows the convergence history for uniform and adaptive refinement. The initial triangulation is that from Figure 9.2. Any choice of $J \subseteq \{3, 4\}$ leads to the optimal convergence rate of the adaptive algorithm, while uniform refinement yields sub-optimal convergence rates.

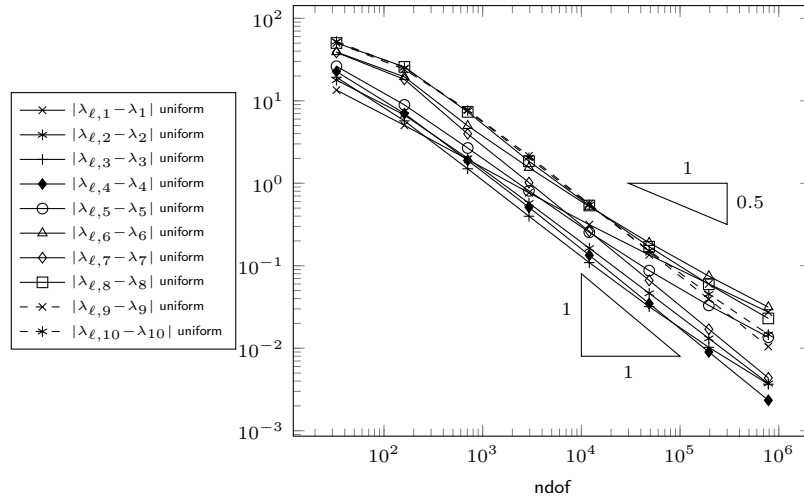


Figure 9.13.: Convergence history for the eigenvalues of the Stokes system on the L-shaped domain with uniform mesh-refinement.

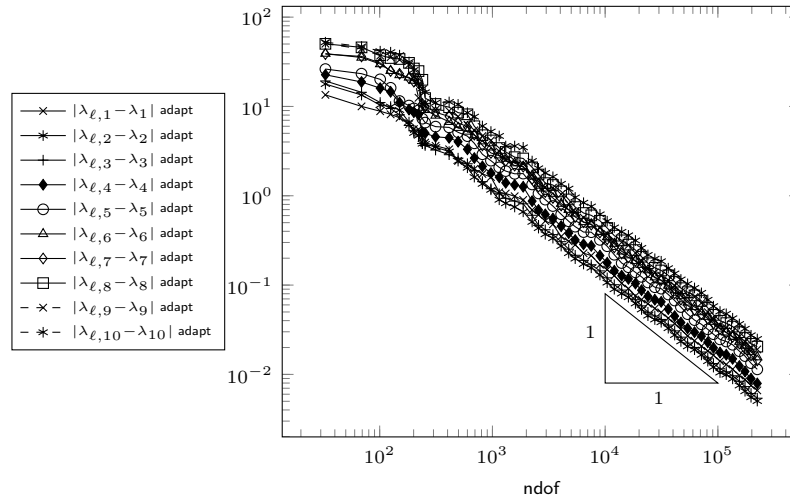


Figure 9.14.: Convergence history for the eigenvalues of the Stokes system on the L-shaped domain with adaptive mesh-refinement.

ndof Morley	$\lambda_{\ell,1}$ Morley	GLB	GUB	ndof BFS
5	8.5131670	1.4006877		
33	18.654900	4.9328469	34.495588	20
161	27.094348	13.479371	33.065887	132
705	30.187241	23.559113	32.537366	644
2 945	31.366099	29.229924	32.320020	2 820
12 033	31.817635	31.238674	32.220444	11 780
48 641	31.997285	31.848884	32.173905	48 132
195 585	32.072453	32.035048	32.152062	194 564
784 385	32.105273	32.095895	32.141798	782 340
3 141 633	32.120034	32.117687	32.136972	3 137 540

Table 9.4.: Guaranteed upper (GUB) and lower (GLB) eigenvalue bounds for the first eigenvalue of the Stokes system on the L-shaped domain on uniformly refined meshes. The extrapolated eigenvalue is $\lambda_1 = 32.132687$.

9. Numerical Experiments

$ndof$	$\lambda_{\ell,3}$ from BFS FEM	extrapolation λ_3	$\lambda_{\ell,4}$ from BFS FEM	extrapolation λ_4
64 004	49.828449	49.706886	49.837677	49.716130
259 076	49.770659	49.710781	49.779927	49.720063
1 042 436	49.741508	49.711837	49.750792	49.721131
4 182 020	49.726872	49.712114	49.736164	49.721410

Table 9.5.: Aitken extrapolation of the Stokes eigenvalues on the square with perturbed slits.

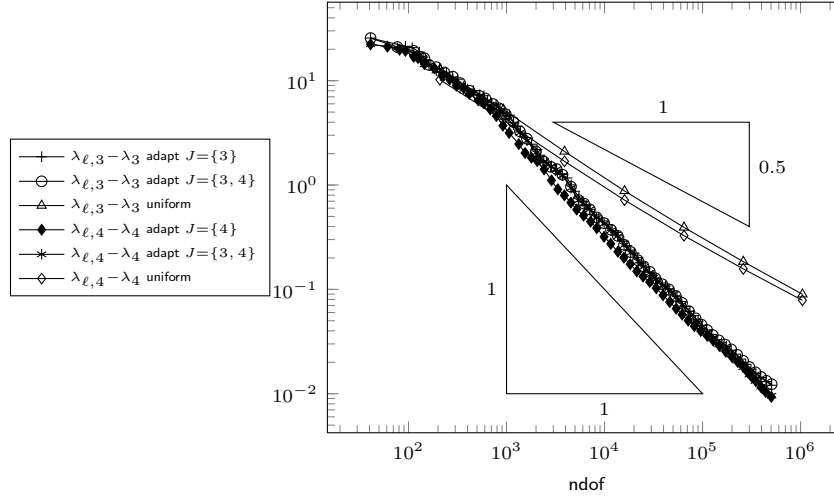


Figure 9.15.: Convergence history for the eigenvalues of the Stokes system on the square with perturbed slits. Adaptive mesh refinement is based on $J \subseteq \{3, 4\}$.

9.4. Eigenvalues of the Biharmonic Operator

This section presents adaptive eigenvalue computations for the biharmonic operator on the L-shaped domain for mixed boundary conditions and on the domain with perturbed slits for clamped boundary conditions with the Morley FEM.

L-shaped Domain with Mixed Boundary Conditions

This subsection considers the eigenvalues of the biharmonic operator on the L-shaped domain with mixed boundary conditions from Figure 9.1c. The Bogner-Fox-Schmit FEM and Aitken extrapolation lead to the reference approximations of the first 10 eigenvalues

$$\begin{aligned}
 \lambda_1 &= 252.034 & \lambda_6 &= 1591.352 \\
 \lambda_2 &= 301.976 & \lambda_7 &= 2189.758 \\
 \lambda_3 &= 483.583 & \lambda_8 &= 2616.840 \\
 \lambda_4 &= 673.674 & \lambda_9 &= 3060.011 \\
 \lambda_5 &= 965.351 & \lambda_{10} &= 3176.759.
 \end{aligned}$$

Table 9.6 gives some insight for the extrapolated eigenvalue number 10 and suggests that at least the first four displayed digits are accurate.

The strongly reduced convergence rate for uniform mesh-refinement can be seen in Figure 9.16. Figure 9.17 displays the convergence history for the simultaneous adaptive approximation of the first 10 eigenvalues computed by the Morley finite element method.

$ndof$	$\lambda_{\ell,10}$ from BFS FEM	extrapolation
48 8910	3 194.9618	3 178.9983
196 091	3 187.5656	3 177.4358
785 403	3 183.2050	3 176.9411
3 143 675	3 180.6040	3 176.7595

Table 9.6.: Extrapolation of the 10th eigenvalue of the biharmonic operator on the L-shaped domain.

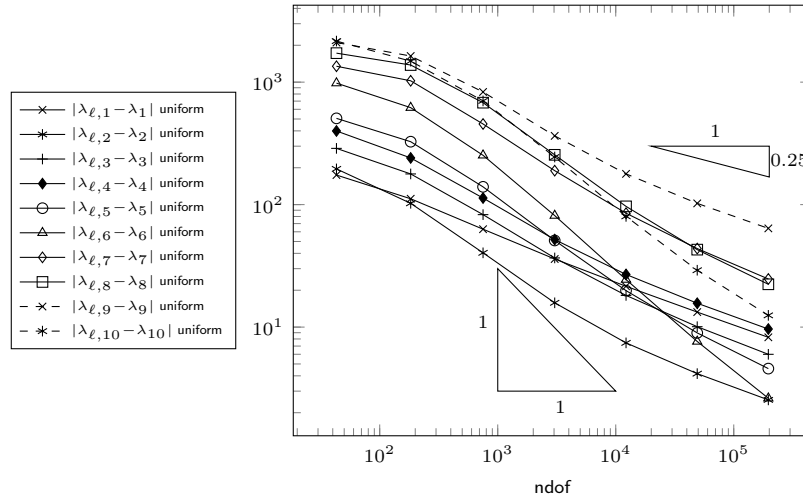


Figure 9.16.: Convergence history for the eigenvalues of the biharmonic operator on the L-shaped domain with mixed boundary conditions under uniform mesh refinement.

In contrast to uniform mesh-refinement, the adaptive algorithm yields the optimal convergence rate. The initial mesh is obtained by one red-refinement of the triangular mesh in Figure 9.1.

Guaranteed upper and lower bounds for the first eigenvalue under uniform mesh-refinement are displayed in Table 9.7.

Perturbed Geometry

On the square with perturbed slits, the eigenvalues 9 to 13 of the biharmonic operator read as

$$\lambda_9 = 5232.282 \quad \lambda_{10} = 5280.960 \quad \lambda_{11} = 5281.125 \quad \lambda_{12} = 5340.869.$$

These values are obtained with the Bogner-Fox-Schmit finite element and Aitken extrapolation. The values from Table 9.8 suggest that at least the first three displayed digits are accurate.

Figure 9.18 displays the convergence of the eigenvalues for the simultaneous marking and for uniform refinement. The adaptive approximation has the optimal rate. The convergence history for marking based on only one eigenfunction is plotted in Figure 9.19. The approximation of the eigenvalue λ_{12} shows a plateau up to 80 000 degrees of freedom. The discussion from Section 9.2 gives some explanation for this pre-asymptotic regime in the case of single marking. If the initial triangulation is finer (one red-refinement), the convergence rate in Figure 9.20 appears optimal from the very beginning.

9. Numerical Experiments

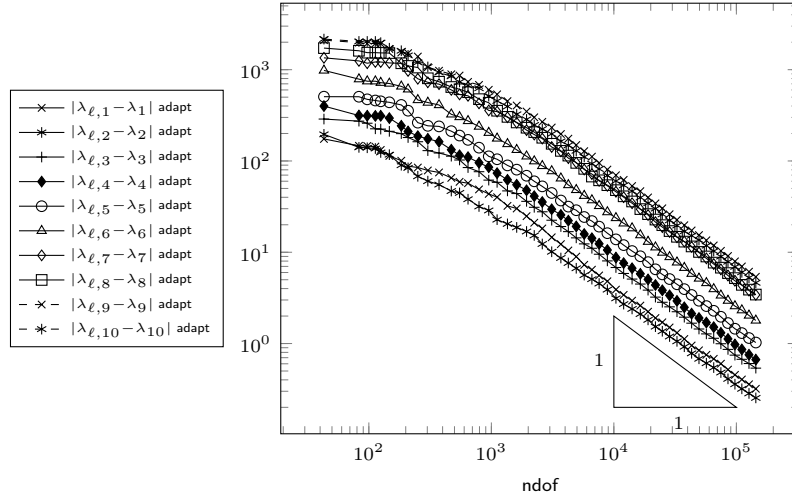


Figure 9.17.: Convergence history for the eigenvalue of the biharmonic operator on the L-shaped domain with mixed boundary conditions; adaptive mesh-refinement based on $J = \{1, \dots, 10\}$.

ndof Morley	$\lambda_{\ell,1}$ Morley	GLB	GUB	ndof BFS
9	58.388488	3.5427722		
43	77.660939	33.958600	292.79805	35
183	140.41084	122.58427	276.22677	171
751	189.03610	186.75092	266.77337	731
3 039	216.05160	215.86292	260.76379	3 003
12 223	230.49237	230.47894	257.14071	12 155
49 023	238.77276	238.77186	255.01258	48 891
196 351	243.78144	243.78138	253.77306	196 091
785 919	246.87870	246.87869	253.05114	785 403
3 144 703	248.80626	248.80626	252.62894	3 143 675

Table 9.7.: Guaranteed upper (GUB) and lower (GLB) eigenvalue bounds for the first eigenvalue of the biharmonic operator on the L-shaped domain with mixed boundary conditions. The extrapolated exact eigenvalue is $\lambda_1 = 252.03427$.

ndof	$\lambda_{\ell,9}$ from BFS FEM	extrapolation λ_9	$\lambda_{\ell,10}$ from BFS FEM	extrapolation λ_{10}
64 004	5 241.3517	5 232.0912	5 286.8069	5 281.0008
259 076	5 236.8542	5 232.1728	5 283.9187	5 280.8965
1 042 436	5 234.5807	5 232.2567	5 282.4524	5 280.9402
4 182 020	5 233.4377	5 232.2820	5 281.7129	5 280.9606
ndof	$\lambda_{\ell,11}$ from BFS FEM	extrapolation λ_{11}	$\lambda_{\ell,12}$ from BFS FEM	extrapolation λ_{12}
64 004	5 287.0464	5 281.1390	5 342.5530	5 341.1561
259 076	5 284.0996	5 281.0680	5 341.7129	5 340.8877
1 044 360	5 282.6166	5 281.1140	5 341.2920	5 340.8692
4 182 020	5 281.8732	5 281.1259	5 341.0811	5 340.8696

Table 9.8.: Aitken extrapolation of eigenvalues of the biharmonic operator on the square with perturbed slits.

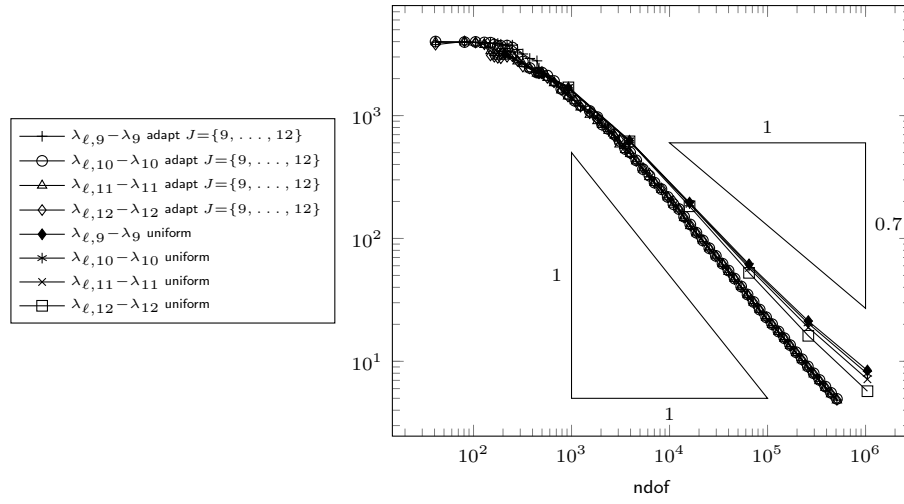


Figure 9.18.: Convergence history for the eigenvalues of the biharmonic operator on the square with perturbed slits based on $J = \{9, \dots, 12\}$ and a coarse initial mesh with 41 degrees of freedom.

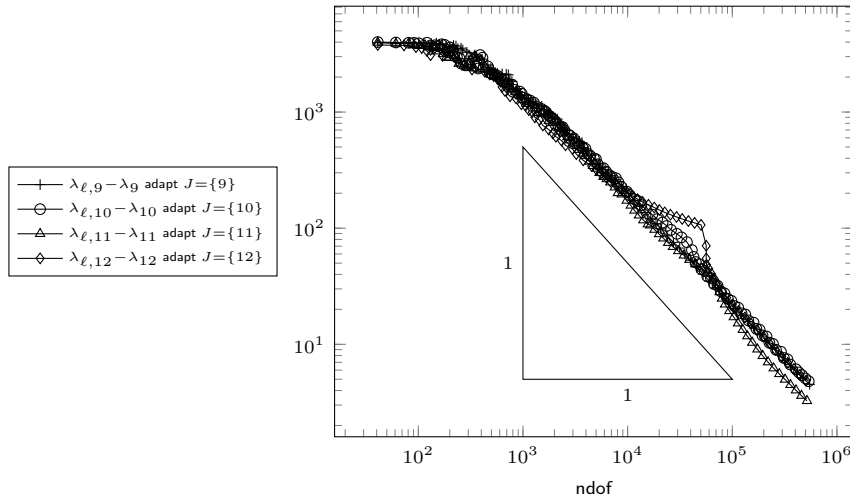


Figure 9.19.: Convergence history for the eigenvalues of the biharmonic operator on the square with perturbed slits based on $J \subseteq \{9, \dots, 12\}$ and a coarse initial mesh with 41 degrees of freedom.

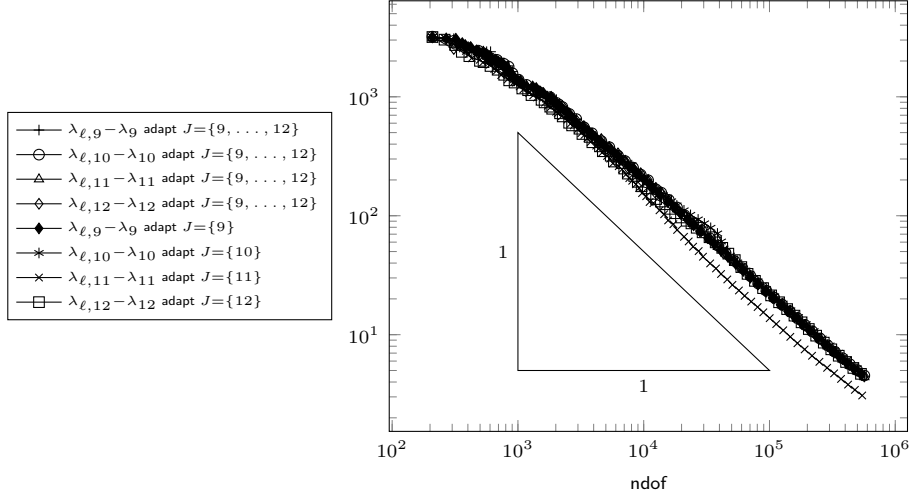


Figure 9.20.: Convergence history for the eigenvalues of the biharmonic operator on the square with perturbed slits based on $J \subseteq \{9, \dots, 12\}$ and an initial mesh with 209 degrees of freedom.

9.5. Inexact Solution of the Algebraic Eigenvalue Problems

This section gives an outlook how to include the linear-algebraic error in the adaptive algorithm. The computation of eigenvalues requires iterative schemes; an approximation up to machine precision is not realistic. The optimality analysis of this thesis can be extended to Algorithm 3.17 under the condition that the parameter $\varkappa \ll 1$ which controls the accuracy of the linear-algebraic solve is sufficiently small. This type of perturbation arguments has been carried out in [Carstensen and Gedicke, 2012, Carstensen, Gallistl, and Schedensack, 2014c], but the smallness of \varkappa is not quantified.

The purpose of this section is to present a very basic practical algorithm for the conforming finite element discretisation of the Laplacian that includes the linear-algebraic error and to investigate suitable values of \varkappa and how these values are related to the required parameters in the linear-algebraic eigenvalue solver.

Iterative Algorithm

The proposed algorithm includes the spectral gap. Given the eigenvalue cluster J and eigenpair approximations $(\tilde{\lambda}_{\ell,j}, \tilde{u}_{\ell,j})$ define

$$d := \begin{cases} \min_{j \in J} \min_{k \notin J} |\tilde{\lambda}_{\ell,j} - \lambda_{\ell,k}| & \text{if the cluster } \text{conv}\{\tilde{\lambda}_{\ell,j} \mid j \in J\} \text{ does not contain} \\ & \text{eigenvalues } \lambda_{\ell,k} \text{ for } k \notin J, \\ -1 & \text{else.} \end{cases}$$

The Matlab routine `eigs` is based on ARPACK [Lehoucq et al., 1998] which realises the implicitly restarted Arnoldi method. The proposed algorithm improves the eigenvalue approximation by increasing the dimension of the Krylov subspace. The pseudocode reads as follows.

Algorithm 9.1 (practical AFEM with iterative solve).

Input: Initial triangulation \mathcal{T}_0 , bulk parameter $0 < \theta \leq 1$, parameter $0 < \varkappa < \infty$, maximum size of Krylov space dimension `pmax`, `eigs` parameters `maxit` and `tol`.

for $\ell = 0, 1, 2, \dots$ **do**

$p := n + N$

repeat

Increase $p := p + 1$.

Compute approximations $(\tilde{\lambda}_{\ell,j}, \tilde{u}_{\ell,j})_{j \in J}$ to the discrete eigenpairs $(\lambda_{\ell,j}, u_{\ell,j})_{j \in J}$ using `eigs` with Krylov space dimension p and parameters `maxit` and `tol` from input as well as `issym` := 1 and `isreal` := 1.

Compute local contributions of the error estimator $(\eta_\ell^2(T))_{T \in \mathcal{T}_\ell}$ based on the quantities $(\tilde{\lambda}_{\ell,j}, \tilde{u}_{\ell,j})_{j \in J}$.

until $p > \text{pmax}$ or (with $\eta_{-1}^2 := \infty$)

$$\sum_{j \in J} \|a(\tilde{u}_{\ell,j}, \cdot) - \tilde{\lambda}_{\ell,j} b(\tilde{u}_{\ell,j}, \cdot)\|_{V_\ell^*}^2 \leq \text{sign}(d) d^2 \varkappa \min\{\eta_\ell^2, \eta_{\ell-1}^2\}. \quad (9.2)$$

Mark. Choose a minimal subset $\mathcal{M}_\ell \subseteq \mathcal{T}_\ell$ such that $\theta \eta_\ell^2(\mathcal{T}_\ell) \leq \eta_\ell^2(\mathcal{M}_\ell)$.

Refine. Generate $\mathcal{T}_{\ell+1} := \text{refine}(\mathcal{T}_\ell, \mathcal{M}_\ell)$ with Algorithm 2.15.

end for

Output: Approximate discrete eigenpairs $((\tilde{\lambda}_{\ell,j}, \tilde{u}_{\ell,j})_{j \in J})_\ell$. ◆

In (9.2), $\|\cdot\|_{V_\ell^*}$ denotes the dual norm, i.e.,

$$\|F\|_{V_\ell^*} := \sup_{v_\ell \in V_\ell \setminus \{0\}} \frac{|F(v_\ell)|}{\|v_\ell\|} \quad \text{for any } F \in V_\ell^*.$$

Remark 9.2. Algorithm 9.1 is designed to identify sharp bounds on the critical value of \varkappa for which one obtains the optimal convergence rate. In practice, where one is interested in optimal computational complexity, such empirical values for \varkappa have to be combined with some proper parameter choice for the eigensolver and appropriate spectrally equivalent preconditioning (e.g., multigrid) as in [Carstensen and Gedicke, 2012]. ◆

Remark 9.3. Algorithm 9.1 employs a very simple criterion to improve the discrete eigen-solution, namely it increases the number of Arnoldi vectors while the maximum number of implicit restarts `maxit` is fixed. In the computations of this section the maximum Krylov space dimension is set `pmax` = 30. ◆

Remark 9.4. The parameter `tol` in `eigs` gives a criterion whether the eigenvalue approximation is appropriate. If `eigs` detects “no convergence”, the output is NaN. In order to avoid any influence of this criterion on the termination criterion (9.2), the implementation increases the parameter `tol` until `eigs` outputs some finite eigenvalue approximations. The quality of the approximation is validated via (9.2). ◆

Remark 9.5. Note that, if d is negative, the right-hand side of (9.2) is also negative. The computation of the gap d requires some information on the spectrum such as lower eigenvalue bounds. In order to keep the implementation simple, the extrapolated exact eigenvalue of the Laplacian is provided to compute an approximation for the gap by

$$d \stackrel{\text{approx}}{=} \min\{\lambda_{n+N+1} - \tilde{\lambda}_{\ell,n+N}, \tilde{\lambda}_{\ell,n+1} - \tilde{\lambda}_{\ell,n}, \tilde{\lambda}_{\ell,n+1} - \lambda_{\ell,n}\}. \quad \text{◆}$$

The implementation of the iterative loop is displayed in Figure 9.21.

```

p = cluster_upper;
termination = false;
while (~termination)
    p = p+1; opts.p = p;
    opts.maxit = maxit; opts.tol = tol; opts.isreal = 1; opts.issymm = 1;
    eVect = zeros(nrNodes,nEig);

    while(true)
        [V,D] = eigs(A(dof,dof),B(dof,dof),cluster_upper,'sm',opts);
        [D,ind] = sort(diag(D));
        eVect(dof,:) = V(:,ind(cluster_lower:cluster_upper));
        eVal = D(cluster_lower:cluster_upper);
        if isnan(prod(eVal))
            opts.tol=10*opts.tol;
        else
            break
        end
    end

    % Evaluate error estimator
    for ell=1:nEig
        cur_eta4e = estimatePlevpEtaElements(eVal(ell),eVect(:,ell),...
            c4n,n4e,n4sDb,n4sNb);
        eta4e = eta4e + cur_eta4e;
    end
    totalestSq = sum(eta4e);

    % compute gap
    d = exactEVs(cluster_upper+1)-D(cluster_upper);
    if cluster_lower == 1
        d=min(d,D(cluster_lower));
    else
        d=min(d,D(cluster_lower)-exactEVs(cluster_lower-1));
        d=min(d,D(cluster_lower)-D(cluster_lower-1));
    end

    if(isnan(d))
        d=-1;
    end

    % Compute the residual
    r = A(dof,dof)*eVect(dof,:)- B(dof,dof)*eVect(dof,:)*diag(eVal);
    R = sum(diag(r'*(A(dof,dof)\r)))/d^2;

    % Check termination criterion
    if p>=min(ndof,pmax), break ,end

    termination = (R<sign(d)*term_param*min(totalestSq,eta_oldSq));
end

```

Figure 9.21.: Matlab implementation of the loop of Algorithm 9.1.

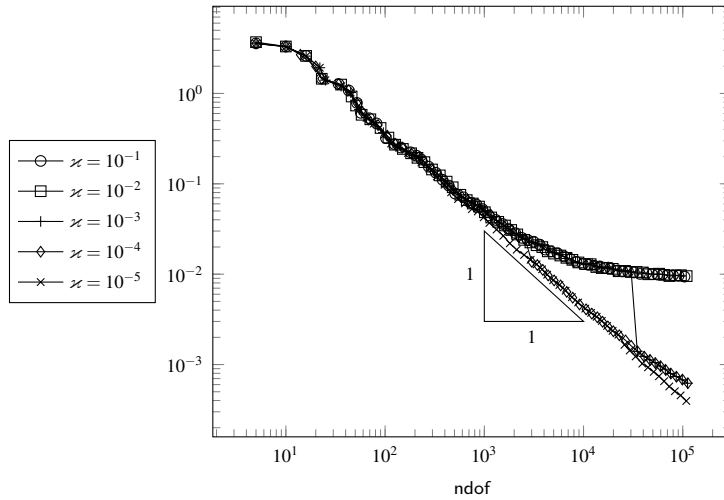


Figure 9.22.: Convergence history for the adaptive inexact computation of the first eigenvalue of the Laplacian on the L-shaped domain for different values of \varkappa .

First Eigenvalue on the L-Shaped Domain

The first computational example with inexact solve considers the first eigenvalue on the L-shaped domain from Figure 9.1. In this example, no implicit restart is used, $\text{maxit} = 1$. Figure 9.22 displays the convergence history for different values of \varkappa ranging from 10^{-1} to 10^{-5} . The choice $\varkappa \in \{10^{-1}, 10^{-2}\}$ does not lead to convergence, the Krylov spaces have dimension 2 on all levels of the AFEM. For the choice $\varkappa = 10^{-3}$ one can observe the optimal convergence rate after 30 000 degrees of freedom only. This is exactly the point where the dimension of the Krylov spaces enforced by \varkappa changes from 2 to 3. The values of Table 9.9 show that tremendous improvement of the error by a factor between 7 and 8 when one more Arnoldi vector is utilised and the degrees of freedom are increased by a factor 1.15. This indicates that the use of 2 Arnoldi vectors up to this point leads to an adaptive mesh whose quality is comparable with meshes generated with higher accuracy.

AFEM level	ndof	Arnoldi vectors	$ \tilde{\lambda}_{\ell,1} - \lambda_1 $
48	23 076	2	0.0111099
49	26 549	2	0.0109337
50	30 223	2	0.0105784
51	34 835	3	0.00139945
52	40 728	3	0.00123130

Table 9.9.: Convergence history on the L-shaped domain using `eigs` with $\varkappa = 0.001$.

The smaller values $\varkappa \in \{10^{-4}, 10^{-5}\}$ lead to the optimal convergence rate. The corresponding Krylov spaces typically have dimension $p = 3$ for $\varkappa = 10^{-4}$ and $p = 4$ for $\varkappa = 10^{-5}$. The fact that $p = 3$ suffices to produce the optimal rate in the considered range has also been observed in [Mehrmann and Miedlar, 2011].

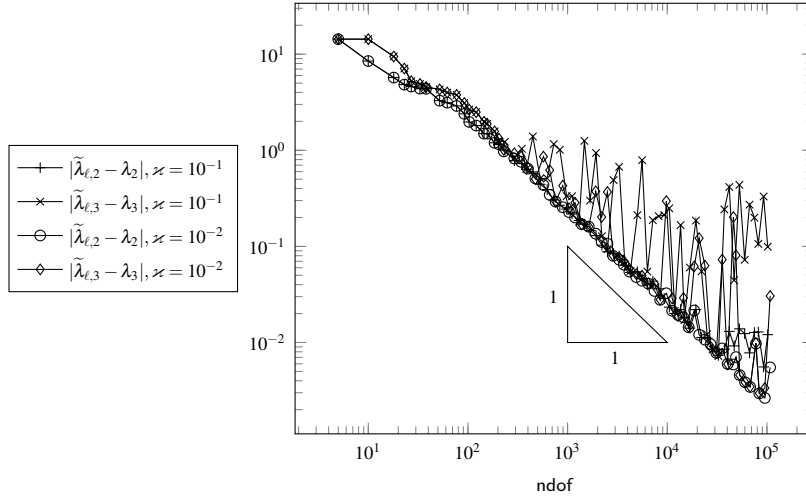


Figure 9.23.: Convergence history for the adaptive inexact computation of the eigenvalues number 2 and 3 of the Laplacian on the square with perturbed slits using eigs with maxit = 1 and the parameter $\kappa \in \{10^{-1}, 10^{-2}\}$.

Clustered Eigenvalues on the Square with Perturbed Slits

This example revisits the eigenvalue cluster $J = \{2, 3\}$ of the Laplacian on the perturbed slit domain from Figure 9.2. In a first test, the parameters are set maxit = 1 and tol = 10^{60} , which means no implicit restart and a large tolerance in order to prevent Matlab from reporting “no convergence”. Figure 9.23 displays the convergence history of the computed eigenvalues $\tilde{\lambda}_{\ell,2}$ and $\tilde{\lambda}_{\ell,3}$ for $\kappa \in \{10^{-1}, 10^{-2}\}$. The choice $\kappa = 10^{-1}$ enforces the use of 12 to 13 Arnoldi vectors while for $\kappa = 10^{-2}$ the number of Arnoldi vectors varies from 13 to 14. Both choices of κ do not lead to convergence, but $\kappa \in 10^{-2}$ shows satisfactory results up to 20000 degrees of freedom. For $\kappa \in \{10^{-3}, 10^{-4}\}$ the optimal convergence rate can be observed in the convergence history of Figure 9.24 The number of Arnoldi vectors ranges from 13 to 15.

In a second test, the parameters are set maxit = 10 and tol = 10^{-6} which means that up to 9 implicit restarts are used. Figure 9.25 displays the convergence rates for $\kappa \in \{10^{-1}, 10^{-3}\}$. For any choice of κ the observed convergence rate is optimal. While on coarse meshes the criterion including the spectral gap enforces high-accuracy solutions, for all numbers of degrees of freedom beyond 145, the number of Arnoldi vectors is constantly 6 for any choice of κ . In other words, the termination criterion seems to be guaranteed by 6 Arnoldi vectors for all κ in the considered range. This means that the criterion (9.2) for $\kappa = 0.1$ implies the termination criterion also for some smaller values of κ . This shows that, dependent on the eigensolver at hand, one can obtain good results also for large values of κ .

Comparison with LOBPCG

The abstract Algorithm 3.17 does not make use of any property of the linear-algebraic eigenvalue solver which is rather assumed to be a “black box” eigensolver. For comparison, this subsection presents a computation on the slitted square domain from Figure 9.2 where the algebraic eigenvalue problem is solved inexactly with A. Knyazev’s Matlab im-

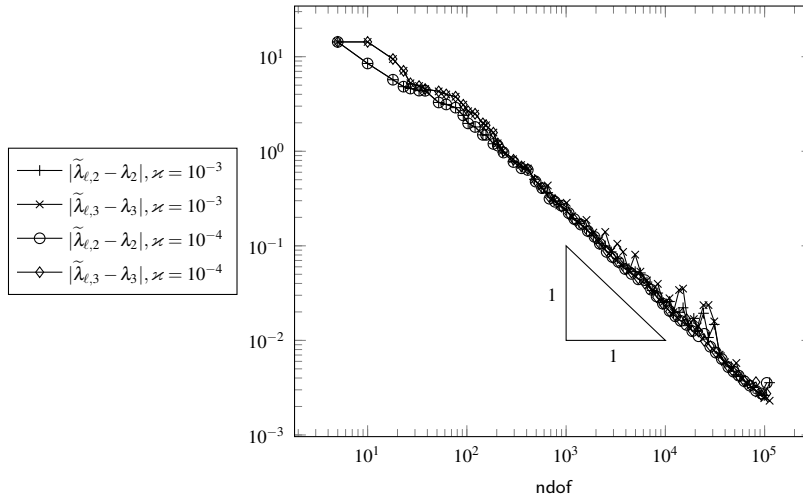


Figure 9.24.: Convergence history for the adaptive inexact computation of the eigenvalues number 2 and 3 of the Laplacian on the square with perturbed slits using eigs with maxit = 1 and the parameter $\varkappa \in \{10^{-3}, 10^{-4}\}$.

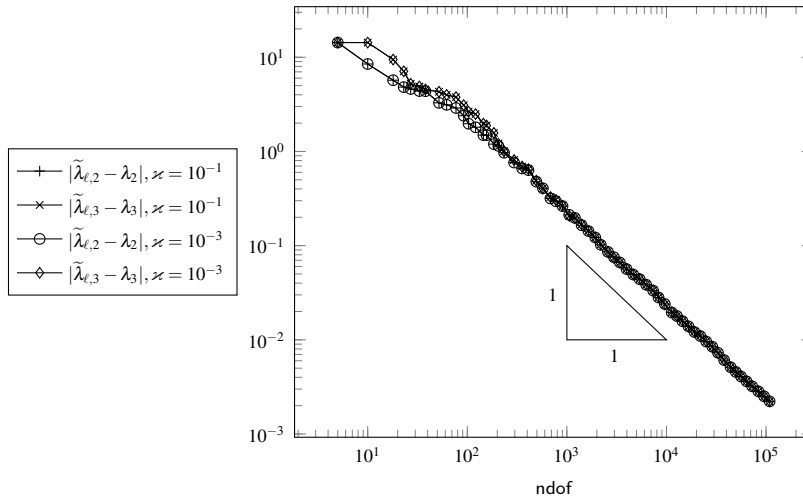


Figure 9.25.: Convergence history for the adaptive inexact computation of the eigenvalues number 2 and 3 of the Laplacian on the square with perturbed slits with 9 implicit restarts in eigs.

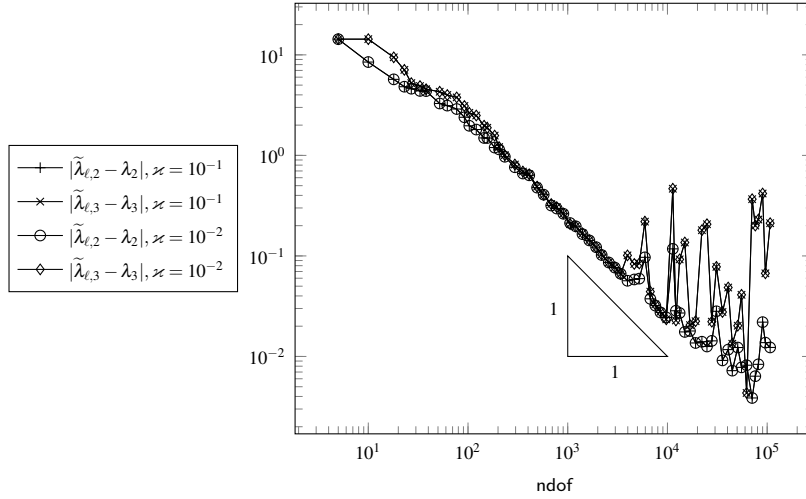


Figure 9.26.: Convergence history for the adaptive inexact computation of the eigenvalues number 2 and 3 of the Laplacian on the square with perturbed slits and parameter $\varkappa \in \{10^{-3}, 10^{-4}\}$ with LOBPCG.

plementation of the Locally Optimal Block Preconditioned Conjugate Gradient Method (LOBPCG) [Knyazev, 2001, 2011]. The block-size is chosen as 4 and the number of iterations is increased as long as the termination criterion is not satisfied. This increase of iterations should give a rather sharp bound on the required value of \varkappa . For simplicity, no preconditioning is utilised. The convergence history for the approximation of the eigenvalues 2 and 3 with $\varkappa \in \{10^{-1}, 10^{-2}\}$ is displayed in Figure 9.26. The error decays optimally in the range up to 10^4 degrees of freedom and oscillates for higher levels of the AFEM. For the choice $\varkappa \in \{10^{-3}, 10^{-4}\}$ one observes the optimal convergence rate in Figure 9.27. This coincides with the values observed for `eigs` when the number of Arnoldi vectors is increased without implicit restarts.

9.6. Conclusions from the Computational Experiments

General observations. The bulk parameter $\theta = 0.1$ leads to optimal convergence rates in all test examples, provided that the cluster is resolved by a simultaneous marking. The initial mesh that results from one red-refinement of the triangulation in Figure 9.2 appears to be sufficiently fine for the case of marking with respect to a single eigenfunction whereas the coarse initial mesh of Figure 9.2 itself leads to a large pre-asymptotic range in the examples of Section 9.2 and 9.4.

Single marking vs. simultaneous marking. In the case that the eigenvalue cluster is not resolved by the initial triangulation, the simultaneous approximation seems to be superior compared to the use of an adaptive scheme for each eigenvalue separately, even if all eigenvalues on the continuous level are simple. While the use of a coarse initial mesh in the example with the latter strategy leads to a wide pre-asymptotic regime for the conforming \mathcal{P}_1 FEM for the Laplacian and for the Morley FEM for the biharmonic operator, the simultaneous approximation produces optimal rates from the very beginning.

Observed required initial mesh-size. It is evident from the convergence history plot in

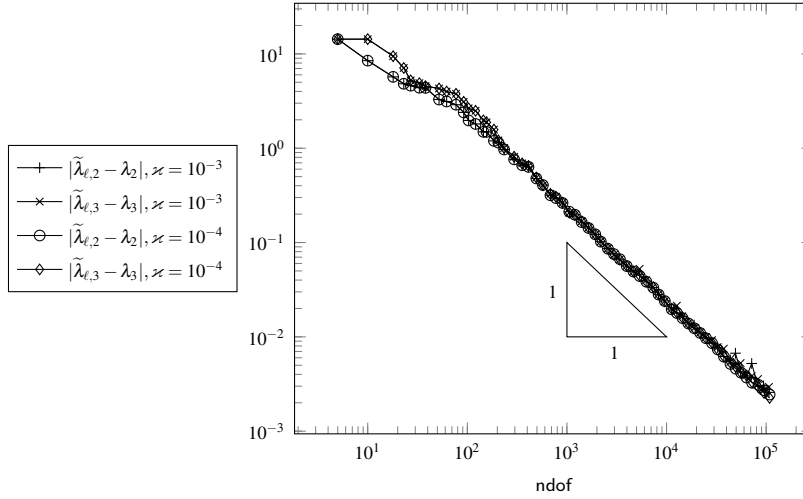


Figure 9.27.: Convergence history for the adaptive inexact computation of the eigenvalues number 2 and 3 of the Laplacian on the square with perturbed slits and parameter $\varkappa \in \{10^{-3}, 10^{-4}\}$ with LOBPCG.

Figure 9.8 that the initial separation of the eigenvalue cluster has a strong influence on the quality of the adaptive approximation. The critical quantity is the separation of the cluster from the remaining spectrum and not a full resolution of the multiplicities within the cluster. The separation of the cluster is a more relaxed condition than the separation of a single eigenvalue. Accordingly, the simultaneous marking strategy yields better results. The further assumptions on sufficiently small initial mesh-sizes seemingly indicate that a uniform refinement might be competitive with an adaptive mesh-refinement at least in a large pre-asymptotic regime. This is indeed untrue as seen in the numerical examples for simultaneous marking. While the remaining theoretical conditions on the initial mesh-size are vital for the analysis, the numerical tests for the simultaneous marking strategy yield optimal results in all examples.

Discussion of initial mesh-size. The optimal convergence rates proven in this thesis are of asymptotic nature and do not quantify the pre-asymptotic range. The results of Garau et al. [2009] state (at least for conforming FEMs) that for any arbitrarily coarse initial mesh \mathcal{T}_0 there is convergence towards *some* eigenpair and the global mesh-size $\|h_\ell\|_{L^\infty(\Omega)} \rightarrow 0$ tends to zero. The combination with the results of this thesis implies that at some point the global mesh-size is small enough to allow for the optimal convergence rate. The quasi-optimality results in this thesis, however, cannot dispense with the restrictions on the initial mesh-size because the involved constant (e.g., C_{opt} in Theorem 4.6) has a universal character in that it only depends on the domain and the shape-regularity of the triangulations. Without any restrictions on the mesh-size one also eventually obtains the optimal convergence rate, but with an unquantified constant that may be sensitive with respect to the eigenvalue of interest or the angles in the initial triangulation. Furthermore, it is clear that the separation constant M_J heavily depends on the definition of the cluster J and the numerical experiments show that the separation has influence on the width of the pre-asymptotic range.

Inexact solve. The inexact solution of the linear-algebraic problem can be included in the adaptive algorithm and the convergence rate appears optimal for a moderate size of

9. Numerical Experiments

Krylov subspaces (for the first eigenvalue, $p = 3$ seems to be sufficient up to 10^5 degrees of freedom). For eigenvalue clusters, the inexact solve in the adaptive algorithm requires a termination criterion that includes the spectral gap. Algorithm 9.1 includes one possible realisation of such a criterion. In the numerical experiments, the algorithms `eigs` with no implicit restart, `eigs` with 10 implicit restarts and LOBPCG with block size 4 show the optimal convergence rate for a moderate choice of $\varkappa \in \{10^{-3}, 10^{-4}\}$. The optimality results of this thesis can be extended to the case of inexact solve provided the parameter $\varkappa \ll 1$ is sufficiently small.

Bibliography

- G. Acosta, R. G. Durán, and M. A. Muschietti. Solutions of the divergence operator on John domains. *Adv. Math.*, 206(2):373–401, 2006.
- R. A. Adams and J. J. F. Fournier. *Sobolev Spaces*, volume 140 of *Pure and Applied Mathematics (Amsterdam)*. Elsevier/Academic Press, Amsterdam, second edition, 2003.
- J. Albery, C. Carstensen, and S. A. Funken. Remarks around 50 lines of Matlab: short finite element implementation. *Numer. Algorithms*, 20(2-3):117–137, 1999.
- T. Apel, V. Mehrmann, and D. Watkins. Structured eigenvalue methods for the computation of corner singularities in 3D anisotropic elastic structures. *Comput. Methods Appl. Mech. Eng.*, 191(39-40):4459–4473, 2002.
- M. G. Armentano and R. G. Durán. Asymptotic lower bounds for eigenvalues by nonconforming finite element methods. *Electron. Trans. Numer. Anal.*, 17:93–101, 2004.
- D. N. Arnold and R. S. Falk. A uniformly accurate finite element method for the Reissner-Mindlin plate. *SIAM J. Numer. Anal.*, 26(6):1276–1290, 1989.
- I. Babuška and J. Osborn. Eigenvalue problems. In *Handbook of Numerical Analysis*, volume II, pages 641–787. North-Holland, Amsterdam, 1991.
- C. Bahriawati and C. Carstensen. Three MATLAB implementations of the lowest-order Raviart-Thomas MFEM with a posteriori error control. *Comput. Methods Appl. Math.*, 5(4):333–361, 2005.
- R. Becker and S. Mao. An optimally convergent adaptive mixed finite element method. *Numer. Math.*, 111(1):35–54, 2008.
- R. Becker and S. Mao. Convergence and quasi-optimal complexity of a simple adaptive finite element method. *M2AN Math. Model. Numer. Anal.*, 43(6):1203–1219, 2009.
- R. Becker and S. Mao. Quasi-optimality of adaptive nonconforming finite element methods for the Stokes equations. *SIAM J. Numer. Anal.*, 49(3):970–991, 2011.
- R. Becker, S. Mao, and Z. Shi. A convergent nonconforming adaptive finite element method with quasi-optimal complexity. *SIAM J. Numer. Anal.*, 47(6):4639–4659, 2010.
- L. Beirão da Veiga, J. Niiranen, and R. Stenberg. A posteriori error estimates for the Morley plate bending element. *Numer. Math.*, 106(2):165–179, 2007.
- L. Beirão da Veiga, J. Niiranen, and R. Stenberg. A posteriori error analysis for the Morley plate element with general boundary conditions. *Internat. J. Numer. Methods Engrg.*, 83(1):1–26, 2010.

BIBLIOGRAPHY

- P. Binev, W. Dahmen, and R. DeVore. Adaptive finite element methods with convergence rates. *Numer. Math.*, 97(2):219–268, 2004.
- H. Blum and R. Rannacher. On the boundary value problem of the biharmonic operator on domains with angular corners. *Math. Methods Appl. Sci.*, 2(4):556–581, 1980.
- D. Boffi. Finite element approximation of eigenvalue problems. *Acta Numer.*, 19:1–120, 2010.
- D. Boffi, F. Brezzi, and M. Fortin. *Mixed Finite Element Methods and Applications*, volume 44 of *Springer Series in Computational Mathematics*. Springer, Heidelberg, 2013.
- D. Boffi, R. G. Duran, F. Gardini, and L. Gastaldi. A posteriori error analysis for nonconforming approximation of multiple eigenvalues. *arXiv e-Prints*, 1404.5560, 2014. URL <http://arxiv.org/abs/1404.5560>.
- D. Braess. *Finite Elements. Theory, Fast Solvers, and Applications in Elasticity Theory*. Cambridge University Press, Cambridge, third edition, 2007.
- D. Braess. An a posteriori error estimate and a comparison theorem for the nonconforming P_1 element. *Calcolo*, 46(2):149–155, 2009.
- S. C. Brenner. A two-level additive Schwarz preconditioner for the stationary Stokes equations. *Adv. Comput. Math.*, 4(1-2):111–126, 1995.
- S. C. Brenner. Two-level additive Schwarz preconditioners for nonconforming finite element methods. *Math. Comp.*, 65(215):897–921, 1996.
- S. C. Brenner. Poincaré-Friedrichs inequalities for piecewise H^1 functions. *SIAM J. Numer. Anal.*, 41(1):306–324, 2003.
- S. C. Brenner and L. R. Scott. *The Mathematical Theory of Finite Element Methods*, volume 15 of *Texts in Applied Mathematics*. Springer, New York, third edition, 2008.
- S. C. Brenner, T. Gudi, and L.-Y. Sung. An a posteriori error estimator for a quadratic C^0 -interior penalty method for the biharmonic problem. *IMA J. Numer. Anal.*, 30(3):777–798, 2010.
- A. Buffa and C. Ortner. Compact embeddings of broken Sobolev spaces and applications. *IMA J. Numer. Anal.*, 29(4):827–855, 2009.
- C. Carstensen and J. Gedicke. An oscillation-free adaptive FEM for symmetric eigenvalue problems. *Numer. Math.*, 118(3):401–427, 2011.
- C. Carstensen and S. A. Funken. Constants in Clément-interpolation error and residual based a posteriori error estimates in finite element methods. *East-West J. Numer. Math.*, 8(3):153–175, 2000.
- C. Carstensen and D. Gallistl. Guaranteed lower eigenvalue bounds for the biharmonic equation. *Numer. Math.*, 126(1):33–51, 2014.
- C. Carstensen and J. Gedicke. An adaptive finite element eigenvalue solver of quasi-optimal computational complexity. *SIAM J. Numer. Anal.*, 50(3):1029–1057, 2012.

- C. Carstensen and J. Gedicke. Guaranteed lower bounds for eigenvalues. *Math. Comp.*, 2014. doi: 10.1090/S0025-5718-2014-02833-0. In print.
- C. Carstensen and R. H. W. Hoppe. Convergence analysis of an adaptive nonconforming finite element method. *Numer. Math.*, 103(2):251–266, 2006.
- C. Carstensen and E.-J. Park. Convergence and optimality of adaptive least squares finite element methods. 2013. In preparation.
- C. Carstensen, J. Gedicke, V. Mehrmann, and A. Miedlar. An adaptive homotopy approach for non-selfadjoint eigenvalue problems. *Numer. Math.*, 119(3):557–583, 2011.
- C. Carstensen, M. Eigel, R. Hoppe, and C. Löbhard. A review of unified a posteriori finite element error control. *Numer. Math. Theory Methods Appl.*, 5(4):509–558, 2012a.
- C. Carstensen, D. Peterseim, and M. Schedensack. Comparison results of finite element methods for the Poisson model problem. *SIAM J. Numer. Anal.*, 50(6):2803–2823, 2012b.
- C. Carstensen, D. Gallistl, and M. Schedensack. Discrete reliability for Crouzeix-Raviart FEMs. *SIAM J. Numer. Anal.*, 51(5):2935–2955, 2013a.
- C. Carstensen, D. Peterseim, and H. Rabus. Optimal adaptive nonconforming FEM for the Stokes problem. *Numer. Math.*, 123(2):291–308, 2013b.
- C. Carstensen, M. Feischl, M. Page, and D. Praetorius. Axioms of adaptivity. *Comput. Math. Appl.*, 67(6):1195–1253, 2014a.
- C. Carstensen, D. Gallistl, and J. Hu. A discrete Helmholtz decomposition with Morley finite element functions and the optimality of adaptive finite element schemes. *Comput. Math. Appl.*, 2014b. Submitted for publication.
- C. Carstensen, D. Gallistl, and M. Schedensack. Adaptive nonconforming Crouzeix-Raviart FEM for eigenvalue problems. *Math. Comp.*, 2014c. In print.
- C. Carstensen, J. Gedicke, V. Mehrmann, and A. Miedlar. An adaptive finite element method with asymptotic saturation for eigenvalue problems. *Numer. Math.*, 2014d. doi: 10.1007/s00211-014-0624-2. In print.
- C. Carstensen, D. Peterseim, K. Köhler, and M. Schedensack. Comparison results for the Stokes equations. *Appl. Numer. Math.*, 2014e. doi: 10.1016/j.apnum.2013.12.005. In print.
- C. Carstensen et al. AFEM software package and documentaion. Humboldt-Universität zu Berlin, unpublished, 2009.
- J. Cascon, C. Kreuzer, R. H. Nochetto, and K. G. Siebert. Quasi-optimal convergence rate for an adaptive finite element method. *SIAM J. Numer. Anal.*, 46(5):2524–2550, 2008.
- F. Chatelin. *Spectral Approximation of Linear Operators*. Computer Science and Applied Mathematics. Academic Press Inc., New York, 1983.

BIBLIOGRAPHY

- P. G. Ciarlet. *The Finite Element Method for Elliptic Problems*, volume 4 of *Studies in Mathematics and its Applications*. North-Holland, Amsterdam, 1978.
- M. Crouzeix and P.-A. Raviart. Conforming and nonconforming finite element methods for solving the stationary Stokes equations. I. *Rev. Française Automat. Informat. Recherche Opérationnelle Sér. Rouge*, 7(R-3):33–75, 1973.
- X. Dai, J. Xu, and A. Zhou. Convergence and optimal complexity of adaptive finite element eigenvalue computations. *Numer. Math.*, 110(3):313–355, 2008.
- X. Dai, L. He, and A. Zhou. Convergence rate and quasi-optimal complexity of adaptive finite element computations for multiple eigenvalues. *arXiv e-Prints*, 1210.1846v2, 2013. URL <http://arxiv.org/pdf/1210.1846v2>.
- E. Dari, R. Durán, and C. Padra. Error estimators for nonconforming finite element approximations of the Stokes problem. *Math. Comp.*, 64(211):1017–1033, 1995.
- E. Dari, R. Duran, C. Padra, and V. Vampa. A posteriori error estimators for nonconforming finite element methods. *RAIRO Modél. Math. Anal. Numér.*, 30(4):385–400, 1996.
- E. A. Dari, R. G. Durán, and C. Padra. A posteriori error estimates for non-conforming approximation of eigenvalue problems. *Appl. Numer. Math.*, 62(5):580–591, 2012.
- C. Davis and W. M. Kahan. The rotation of eigenvectors by a perturbation. III. *SIAM J. Numer. Anal.*, 7:1–46, 1970.
- D. A. Di Pietro and A. Ern. *Mathematical Aspects of Discontinuous Galerkin Methods*, volume 69 of *Mathématiques & Applications (Berlin)*. Springer, Heidelberg, 2012.
- R. G. Durán, C. Padra, and R. Rodríguez. A posteriori error estimates for the finite element approximation of eigenvalue problems. *Math. Models Methods Appl. Sci.*, 13(8):1219–1229, 2003.
- L. C. Evans. *Partial Differential Equations*, volume 19 of *Graduate Studies in Mathematics*. American Mathematical Society, Providence, RI, second edition, 2010.
- E. B. Fabes, C. E. Kenig, and G. C. Verchota. The Dirichlet problem for the Stokes system on Lipschitz domains. *Duke Math. J.*, 57(3):769–793, 1988.
- R. S. Falk and M. E. Morley. Equivalence of finite element methods for problems in elasticity. *SIAM J. Numer. Anal.*, 27(6):1486–1505, 1990.
- S. Funken, D. Praetorius, and P. Wissgott. Efficient implementation of adaptive P1-FEM in Matlab. *Comput. Methods Appl. Math.*, 11(4):460–490, 2011.
- E. M. Garau, P. Morin, and C. Zuppa. Convergence of adaptive finite element methods for eigenvalue problems. *Math. Models Methods Appl. Sci.*, 19(5):721–747, 2009.
- S. Giani and I. G. Graham. A convergent adaptive method for elliptic eigenvalue problems. *SIAM J. Numer. Anal.*, 47(2):1067–1091, 2009.

- V. Girault and P.-A. Raviart. *Finite Element Methods for Navier-Stokes Equations. Theory and Algorithms*, volume 5 of *Springer Series in Computational Mathematics*. Springer-Verlag, Berlin, 1986.
- P. Grisvard. *Elliptic Problems in Nonsmooth Domains*, volume 24 of *Monographs and Studies in Mathematics*. Pitman, Boston, MA, 1985.
- T. Gudi. A new error analysis for discontinuous finite element methods for linear elliptic problems. *Math. Comp.*, 79(272):2169–2189, 2010.
- J. Guzmán and M. Neilan. Conforming and divergence-free Stokes elements on general triangular meshes. *Math. Comp.*, 83(285):15–36, 2014.
- V. Heuveline and R. Rannacher. A posteriori error control for finite approximations of elliptic eigenvalue problems. *Adv. Comput. Math.*, 15(1-4), 2001.
- J. Hu and Z. Shi. A new a posteriori error estimate for the Morley element. *Numer. Math.*, 112(1):25–40, 2009.
- J. Hu and J. Xu. Convergence and optimality of the adaptive nonconforming linear element method for the Stokes problem. *J. Sci. Comput.*, 55(1):125–148, 2013a.
- J. Hu and J. Xu. Convergence and optimality of the adaptive nonconforming linear element method for the Stokes problem. *arXiv e-Prints*, 1309.3608v1, 2013b. URL <http://arxiv.org/abs/1309.3608v1>.
- J. Hu, Z. Shi, and J. Xu. Convergence and optimality of the adaptive Morley element method. *Numer. Math.*, 121(4):731–752, 2012.
- J. Hu, Z. Shi, and J. Xu. Convergence and optimality of the adaptive Morley element method. *arXiv e-Prints*, 1309.3606, 2013. URL <http://arxiv.org/abs/1309.3606>.
- T. Kato. *Perturbation Theory for Linear Operators*, volume 132 of *Die Grundlehren der mathematischen Wissenschaften*. Springer-Verlag, New York, 1966.
- A. Knyazev. *lobpcg.m*. 2011. URL <http://www.mathworks.com/matlabcentral/fileexchange/48-lobpcg-m>. 25 May 2000 (Updated 17 Oct 2011).
- A. V. Knyazev. Toward the optimal preconditioned eigensolver: locally optimal block preconditioned conjugate gradient method. *SIAM J. Sci. Comput.*, 23(2):517–541, 2001.
- A. V. Knyazev and J. E. Osborn. New a priori FEM error estimates for eigenvalues. *SIAM J. Numer. Anal.*, 43(6):2647–2667, 2006.
- Y. A. Kuznetsov and S. I. Repin. Guaranteed lower bounds of the smallest eigenvalues of elliptic differential operators. *J. Numer. Math.*, 21(2):135–156, 2013.
- M. G. Larson. A posteriori and a priori error analysis for finite element approximations of self-adjoint elliptic eigenvalue problems. *SIAM J. Numer. Anal.*, 38(2):608–625, 2000.
- P. Lascaux and P. Lesaint. Some nonconforming finite elements for the plate bending problem. *Rev. Française Automat. Informat. Recherche Operationnelle*, 9(R-1):9–53, 1975.

BIBLIOGRAPHY

- R. S. Laugesen and B. A. Siudeja. Minimizing Neumann fundamental tones of triangles: an optimal Poincaré inequality. *J. Differential Equations*, 249(1):118–135, 2010.
- R. B. Lehoucq, D. C. Sorensen, and C. Yang. *ARPACK users' guide*, volume 6 of *Software, Environments, and Tools*. Society for Industrial and Applied Mathematics (SIAM), Philadelphia, PA, 1998.
- X. Liu and S. Oishi. Verified eigenvalue evaluation for the Laplacian over polygonal domains of arbitrary shape. *SIAM J. Numer. Anal.*, 51(3):1634–1654, 2013.
- S. Mao and Z. Shi. On the error bounds of nonconforming finite elements. *Sci. China Math.*, 53(11):2917–2926, 2010.
- J. M. Maubach. Local bisection refinement for n -simplicial grids generated by reflection. *SIAM J. Sci. Comput.*, 16(1):210–227, 1995.
- V. Mehrmann and A. Miedlar. Adaptive computation of smallest eigenvalues of self-adjoint elliptic partial differential equations. *Numer. Linear Algebra Appl.*, 18(3):387–409, 2011.
- H. Melzer and R. Rannacher. Spannungskonzentrationen in Eckpunkten der Kirchhoffschen Platte. *Bauingenieur*, 55:181–184, 1980.
- A. Meyer. A simplified calculation of reduced HCT-basis functions in a finite element context. *Comput. Methods Appl. Math.*, 12(4):486–499, 2012.
- A. Miedlar. Functional perturbation results and the balanced AFEM algorithm for self-adjoint PDE eigenvalue problems. *Matheon Preprint*, #817, 2011. URL <http://opus4.kobv.de/opus4-matheon/files/897/Mie11.pdf>.
- L. S. D. Morley. The triangular equilibrium element in the solution of plate bending problems. *Aeronaut. Quart.*, 19:149–169, 1968.
- E. Ovtchinnikov. Cluster robust error estimates for the Rayleigh-Ritz approximation. I. Estimates for invariant subspaces. *Linear Algebra Appl.*, 415(1):167–187, 2006a.
- E. Ovtchinnikov. Cluster robust error estimates for the Rayleigh-Ritz approximation. II. Estimates for eigenvalues. *Linear Algebra Appl.*, 415(1):188–209, 2006b.
- B. N. Parlett. *The Symmetric Eigenvalue Problem*, volume 20 of *Classics in Applied Mathematics*. Society for Industrial and Applied Mathematics (SIAM), Philadelphia, PA, 1998.
- H. Rabus. A natural adaptive nonconforming FEM of quasi-optimal complexity. *Comput. Methods Appl. Math.*, 10(3):315–325, 2010.
- R. Rannacher. Nonconforming finite element methods for eigenvalue problems in linear plate theory. *Numer. Math.*, 33(1):23–42, 1979.
- G. Savaré. Regularity results for elliptic equations in Lipschitz domains. *J. Funct. Anal.*, 152(1):176–201, 1998.

- L. R. Scott and M. Vogelius. Norm estimates for a maximal right inverse of the divergence operator in spaces of piecewise polynomials. *RAIRO Modél. Math. Anal. Numér.*, 19(1): 111–143, 1985.
- L. R. Scott and S. Zhang. Finite element interpolation of nonsmooth functions satisfying boundary conditions. *Math. Comp.*, 54(190):483–493, 1990.
- R. Stevenson. Optimality of a standard adaptive finite element method. *Found. Comput. Math.*, 7(2):245–269, 2007.
- R. Stevenson. The completion of locally refined simplicial partitions created by bisection. *Math. Comp.*, 77(261):227–241, 2008.
- R. Stevenson. Private communication. Korteweg-de Vries Institute for Mathematics, Amsterdam, 2013.
- J. Stoer and R. Bulirsch. *Introduction to Numerical Analysis*, volume 12 of *Texts in Applied Mathematics*. Springer-Verlag, New York, third edition, 2002.
- G. Strang and G. J. Fix. *An Analysis of the Finite Element Method*. Prentice-Hall Series in Automatic Computation. Prentice-Hall Inc., Englewood Cliffs, N. J., 1973.
- The MathWorks, Inc. *Matlab version 7.14.0.739 (R2012a)*. Natick, Massachusetts, United States., 2012.
- S. Timoshenko and J. Gere. *Theory of Elastic Stability*. Engineering Societies Monographs. MacGraw-Hill International, Auckland, 1985.
- C. T. Traxler. An algorithm for adaptive mesh refinement in n dimensions. *Computing*, 59(2):115–137, 1997.
- R. Verfürth. A posteriori error estimates for nonlinear problems. Finite element discretizations of elliptic equations. *Math. Comp.*, 62(206):445–475, 1994.
- R. Verfürth. *A Review of a Posteriori Error Estimation and Adaptive Mesh-Refinement Techniques*. Advances in numerical mathematics. John Wiley & Sons., Chichester, 1996.
- M. Wang and J. Xu. The Morley element for fourth order elliptic equations in any dimensions. *Numer. Math.*, 103(1):155–169, 2006.
- A. Weinstein and W. Stenger. *Methods of Intermediate Problems for Eigenvalues*, volume 89 of *Theory and Ramifications, Mathematics in Science and Engineering*. Academic Press, New York, 1972.

A. Table of Common Notation

Elementary Notation

\bullet or \cdot	identity mapping
\mathbb{N}	positive integers, i.e., $\{1, 2, 3, \dots\}$
\mathbb{N}_0	nonnegative integers, i.e., $\mathbb{N} \cup \{0\}$
\mathbb{R}	field of real numbers
\mathbb{C}	field of complex numbers
$m \bmod n$	m modulo n , i.e., $m \bmod n$ is the remainder of the Euclidean division of m by n
$\mathbb{R}^{m \times n}$	space of $m \times n$ matrices with real coefficients
A^\top	transpose of the matrix A
d	(physical) space dimension
$\text{sym}(A)$	symmetric part of $A \in \mathbb{R}^{n \times n}$, i.e., $\text{sym}(A) = 1/2(A + A^\top)$
\mathbb{S}	space of symmetric matrices of $\mathbb{R}^{d \times d}$
$1_{n \times n}$	$n \times n$ unit matrix
$\text{tr}(A)$	trace of $A \in \mathbb{R}^{n \times n}$, i.e., $\text{tr}(A) = \sum_{j=1}^n A_{jj}$
$\text{dev}(A)$	deviatoric part of $A \in \mathbb{R}^{n \times n}$, i.e., $\text{dev}(A) = A - 1/n \text{tr}(A) 1_{n \times n}$
δ_{jk}	Kronecker δ , i.e., $\delta_{jk} = \begin{cases} 1 & \text{if } j = k \\ 0 & \text{else} \end{cases}$
$x \cdot y$	Euclidean scalar product of two elements of \mathbb{R}^n , i.e., $x \cdot y = \sum_{j=1}^n x_j y_j$
$ x $	Euclidean length of $x \in \mathbb{R}^n$, i.e., $ x = \sqrt{x \cdot x}$ or length of a multi-index $x \in \mathbb{N}_0^n$, i.e., $ x = \sum_{j=1}^n x_j$ (clear from the context)
$(a, b), [a, b]$	open (resp. closed) real intervals
X^*	topological dual of a normed space X
$\sin_{a, \text{NC}} \angle(x, y), \sin_a \angle(x, y)$	sine of the angle between two vectors x and y ; measured in the scalar product a_{NC} or a
$\sin_{a, \text{NC}} \angle(X, Y), \sin_a \angle(X, Y)$	sine of the largest principal angle from X to Y for finite-dimensional spaces X and Y ; measured in the scalar product a_{NC} or a

Set-Related Notation

\emptyset	the empty set
$X \subseteq Y$	X is a subset of Y
$X \subsetneq Y$	$X \subseteq Y$ and $X \neq Y$
2^X	power set of the set X
$\text{card}(X)$	cardinality of a set X
$\overline{\omega}$	closure of the set $\omega \subseteq \mathbb{R}^d$ with respect to the topology of the Euclidean space
$\partial\omega$	boundary of the set $\omega \subseteq \mathbb{R}^d$ with respect to the topology of the Euclidean space
$\text{int}(\omega)$	interior of the set $\omega \subseteq \mathbb{R}^d$ with respect to the topology of the Euclidean space
$\text{conv}(\omega)$	convex hull of the set $\omega \subseteq \mathbb{R}^d$
$\text{span}(\omega)$	linear hull of $\omega \subseteq \mathbb{R}^n$

Geometrical and Measure-Theoretical Notation

$\text{dist}(x, X)$	Euclidean distance of $x \in \mathbb{R}^d$ to the set $X \subseteq \mathbb{R}^d$, i.e., $\text{dist}(x, X) = \inf_{y \in X} x - y $
$\text{dist}(X, Y)$	Euclidean distance of the subsets $(X, Y) \in (\mathbb{R}^d)^2$, i.e., $\text{dist}(X, Y) = \inf_{(x, y) \in X \times Y} x - y $
$\text{diam}(X)$	diameter of the set $X \subseteq \mathbb{R}^d$, i.e., $\text{diam}(X) = \sup_{(x, y) \in X^2} x - y $
$\text{meas}(X)$	d -dimensional Lebesgue measure of $X \subseteq \mathbb{R}^d$
$\text{meas}_{d-1}(X)$	$(d-1)$ -dimensional Hausdorff measure of $X \subseteq \mathbb{R}^d$
$\int_{\omega} f dx$ or $\int_{\omega} f(\xi) dx(\xi)$	d -dimensional Lebesgue integral of f over ω
$\int_{\omega} f ds$	$(d-1)$ -dimensional surface integral of f over ω
\bar{f}	mean value integral
$\int_{\Gamma} f(z) dz$	complex contour integral over Γ
$L^2(\omega), L^2(\omega; X)$	square-integrable functions over ω (measure clear from the context)
$L_0^2(\omega), L_0^2(\omega; X)$	square-integrable functions over ω with vanishing integral
$\ f\ _{L^2(\omega)}$	L^2 norm of f over ω
$\ f\ $	$:= \ f\ _{L^2(\Omega)}$
$(f, g)_{L^2(\omega)}$	L^2 scalar product of f and g
$L^{\infty}(\omega), L^{\infty}(\omega; X)$	essentially bounded measurable functions (measure clear from the context)
$\ f\ _{L^{\infty}(\omega)}$	essential supremum of f over ω

$\ f\ _\infty$	$:= \ f\ _{L^\infty(\Omega)}$
$H^k(\omega), H^k(\omega; X)$	Sobolev space of k -times weakly differentiable L^2 functions with weak derivatives in L^2
$H^{k+s}(\omega), H^{k+s}(\omega; X)$	fractional-order Sobolev space
$\ f\ _{H^k(\omega)}, \ f\ _{H^{k+s}(\omega)}$	Sobolev norms
$\mathcal{D}(\omega), \mathcal{D}(\omega; X)$	smooth functions with compact support in ω
$H_0^k(\omega), H_0^k(\omega; X)$	closure of $\mathcal{D}(\omega)$ (resp. $\mathcal{D}(\omega; X)$) with respect to $\ \cdot\ _{H^k(\omega)}$
$H^{-k}(\omega), H^{-k}(\omega; X)$	dual space of $H_0^k(\omega)$ resp. $H_0^k(\omega; X)$
$\ \cdot\ _{H^{-k}(\omega)}$	operator norm in $H^{-k}(\omega)$
$\mathcal{P}_k(\omega), \mathcal{P}_k(\omega; X)$	polynomial functions on ω of total degree $\leq k$ (understood component-wise, if X -valued)
$\mathcal{Q}_k(\omega), \mathcal{Q}_k(\omega; X)$	polynomial functions on ω of partial degree $\leq k$ (understood component-wise, if X -valued)

Differential Operators

D, D^2	derivative, Hessian
Δ, Δ^2	Laplacian, biharmonic operator (bi-Laplacian)
div	divergence, applied row-wise to tensor-fields
Curl	Curl operator in 2 dimensions, i.e., $\text{Curl} f := (-\partial f / \partial x_2 \ \partial f / \partial x_1)$; applied row-wise to tensor-fields (cf. Definition 2.3)
$\partial f / \partial \rho$	directional derivative with respect to $\rho \in \mathbb{R}^d$
NC	subscript index to indicate the piecewise action of a differential operator

Triangulations

$\mathbb{T}(\mathcal{T})$	set of admissible triangulations refined from the initial triangulation \mathcal{T}
\mathbb{T}	$:= \mathbb{T}(\mathcal{T}_0)$
$\mathbb{T}(m)$	$:= \{\mathcal{T} \in \mathbb{T} \mid \text{card}(\mathcal{T}) - \text{card}(\mathcal{T}_0) \leq m\}$
$\mathcal{T}_1 \otimes \mathcal{T}_2$	overlay of $(\mathcal{T}_1, \mathcal{T}_2) \in \mathbb{T}^2$
$\mathcal{F}(T)$	hyper-faces of the simplex T
$\mathcal{F}_\ell := \mathcal{F}(\mathcal{T}_\ell)$	hyper-faces of the triangulation \mathcal{T}_ℓ
$\mathcal{F}_\ell(\Omega)$	interior hyper-faces of \mathcal{T}_ℓ
$[v]_F$	jump of a function v across the hyper-face F
\mathbf{v}_F	unit normal vector of the hyper-face F
$\boldsymbol{\tau}_F$	unit tangent vector of the hyper-face F (for $d = 2$)
$\mathcal{N}(T)$	vertices of the simplex T
$\mathcal{N}_\ell := \mathcal{N}(\mathcal{T}_\ell)$	vertices of \mathcal{T}_ℓ
$\text{mid}(T), \text{mid}(F),$	midpoint (barycentre) of a simplex T or a hyper-face F
h_T	$:= \text{meas}(T)^{1/d}$ for a simplex $T \in \mathcal{T}$

A. Table of Common Notation

$h_{\mathcal{T}_\ell}, h_\ell$	mesh-size function, $h_{\mathcal{T}_\ell} _T := h_T$ for any $T \in \mathcal{T}$
h_F	$:= \text{diam}(F)$ for a hyper-face $F \in \mathcal{F}(\mathcal{T})$
$\mathcal{P}_k(\mathcal{T}_\ell), \mathcal{P}_k(\mathcal{T}_\ell; X)$	piecewise polynomials of total degree $\leq k$
$\mathcal{Q}_k(\mathcal{T}_\ell), \mathcal{Q}_k(\mathcal{T}_\ell; X)$	piecewise polynomials of partial degree $\leq k$
Π_ℓ^p	L^2 projection onto $\mathcal{P}_p(\mathcal{T}_\ell)$
$\text{osc}_{p,k}^2(f, \mathcal{T}_\ell)$	oscillations, i.e., $\ h_\ell^k(1 - \Pi_\ell^p)f\ _{L^2(\Omega)}^2$

Approximation of Eigenvalue Clusters

$J = \{n+1, \dots, n+N\}$	index set that describes the eigenvalue cluster
λ_j, u_j, p_j	exact eigenvalues and fixed orthonormal set of eigenfunctions u_j (and pressures p_j in case of the Stokes problem)
$\lambda_{\ell,j}, u_{\ell,j}$	discrete eigenvalues, orthonormal set of discrete eigenfunctions with respect to the finite element space V_ℓ
$R_\ell, R_{\mathcal{T}_\ell}$	(quasi-) Ritz projection onto V_ℓ
$P_\ell, P_{\mathcal{T}_\ell}$	L^2 -orthogonal projection onto $\text{span}\{u_{\ell,j} \mid j \in J\}$
$\Lambda_\ell, \Lambda_{\mathcal{T}_\ell}$	$:= P_{\mathcal{T}_\ell} \circ R_{\mathcal{T}_\ell}$
$[A, B]$	real interval that contains the eigenvalue cluster
$a \lesssim b$	$a \leq Cb$ for a constant C that does not depend on the mesh-size or the eigenvalue cluster
$a \approx b$	$a \lesssim b \lesssim a$
$a \ll b$	a sufficiently small relative to b

B. Implementation

This appendix chapter gives an overview of the Matlab implementation for the numerical examples from Chapter 9. The implementation is based on the AFEM software package [Carstensen et al., 2009] maintained by the Numerical Analysis Group at HU Berlin.

B.1. Structure of the Implementation

Problem-Specific Functions

The conforming and nonconforming \mathcal{P}_1 FEM for the Poisson eigenvalue problem are adopted from the AFEM package and implemented as

```
function [eVect,eVal,ndof,A,B] = solveP1PoissonEVPcluster(cluster_lower,...
    cluster_upper,c4n,n4e,n4sDb,n4sNb)
function [eVect,eVal,ndof,A,B] = solveCRPoissonEVPcluster(...
    cluster_lower,cluster_upper,c4n,n4e,n4sDb,n4sNb)
```

The \mathcal{P}_2 FEM for the computation of reference eigenvalues is implemented as

```
function [eVect,eVal,ndof] = solveP2PoissonEVPcluster(cluster_lower,...
    cluster_upper,c4n,n4e,n4sDb,n4sNb)
```

The Morley FEM and the BFS FEM for fourth-order problems are implemented as

```
function [eVect,eVal,ndof,Hess4e,Blocal] = solveMorleyEVPcluster(...
    cluster_lower,cluster_upper,RHS,c4n,n4e,n4sCb,n4sSb)
function [eVect,eVal,ndof] = solveBFSEVPcluster(cluster_lower,...
    cluster_upper,RHS,c4n,n4e,n4sCb,n4sSb)
```

The conforming \mathcal{P}_1 FEM with inexact solve is implemented as

```
function [eVect,eVal,ndof,A,B,p] = solveP1PoissonEVPcluster_eigs(...
    cluster_lower,cluster_upper,c4n,n4e,n4sDb,n4sNb,exEVfile,...
    term_crit,term_param,maxit,tol,eta_oldSq,printinfo)
function [eVect,eVal,ndof,A,B,niter] = solveP1PoissonEVPcluster_lobpcg(...
    cluster_lower,cluster_upper,c4n,n4e,n4sDb,n4sNb,exEVfile,...
    term_param,niter,maxiter,tol,eta_oldSq)
```

Error Estimation

The error estimators are similar to those of the linear problems implemented in the AFEM package. For the Laplace eigenvalue problem the corresponding functions are

```
function eta4eSq = estimateCREvpEtaElements(eVal,eVect,c4n,n4e,n4sDb,n4sNb)
function eta4eSq = estimateP1evpEtaElements(eVal,eVect,c4n,n4e,n4sDb,n4sNb)
```

The error estimator contributions for the Morley FEM are computed by

```
function eta4eSq = estimateMorleyEtaElements(lambda,u,c4n,n4e,n4sCb,...
    n4sSb,RHS,Hess4e,Blocal)
```

Mesh-Refinement

The routines for triangular mesh-refinement are taken from the AFEM package without modifications

```
function n4sMarked = markBulk(n4p,eta4p,OPTtheta)
function [c4nNew,n4eNew,n4sDbNew,n4sNbNew] = ...
    refineBi3GB(c4n,n4e,n4sDb,n4sNb,n4sMarked
    )
function n4sRefine = closure(n4e, n4sMarked)
function [c4nNew,n4eNew,n4sDbNew,n4sNbNew] = refineUniformRed(c4n,n4e,n4sDb,
    n4sNb)
```

For rectangular partitions, the uniform red-refinement is implemented as

```
function [c4nNew,n4eNew,n4sDbNew,n4sNbNew] = refineUniformRed_rect(c4n,...
    n4e,n4sDb,n4sNb)
```

Computation of Data Structures

The following functions for the computation of geometrical quantities and data structures are taken from the AFEM package without modifications

```
function area4e = computeArea4e(c4n,n4e)
function e4n = computeE4n(n4e)
function e4s = computeE4s(n4e)
function length4s = computeLength4s(c4n,n4s)
function mid4s = computeMid4s(c4n, n4s)
function n4s = computeN4s(n4e)
function normal4e = computeNormal4e(c4n,n4e)
function normal4s = computeNormal4s(c4n,n4s)
function s4e = computeS4e(n4e)
function s4n = computeS4n(n4e)
function tangent4e = computeTangent4e(c4n,n4e)
function tangent4s = computeTangent4s(c4n,n4s)
function jump4s = P0NormalJump(c4n,n4e,n4sDb,n4sNb,sigma4e,g)
function jump4s = P0TangentJump(c4n,n4e,n4sDb,n4sNb,sigma4e,u4Db)
```

AFEM Loop

The main programs that realise the AFEM loop for the eigenvalues of the Laplacian are

```
function afemCRPoissonEVPcluster(geom,nrRedRefinements,theta,minndof,...
    cluster_lower,cluster_upper,exEVfile,foldername)
function afemP1PoissonEVPcluster(geom,nrRedRefinements,theta,minndof,...
    cluster_lower,cluster_upper,exEVfile,foldername)
```

The adaptive Morley FEM is implemented as

```
function afemMorleyEVPcluster(geom,nrRedRefinements,theta,minndof,...
    cluster_lower,cluster_upper,RHS,exEVfile,foldername)
```

The conforming \mathcal{P}_1 AFEM loop with inexact solve is implemented as

```
function afemP1PoissonEVPcluster_inx(geom,nrRedRefinements,theta,...
    minndof,cluster_lower,cluster_upper,exEVfile,method,term_crit,...
    term_param,maxit,tol,foldername)
```

Further Programs

The following programs compute eigenvalues on uniformly-refined meshes with the conforming \mathcal{P}_2 FEM and the BFS FEM

```
function P2EVPcluster(geom,nrRedRefinements,minndof,cluster_lower,...
    cluster_upper,exEVfile,foldername)
function BFSEVPcluster(geom,nrRedRefinements,minndof,cluster_lower,...
    cluster_upper,RHS,exEVfile,foldername)
```

The reference eigenvalues can be extrapolated with the Aitken method

```
function val = aitken(x)
```

The following three plot routines are taken from the AFEM package without modification

```
function plotConvergence(nrDoF4lvl, error4lvl, OPTname)
function plotCR(c4n, n4e, x, OPTtitle)
function plotP1(c4n, n4e, x, OPTtitle)
```

Surface plots and mesh plots for triangular or rectangular partitions can be generated with

```
function plot4vert(c4n,n4e,x,nrVertices,OPTtitle)
function plotTriangulation (c4n,n4e)
```

Geometrical data can be loaded with

```
function [c4n n4e n4sDb n4sNb] = loadGeometry(name, OPTRefinementLevel)
function [c4n,n4e,n4sDb,n4sNb] = loadGeometry_rect(name,OPTRefinementLevel)
```

The following function writes the computed data into *.dat files

```
function saveInformation(folder,cluster_lower,cluster_upper,nEig,geom,...
    theta,ndofList,eVallList,hmaxlist,infostring)
```

B.2. Reproduction of the Numerical Experiments

This section briefly describes how to reproduce the computational experiments from Chapter 9 by providing sample calls of the functions that perform the AFEM loop (named `afem*.m`).

Laplacian

Since the syntax for the conforming and nonconforming \mathcal{P}_1 FEM is identical, the example only concerns the conforming version.

The simultaneous adaptive computation of the first 10 eigenvalues on the L-shaped domain with one red-refinement for the coarse triangulation is performed by a call of

```
afemP1PoissonEVPcluster('Lshape',1,0.1,10^5,1,10,Lshape_EVs_Poisson.dat','tmp',)
```

The example for the perturbed slit domain and $J = \{2\}$, $\theta = 1$ and no initial refinement of the domain can be reproduced by calling

```
afemP1PoissonEVPcluster('PerturbSlit',0,0.1,10^5,2,2,'PerturbSlit_EVs_Poisson.dat','tmp')
```

B. Implementation

The reference eigenvalues (here for example the second) can be computed with

```
P2EVPcluster('PerturbSlit',2,10^5,1,10,'','tmp')
evallist1 = load('tmp/EvallList1.dat');
extrapol_evallist1 = aitken(evallist1);
```

Laplacian with Inexact Solve

The example for the perturbed slit domain and $J = \{2, 3\}$, $\theta = 0.1$, $\varkappa = 0.01$ and no initial refinement of the domain and eigs options $\text{tol} = 10^{-6}$ and $\text{maxit} = 10$ can be reproduced by calling

```
afemP1PoissonEVPcluster_inx('PerturbSlit',0,0.1,6*10^4,2,3,'
    PerturbSlit_EVs_Poisson.dat','eigs','kappa',0.01,10,10^-6,'tmp')
```

Stokes System

The first 10 Stokes eigenvalues on the L-shaped domain with one red-refinement for the coarse triangulation and $\theta = 0.1$ are computed by

```
afemMorleyEVPcluster('Lshape',1,0.1,10^5,1,10,'grad','
    Lshape_EVs_clamped_Buckling.dat','tmp')
```

The reference eigenvalues (here for example the first) can be computed with

```
BFSEVPcluster('Lshape',2,10^5,1,10,'grad','','tmp')
evallist1 = load('tmp/EvallList1.dat');
extrapol_evallist1 = aitken(evallist1);
```

Biharmonic operator

The eigenvalues 9–12 of the biharmonic operator on the perturbed slit domain with adaptive refinement ($\theta = 0.1$) and $J = \{9, \dots, 12\}$ are computed by

```
afemMorleyEVPcluster('PerturbSlit',0,0.1,10^5,9,12,'mass','
    PerturbSlit_EVs_clamped_bih.dat','tmp')
```

The reference eigenvalues (here for example the 9th) can be computed with

```
BFSEVPcluster('PerturbSlit',2,10^5,1,12,'mass','','tmp')
evallist1 = load('tmp/EvallList9.dat');
extrapol_evallist9 = aitken(evallist9);
```

C. Data Medium Containing the Software

The online version of this document contains the software as embedded tar-file. Please use an appropriate pdf viewer to extract the file, such as KDE Okular or Adobe Reader. In contrast to the thesis' text, the code (except lobpcg.m) is provided under the terms of the GNU General Public License as published by the Free Software Foundation, either version 3 of the License, or (at your option) any later version. Refer to the file LICENSE.txt in the software archive for more information.

Content of the Software Archive

```

  afemCRPoissonEVPcluster.m      P2EVPcluster.m
  afemMorleyEVPcluster.m        plot4vert.m
  afemP1PoissonEVPcluster.m     plotTriangulation.m
  afemP1PoissonEVPcluster_inx.m refineUniformRed_rect.m
  aitken.m                      saveInformation.m
  BFSEVPcluster.m              solveBFSEVPcluster.m
  estimateCRvpEtaElements.m     solveCRPoissonEVPcluster.m
  estimateMorleyEtaElements.m   solveMorleyEVPcluster.m
  estimateP1evpEtaElements.m    solveP1PoissonEVPcluster.m
  GNUGPLv3.txt                 solveP1PoissonEVPcluster_eigs.m
  integrate.m                  solveP1PoissonEVPcluster_lobpcg.m
  LICENSE.txt                  solveP2PoissonEVPcluster.m
  loadGeometry_rect.m

  afem-base ..... files taken from AFEM [Carstensen et al., 2009]
  └─ closure.m          computeN4s.m      computeTangent4s.m  plotCR.m
    computeArea4e.m     computeNormal4e.m  loadGeometry.m      plotP1.m
    computeE4n.m        computeNormal4s.m  markBulk.m          refineBi3GB.m
    computeE4s.m        computeS4e.m       P0NormalJump.m      refineUniformRed.m
    computeLength4s.m   computeS4n.m       P0TangentJump.m
    computeMid4s.m      computeTangent4e.m  plotConvergence.m

  data ..... contains *.dat-files with reference eigenvalues
  extern ..... LOBPCG eigensolver
  └─ license.txt
    lobpcg.m ..... Author: A. Knyazev [Knyazev, 2011]
  geometries ..... subfolders contain *.dat-files with geometrical data
  └─ Lshape
    └─ Lshape_mixedBC
      └─ Lshape_mixedBC_rect
        └─ Lshape_rect
          └─ PerturbSlit
            └─ PerturbSlit_rect

```


List of Figures

1.1. Convergence history for the first eigenvalue of the biharmonic operator and guaranteed lower bound on the L-shaped domain.	1
1.2. Numerical test on a perturbed geometry.	2
1.3. Mnemonic diagrams of some finite elements.	3
2.1. Possible refinements of a triangle T in one level in 2D.	12
5.1. Triangulation, refinement and intermediate triangulation.	51
7.1. Mnemonic diagrams of two finite elements for the biharmonic equation. . .	80
8.1. Mappings between the spaces \widehat{V}_ℓ , $\widehat{V}_{\ell+m}$, V , V_ℓ and $V_{\ell+m}$	102
9.1. Initial partitions and boundary conditions for the L-shaped domain.	113
9.2. Square domain with perturbed slits.	114
9.3. The Bogner-Fox-Schmit bicubic finite element.	115
9.4. Convergence history for the eigenvalues of the Laplacian on the L-shaped domain for the conforming \mathcal{P}_1 method with uniform mesh-refinement. . .	117
9.5. Convergence history for the eigenvalues of the Laplacian on the L-shaped domain for the conforming \mathcal{P}_1 method with adaptive mesh-refinement. . .	118
9.6. Convergence history for the eigenvalues of the Laplacian on the L-shaped domain for the nonconforming \mathcal{P}_1 method with uniform mesh-refinement. .	118
9.7. Convergence history for the eigenvalues of the Laplacian on the L-shaped domain for the nonconforming \mathcal{P}_1 method with adaptive mesh-refinement. .	119
9.8. Convergence history of the conforming \mathcal{P}_1 method on the square with perturbed slits.	120
9.9. Convergence history of the nonconforming \mathcal{P}_1 method on the square with perturbed slits.	120
9.10. Approximation of the eigenmodes u_2 and u_3 of the Laplacian on the perturbed slit domain.	121
9.11. Adaptive approximation of the eigenmodes u_2 and u_3 of the Laplacian on the perturbed slit domain.	121
9.12. Adaptive meshes for the perturbed slit domain.	121
9.13. Convergence history for the eigenvalues of the Stokes system on the L-shaped domain with uniform mesh-refinement.	123
9.14. Convergence history for the eigenvalues of the Stokes system on the L-shaped domain with adaptive mesh-refinement.	123
9.15. Convergence history for the eigenvalues of the Stokes system on the square with perturbed slits.	124

LIST OF FIGURES

9.16. Convergence history for the eigenvalues of the biharmonic operator on the L-shaped domain with mixed boundary conditions under uniform mesh refinement.	125
9.17. Convergence history for the eigenvalue of the biharmonic operator on the L-shaped domain with mixed boundary conditions; adaptive mesh-refinement based on $J = \{1, \dots, 10\}$	126
9.18. Convergence history for the eigenvalues of the biharmonic operator on the square with perturbed slits based on $J = \{9, \dots, 12\}$ and a coarse initial mesh with 41 degrees of freedom.	127
9.19. Convergence history for the eigenvalues of the biharmonic operator on the square with perturbed slits based on $J \subseteq \{9, \dots, 12\}$ and a coarse initial mesh with 41 degrees of freedom.	127
9.20. Convergence history for the eigenvalues of the biharmonic operator on the square with perturbed slits based on $J \subseteq \{9, \dots, 12\}$ and an initial mesh with 209 degrees of freedom.	128
9.21. Matlab implementation of the loop of Algorithm 9.1.	130
9.22. Convergence history for the adaptive inexact computation of the first eigenvalue of the Laplacian on the L-shaped domain.	131
9.23. Convergence history for the adaptive inexact computation of the eigenvalues number 2 and 3 of the Laplacian on the square with perturbed slits using eigs with maxit = 1 and the parameter $\varkappa \in \{10^{-1}, 10^{-2}\}$	132
9.24. Convergence history for the adaptive inexact computation of the eigenvalues number 2 and 3 of the Laplacian on the square with perturbed slits using eigs with maxit = 1 and the parameter $\varkappa \in \{10^{-3}, 10^{-4}\}$	133
9.25. Convergence history for the adaptive inexact computation of the eigenvalues number 2 and 3 of the Laplacian on the square with perturbed slits with 9 implicit restarts in eigs.	133
9.26. Convergence history for the adaptive inexact computation of the eigenvalues number 2 and 3 of the Laplacian on the square with perturbed slits and parameter $\varkappa \in \{10^{-3}, 10^{-4}\}$ with LOBPCG.	134
9.27. Convergence history for the adaptive inexact computation of the eigenvalues number 2 and 3 of the Laplacian on the square with perturbed slits and parameter $\varkappa \in \{10^{-3}, 10^{-4}\}$ with LOBPCG.	135

List of Tables

4.1. Overview of assumptions on the initial mesh-size for the conforming \mathcal{P}_1 finite element method and their first occurrence in this thesis. B acts as upper bound for all $(\lambda_j \mid j \in J)$	36
9.1. Aitken extrapolation of the 10th eigenvalue of the Laplacian on the L-shaped domain.	117
9.2. Aitken extrapolation of eigenvalues of the Laplacian on the square with perturbed slits.	118
9.3. Extrapolation of the 10th eigenvalue of the Stokes system on the L-shaped domain.	122
9.4. Guaranteed upper (GUB) and lower (GLB) eigenvalue bounds for the first eigenvalue of the Stokes system on the L-shaped domain on uniformly refined meshes. The extrapolated eigenvalue is $\lambda_1 = 32.132687$	123
9.5. Aitken extrapolation of the Stokes eigenvalues on the square with perturbed slits.	124
9.6. Extrapolation of the 10th eigenvalue of the biharmonic operator on the L-shaped domain.	125
9.7. Guaranteed upper (GUB) and lower (GLB) eigenvalue bounds for the first eigenvalue of the biharmonic operator on the L-shaped domain with mixed boundary conditions.	126
9.8. Aitken extrapolation of eigenvalues of the biharmonic operator on the slit- ted square.	126
9.9. Convergence history on the L-shaped domain using <code>eigs</code> with $\varkappa = 0.001$	131

Erklärung

Ich erkläre, dass ich die vorliegende Arbeit selbständig und nur unter Verwendung der angegebenen Literatur und Hilfsmittel angefertigt habe.

Berlin, den 05. März 2014

Dietmar Gallistl